Levetiracetam and Brivaracetam:

Synthesis of Radioligands as Pharmacological Tools

for

Studying Their Interactions with Target Proteins

Dissertation

zur

Erlangung des Doktorgrades (Dr. rer. nat.)

der

Mathematisch-Naturwissenschaftlichen Fakultät

der

Rheinischen Friedrich-Wilhelms-Universität Bonn

vorgelegt von

Simone Hildenbrand

aus

Krefeld

Bonn 2012

Angefertigt mit Genehmigung der Mathematisch-Naturwissenschaftlichen Fakultät der Rheinischen Friedrich-Wilhelms-Universität Bonn.

Die vorliegende Arbeit wurde in der Zeit von Mai 2008 bis April 2012 am Pharmazeutischen Institut der Rheinischen Friedrich-Wilhelms-Universität Bonn unter der Leitung von Frau Prof. Dr. Christa E. Müller durchgeführt.

Meinen Eltern

Abstract

Epilepsy is one of the most common neurological disorders affecting more than 50 million people worldwide. Despite extensive efforts in antiepileptic drug (AED) development it is estimated that around 30% of all epileptic patients remain resistant to current AED therapy. In addition, the majority of conventional AEDs exhibits a large spectrum of side effects and a high potential of drug interactions (cytochrome P450), which restrict their applicability. In 1999, the antiepileptic drug levetiracetam (LEV, (2S)-2-(2-oxopyrrolidin-1-yl)butanamide, Keppra[®]) was launched on the market and soon became one of the most successful AEDs of the newer generation. It binds to the synaptic vesicle protein SV2A and thus appears to exert its potent antiepileptic effect via a unique mechanism of action that is, however, still not well understood. Its analogue brivaracetam (BRV), which possesses a 10- to 20-fold higher affinity to the SV2A protein, is currently in late stages of phase III clinical trials.

In the present study, synthetic pathways were devised for precursor molecules of LEV and BRV suitable for generating ³H-labeled forms of both AEDs with high specific activity (94-98 Ci/mmol). In a reductive amination reaction mucochloric acid and previously prepared (S)-2-aminobutanamide were applied in the presence of sodium triacetoxyborohydride and acetic acid to synthesize (S)-2-(3,4-dichloro-2,5-dihydro-2-oxo-1H-pyrrol-1-yl)butanamide, which served as precursor for the preparation of [³H]LEV. The second precursor molecule was prepared via the intermediate 4-allyl-5-hydroxyfuran-2(5H)-one, obtained in a Mannich type reaction of glyoxylic acid and pent-4-enal in the presence of morpholine hydro-chloride, which was subsequently utilized in a reductive amination reaction with (S)-2-aminobutanamide for the preparation of (S)-2-(4-allyl-2-oxo-2,5-dihydro-1H-pyrrol-1-yl)butanamide. This precursor molecule allowed the generation of [³H]BRV and its diastereomer [³H]isoBRV. In subsequent binding studies the applicability of the new radioligands was confirmed. [³H]BRV, exhibiting the highest target affinity, proved to be highly useful for the screening of ligands that compete with its binding, as well as for examinations of rare clinical brain samples of epileptic patients. Binding studies with [³H]BRV at recombinantly expressed SV2A protein variants revealed that the long cytoplasmic loop of the SV2A protein could potentially be involved in ligand-binding interactions. A previously postulated direct interaction of LEV with AMPA receptors could not be confirmed in our binding studies so far. Initial experiments at brain membrane preparations of SV2A KO mice were performed to investigate [³H]BRV binding in the absence of SV2A with the intention to identify potential low-abundant target sites. Due to its high specific activity the new radioligand [³H]BRV represents a most valuable tool for the extension of these studies with the goal to identify potential novel, low-abundant targets.

Keywords: levetiracetam, brivaracetam, SV2A protein, radioligand binding studies, epilepsy, AMPA receptor

Table of contents

1 Introduction

1.1 Epilepsy

Epilepsy (Greek ἐπιληψία, *epilēpsía* – "seizure") is one of the most common neurological disorders. It affects an estimated percentage of about 0.5 to 1% of the world's population, currently at least 50 million people worldwide, with an incidence of approximately 50-80/100,000/year.[1–5] While the onset can occur at any age, it is most common among young and elderly (> 65 years) people (see **Figure 1**).[6,7]
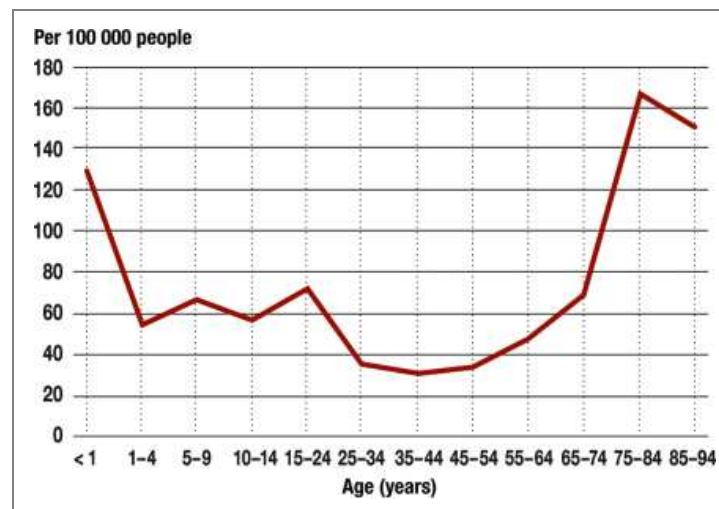
Figure 1: Incidence of epileptic seizures, published by Werhahn[8] based on data from Olafsson et al.[6]

Epilepsy is characterized by the occurrence of epileptic seizures – spontaneous and paroxysmal impairments of the physiological brain function. It is estimated that about 10% of the whole population is affected by an isolated epileptic seizure during the course of one's life.[2,4] According to the ILAE (International League Against Epilepsy)[9], these epileptic seizures, representing "transient occurrences of signs and/or symptoms", have to be distinguished from the term "epilepsy", which refers to a cerebral disorder comprising an "enduring predisposition to generate epileptic seizures" along with several physical and mental consequences of this condition. However, according to the ILAE, already one epileptic seizure might be sufficient for the diagnosis of epilepsy, if corresponding medical results (e.g. MRT or EEG) support an increased receptiveness for seizures.

The proper functioning of the central nervous system (CNS) is depending on a well-coordinated interaction between inhibitory and excitatory neurotransmitters. This is essential for the maintenance of the membrane potential as well as for a specific and

efficient transmission of neuronal signals. In epileptic conditions the normal electrical activity of the brain is impaired, which results in a lowered seizure threshold due to instabilities of the membrane potential. Consequently, neuronal networks of the brain become more susceptible to uncontrolled electrical activity and exhibit a higher risk for the development of recurrent seizures, which emerge from abnormal, synchronic and excessive discharges of cerebral groups of neurons.[10,11]

With regard to the etiology, several risk factors are known today that increase the chances of developing epilepsy. These encompass neurologic disorders (e.g. strokes and neurodegenerative diseases) as well as brain malformations, head injuries, tumors, encephalitis and metabolic disorders.[4,8] Besides external influence factors it is known that several types of epilepsy are caused by genetic disposition, like e.g. defects in genes encoding for ion channels.[5,12,13] A further group of epilepsies is of unknown etiology, which in elderly patients sums up to one-third of all cases.[14]

Epileptic conditions and associated manifestations represent a very heterogeneous symptom complex. Various efforts have been made for a structured categorization (reviewed by Reynolds and Rodin)[15] from which the Classifications of Seizures determined by the ILAE in 1981 and 1989 has become widely accepted.[16,17] In general, seizures are primarily distinguished by their local origin, wherein (1) partial seizures comprise locally restricted seizures of limited extension in one hemisphere and (2) generalized seizures include origins that are distributed over the whole brain area. Furthermore, one differentiates between "symptomatic" seizures (as a consequence of a primary condition, e.g. a tumor), "idiopathic" seizures (presumably of genetic etiology) and "cryptogenic" seizures (of unknown cause, but presumably symptomatic). The complexity of this multifaceted disorder is additionally reflected by numerous further definitions, which for example refer to the affection of consciousness (simple partial or complex partial), seizure propagation (secondary generalized), physical manifestation (tonic, clonic, myoclonic, absence) as well as a number of epilepsy syndroms (e.g. Lennox-Gastaut syndrome). The precise characterization of the epilepsy in combination with the epileptic seizure type is especially important with regard to the choice of the medical treatment, which ideally aims at freedom from seizures.[4,18]

1.2   Antiepileptic pharmacotherapy

Pharmacological therapy plays an important role in the treatment of epilepsy. However, despite a continuous effort to develop new AEDs, pharmacotherapy is still mainly limited to the suppression of emerging seizures by elevating a lowered seizure threshold. Up to now, a curative treatment with currently available AEDs is not possible.[19]

Initial pharmacological treatment, which is preferably given as a monotherapy, is selected based on various factors, e.g. seizure type, age, sex and concomitant conditions and medications. It is estimated that around 50% of all epileptic patients experience freedom from seizures by this first medication. A further 20% of the patients respond to the second medication (another AED or polytherapy), while an approximate percentage of 30% remains resistant to available pharmacotherapy.[20–22] Due to a significant relapse rate about two thirds of the patients have to take antiepileptic medication for the rest of their life.[4]

Until today, more than 20 drugs have been approved for the treatment of epilepsy (see also **Table 1**). As AEDs of the first generation, compounds such as phenytoin, ethosuximide, carbamazepine, valproic acid and phenobarbital have been successfully introduced into antiepileptic treatment. Although these drugs still play an important role in modern antiepileptic pharmacotherapy, their application is strongly limited by several unfavorable characteristics. For most of them a long list of severe side effects has been documented, which include teratogenicity, hepatotoxicity, hair loss, weight gain, tremor (e.g. valproic acid), fatigue, dizziness, diplopia, blood count changes (e.g. carbamazepine) and many more. Moreover, a high interaction potential (metabolism via cytochrome systems) and pharmacokinetic drawbacks affect the possibility of a broad application. Considering that for the majority of epileptics continuous medication is needed for the suppression of seizures, it is obvious that these conventional AEDs do not provide a satisfying profile. With a deeper understanding in processes of neurotransmission and the pathology of epilepsy, drugs of the second generation, including lamotrigine, vigabatrine, felbamate, gabapentin, topiramate, tiagabine, oxcarbazepine, levetiracetam, pregabalin, and zonisamide, were developed. In general, the newer AEDs are better tolerated. Nevertheless, despite the achieved improvement of AED therapy, there are still several drawbacks that ongoing research might overcome with AEDs of the next generations. Apart from improved efficacy and tolerability,

especially drugs with potent antiepileptogenic and disease-modifying effects (prevention or control of epileptogenesis) would represent a milestone in the therapy of epilepsy.[8,11,18,23–25]

1.2.1 Target structures for antiepileptic drugs

In general, antiepileptic pharmacotherapy aims at elevating the seizure threshold, which is lowered in epileptic conditions due to an abnormally high excitability of the neuronal network. This can either be achieved by enhancing inhibitory or by inhibiting excitatory mechanisms. Based on this principle, common targets of antiepileptic drugs include (1) voltage-gated ion channels, (2) the inhibitory GABAergic neurotransmitter system, and (3) the excitatory glutamatergic neurotransmitter system.[10,11,18] The challenge of designing specifically acting AEDs can be derived from the fact that more or less all current AEDs seem to convey their effects via multiple mechanisms by acting at different target structures. In the following paragraphs the most common targets of AEDs will be briefly summarized and selected examples for each target will be given.

Voltage-gated ion channels[26] are essential for the maintenance of the membrane potential, for the production and propagation of action potentials as well as for neurotransmitter release into the synaptic cleft. Therefore, they play a role in the generation of epileptic seizures. Several AEDs are interacting with voltage-gated sodium, calcium and potassium channels and thereby either inhibit the influx or stimulate the efflux of cations, which, in turn, stabilizes the membrane potential. Sodium channels,[27] which contribute to the generation of action potentials, represent the main target for several AEDs. Among these are phenytoin, lamotrigine, carbamazepine and oxcarbazepine, which stabilize the channels in their inactive state.[28] Calcium channels[29] can be subdivided into high-voltage activated (HVA) and low-voltage activated (LVA) channels, based on the degree of depolarization at which the channel opens. The group of HVA calcium channels comprises L-, P/Q- and N-type channels. While L-type channels are mainly expressed postsynaptically, N- and P/Q-type channels are located presynaptically and are therefore involved in the regulation of transmitter release. Gabapentin and pregabalin most likely exert their antiepileptic effects by a blockade of HVA calcium channels; their interaction with the $\alpha_2\delta$ auxiliary subunit proteins could be demonstrated.[30,31] LVA calcium channels are T-type channels, which are integrally involved in the abnormal conditions during generalized absence

seizures.[32] They presumably present the molecular target structure for ethosuximide.[33] Potassium channels are also voltage-gated ion channels, which are essential for the maintenance of the resting potential and important in cellular excitability; they therefore represent potential targets for antiepileptic therapy.[34] The novel antiepileptic drug retigabine, which has been approved in 2011, appears to be the first AED interacting with potassium channels. Being a positive allosteric modulator, which binds to KCNQ2/3 potassium channels, the drug is capable of opening the channel, and thus initiating an efflux of potassium ions.[35,36]

GABA (γ-amino butyric acid), the most important neurotransmitter of the inhibitory nervous system, plays another important role in epileptic conditions.[37] After release into the synaptic cleft, it binds to three different GABA receptors (type A, B and C) from which the ionotropic (chloride) GABA$_A$ receptor represents a major target in antiepileptic pharmacotherapy. Benzodiazepines are positive allosteric modulators of the GABA$_A$ receptor. They interact with subtypes that contain certain α and γ subunits, thereby increasing the sensitivity of the receptor for its endogenous ligand GABA.[38] Besides benzodiazepines, barbiturates are also interacting with GABA$_A$ receptors.[39] By positive allosteric modulation via the β subunit the channel remains in its opened state for an extended period of time in the presence of barbiturates. The supply with GABA *in vivo* is regulated by the enzyme glutamate decarboxylase (GAD), which converts the amino acid glutamate into GABA (see **Figure 2**). It has been supposed (although controversially discussed) that one of the many mechanisms of valproic acid might be a modulation of this enzyme leading to an increased synthesis of GABA.[40] The concentration of GABA can be further increased by the AED vigabatrin, which irreversibly inhibits the enzyme GABA transaminase (GABAT).[41,42] Thus, the degradation of GABA to succinic semialdehyde along with the simultaneous conversion of 2-oxoglutarate to glutamate is inhibited (see **Figure 2**). Furthermore, GABAergic signaling can be enhanced by the drug tiagabine.[43] This AED binds with high affinity to the GABA transporter GAT-1, inhibits the reuptake of released GABA from the synaptic cleft and increases its concentration and duration of action.
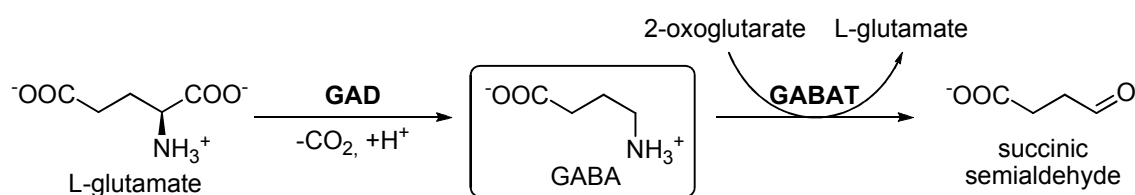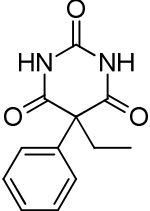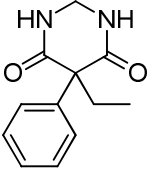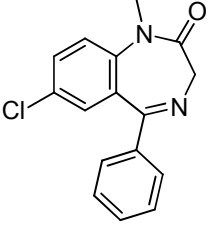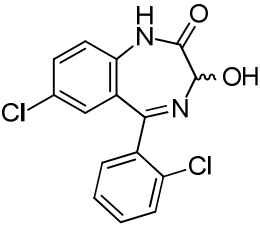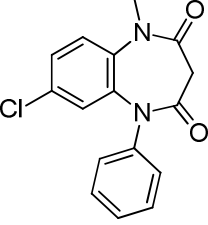
Figure 2: Metabolism of GABA; GAD: glutamate decarboxylase; GABAT: GABA transaminase.
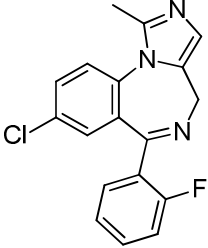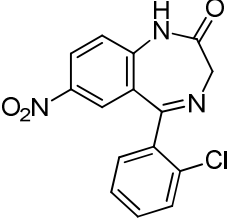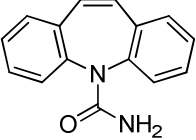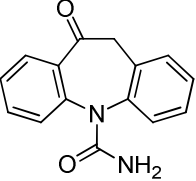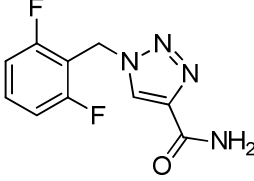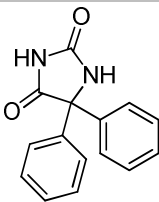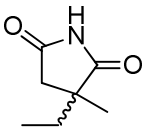
The amino acid glutamate represents the major excitatory neurotransmitter of the central nervous system.[44] Its receptors can be subdivided into ionotropic (glutamate-gated cation channels) and metabotropic (G protein-coupled) receptors. While the latter ones currently do not represent targets for antiepileptic pharmacotherapy, ionotropic glutamate receptors are addressed by several AEDs. Three types of ionotropic glutamate receptors are known, which have been named after pharmacological agonists that selectively bind to and activate the corresponding subtype. NMDA (*N*-methyl-*D*-aspartate) receptors are permeable for sodium, potassium and calcium ions. During the resting potential the channel is closed by magnesium and only opens upon glutamate stimulus, if the co-agonist glycine is bound to its allosteric binding site.[45] The AED felbamate might – at least in parts – convey its effect by inhibiting NMDA receptors.[46] AMPA (α-amino-3-hydroxy-5-methyl-4-isoxazole propionate) receptors,[47] another type of ionotropic glutamate receptors, will be discussed in more detail in chapter 1.4. They are involved in seizure spread and therefore may play an important role in antiepileptic pharmacotherapy. Compounds like perampanel, which is currently in late stages of clinical trials, are interacting with AMPA receptors as non-competitive, highly selective antagonists.[48] KA (kainic acid) receptors are the third group of ionotropic glutamate receptors, which represent one of the several target sites for the AED topiramate.[49]
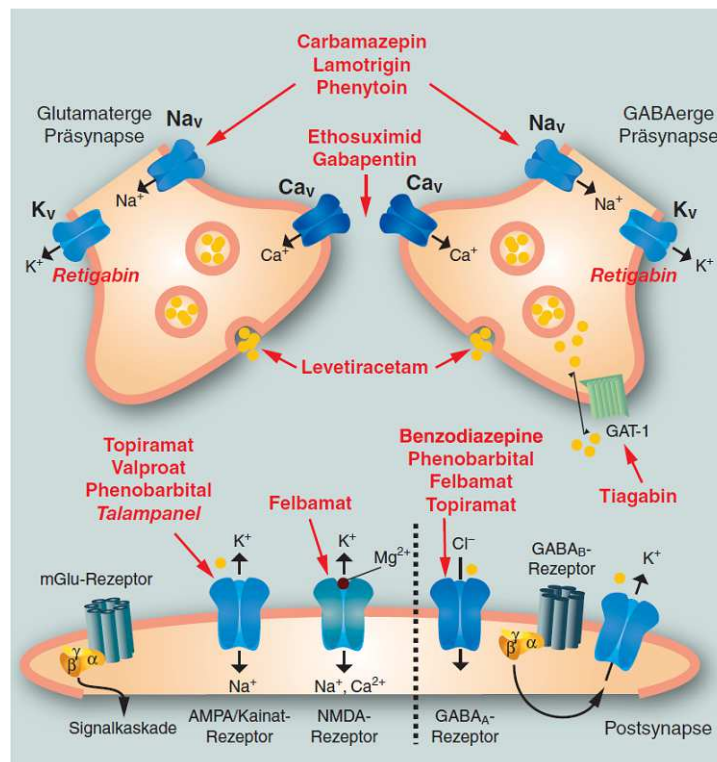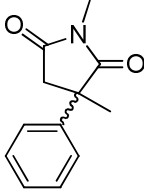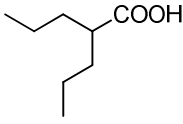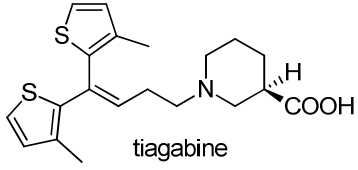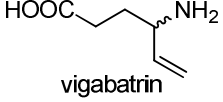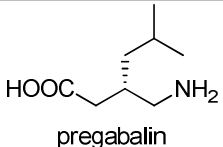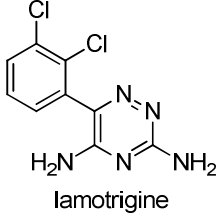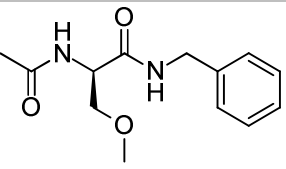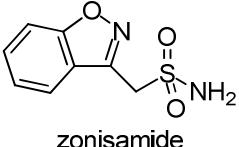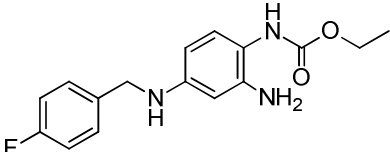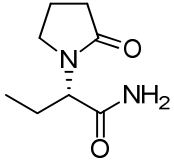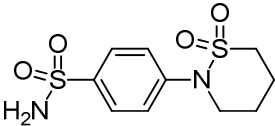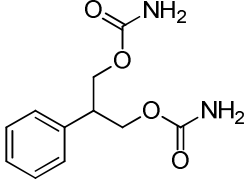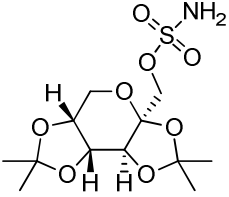
Figure 3: Schematic drawing of the most important target structures of AEDs (from Böhme and Lüddens).[10] Na_v, Ca_v, K_v: voltage-gated sodium, calcium and potassium channels; GAT-1: GABA transporter 1.

Table 1: Mechanisms of action and therapeutic plasma concentrations of antiepileptic drugs.[23,50–53] Therapeutic plasma concentrations have been taken from Micromedex® Healthcare Series;[54] nd: no data.

Antiepileptic drug	Mechanisms of action	Therapeutic plasma concentration
phenobarbital	GABA$_A$ receptor (positive allosteric modulation)	10-40 µg/ml
primidone	GABA$_A$ receptor (positive allosteric modulation)	5-12 µg/ml
diazepam	GABA$_A$ receptor (positive allosteric modulation)	nd
lorazepam	GABA$_A$ receptor (positive allosteric modulation)	nd
clobazam	GABA$_A$ receptor (positive allosteric modulation)	0.1-0.4 µg/ml of active metabolite desmethylclobazam

Antiepileptic drug	Mechanisms of action	Therapeutic plasma concentration
midazolam	GABA$_A$ receptor (positive allosteric modulation)	nd (no direct correlation between clinical effects and plasma concentrations)
clonazepam	GABA$_A$ receptor (positive allosteric modulation)	25-30 ng/ml
carbamazepine	Na$^+$-channel blockade	4-12 µg/ml
oxcarbazepine	Na$^+$-channel blockade Ca^{2+}-channel blockade	nd
rufinamide	Na$^+$-channel blockade	nd
phenytoin	Na$^+$-channel blockade	10-20 µg/ml
ethosuximide	Ca^{2+}-channel blockade	40-100 µg/ml

Antiepileptic drug	Mechanisms of action	Therapeutic plasma concentration
methsuximide	Ca^{2+}-channel blockade	10-40 µg/ml
valproic acid	Na^+-channel blockade Ca^{2+}-channel blockade GABA supply ↑	50-100 µg/ml
tiagabine	GABA transporter (GAT-1) inhibition	not well established (1-234 ng/ml observed)
vigabatrin	GABA transaminase (GABAT) inhibition, irreversible	nd
gabapentin	Ca^{2+}-channel blockade ($\alpha_2\delta$ subunit)	≥ 2 µg/ml
pregabalin	Ca^{2+}-channel blockade ($\alpha_2\delta$ subunit)	nd
lamotrigine	Na^+-channel blockade Ca^{2+}-channel blockade	1-4 µg/ml
lacosamide	Na^+-channel blockade	nd
zonisamide	Na^+-channel blockade Ca^{2+}-channel blockade	20-30 µg/ml

Antiepileptic drug	Mechanisms of action	Therapeutic plasma concentration
retigabine	K$^+$-channel opener	nd
levetiracetam	SV2A protein interaction Ca^{2+}-channel blockade GABA$_A$ receptor modulation	7-40 µg/ml
sultiame	carboanhydrase inhibition	nd
felbamate	NMDA receptor blockade Na$^+$-channel blockade Ca^{2+}-channel blockade GABA modification	18-83 µg/ml
topiramate	KA/AMPA receptor Na$^+$-channel Ca^{2+}- channel GABA modification carboanhydrase inhibition	10.5 µg/ml

1.2.2 Levetiracetam and analogues

In the 1960s, there were increased efforts to develop sedatives that were supposed to act via the inhibitory effect of the GABAergic system. For this purpose several pyrrolidone derivatives were synthesized with the rationale to design cyclic analogues of γ-aminobutyric acid. However, in animal studies it was found, that some of these compounds possessed cognitive enhancing effects instead of sedative properties. In this context piracetam was discovered, which represents the first nootropic drug that was applied in clinical therapy.[55] In 1992, the potent effect of the pyrrolidone drug levetiracetam (LEV) was discovered. By random screening Alma Gower (UCB, Belgium) found that this (*S*)-configured ethyl derivative ((2*S*)-α-ethyl-2-oxo-1-pyrrolidine acetamide) of piracetam possesses pronounced anticonvulsive effects, which became evident by tests involving acoustically induced seizures in sound-sensitive mice.[56] Subsequent investigations suggested a specific profile for LEV distinct from that of other AEDs. While LEV showed potent antiepileptic effects in several animal models of epilepsy, it was lacking potency in two of the widely used screening tests for AEDs: the maximal electroshock (MES) test and the subcutaneous pentylenetetrazol (s.c. PTZ) test. All other clinically applied AEDs possess activity in at least one of these two screening tests. Furthermore, the examinations brought forward that LEV might possess antiepileptogenic effects, and thus could also be effective in inhibiting the progression of the disease. In addition, the absence of severe side effects adds to the most promising profile, which was determined for the compound.[56–58] LEV underwent clinical trials and eventually was approved by the FDA under the trade name Keppra[®] in November 1999.[59] At that time, not much was known regarding the molecular mechanism of action and the target of LEV, for which Noyer et al. supposed a highly abundant protein located in synaptic vesicle membranes of the central nervous system.[60] Five years after its approval, in 2004, this site was identified by Lynch et al. as the synaptic vesicle protein SV2A, a glycoprotein of nearly ubiquitous distribution in the brain (see chapter 1.3).[61] Thus, it became evident that LEV most likely exerted its antiepileptic effects via a novel mechanism of action and thus might represent the first compound of a potential new class of AEDs.[62] Today, Keppra[®] belongs to the most successful of the newer AEDs, being widely prescribed for partial as well as generalized seizures, as a monotherapy and as an add-on medication.[63–68] With the aim to identify a drug with even higher potency, about 12000 compounds were screened for their affinity to the SV2A protein in radioligand binding studies versus [³H](2*S*)-2-[4-(3-

azidophenyl)-2-oxopyrrolidin-1-yl]butanamide, [³H]ucb30889 (see **Figure 8**) by UCB Pharma SA, Belgium. This effort led to the discovery of brivaracetam (BRV), the (*4R*)-4-propylpyrrolidinyl analogue of LEV. It possesses a 10- to 20-fold higher affinity for the SV2A protein than LEV, and through potential additional antiepileptic mechanisms of action might not only be a more potent, but also a more effective AED in comparison with LEV. Moreover, it appears to have a side effect profile indistinguishable from placebo. Currently, BRV is undergoing late stages of phase III clinical trials.[69–74] A pivotal role of the SV2A protein in the antiepileptic effects of the pyrrolidone derivatives has been postulated. For several LEV derivatives binding affinities to the SV2A protein (determined in competition binding experiments versus the radioligand [³H]ucb30889) showed a positive correlation with their antiepileptic potency in several animal models of epilepsy after i.p. administration of the test compounds.[61,75] However, it has been criticized that in these studies the cerebrospinal fluid (CSF) levels of the investigated AEDs had not been determined; thus, it cannot be excluded that the CSF concentrations of the drugs may have differed considerably.[76]

Apart from the known interaction with the SV2A protein, LEV appears to evoke additional effects, which were observed in several *in vitro* and *in vivo* studies. In this context a reduction of cation currents has been described including N- and P/Q-type calcium currents[77,78] as well as certain potassium currents.[79] Concerning sodium currents no modulation could be observed.[80] Furthermore, LEV appears to have an influence on intraneuronal calcium stores, where it is capable of inhibiting the intracellular calcium release.[81] Moreover, a modulation of $GABA_A$ receptors could be demonstrated: LEV reversed the effect of zinc that can be applied as an allosteric modulator to reduce the inhibitory effect of GABA in epileptic brain tissue.[82] In addition, LEV also appears to have an influence on the glutamatergic system, since a reversible inhibition of AMPA currents in the presence of LEV could be shown.[83] So far, for none of these effects a mechanism of action or a specific target site has been identified. Whether these effects are related to the interaction with the SV2A protein or whether they are evoked by an SV2A-independent pathway is not clear yet. Also, it remains to be elucidated to which extent these effects contribute to the unique antiepileptic effects of LEV.

1.3   SV2A protein

The identification of the putative molecular target structure of LEV[61] led to increased interest in the synaptic vesicle proteins SV2 in epilepsy research. The SV2 proteins are membrane proteins, which are present in all synaptic vesicles of neurons and endocrine cells of vertebrates.[75,84–86] Encoded by different genes three highly homologous isoforms exist, termed SV2A, SV2B and SV2C.[87–90] The SV2A protein is the most abundantly expressed isoform, which is present on all presynaptic terminals of neurons, independent of their neurotransmitter type. The distribution pattern of the second most abundant isoform SV2B is more restricted and the SV2C isoform is only expressed in certain evolutionarily older brain regions.[86,90] SV2 proteins are composed of 12 transmembrane domains (TMDs), which are flanked by cytoplasmic N- and C-termini (see **Figure 4**). In general the loops between the TMDs are relatively short with two exceptions: SV2 proteins possess a long cytoplasmic loop between the TMDs 6 and 7, and a long luminal loop between TMDs 7 and 8 with *N*-glycosylation sites in three positions.[87–89] It has been suggested that the sugar chains might function as a stabilizing gel in the intravesicular space.[85,91,92] The three isoforms exhibit a high sequence homology within the 12 TMDs and to a somewhat lesser extent also within the long cytoplasmic loop, whereas the sequences of the N-terminus as well as the long intravesicular loop are less well conserved among the isoforms.[90]

Apart from the SV2 proteins a more distantly related protein was identified, the SVOP (<u>SV</u>tw<u>o</u>-related <u>p</u>rotein), which beyond vertebrates is conserved in all multicellular organisms that have been examined so far.[92] It is suggested to be a potential evolutionary precursor of the SV2 proteins (SV2 proteins, in contrast, have only been found in vertebrates) possessing a similar transmembrane structure, but lacking both long loops present in the SV2 proteins. Within their transmembrane structure SVOP as well as SV2 proteins exhibit significant homology to mammalian organic cation and anion transporters and more distantly also to sugar transporter proteins in eukaryotes and bacteria.[87,88,92] Being located in the membranes of synaptic vesicles, initially it was proposed that SV2 proteins might function as transporters for the uptake of neurotransmitters into the vesicles.[88] However, due to the ubiquitous presence of the SV2 proteins in synapses with different types of neurotransmitters this hypothesis was discarded.[86]
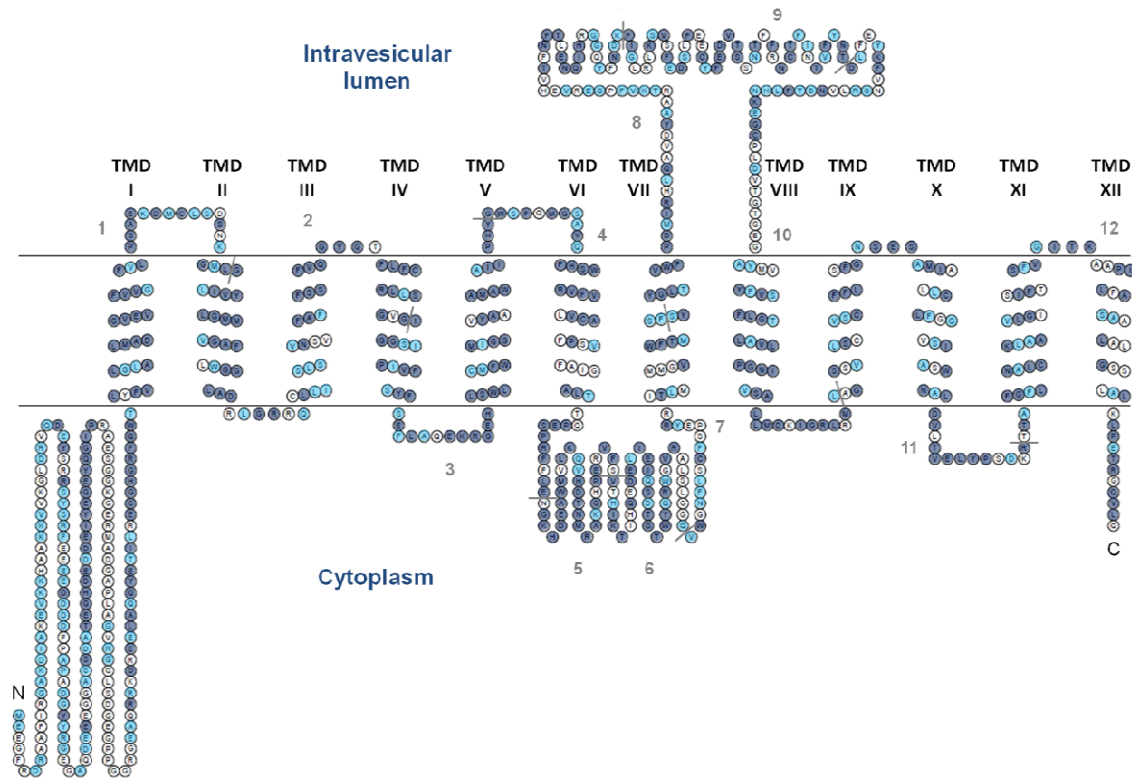
Figure 4: Topology model of the rat SV2A protein. The snakeplot diagram was drawn with TOPO2 with prediction of transmembrane domains based on TMHMM software[93,94] (see 8.1.1). Transmembrane domains are numbered TMD I to XII, exons are numbered in grey Arabic numbers from 1 to 12 and separated by lines, N- and C-termini are labeled with the corresponding letters. Amino acids colored in dark blue represent residues that are conserved among all three isoforms (SV2A, SV2B and SV2C), light blue colored ones are conserved in one other isoform besides SV2A, and white colored ones are non-conserved and only present in the SV2A isoform. For an enlarged view see **Figure 35**.

Recently, two conformations of the SV2A protein were determined by protein tomography (an electron microscopic-based technique for the three-dimensional visualization of proteins).[95] By this analysis it could be shown that the protein can be present either in a compact funnel structure with a pore-like opening towards the cytoplasm or in a more open, V-shaped structure with a cleft-like opening towards the intravesicular space. Based on these findings it seems conceivable that SV2 proteins could actually perform a function as transporters. Many hypotheses have been put forward as to which small molecules might represent potential substrates.[86,88,96–98] However, until today it was not possible to identify any substrate that is recognized and transported by the SV2 proteins. On the other hand, SV2 proteins, although they might have emerged from transporter proteins, may perform a transporter-independent function, as it is the case e.g. for the adenylyl cyclases.[99]

Very recently the structural similarity of SV2 proteins to transporter proteins has been taken as a basis for combined modeling and mutagenesis studies to identify amino acids that may be involved in the interaction with the pyrrolidone drugs.[100] Therefore, point mutants of the SV2A protein have been created in positions corresponding to functional residues in related transporter proteins. By binding studies with pyrrolidone radio-ligands, 14 amino acids were identified, which supposedly are involved in the binding interaction. Since the investigated transporter proteins (lactose permease LacY, rat and human organic anion transporters) do not possess long TMD-connecting loops, the identified amino acids are mainly located within the TMDs. So far this study provides the only available information concerning the putative SV2A-pyrrolidone interaction site and suggests that the ligands may bind in the central cavity of the SV2A protein.

Whereas a lot of uncertainties remain concerning the transporter function, it is known that SV2 proteins represent the neuronal receptor for botulinum toxin A.[101,102] This peptide is interacting with SV2 proteins by binding to the intravesicular *N*-glycosylated loop between TMDs 7 and 8 during the release of the vesicle content into the synaptic cleft. After endocytotic internalization botulinum toxins inhibit further neurotransmitter release by cleaving essential fusion-mediating proteins. Moreover, an involvement of SV2 proteins in regulated insulin secretion has been suggested, presumably by controlling the glucose-evoked insulin granule recruitment to the plasma membrane.[97]

To further elucidate potential functions of the SV2 proteins studies with KO mice have been performed, which revealed that SV2 proteins are essential for survival and normal brain function.[96,103] SV2A KO mice (-/-), lacking the primary SV2 isoform, appear normal at birth. However, they do not grow, exhibit severe seizures and die within the second or third week after birth. SV2B KO mice do not show this phenotype, why it has been suggested that the function of the SV2B protein can be taken over by the ubiquitously present SV2A isoform. SV2C proteins were not considered in these studies due to their limited overall expression.[96] Heterozygous SV2A KO mice (+/-) develop normally, but exhibit an increased seizure susceptibility.[104] Effects on neurotransmitter secretion, which are caused by a knockout of the SV2 genes have been described and discussed. Most of the studies suggest a decreased secretion of neurotransmitters in SV2A KO[103,105] as well as in SV2B KO[106] mice. In contrast, increased excitatory neurotransmission was observed in SV2A KO mice in one study.[96] Other studies, applying cultured neurons of SV2A KO mice, support the idea that neurotransmission is

decreased in the absence of the SV2A protein.[107] Furthermore, it was observed that only action potential-dependent (and thus Ca^{2+}-dependent), but not action potential-independent neurotransmission was impaired in SV2A KO mice.[103] Thus, a functional role of the SV2 protein in Ca^{2+}-regulated exocytosis was suggested. Moreover, a binding site for the synaptic vesicle protein synaptotagmin was identified: the amino termini of the SV2A and SV2C isoforms are interacting with the synaptotagmin protein, which represents a calcium-sensor in neurotransmitter exocytosis.[108–110] The process of exocytosis in synapses, which is part of the synaptic vesicle cycle, involves several steps: initially, vesicles that are filled with neurotransmitters interact with the active zone, which lies opposite to the synaptic cleft (docking). Thereupon, vesicles undergo a maturation step, which makes them competent for Ca^{2+}-induced fusion with the synaptic membrane (priming). Finally, exocytosis occurs upon an action potential-evoked Ca^{2+}-influx (fusion).[111,112] Chang and Südhof suggested that the SV2A protein is regulating neurotransmitter release by being involved in a yet unidentified process downstream of vesicle priming, but before Ca^{2+}-triggered fusion. In this context enhancement of the Ca^{2+}-responsiveness of synaptic vesicles was proposed as a role of the SV2A protein.[113]

Despite many efforts, it has not been possible to elucidate the exact role of the SV2 proteins in neurotransmitter release to date. Since the AED levetiracetam (LEV) is only interacting with the SV2A isoform,[61] a prominent role for this isoform in neurotransmitter release has to be presumed. The ubiquitous expression of the SV2A isoform, however, makes it difficult to interpret the effect that is caused by binding of LEV to this protein. For instance, Yang et al. suggested that the interaction of LEV with the SV2A protein evokes reduced neurotransmitter release.[114] However, the broad expression of the SV2A protein – in excitatory as well as inhibitory synapses – is only hardly compatible with the distinct antiepileptic effects conveyed by LEV. Even though several studies indicate that SV2A is the main target and responsible for LEV's pharmacological action,[61,72] it cannot be excluded that further targets, which potentially are much less abundant, contribute to some extent to LEV's potent antiepileptic effects. In this context it has been postulated that LEV is also binding to AMPA receptors, a glutamate receptor subtype (see chapter 1.4).[115] Since these receptors are much less abundant than the SV2 proteins, it is conceivable that previous investigations may have failed in determining interactions with such low abundant targets due to limited sensitivity of the employed analytical methods.

1.4 AMPA receptors – glutamate receptor subtypes

1.4.1 Glutamate receptor subtypes

The amino acid L-glutamate represents the major excitatory neurotransmitter of the central nervous system.[44] With the arrival of an action potential (transmitted by voltage-gated sodium and potassium channels) at the presynaptic site of a glutamatergic synapse, voltage-gated calcium channels are opened and calcium flows into the cell. Upon this stimulus glutamate-filled vesicles are released via exocytosis. After diffusion across the synaptic cleft, glutamate is interacting with several glutamate receptors, which can be assigned to two main groups: metabotropic (G protein-coupled) and ionotropic (ligand-gated ion channel) receptors.[116] Metabotropic glutamate receptors mediate the slow excitatory neurotransmission and are involved in multiple biochemical pathways.[117,118] The fast excitatory neurotransmission (on a millisecond time scale)[119] is mediated by ionotropic glutamate receptors, which are ligand-gated cation channels.[120] Ionotropic glutamate receptors are further subdivided into NMDA receptors and the two non-NMDA receptors AMPA receptor and kainate receptor. Their names originate from pharmacologic agonists that selectively bind to and activate the corresponding receptor: *N*-methyl-*D*-aspartate (NMDA), α-amino-3-hydroxy-5-methyl-4-isoxazole propionate (AMPA) and kainic acid (KA), which are all structurally related to the endogenous agonist glutamate (see **Figure 5**).
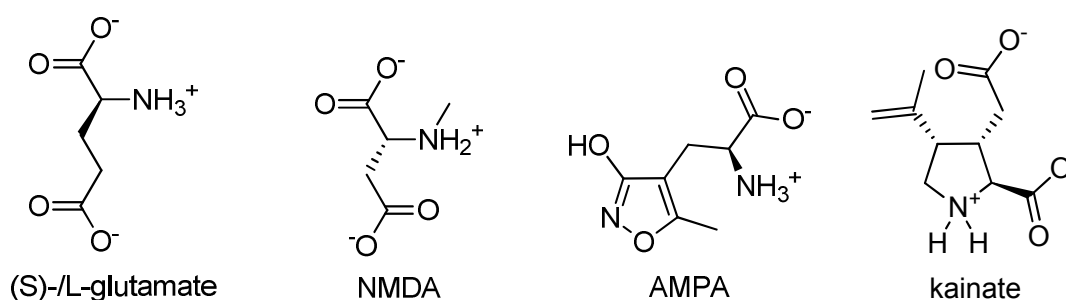
Figure 5: Chemical structures of L-glutamate and its analogues NMDA, AMPA and kainate.

1.4.2 AMPA receptors

Molecular cloning of glutamate receptors has contributed greatly to the understanding of the structure and function of AMPA receptors (AMPARs).[47,121,122] Further information was obtained by several crystal structure studies of AMPAR subtypes, which have been published during the last 10 years.[123–126] Four subunits have been identified (GluR1-GluR4, also named GluA1-GluA4 after <u>A</u>MPA), which are encoded

by the genes *Gria1-4*. The subunits, which posses a length of about 900 amino acids, share a sequence homology of approximately 70%.[47] All of the four subunits are composed of an extracellular amino-terminal domain (N-terminus), a ligand-binding domain (D1 and D2), the transmembrane domain (consisting of three membrane-spanning domains M1, M3 and M4, and one intramembraneous re-entrant loop M2), and a cytoplasmic carboxy-terminal domain (C-terminus), as depicted in **Figure 6**.
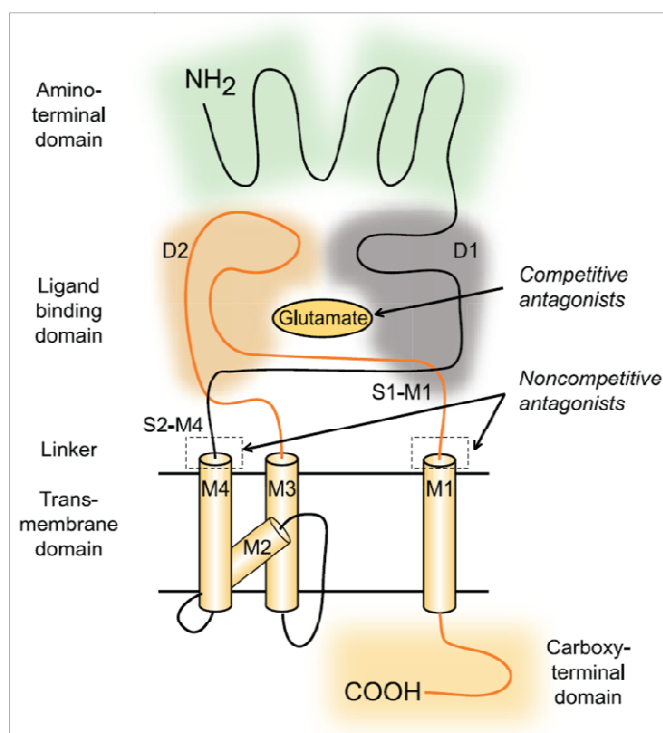
Figure 6: Schematic model of the domain structure of a single receptor subunit of AMPARs (modified from Rogawski).[127] The subunit is composed of an extracellular amino-terminal and ligand-binding (D1 and D2) domain that represents the binding site for the endogenous agonist glutamate, a transmembrane domain (comprising three membrane-spanning domains M1, M3 and M4, and a re-entrant loop M2), and a cytoplasmic carboxy-terminal domain. In the region of the linker sequences S1-M1 and S2-M4 binding sites for noncompetitive antagonists are assumed.

The long extracellular amino-terminal domain, which is *N*-glycosylated at several positions,[128] is suggested to be involved in subunit dimerization and subtype-specific assembly.[129] Also on the extracellular site is the ligand binding site (D1 and D2), which represents the binding site for the endogenous agonist glutamate as well as for AMPA. It has been suggested that the agonist initially interacts with the D1 lobe, whereupon the D2 lobe moves towards the D1 lobe and interacts with the ligand. This conformational change is transmitted via the linker sequences to the transmembrane domain, thus causing the channel to open.[130,131] Within the region of the linker sequences S1-M1 and S2-M4 the binding sites for noncompetitive antagonists are suggested. It is assumed that

those negative allosteric modulators stabilize the conformation of the receptor by hindering the linker domains to transfer the conformational change onto the transmembrane domain and thus impair the opening of the channel.[132] The transmembrane domain comprises three hydrophobic domains that are spanning the membrane (M1, M3 and M4) and a fourth domain (M2), which represents an intramembraneous re-entrant loop. This re-entrant loop forms the ion channel pore.[133] Within the intracellular carboxy-terminal domain the four subunits exhibit the largest sequence differences. This region interacts with many different proteins, and thus, among other functions, is responsible for targeting the receptor to synapses.[134]

All of the four AMPAR subunits exist in two variants, called flip and flop, which are products of alternative splicing.[121] This flip/flop region is located on the extracellular site in close proximity to the transmembrane domain indicated as M1 in **Figure 6**. It is encoded by neighbored exons of the subunit gene, which comprise 115 bp. Among different subunits these segments are quite similar, exhibiting differences in the peptide sequence between flip and flop in 9 to 11 amino acids. The flip and flop variants are present in different expression levels during the development of the brain and also exhibit a distinct, but partly overlapping expression pattern throughout diverse brain structures.[135] They functionally differ from each other by their kinetic properties: in general, the flop variant desensitizes faster than the flip variant in the presence of glutamate.[121,136,137]

A functional AMPAR that exhibits two agonist binding sites is composed of four subunits forming a tetrameric receptor structure, which consists of two dimers of the subunits GluR1 to GluR4.[47,138,139] While homotetramers represent functional receptors, native receptors are almost exclusively heterotetramers (consisting of two different subunits each in dimer pairs).[140] The assembly of AMPARs varies depending on developmental stage and subcellular localization. However, the majority of AMPARs in the adult brain appears to consist of GluR1/GluR2 and GluR2/GluR3 subunit combinations.[141,142]

1.4.3   The AMPA receptor subunit GluR2

Among the four subunits, the GluR2 subunit plays a central role for AMPARs. It is widely expressed in the central nervous system, being present within the majority of all

AMPARs.[47,135,142–144] GluR2 is the only subunit that carries a so-called Q/R-editing site, which is located in the re-entrant loop forming the ion channel pore (indicated as M2 in **Figure 6**).[145–147] This site has an essential function in the regulation of cation permeability of the channel. By posttranscriptional RNA-editing the genetically encoded amino acid glutamine (Q) at position 607 is exchanged by the amino acid arginine (R) in almost all GluR2 subunits. This is mediated by the enzyme adenosine deaminase ADAR2, which is converting adenosine to inosine by hydrolytic deamination, thereby changing the codon CAG to CIG.[148] This inosine is read by RNA-dependent RNA-polymerases as guanosine, which changes the codon to CGG. Subsequently, arginine (CGG) instead of glutamine (CAG) is integrated into the channel forming domain. Due to the positive charge and the steric hindrance by this residue, AMPARs possessing the edited GluR2 subunits are impermeable for calcium and hence only allow monovalent ions (sodium and potassium) to pass the channel.[146,149,150]

In genetically modified mouse models lacking the GluR2 subunit it could be shown that this subunit has an integral role in development and function of the brain. In the absence of GluR2, the mice show several behavioral abnormalities and an overall increased mortality.[151,152] Furthermore, it was demonstrated that mice, which express the unedited GluR2 subunit (heterozygous), exhibit a particular phenotype: due to unhindered calcium permeability they develop epileptic seizures and die shortly after birth.[153,154] Similar observations were made with mice (homozygous) lacking the editing-responsible enzyme ADAR2.[148]

AMPARs represent the major mediator of excitatory neurotransmission and thus are integrally involved in the generation and spread of epileptic seizures.[127] Given the fact that the GluR2 subunit is present in the majority of AMPARs together with its dominant role in calcium permeability and the effects observed in mice lacking edited GluR2 subunits, it becomes evident that this subunit crucially contributes to the physiological functioning of AMPARs and thus very likely also in their role in seizure propagation. Consequently, it might be conceivable that a potential interaction of LEV and its analogues with AMPARs in a negative allosteric manner could contribute to their antiepileptic effects. Due to a much lower abundance than the highly expressed SV2A protein the detection of these receptors might be much more difficult and hence require more sensitive techniques than those applied in previous studies.

1.5 Objectives

Levetiracetam (LEV) is one of the most successful of the newer antiepileptic drugs (AEDs) exhibiting a novel, unique mechanism of action. In 2004, the synaptic vesicle protein SV2A has been postulated to be the molecular target for LEV and related pyrrolidone drugs,[61] since LEV was shown to specifically bind to SV2A with an affinity of around $1\,\mu M$. Very recently, several amino acids of the SV2A protein were suggested to be involved in ligand binding,[100] however, the exact binding site is still unknown. So far the exact effects that LEV may evoke upon binding to this protein and thus the mechanism of action of LEV are not well understood. Several effects have been determined for LEV *in vivo* as well as *in vitro*, e.g., on ion currents, which cannot be readily explained by an interaction with the SV2A protein. In this context, the question remains whether the ubiquitously expressed SV2A protein represents the exclusive target for LEV, or whether other targets are involved in its potent antiepileptic effects.

The present study was aimed at (1) contributing to the identification of the binding site of the pyrrolidone drugs at the SV2A protein and (2) searching for potentially new binding sites of LEV and BRV besides the broadly and highly expressed SV2A protein. Considering that potential, but so far unidentified target structures for LEV besides the SV2A protein may exist, it can be assumed that they would probably be present at much lower expression levels than the SV2A protein. Therefore sensitive detection methods are needed. For this purpose, the first goal of this project was to devise synthetic strategies, which would allow the generation of a radioligand labeled with tritium with high specific activity. Besides [³H]LEV, its analogue brivaracetam (BRV) was to be prepared as a tritiated radioligand as well, since it possesses higher affinity for the target structure (SV2A) and therefore would represent an improved investigational tool. Subsequently, a valuable and reproducible assay was to be established, in which the new radioligands could be characterized. Taking this assay system as a basis, it was further planned to investigate binding to different tissue samples including pathological tissues from epileptic patients.

In order to contribute to the identification of the binding site of the pyrrolidone drugs, several SV2 variants were to be obtained by molecular cloning and heterologous expression, which afterwards should be investigated in binding studies using the new radioligands. The effects of certain mutations on the binding behavior of the radioligands were to be investigated.

Based on the results of published radioligand binding studies it was postulated that LEV and its analogues exclusively bind to the SV2A protein, since no binding could be detected in membrane preparations from SV2A KO mice.[61,72]
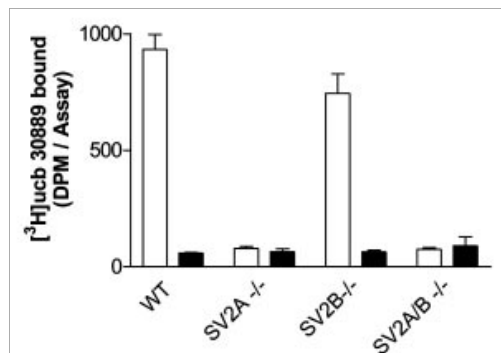
Figure 7: Binding of [³H]ucb30889 to brain membranes of wild-type (WT) and SV2A/B KO mice in dpm from Lynch et al.[61] Bars demonstrate total binding (white) and non-specific binding determined in the presence of 1 mM levetiracetam (black).

However, these studies were limited by a moderate to low specific activity of the applied radioligands. Thus, binding sites with much lower expression levels than that of SV2A, which would for example be the expected expression levels of ion channels or many membrane receptors, could not have been detected by the applied method.[61,72] It has been suggested that LEV may interact with AMPA receptors,[83,115] but the published studies would have failed detecting this interaction due to the low specific activity of the applied radioligand and the low expression levels of AMPA receptors in comparison to that of the SV2A protein (at least 10-fold difference). It was a further objective of this study to investigate, whether direct binding of the new radioligands to recombinantly expressed AMPA receptors could be determined. Furthermore, radioligand binding studies with membrane preparations of SV2A KO mice were to be performed with radioligands of high specific activity in order to have a chance to identify potential low-abundant binding sites for LEV and BRV.

2 Syntheses

2.1 Introduction

As mentioned above (see 1.2.2), due to various beneficial properties, levetiracetam (LEV) belongs to the most successful newer generation antiepileptic drugs. The newer analogue brivaracetam (BRV), which is currently in phase III clinical studies, raises even higher expectations. However, the question of the mode of action of these pyrrolidone drugs still needs to be clarified.

A very powerful technique to investigate drug-target interactions is the performance of radioligand binding studies.[155–158] If a certain drug is available as a radioligand (radioactively labeled compound), it represents an extremely valuable tool for examination of the drug's binding behavior in various scientific problems. LEV[60] and BRV[72] have already been published as tritium-labeled radioligands. They, as well as the structurally related radioligand [³H]ucb30889[61,75,104,159–161] (see **Figure 8**), have been applied for answering various scientific questions including investigations on the binding behavior in diverse brain regions and peripheral tissues, binding to tissue preparations from different species (rat, mouse, human), competitive binding behavior in the presence of inhibitors, binding to recombinantly expressed SV2 proteins, autoradiography and binding to brain membranes of SV2A KO mice.
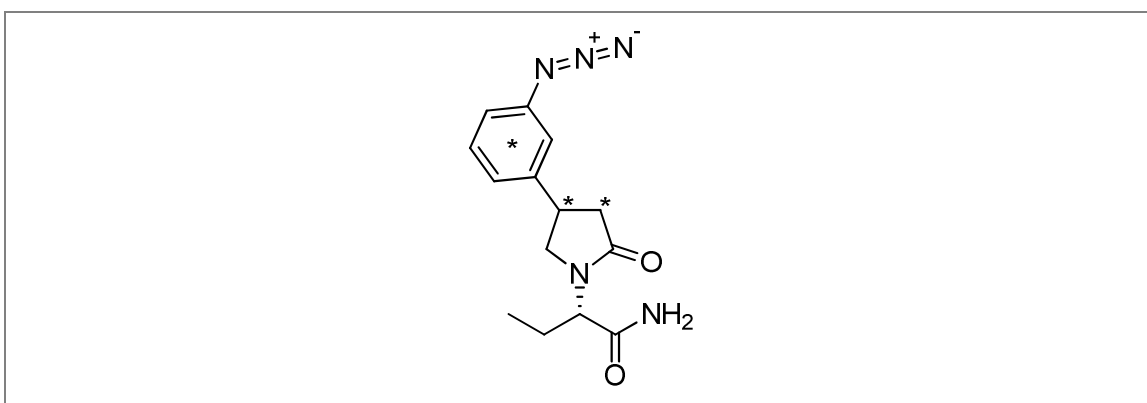
Figure 8: Chemical structure of [³H]ucb30889 (*denotes positions of ³H).

Based on these experiments, a wealth of information has been obtained that contributes to the understanding of LEV's mode of action. However, there is one major drawback that has to be brought forward concerning these formerly published radioligands: they all possess only moderate ([³H]LEV: 36.6 Ci/mmol)[60] to low ([³H]BRV: 8 Ci/mmol)[72] specific activity and thus might not be sufficient for answering all of the posed scientific

questions – especially concerning the hypothesis that the SV2A protein might not be the only target structure for LEV. Assuming that further target structures with much lower abundance exist in concomitance with the SV2A protein, a radioligand with low specific activity might not be sufficient for determining a potential interaction. This becomes particularly evident in previously published data, in which binding of the radioligands to brain membranes of SV2A KO mice has been investigated.[61] Within these experiments even in controls (wild-type mice) only relatively low signals have been detected, raising the question, if the given evaluation range was still big enough for the detection of potential low abundant targets. In a recently published repetition of this experiment (saturation binding to brain membrane preparations of SV2A KO mice),[72] the applied radioligand only possessed a specific activity of 8 Ci/mmol. These examples emphasize that radioligands with considerably higher specific activity are required as powerful tools for definite clarification of this matter, as well as for further investigations regarding the interaction sites of LEV and its analogues.

Concerning the radioactive isotope, there are several arguments, which support the choice of tritium (^{3}H) for labeling of the ligands.[156,157,162] Labeling with ^{3}H (in contrast to e.g. ^{125}I) offers the advantage of providing radioligands that can be considered biologically identical to their unlabeled (hydrogen-containing) analogues. With a half life of 12.5 years, tritium enables the preparation of storable radioligands. The maximum theoretical specific activity, which is obtainable with one ^{3}H atom is 28.76 Ci/mmol. Thus, it is possible to achieve sufficient specific activity of a radioligand by introduction of three or four ^{3}H atoms per molecule. Ideally. tritium-labeled radioligands should have affinities in the low nanomolar range. Due to the fact that LEV in this matter does not fulfill the optimal demand of a radioligand, besides LEV it was decided to additionally prepare its more potent analogue BRV as a tritium-labeled ligand for binding studies (see **Figure 9**).
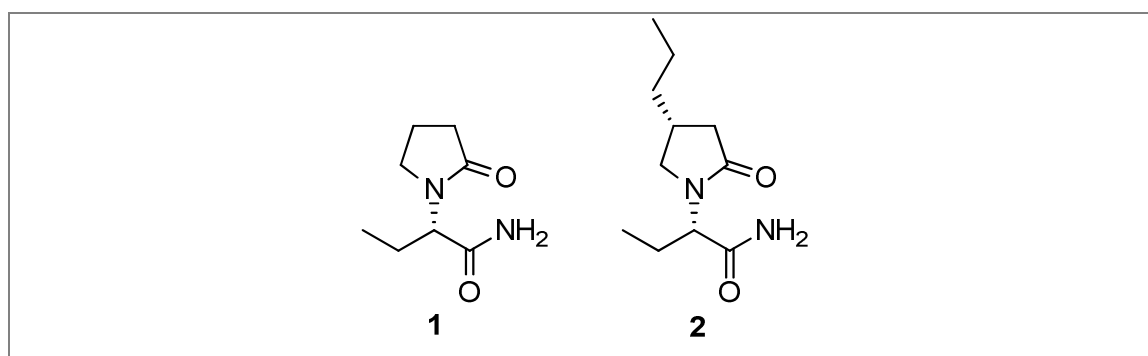
Figure 9: Chemical structures of levetiracetam (**1**) and brivaracetam (**2**).

The objective of the first part of this study was to devise a synthetic route, which allowed for the preparation of tritium-labeled radioligands (of LEV and BRV) with high specific activity. An alternative convenient technique of labeling molecules with tritium would have been an isotope exchange e.g. by exposure of organic compounds to tritium gas (Wilzbach procedure).[163] However, this technique was not taken into account, since radiolabeled compounds obtained by this method are labeled randomly with often only moderate specific activity and furthermore need rigorous purification due to the formation of a considerable amount of tritiated by-products.[164] Instead, a synthetic pathway had to be elaborated by which a reactive group could be introduced into the molecule that in the following step enabled the possibility to be transformed with tritium gas into the required functionality. In general, potential reactive groups that serve for this purpose are e.g. unsaturated hydrocarbons like alkenes and alkynes as well as aryl halogenides. By reduction of an unsaturated hydrocarbon to an alkane, or by substitution of an aryl halogenide, respectively, the controlled introduction of tritium into the molecule is possible.

2.2   Synthesis of [³H]LEV

The synthetic strategy that was used for the synthesis of the radioligand [³H]LEV (**3**) is based on a procedure described by Das Sarma et al.[165] The key step of this synthesis is a reductive amination reaction using mucochloric acid. As shown in **Scheme 1** (mechanism of reductive amination as proposed by Zhang et al.)[166] during the course of this reaction mucochloric acid is cleaved into its ring open form catalyzed by acetic acid. After nucleophilic attack by the amine a hemiaminal is formed, which is transformed into the corresponding iminium ion under elimination of H_2O. Subsequently, it is reduced to the secondary amine in the presence of $NaBH(OAc)_3$. The ring closure is then initiated by an intramolecular nucleophilic attack of the secondary amine at the carbonyl carbon atom. Thus, it is possible to introduce the lactam scaffold containing an unsaturated double bond twice substituted by chlorine atoms. This motive represents an ideal element for the introduction of tritium by catalytic hydrogenation in the last step.
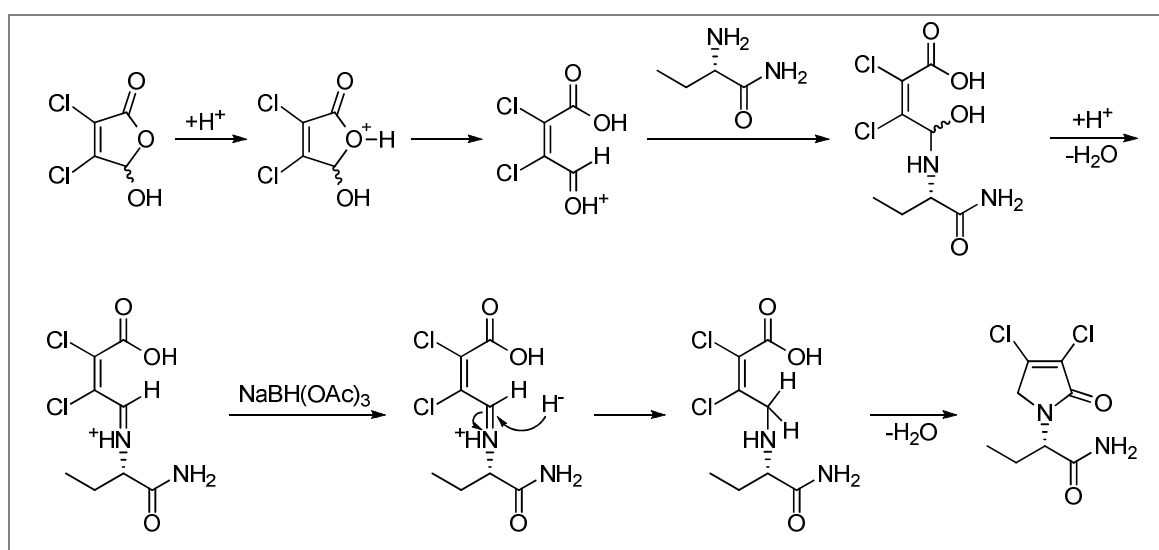
Scheme 1: Proposed mechanism of reductive amination with mucochloric acid.[166]

The synthesis of the radioligand [³H]LEV (**3**) was performed as depicted in **Scheme 2**. The starting compound (*S*)-2-aminobutyric acid (**4**) was reacted with thionyl chloride in methanol to yield the methyl ester **5** in analogy to Klieger and Gibian.[167] In a subsequent microwave reaction using ammonia in methanol the methyl ester was transformed into the corresponding primary amide **6**. This amino acid amide was applied in the above mentioned reductive amination reaction together with mucochloric acid (**7**) in the presence of sodium triacetoxyborohydride and catalytic amounts of acetic acid in chloroform to form the desired lactam **8**,[165] which represents a suitable precursor

molecule for the generation of the radioligand **3**. Compound **8** (precursor) was custom-labeled by Quotient Bioresearch (UK) by catalytic hydrogenation with tritium gas in the presence of palladium on charcoal as a catalyst. The herein described synthesis of [³H]LEV was published in the *Journal of Labelled Compounds and Radiopharmaceuticals*.[168]
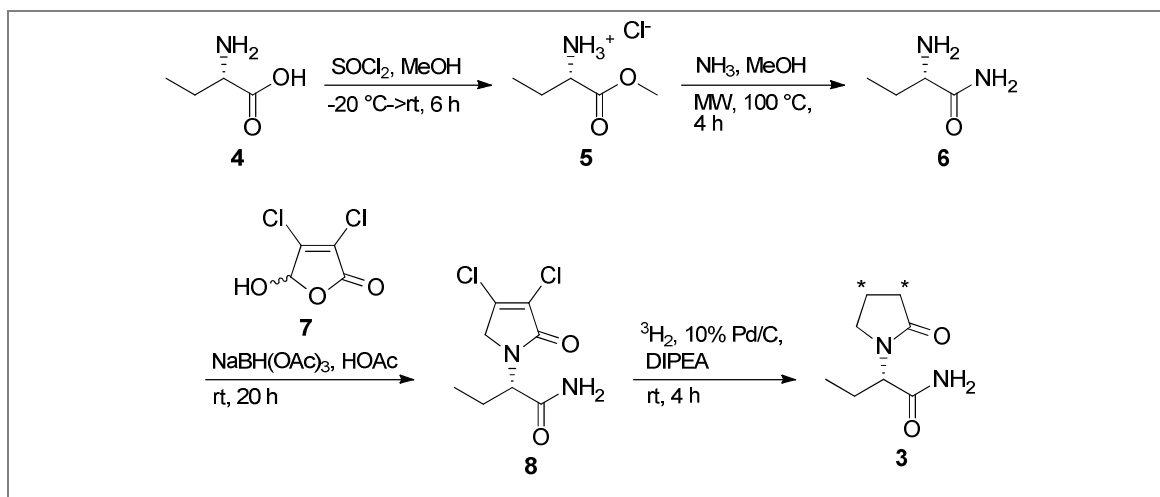
Scheme 2: Synthesis of [³H]LEV; MW: microwave, DIPEA: *N,N*-diisopropylethylamine (*denotes positions of ³H).

2.3 Synthesis of [³H]BRV

For the elaboration of a synthetic route for the preparation of [³H]BRV (**9**), initially a synthetic strategy for the unlabeled BRV was developed (see **Scheme 3**). This synthetic pathway provides the opportunity to introduce a non-saturated structure by replacing the propyl Grignard reagent **11** by the corresponding alkinyl or alkenyl Grignard reagent. Thus, a compound would be obtained that could be labeled by catalytic hydrogenation with ³H₂ gas.
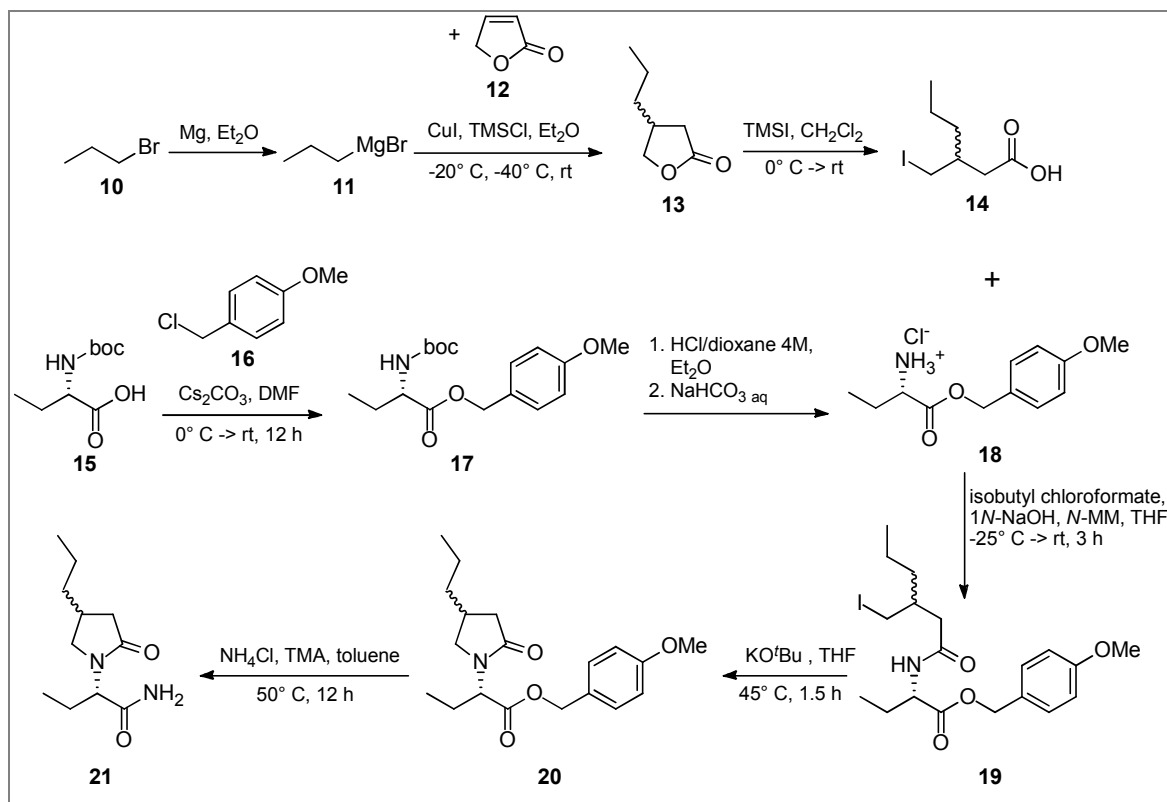
Scheme 3: Synthesis of BRV (**21**) (diastereomeric mixture); TMSCl: trimethylsilyl chloride, TMSI: trimethylsilyl iodide, *N*-MM: *N*-methylmorpholine, TMA: trimethylaluminum.

Following the above depicted synthetic pathway, 3-(iodomethyl) hexanoic acid (**14**) was synthesized as previously described by Kenda et al.[70] The propyl Grignard reagent **11** was prepared from *n*-propyl bromide (**10**). It was directly used for the synthesis of 4-*n*-propylbutyrolactone (**13**) with furanone (**12**) in a conjugate addition reaction in the presence of copper(I) iodide and trimethylsilyl chloride (TMSCl). Thereby a C-C-bond is formed between the alkyl moiety of the organometallic Grignard reagent **11** and the electron-deficient ß-carbon of the vinylogous compound **12**. The regioselectivity of this synthetic step is further improved by the presence of CuI, which is directing almost exclusively towards 1,4-addition reactions.[169] Furthermore, TMSCl supports regioselective 1,4-addition over the non-desired 1,2-addition, presumably by trapping the reactive enolate intermediate of the vinylogous keto compound and thus preventing reactions with the α-position.[170–172] The formation of unwanted side products, like e.g. by intermolecular coupling reactions of the Grignard reagents (2 R-MgX → R-R), as well as by other reactions, can further be influenced by factors like temperature, excess of reagents, and velocity of addition.[173] Thus, compound **13** was obtained, which was cleaved with trimethylsilyl iodide (TMSI) leading to compound **14** (3-(iodomethyl) hexanoic acid).

For the preparation of the amino acid ester **18** (*S*)-2-aminobutyric acid (**4**) was *N*-boc-protected (**15**) and thereafter esterified with 4-methoxybenzyl chloride (**16**) using Cs_2CO_3 as a base according to a general esterification procedure described by Dutton et al.[174] After deprotection of **17** by addition of HCl (4 M) in dioxane the amino acid ester **18** was reacted with the freshly prepared iodohexanoic acid **14** in an amide coupling reaction. Therefore, the carboxylic group of **14** was activated as mixed anhydride using isobutyl chloroformate in the presence of *N*-methylmorpholine based on the conditions described by Herrmann et al.[175] The obtained amide **19** was cyclized to the lactam **20** with potassium *tert*-butoxide as a base inspired by a cyclization procedure described by Sánchez et al.[176] In the last step the ester of compound **20** was transformed into the corresponding amide with an aluminum amide reagent, *in situ* prepared from trimethylaluminum and NH_4Cl applying similar conditions as described in former publications.[177,178] By means of the above described synthetic route it was possible to obtain the diastereomeric mixture of BRV in a ratio of 1 : 1 (*S*,*R* and *S*,*S*, **21**).

Subsequently, it was planned to repeat the whole synthetic route (**Scheme 3**), replacing the propyl Grignard reagent **11** by an unsaturated analogue (propenyl or propinyl residue) to obtain a suitable precursor molecule for tritium-labeling in the last step. However, even though the C-C coupling reaction was tried in various attempts making use of different mechanistic reaction principles, it was not possible to isolate the desired product (propenyl or propinyl lactone) in satisfying yields.

A further approach that was taken into account, was the introduction of the unsaturated structure within the amino acid part, namely by synthesizing 2-aminobut-3-enoic acid[179] (see **Figure 10**), which would be employed instead of the saturated compound (*S*)-2-aminobutyric acid (**4**).
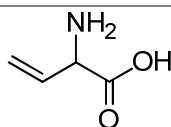
Figure 10: Chemical structure of 2-aminobut-3-enoic acid.

Being aware of the fact that this strategy would lead to a mixture of diastereomers in both stereocenters and would only allow the introduction of two ³H atoms, it was rejected for the sake of another strategy, which led to the desired result:

In contrast to the above listed strategies, the following synthetic pathway allows the introduction of four ³H atoms. Diastereomeric separation of the radioactively labeled

compounds, which emerge during the labeling reaction, is performed after radiolabeling. This presents an effective and convenient method for the preparation of a precursor molecule, which can be used for production of a radioligand labeled to a high specific activity.

In order to synthesize an adequate precursor molecule for the radioligand [³H]BRV (**9**), initially compound **22** (4-allyl-5-hydroxyfuran-2(5*H*)-one) was prepared in analogy to the procedure described by Bourguignon and Wermuth.[180] Glyoxylic acid (**23**) and pent-4-enal (**24**) were used as building blocks to be applied in a Mannich-type reaction in the presence of morpholine hydrochloride (**25**). According to the proposed reaction mechanism (see **Scheme 4**) an intermediate iminium ion was formed by reaction of morpholine hydrochloride with glyoxylic acid, which then reacted (nucleophilic attack) with the ß-carbon atom of the CH-acidic aldehyde **24**. After intramolecular cyclization the lactone **26** was obtained. Elimination of morpholine under acidic conditions provided the product **22**.
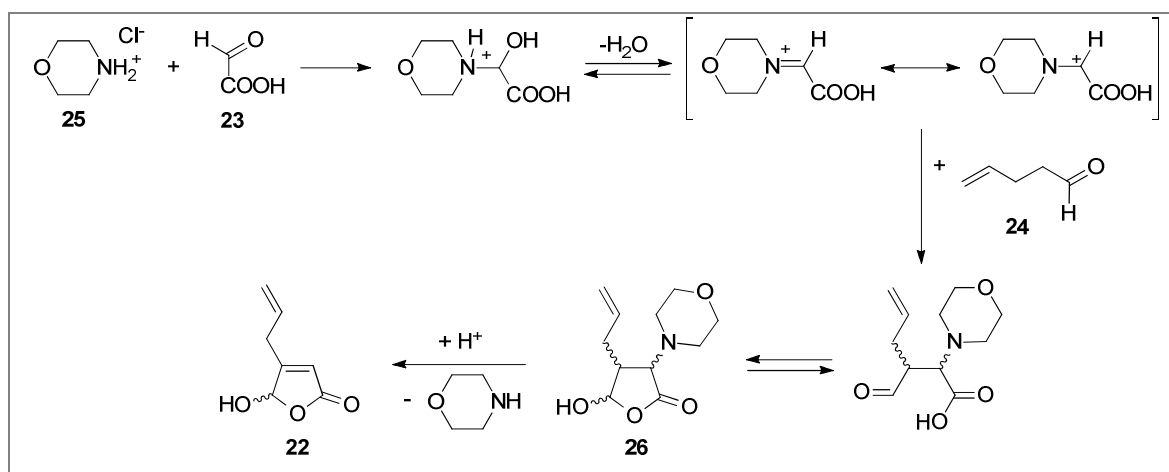
Scheme 4: Proposed mechanism of the synthesis of 4-allyl-5-hydroxyfuran-2(5*H*)-one (**22**).

Compound **22** together with the amino acid amide **6** were then applied for the synthesis of the precursor molecule **27** via a reductive amination reaction (see **Scheme 1**) as described above.[165] The hereby obtained precursor molecule **27** was custom-labeled by Quotient Bioresearch (UK) by catalytic reduction with tritium gas in the presence of palladium on charcoal as a catalyst.
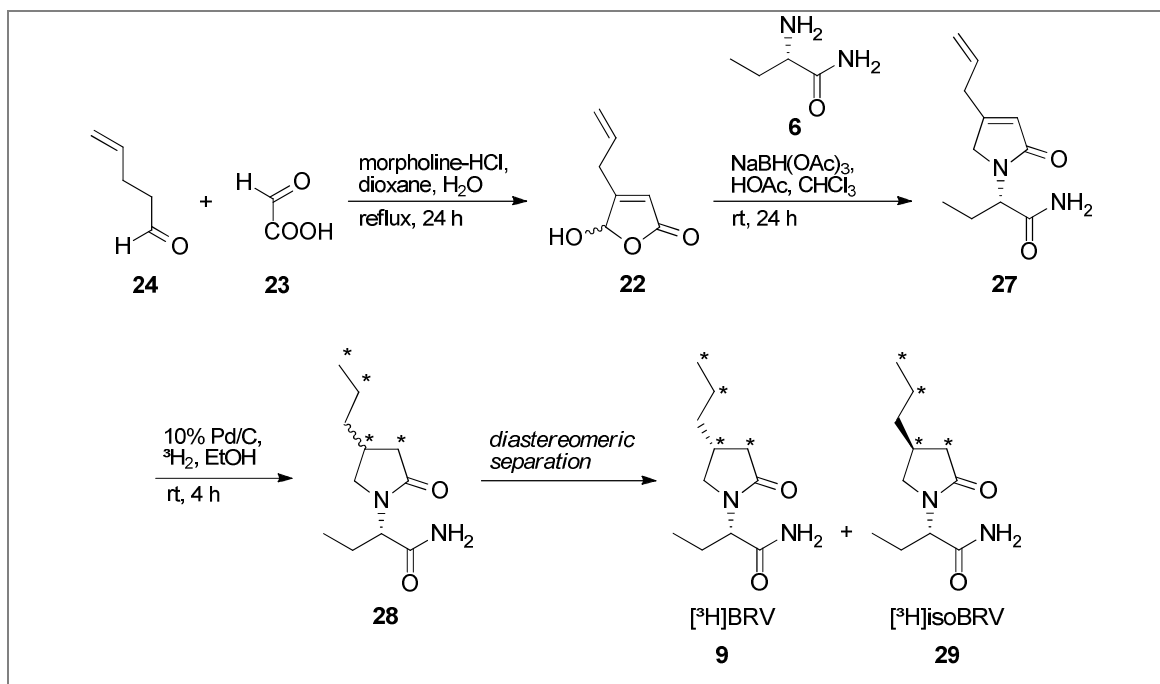
Scheme 5: Synthesis of [³H]BRV/[³H]isoBRV (diastereomeric mixture, **28**); *denotes positions of ³H.

As mentioned above, during the labeling reaction a diastereomeric mixture of the radiolabeled compound evolves (**28**) comprising the *S,R*- as well as the *S,S*-diastereomer. Consequently, diastereomeric separation of the mixture by chiral HPLC was necessary, leading to the radioligands [³H]BRV (**9**) and [³H]isoBRV (**29**) in their enantiopure form.
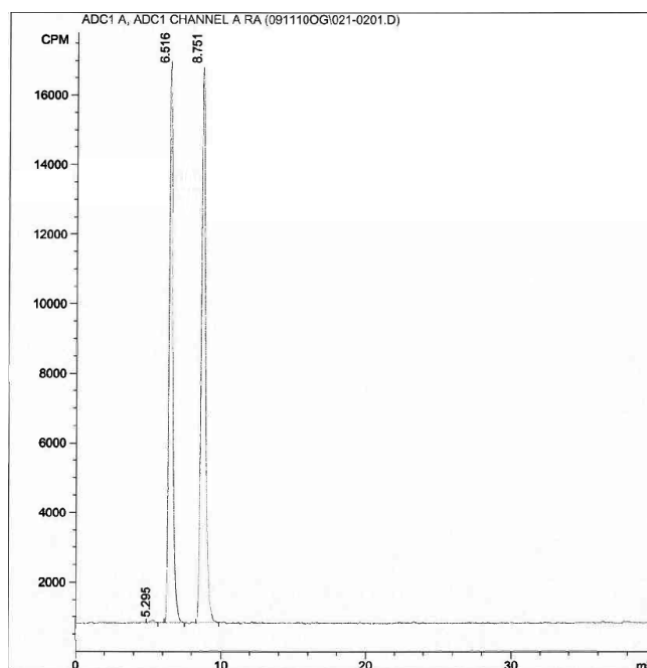
Figure 11: Chromatogram of diastereomeric separation of [³H]isoBRV (retention time: 6.516 min) and [³H]BRV (retention time: 8.751 min) by chiral HPLC. Chromatographic separation was performed by Quotient Bioresearch (Chiralpak AD-H 5 µm, 250 x 46 mm column, isocratic elution with ethanol : hexane (55 : 45) at 25 °C with a flow rate of 1 ml/min, UV detection at 205 nm).

2.4 Summary

Radioligands represent powerful tools for the clarification of scientific problems related to pharmacological or biochemical issues. They are applied in a broad field of investigational research and are especially helpful to study drug-target interactions. Considering that the mechanism of action of LEV (Keppra®), which is successfully applied as AED, is still not understood, it seems obvious that suitable radioligands represent a valuable tool for further research. Within this study it was one goal to create radioligands that are universally applicable: for general binding studies as well as for the detection of potential low abundant targets. While the so far applied radioligands in this field only possess moderate specific activity and therefore might not be applicable for certain scientific problems, as one part of this study, synthetic strategies had to be devised, which allowed the preparation of radioligands labeled to a high degree. Apart from [³H]LEV (**3**) a synthetic route likewise had to be devised for the preparation of [³H]BRV (**9**). This pyrrolidone analogue exhibits higher affinity to the target structure (SV2A) and thus represents another important investigational tool.

Synthetic strategies for both pyrrolidone drugs were devised leading to the corresponding precursor molecules with functional groups, which allowed the preparation of the desired radioligands by catalytic reduction with tritium. Radiolabeling of the precursor molecules was performed by Quotient Bioresearch. By means of the above described procedures it was possible to obtain the radioligands [³H]LEV (**3**) and [³H]BRV (**9**) as well as its diastereomer [³H]isoBRV (**29**) labeled to a high degree (94-98 Ci/mmol) with tritium (see **Figure 12**).

3   [³H]LEV, [³H]BRV and [³H]isoBRV binding to native proteins

3.1   Introduction

For investigations regarding protein target interactions of LEV and its analogues, radioligands were prepared (described in chapter 2) with high specific activity. Besides the radioligands [³H]LEV and [³H]BRV, for which binding studies with analogues labeled to a much lower degree are already published,[60,72] also [³H]isoBRV – the *S,S*-diastereomer – was obtained (see **Figure 12**). As an initial step it was important to establish radioligand binding assays based on formerly published procedures, which could be applied for the characterization of the present pyrrolidone radioligands. Various experiments were performed to reproduce formerly published results to investigate the radioligand binding to diverse membrane preparations and thereby gain insight into interactions of these radioligands with proteins in native tissue. Furthermore, in the course of these experiments the binding behavior of [³H]LEV and its more potent analogue [³H]BRV were to be compared with each other to assess similarities or differences in their binding behavior.
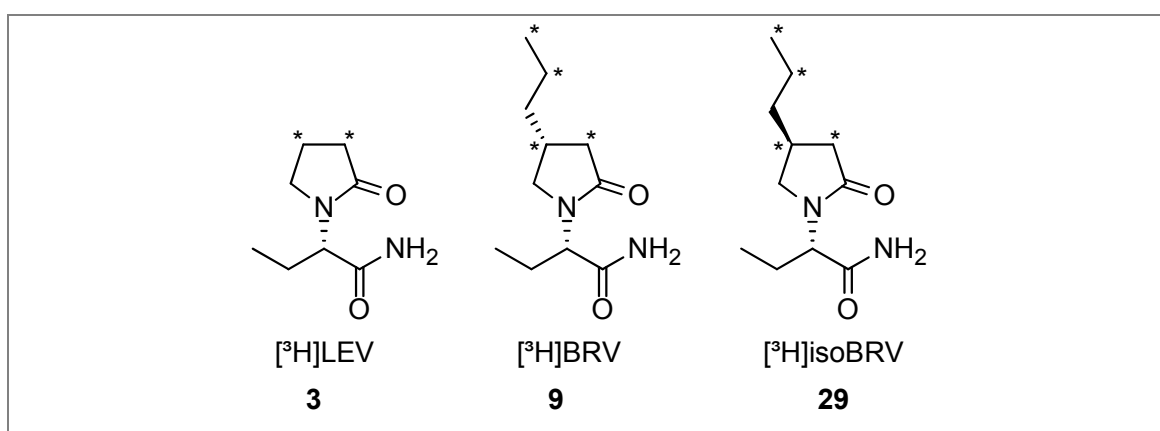
Figure 12: Pyrrolidone radioligands [³H]LEV, [³H]BRV and [³H]isoBRV (*denotes position of ³H).

3.2   Radioligand binding studies

3.2.1   Establishment of binding assays for [³H]LEV, [³H]BRV and [³H]isoBRV

Having the radioligands in hand, it was first necessary to establish a useful and reproducible assay system based on formerly published procedures.[60,159] Therefore, initial experiments were performed to gather information about suitable concentrations of the applied radioligand as well as the amount of protein to be used per well. In

accordance with the reaction conditions described below (see 8.5.4.1.1 and **Table 21**), after an incubation time of 120 min the following results were obtained:
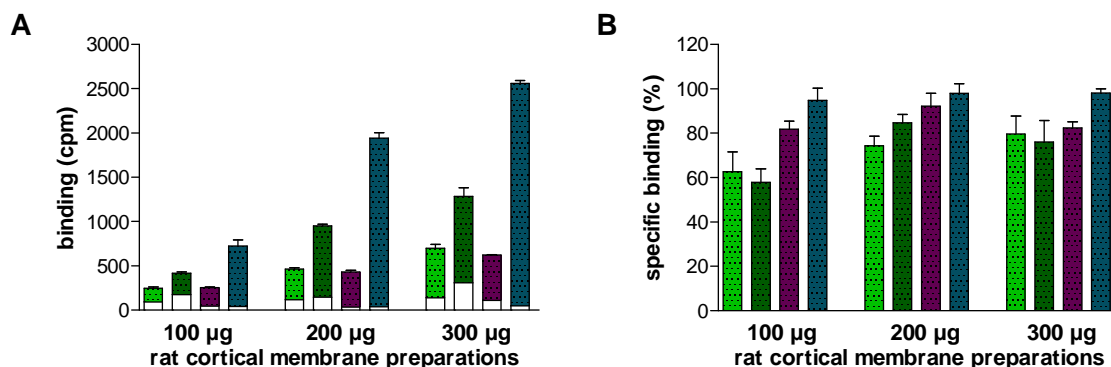
Figure 13: Protein concentration dependent binding of the radioligands [³H]LEV, [³H]isoBRV and [³H]BRV to rat cortical membrane preparations: 100, 200 or 300 µg of protein per well was incubated for 120 min at 4 °C with [³H]LEV 5 nM (light green), [³H]LEV 10 nM (dark green), [³H]isoBRV 1 nM (purple), and [³H]BRV 1 nM (blue), respectively. Non-specific binding (open bars) was determined in the presence of unlabeled LEV (1 mM). Specific binding (dotted bars) was obtained by subtraction of non-specific binding from total binding, which was determined in the absence of unlabeled LEV. All data are means ± SEM of an experiment performed in triplicate. **A:** Specific and non-specific binding in cpm. **B:** Specific binding expressed as a percentage of total binding.

This individual experiment allowed several observations: as assumed, within the investigated ranges binding of the radioligands increased proportionally with the concentration of the protein. Likewise, linearity could also be concluded for the radioligand concentration, as demonstrated by [³H]LEV (5, and 10 nM, respectively), shown in **Figure 13 A**.

Specific binding of [³H]LEV was determined to be $\geq 75\%$ (for protein concentrations of 200 µg and 300 µg per well), while [³H]isoBRV demonstrated specific binding $\geq 80\%$ and [³H]BRV even $\geq 95\%$ for all protein concentrations tested (see **Figure 13 B**). In general, non-specific binding is aimed to be kept as low as possible. Acceptable values for specific binding given in literature are 50% as being considered barely adequate, 70% as good, while 90% is considered as excellent.[156] Based on these data it can be concluded that the radioligands under the applied conditions provide **good to excellent specific binding**.

In order to obtain sufficiently large evaluation ranges it is important to achieve adequate signals for the overall binding. Ideally, the signal should not be lower than 100 cpm for the lowest signal expected in the assay.[155] Confirmed by this preliminary experiment – regarding prospective studies – it was decided to apply [³H]LEV in a concentration of 10 nM and 200 µg of protein (membrane preparations) per well. Since the so far

measured specific binding of [³H]isoBRV was still quite low (around 620 cpm and less), for future studies it was decided to apply the radioligand in a concentration of 5 nM together with 100 µg of protein (membrane preparations) per well. For [³H]BRV a concentration of 1 nM along with 100 µg of protein (membrane preparations) per well was considered to provide sufficient binding and therewith valuable results within future experiments.

Further assay conditions, like the buffer system, assay volume, determination of non-specific binding etc. were adopted from Noyer et al.[60] In a series of experiments it was confirmed that a concentration of 1 mM unlabeled LEV is sufficient for the determination of non-specific binding (data not shown). This is also consistent with data in the literature, which suggest at least an excess of 100 times the K_D concentration.[157] Moreover, it was verified that incubation at 4 °C, as well as keeping the time of the washing procedure as short as possible, whilst using cold washing buffer is essential for the quality of the results. As shown in **Table 2** the allowable separation time shortens remarkably with decreasing K_D values, since dissociation accelerates with lower ligand affinities.

Table 2: Relationship between equilibrium dissociation constant (K_D) and allowable separation time (from: Yamamura et al.).[157]

K_D (M)	allowable separation time (sec)
10^{-9}	~ 100
10^{-8}	10
10^{-7}	0.10
10^{-6}	0.01

It is self-evident that a low temperature buffer and a rapid washing procedure in this context have a remarkable influence. However, concerning the ratio of nonspecific to specific binding, it was further proven that three rinses with a smaller volume provide better results than two rinses with a bigger volume of buffer. Furthermore, it turned out that the use of a double layer of GF/C glass fiber filters for the filtration procedure (from which the upper filter was used for the analysis) led to a reduction of deviations within an assay.

Hence, it can be concluded that all of the three pyrrolidone radioligands can be applied under the above described, optimized conditions for performing standard assays.

3.2.2 Kinetic studies

To investigate the binding of the three radioligands [³H]LEV, [³H]isoBRV and [³H]BRV as a function of time, kinetic experiments were performed using rat cortical membrane preparations (see 8.3.1) according to conditions described in 3.2.2. The following association binding curves were obtained:
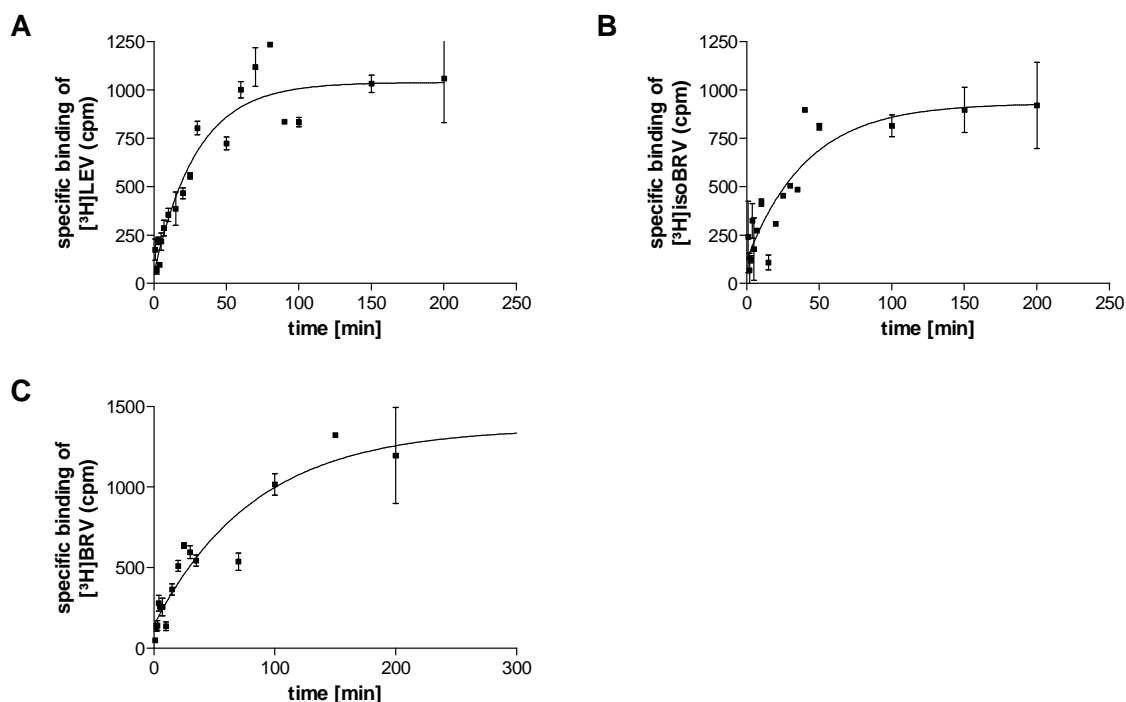
Figure 14: Specific binding of [³H]LEV 10 nM (**A**), [³H]isoBRV 5 nM (**B**) and [³H]BRV 1 nM (**C**) obtained in association binding experiments using rat brain cortical membrane preparations. The radioligand was incubated at 4 °C with membrane preparations (**A**: 200 µg of protein/well; **B**, **C**: 100 µg of protein/well), which were added at different time points. Non-specific binding was determined in the presence of unlabeled LEV (1 mM). Data are representative of 3-4 independent experiments performed in duplicate or triplicate; data points represent means ± SEM.

Table 3: Half time of association $t_{1/2}$ (min) ± SEM of pyrrolidone radioligands obtained in association binding experiments.

	[³H]LEV	[³H]isoBRV	[³H]BRV
$t_{1/2}$ (min)	16 ± 2	29 ± 2	60 ± 1

The given data illustrate the differences in the time interval between the three radioligands until equilibrium of binding was reached. The course of association for all radioligands showed binding to a single site. As expected, at 4 °C [³H]LEV showed the fastest association kinetics ($t_{1/2}$ = 16 ± 2 min), followed by [³H]isoBRV ($t_{1/2}$ = 29 ± 2 min), whereas association proceeded the slowest for [³H]BRV ($t_{1/2}$ = 60 ± 1 min). In the literature, association of [³H]LEV to rat brain membrane preparations is described as

binding to two sites, however with a comparable course of association providing the same time interval until steady-state is reached.[60] Likewise, association of [³H]BRV is characterized as binding to two sites in the literature,[72] but again the overall course of the published association curve is consistent with the one obtained by the here performed association experiment. Based on these results the incubation time (time until steady-state can be assumed) was determined as 120 min for [³H]LEV, 180 min for [³H]isoBRV and 240 min for [³H]BRV.

Besides association studies also dissociation studies for all of the three radioligands have been performed (data not shown). However, the data of the dissociation curves showed considerable deviations, values for k_{off} (calculated with **Equation 4**) were not well reproducible and kinetic K_D values could therefore not be calculated (according to **Equation 6**). Nonetheless, since the K_D value can be calculated from saturation experiments with even higher accuracy, the data from the dissociation experiments were not needed for further calculations, and consequently were discarded.

Concluding the results of the kinetic binding studies, valuable information was obtained concerning the time interval until equilibrium binding was reached by all of the three radioligands. Based on these values, the incubation time for prospective binding studies was determined.

3.2.3 Saturation studies

The three radioligands were further characterized by saturation binding experiments using rat cortical membrane preparations. By means of these experiments the affinity of the radioligands to their binding sites (K_D) as well as the maximum number of binding sites (B_{max}) was determined.
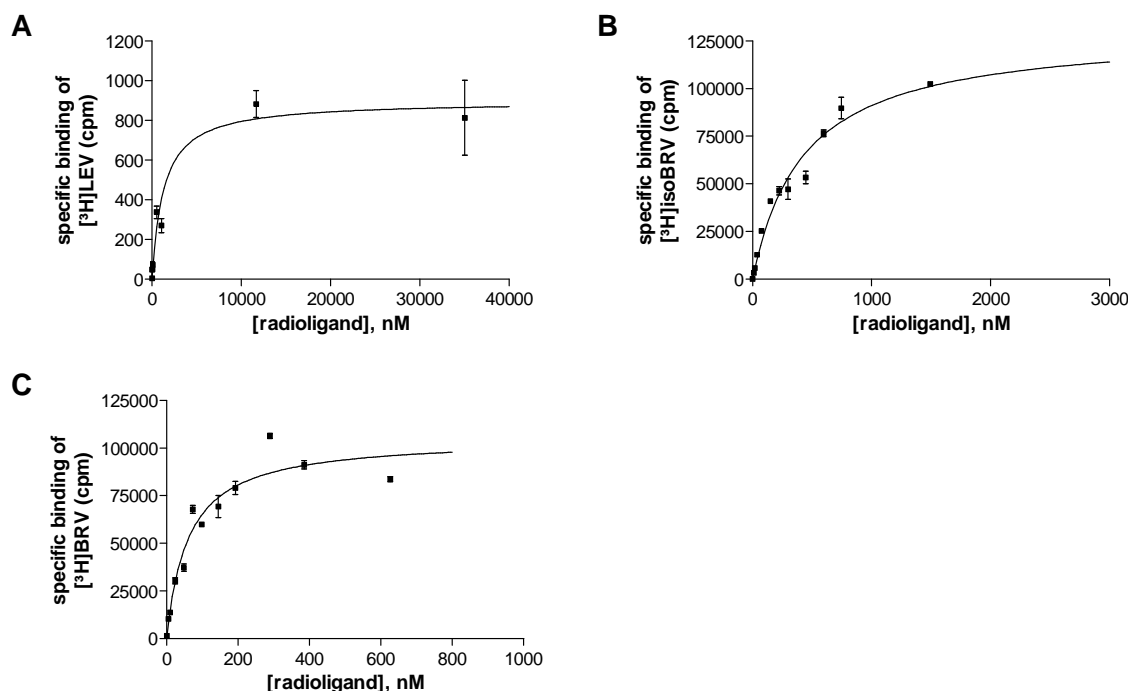
Figure 15: Specific binding of [³H]LEV (**A**), [³H]isoBRV (**B**) and [³H]BRV (**C**) obtained in saturation binding experiments using rat brain cortical membrane preparations. Different concentrations of the radioligand were incubated with membrane preparations (**A**: 200 µg of protein/well; **B**, **C**: 100 µg of protein/well) at 4 °C for 120 min (**A**), 180 min (**B**), or 240 min (**C**), respectively. Non-specific binding was determined for each radioligand concentration in the presence of unlabeled LEV (1 mM). Curves are representative of two independent experiments each performed in triplicate (**A**) or duplicate (**B**, **C**); data points represent means ± SEM.

From the above depicted saturation experiments the following values were obtained (means ± SEM of two individual experiments performed in duplicate or triplicate):

Table 4: K_D and B_{max} values ± SEM of pyrrolidone radioligands obtained in saturation experiments.

	[³H]LEV	[³H]isoBRV	[³H]BRV
K_D (nM)	1115 ± 177	409 ± 23	70.0 ± 8.4
B_{max} (pmol/mg protein)	3.7 ± 0.1	10.4 ± 1.2	8.3 ± 1.5

The saturation experiment of the low affinity ligand [³H]LEV was performed by means of isotopic dilution (see 8.5.3.2.1), which allowed to measure up to concentrations at which a plateau (saturation) was reached. This was not possible for the radioligands

[³H]isoBRV and [³H]BRV, since the corresponding cold ligands were not available. In these cases the saturation binding experiments were performed with non-diluted radioligand, which limited the highest concentration applied in the assay (ideally it should encompass ~0.1 x K_D to ~10 x K_D).[156] Nevertheless, the course of the saturation binding curves was sufficient for determination of the relevant parameters. To increase the accuracy of the saturation studies, the "actual" concentration of radioligand applied in the assay was determined by measuring aliquots of each radioligand dilution. These actual concentrations were used to plot the saturation curve and hence, for the determination of K_D and B_{max} values.

As expected, the obtained data demonstrated increasing affinities of the radioligands to their target site following the order [³H]BRV > [³H]isoBRV > [³H]LEV. Based on these results [³H]BRV showed about 16 times and [³H]isoBRV about 3 times higher affinity than [³H]LEV to their binding site. These determined **K_D values** are in accordance with data from the literature: Gillard et al. determined a K_D value of 62 ± 8 nM for [³H]BRV at rat cortex.[72] For [³H]isoBRV no K_D value has been published so far, however a K_i value (obtained from a heterologous binding experiment vs. [³H]BRV) was determined to be around 320 nM.[72] The K_D value published for [³H]LEV (0.8 ± 0.2 µM), which was obtained by saturation binding to rat hippocampal membrane,[60] is slightly lower than the here determined K_D value. Nevertheless, it is still within the same range, especially since this low affinity ligand is more prone to error in binding experiments.
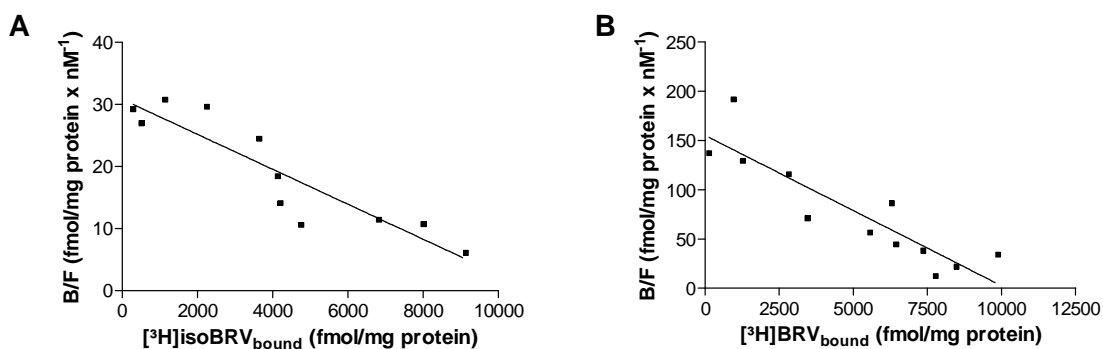
Figure 16: Rosenthal plots from transformed data obtained in saturation experiments with the radioligands [³H]isoBRV (**A**) and [³H]BRV (**B**).

All saturation binding curves describe a **single-phase process** (exemplarily shown by Rosenthal plots for [³H]isoBRV and [³H]BRV in **Figure 16**), and thus demonstrate labeling to a single class of binding sites. This was also suggested by published data from saturation experiments of the radioligand [³H]LEV and [³H]BRV.[60,72] The

determined numbers of binding sites (**B_{max} values**) obtained from these saturation experiments all lie within the low picomolar range. This is in accordance with the B_{max} values of the published saturation experiments (9.1 ± 1.2 and 11 ± 2 pmol/mg protein),[60,72] merely the B_{max} value determined by the radioligand [³H]LEV is slightly lower. This again in parts might be due to higher deviations caused by lower target affinity (leading to a higher dissociative loss) as well as to imprecision in the determination of the B_{max} value from saturation curves with isotopic dilutions.

Summing all up, it can be concluded that all three radioligands provide data compatible with those published in the literature. Even though the low affinity radioligand [³H]LEV is more susceptible for deviations, it provides similar data as formerly suggested.

3.2.4 Competition experiments at rat cortical membrane preparations

As mentioned above (see chapter 1.2), due to an estimated resistance rate of approximately 30%[22,181] regarding AED therapy it becomes of great importance to target novel structures that are distinct from those of the so far known antiepileptic targets. In 2004, Lynch et al. identified the SV2A protein as the molecular target for LEV, thereby supporting the hypothesis that this pyrrolidone drug acts via a unique mechanism.[61] This is further strengthened by the fact that only very few compounds are known that actually compete with the binding of LEV and its analogues,[60,72] some of which were investigated within this study (see **Figure 17**).

One of these compounds is **ethosuximide**, an AED that is predominantly applied in the treatment of generalized absences. It interacts with voltage-gated T-type Ca^{2+}-channels, reducing the influx of Ca^{2+} and therewith inhibiting the formation of an excitatory postsynaptic potential (EPSP). The oral therapy usually starts with increasing doses (250 mg intervals over four to six days) until the typical initial dose (adults: 500 mg per day) is reached. This initial dose is further adapted to a daily dose of generally 20 to 30 mg/kg. The optimum therapeutic index ranges from 40 to 100 µg/ml; concentrations of 160 µg/ml are still tolerated without any severe side effects.[54,182]

Besides anti-convulsive, also pro-convulsive compounds have been identified that compete with LEV and BRV binding. **Pentylenetetrazol**, a respiratory stimulant, presumably acts as a non-competitive antagonist at the $GABA_A$ receptor. In high concentrations it provokes seizures via a yet unknown mechanism. Due to this effect it

is frequently used in epilepsy research to study epileptic seizures in animal models and to investigate the efficacy of potential anticonvulsive compounds (PTZ model). In a *timed intravenous PTZ infusion seizure test* (i.v. PTZ test) the rat or mouse is continuously given PTZ by infusion into the tail vein to determine the dose (mg/kg body weight) at which a certain type of seizure occurs (myoclonic, clonic or tonic). A potential anticonvulsive effect of a test compound, which is administered prior to the infusion of PTZ, can be identified by a delayed occurrence of the formerly observed seizure type. Typical infusion rates are 4-8 mg (rat) or 3 mg (mouse) PTZ per minute. In general, first clonic seizures occur between 30 to 40 mg/kg.[183] With regard to a body weight of 200 g, this corresponds to approximately 43 to 58 µmol per rat. In a further animal model PTZ is administered subcutaneously (s.c. PTZ test) in concentrations of 85 mg/kg body weight and time is measured until clonic seizures occur. Whereas LEV only showed efficacy in the i.v. PTZ test, but not in the s.c. PTZ test, its analogue BRV proved efficacy in both.[69,184]

Bemegride also represents a CNS-active compound with respiratory stimulating effects. It is likewise applied in animal models to evoke convulsions. The dose for inducing clonic seizures is 30 mg/kg body weight i.p., which corresponds to 39 µmol per rat referred to a body weight of 200 g.[185]

Not surprisingly, competitive binding behavior has also been found for structurally related compounds from the class of pyrrolidone drugs. **Piracetam**, the first nootropic drug developed, has been claimed to possess several potential modes of action, including influences on membrane fluidity and neurotransmission as well as enhancement of cerebral blood flow. Besides cognitive disorders, it has several further indications, like e.g. cortical myoclonus and dyslexia. In general, the required doses for therapeutical treatment are very high, such as for treatment of cognitive disorders, which requires dosing between 2.4 and 4.8 g per day. Hereby, following an oral dose of 3.2 g, a plasma level of 84 µg/ml is achieved.[186–189]

Aniracetam is another pyrrolidone drug that likewise possesses cognition enhancing properties. The mechanism of action is still not known yet. It is discussed that aniracetam conveys its effect via positive allosteric modulation of the AMPA receptor, therewith slowing down receptor desensitization, which supposedly results in improved short- and long-term memory storage.[125]

ethosuximide   pentylenetetrazol   bemegride   piracetam   aniracetam
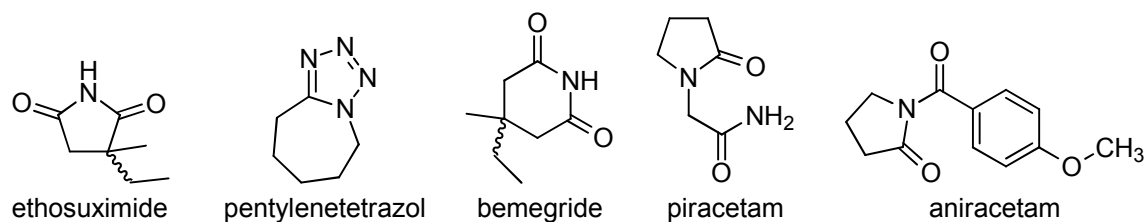
Figure 17: Chemical structures of compounds tested in the present study for competitive behavior vs. [³H]LEV and [³H]BRV.

Within this study, the pyrrolidone radioligands [³H]LEV and [³H]BRV were further characterized by performing competition binding experiments at rat brain cortical membrane preparations, in which initially the unlabeled compound LEV was applied as inhibitor.
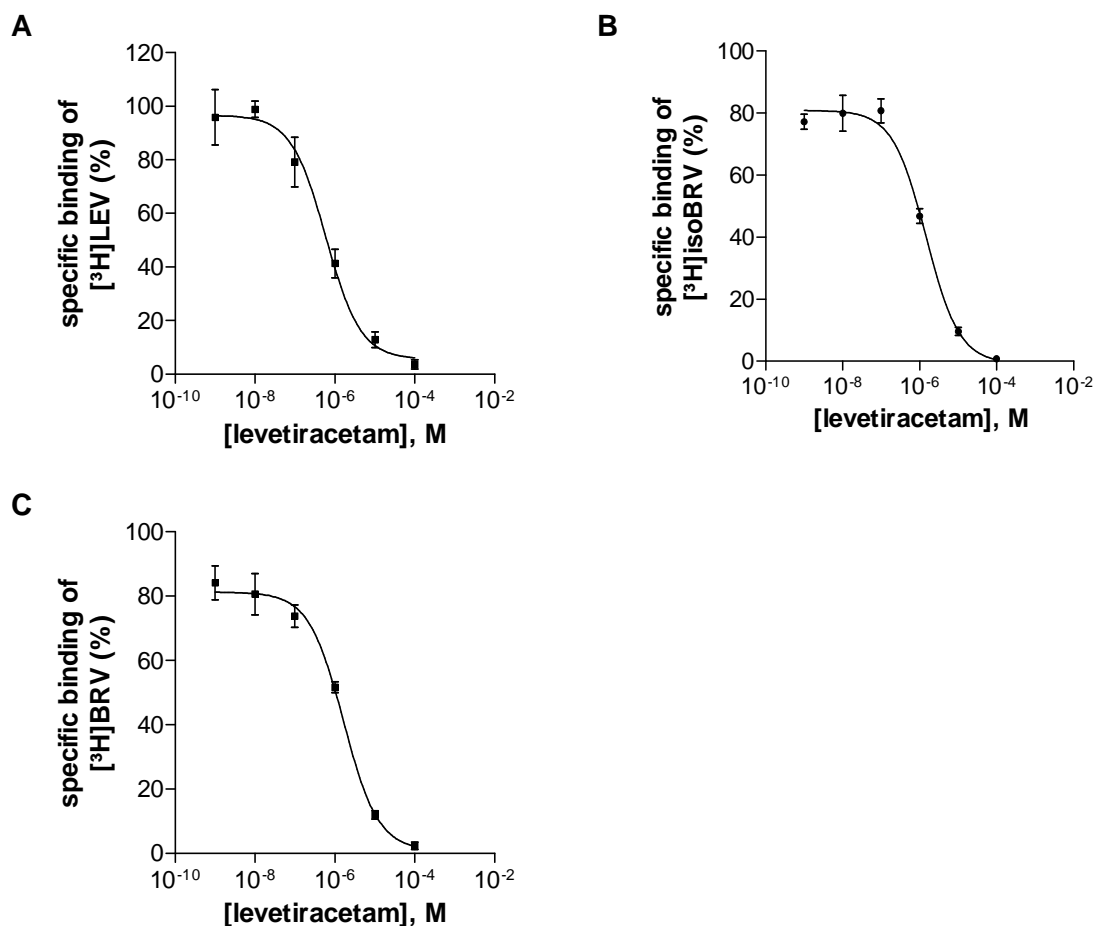
Figure 18: Specific binding of [³H]LEV 10 nM (**A**), [³H]isoBRV 5 nM (**B**) and [³H]BRV 1 nM (**C**) obtained in competition binding experiments with unlabeled LEV using rat brain cortical membrane preparations. Increasing concentrations of unlabeled LEV were incubated with membrane preparations (**A**: 200 µg of protein/well; **B**, **C**: 100 µg of protein/well) and the radioligand at 4 °C for 120 min (**A**), 180 min (**B**), or 240 min (**C**), respectively. Non-specific binding was determined in the presence of unlabeled LEV (1 mM). All data are means ± SEM of 3-5 individual experiments performed in triplicate.

From the homologous binding experiment LEV vs. [³H]LEV, a K_i value of **0.705 ±
0.294 µM** was obtained, which is slightly differing, but still falling within the same
order of magnitude as the K_D value (1.12 ± 0.18 µM) obtained by saturation
experiments. Data published in the literature from rat hippocampal membrane
preparations for both types of binding studies propose values of about 0.8 µM.[60] The
calculated B_{max} value from the above described homologous binding experiment was
2.5 ± 0.9 pmol/mg protein, which is comparable to the B_{max} value that was obtained in
the saturation experiment (3.8 ± 0.1 pmol/mg protein), however lower than the
published B_{max} value of 9.1 ± 1.2 pmol/mg protein.[60] This might still be within the
natural deviation, presumably since [³H]LEV as a low affinity ligand exhibits a fast
dissociation rate and thus the binding equilibrium is more prone to error during the
filtration and washing procedure (dissociative loss). The K_i values for LEV received
from heterologous competition experiments vs. [³H]isoBRV and [³H]BRV were **1.40 ±
0.07 µM** and **1.71 ± 0.23 µM** (literature data for LEV vs. [³H]BRV: 1.26 µM)[72],
respectively.

Apart from LEV several further compounds (described in detail above) were applied in
heterologous competition binding experiments versus the radioligands [³H]LEV and
[³H]BRV to investigate competitive behavior. As mentioned earlier, for these
compounds, which differ in their chemical structure as well as their pharmacological
properties, a competitive effect has been described before.[60,72]
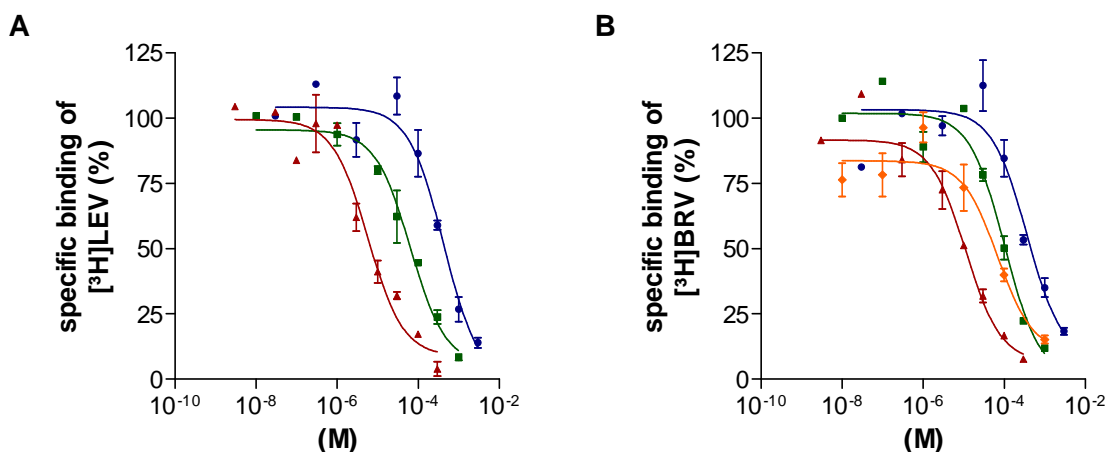
Figure 19: Specific binding of [³H]LEV 10 nM (**A**) and [³H]BRV 1 nM (**B**) obtained in competition
binding experiments with ethosuximide (blue), pentylenetetrazol (green), bemegride (red), and piracetam
(orange), respectively, using rat brain cortical membrane preparations. Increasing concentrations of
competitor were incubated with membrane preparations (**A**: 200 µg of protein/well; **B**: 100 µg of
protein/well) and the radioligand at 4 °C for 120 min (**A**), or 240 min (**B**), respectively. Non-specific
binding was determined in the presence of unlabeled LEV (1 mM). All data are means ± SEM of 3
individual experiments performed in triplicate.

Table 5: K_i values (µM) of different compounds obtained in competition binding experiments at rat cortical membrane preparations, n/a: not available. K_i values in grey originate from published data.

	[³H]LEV	Noyer et al.[60]	[³H]BRV	Gillard et al.[72]
ethosuximide	424 ± 86	316	312 ± 30	
pentylenetetrazol	72.5 ± 18.6	79.4	116 ± 14	126
bemegride	6.68 ± 0.69	10.0	11.9 ± 2.9	25.1
piracetam	n/a	31.6	63.8 ± 22.2	
aniracetam	n/a	1000	> 1000	

Several compounds were tested in competition binding experiments versus the radioligands [³H]LEV and [³H]BRV providing K_i values in the µM range (see **Table 5**). The data are comparable with values that formerly have been published for the compounds.[60,72] Determination of the K_i values of piracetam and aniracetam versus [³H]LEV was not possible due to the presence of DMSO in the assay, which decreased the evaluation range, but was required to solubilize the compounds.

Considering that the effective drug concentration of ethosuximide (40 to 100 µg/ml)[182] corresponds to a concentration of approximately 280 to 700 µM, the obtained data from the competition experiments (see **Table 5**) illustrate that competitive behavior of ethosuximide with LEV and BRV is expectable within applied drug concentrations. This is also the case for piracetam, for which a plasma concentration of 84 µg/ml[189] corresponds to roughly 590 µM and therewith reaches a concentration, where competitive behavior must be expected.

The results from the above described competition experiments demonstrate a reliable and reproducible assay system that therefore proves to be suitable for the screening of compounds. In cases, in which published data from analogous experiments are available, the results are in good accordance and therewith also confirm accuracy. Comparing the results of the corresponding experiments between [³H]LEV and [³H]BRV, it becomes obvious that both radioligands provide quite similar results. With regard to the fact that the radioligand [³H]LEV in general is more prone to errors, it can be concluded that [³H]BRV (due to higher affinity) can be applied as a replacement for LEV in experiments, which are more susceptible for disturbing influences.

3.2.5 Binding to membrane preparations from different species

In further competition experiments binding of LEV using the radioligands [³H]LEV and [³H]BRV to brain membrane preparations of different species was examined. Besides the already applied preparations from rat cortex (RC), also striatal tissue from rat brain (RS) was utilized in these experiments. Brains from Black 6 mice were kindly provided by the group of Prof. Dr. V. Gieselmann and were used for the preparation of whole brain membrane preparations (M). Furthermore, post-mortem human brain samples (thalamus and putamen) were available, which originally were obtained from the University Clinic of Bonn (for additional information on the tissue see 8.3.3).
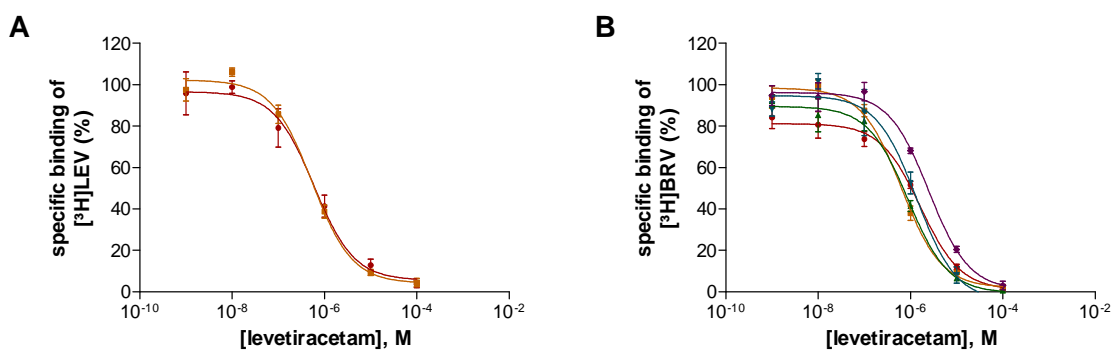
Figure 20: Specific binding of [³H]LEV 10 nM (**A**) and [³H]BRV 1 nM (**B**) obtained in competition binding experiments with unlabeled LEV at membrane preparations of rat cortex (red), rat striatum (brown), mouse brain (green), human thalamus (blue), and human putamen (purple), respectively. Increasing concentrations of LEV were incubated with membrane preparations (100-200 µg of protein/well, see **Table 23**) and the radioligand at 4 °C for 120 min (**A**), or 240 min (**B**), respectively. Non-specific binding was determined in the presence of unlabeled LEV (1 mM). All data are means ± SEM of 3-5 individual experiments performed in triplicate.

Table 6: IC_{50} values (µM) of LEV obtained in competition binding experiments versus the radioligands [³H]LEV and [³H]BRV at membrane preparations from different species. Data in brackets (grey) are B_{max} values (pmol/mg protein) determined in homologous binding experiments; n/a: not available.

	[³H]LEV	[³H]BRV
rat cortex (RC)	0.711 ± 0.297 (2.5 ± 0.9)	1.73 ± 0.23
rat striatum (RS)	0.542 ± 0.070 (3.0 ± 0.4)	0.693 ± 0.131
mouse brain (M)	n/a	0.948 ± 0.144
human thalamus (HT)	n/a	1.43 ± 0.33
human putamen (HP)	n/a	2.69 ± 0.55

In comparing the IC_{50} values obtained from the homologous competition experiment of LEV vs. [³H]LEV at membrane preparations from **rat brain** with each other, quite similar values were determined at RC (0.711 ± 0.297 µM) and at RS (0.542 ± 0.070 µM). This is well comparable with the published IC_{50} value from a homologous

binding experiment (0.8 µM),[60] which was determined at rat hippocampal membrane. Regarding the heterologous competition experiment of LEV vs. [³H]BRV bigger differences between those two rat brain areas were determined. With regard to a published K_i value of the same competition experiment at RC (1.26 µM),[72] the here determined IC_{50} value at RC (1.73 ± 0.23 µM) is slightly higher, while the IC_{50} value determined at RS (0.693 ± 0.131 µM) rather falls into the range of the IC_{50} values obtained from the homologous competition experiments (LEV vs. [³H]LEV) at RC and RS.

Concerning the IC_{50} value obtained from the heterologous competition experiment at **mouse brain** membrane preparations no data from an equivalent experiment has been published in the literature yet. Nevertheless, the value (0.948 ± 0.144 µM) seems to be similar to the IC_{50} values obtained from binding to rat membrane preparations.

The heterologous competition experiments of LEV vs. [³H]BRV at **human brain** membrane preparations provided IC_{50} values of 1.43 ± 0.33 µM at HT and a slightly higher IC_{50} value of 2.69 ± 0.55 µM at HP. With an analogous heterologous competition experiment using membrane preparations of human cortex Gillard et al. determined for LEV a K_i value of 2.00 µM.[72] Hence, it can be concluded that the experimentally determined IC_{50} values from human post-mortem brain are consistent with formerly published results.

Regarding the maximum number of binding sites **B_{max} values** of 2.5-3.0 pmol/mg protein were calculated from the data of the homologous competition experiments at RC and RS. This is in agreement with the B_{max} value obtained from the saturation binding experiment of [³H]LEV at RC (see 3.2.3), though lower than an earlier published value of 9.1 ± 1.2 pmol/mg protein[60] from a saturation experiment of [³H]LEV. As discussed above, this is probably due to the low affinity of the radioligand, which more easily tends to dissociate from its target during the washing procedure and therewith a lower number of binding sites as actually present will be determined. To roughly estimate the present number of binding sites within membrane preparations examined by heterologous competition experiments with [³H]BRV, B_{max} values were calculated approximately. Therefore, a presumable IC_{50} value for BRV had to be used, which was chosen based on data from the literature: in the case of the membrane preparations from murine brain (RC, RS and M) an IC_{50} value of 0.09 µM (calculated from homologous competition experiment at rat cortex)[72] was taken as approximate value. Based on this

value according to **Equation 17** B_{max} values were estimated to be in the range of 13 to 17 pmol/mg protein. Considering that these numbers are only an estimation, they are compatible with a B_{max} value published in the literature (11 ± 2 pmol/mg protein),[72] which was obtained in a saturation experiment of [³H]BRV at rat cortex. In the same way, the approximate B_{max} values for the membrane preparations of the human post-mortem brain were calculated. Therefore, a presumable IC_{50} value for BRV had to be used, which was chosen based on data from the literature as 0.08 µM (calculated from homologous competition experiments at human cortex)[72]. Based on this value according to **Equation 17** B_{max} values were estimated to be in the range of 2 to 3 pmol/mg protein. This is comparable with data from literature (3.5 ± 1.2 pmol/mg protein, determined in a saturation experiment of [³H]BRV at human cortex).[72]

To statistically analyze differences in affinity of LEV to tissue from different brain areas and species, the data of the heterologous competition binding experiments LEV versus [³H]BRV (see **Table 6**, last column) were compared by one-way ANOVA with Tukey's test for multiple comparisons. On the whole, no significant differences were obtained among the five examined tissues ($p > 0.05$), except between HP and RS (**, $p < 0.01$) and between HP and M (*, $p < 0.05$). Hence, these experiments suggest slight differences in the affinity of the pyrrolidone ligands between different brain areas and species within an overall range of 0.7 to 2.7 µM.

Consequently, it can be summarized that the above discussed results – as far as comparable experiments have been described in the literature – are in good accordance with published data. Therewith, the pyrrolidone radioligands once more prove to provide reliable and accurate results. Concerning the obtained data it can be concluded that differences in affinity of LEV to (1) different brain areas as well as to (2) tissue from different species are moderate to low. This is largely consistent with (1) the ubiquitous expression of SV2A within the brain and the previously stated similar binding extent of [³H]LEV to different investigated brain regions (hippocampus, cerebellum, cortex)[60] as well as (2) with the high sequence homology of SV2A from different species (compare **Table 9**). This conclusion will be further proven by analysis of membrane preparations from human brain, which was collected *in vivo* during epilepsy surgery (see 3.2.6).

3.2.6 Binding to membrane preparations from human epileptic brain

Epilepsy surgery may be a solution if epileptic seizures prove to be drug-resistant. The primary aim is to achieve freedom from seizures either by removing the brain section from which the seizures originate or – if not possible – by isolating the affected brain area from its surrounding with a series of incisions. Besides pharmacoresistance a further prerequisite is that all seizures evolve within a locally restricted area within the brain, which can be removed without severe impairments. Within this study several brain samples were investigated, which were kindly provided by the Institute of Neuropathology, University Clinic of Bonn. The brain tissue was resected during epilepsy surgery from people with focal pharmacoresistant epilepsy (for more details see 8.3.3). In six of the eight patients (samples 1-4, 6 and 7) selective amygdala-hippocampectomy[190,191] (in sample 7 together with a resection of two thirds of the temporal lobe) was performed. In one patient (sample 5) a tailored lesionectomy of a cavernoma in the frontal lobe was carried out. Sample 8 was resected from a patient suffering from a glioblastoma in the temporomesial region.

These eight brain tissue samples of pharmacoresistant patients were examined by means of competition binding studies of LEV versus [³H]BRV (and versus [³H]LEV). Three of the samples could further be assigned to subgroups comprising patients that had been treated with Keppra® (levetiracetam) and initially either did respond ("responders") or did not respond ("non-responders") to this medication. In this context, the classification "responder" refers to an initial response of at least six months, while the classification "non-responder" describes patients that never exhibited an effect upon Keppra® treatment. The other five tissue samples derived from patients for which no information existed regarding their response to Keppra®, either due to missing data, or because they had not been treated with this drug before. Regarding the different groups of patients it was of particular interest to investigate, whether the affinity of LEV or the number of binding sites was different among the subgroups of patients.
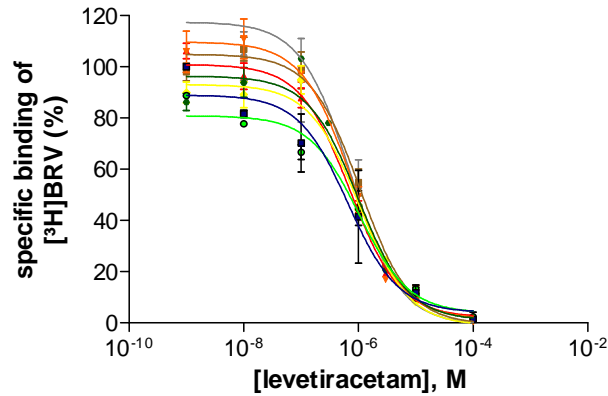
Figure 21: Specific binding of [³H]BRV (1 nM) observed in competition experiments with unlabeled LEV at membrane preparations of different human brain samples obtained by surgery from eight epileptic patients (each shown by a different color). Increasing concentrations of LEV were incubated with membrane preparations (100 µg of protein/well, see **Table 23**) and the radioligand at 4 °C for 240 min. Non-specific binding was determined in the presence of unlabeled LEV (1 mM). All data represent means ± SEM of 2-3 individual experiments performed in triplicate.

Table 7: IC_{50} and B_{max} values of LEV vs. [³H]BRV obtained in competition binding experiments (n = 2-3) at membrane preparations from human brain tissue of people with pharmacoresistant epilepsy. The samples were received by selective amygdala-hippocampectomy (A) in one sample together with a resection of two thirds of the temporal lobe (A/B), by tailored lesionectomy of a cavernoma in the frontal lobe (C), and by resection of a glioblastoma in the temporomesial region (D), respectively. *B_{max} values were calculated assuming an IC_{50} value for BRV of 0.08 µM (based on competition experiments at human cortex);[72] **IC_{50} value determined by a competition experiment of LEV vs. [³H]LEV; nd: no data.

Sample number	Internal code	Tissue type	IC_{50} (µM)	B_{max}* (pmol/mg protein)	Response to Keppra®
1	(TB6883)	A	0.698 ± 0.449	2.5 ± 0.7	not applied
2	(TB6888)	A	1.03 ± 0.07	5.7 ± 0.4	responder
3	(TB6906)	A	0.741 ± 0.102	5.3 ± 0.3	non-responder
4	(TB6863)	A	0.811 ± 0.022	4.3 ± 0.7	not applied
5	(TB6859)	C	1.11 ± 0.06	5.9 ± 1.4	responder
6	(N454/10)	A	1.05 ± 0.09	9.4 ± 1.2	nd
7	(TB5184)	A/B	1.16 ± 0.45	8.8 ± 0.1	nd
8	(TB5257)	D	1.01 ± 0.84 (0.903 ± 0.033)**	6.2 ± 0.2	nd

For all of the eight investigated brain tissue samples highly reproducible competition binding curves could be obtained. Thus, binding of LEV to the target protein SV2A can also be determined in these brain samples of pharmacoresistant patients.

The **IC_{50} values** from the heterologous binding experiments of LEV versus [³H]BRV for all of the eight examined samples ranged from 0.7 to 1.2 µM. These values are comparable to a published K_i value for LEV versus [³H]BRV, which was obtained in a

heterologous competition experiment at human cortex (2.00 µM).[72] Homologous competition experiments (LEV versus [³H]LEV) could only be performed for one sample (sample 8) due to the limited amount of available tissue. From these experiments an IC_{50} value of 0.903 µM was obtained, which is well in agreement with the observed range for IC_{50} values in the heterologous binding experiments (LEV versus [³H]BRV). Moreover, the affinity of LEV for the investigated brain samples all lie within the same range. A statistical analysis of the IC_{50} values obtained from the heterologous competition experiments LEV versus [³H]BRV (see **Table 7**) using a one-way ANOVA with Tukey's test for multiple comparisons revealed that the obtained values show no significant difference ($p > 0.05$). Thus, these experiments demonstrated no differences in the affinity of LEV among the investigated tissue samples, including samples from patients that have been characterized as responder or non-responder to initial Keppra® treatment. Nonetheless, the significance of this study is limited by the small number of samples (including only three patients with characterized response to initial Keppra® therapy) examined so far.

Additionally, the maximal number of binding sites (B_{max}) in these brain samples was calculated as explained above (see 3.2.5). The determined B_{max} values ranged from 2.5 to 9.4 pmol/mg protein. This is on average in the same range as the published B_{max} value obtained in a saturation experiment at human cortex (3.5 ± 1.2 pmol/mg protein).[72] As observed earlier (compare B_{max} values from saturation experiments in 3.2.3), the B_{max} value calculated from the homologous competition experiment with the low affinity ligand [³H]LEV was somewhat lower (1.7 ± 0.3 pmol/mg protein), which may result from the increased dissociative loss during the washing procedure. Overall, these data suggest that differences in the expression level of the target protein (SV2A) might exist among the examined samples. However, this assumption needs to be confirmed with a much larger number of tissue samples. Worth mentioning is the fact that only a marginal difference of B_{max} values was determined between the non-responder (5.3 pmol/mg protein) and the samples of responders (5.7 and 5.9 pmol/mg protein).

It will be required to reproduce and confirm these preliminary data by increasing the number of samples investigated. Especially samples from well characterized patients concerning their response to Keppra® will have to be included in future experiments. Moreover, it should be mentioned that control tissue (in the sense of equivalent brain

samples from healthy humans) is not available for ethical reasons, which limits the control to samples from epileptic patients or tissue as described in 3.2.5. Nevertheless, our preliminary data so far suggest, that a lacking response to Keppra[®] may not be due to altered binding of the drug to its target.

Concerning pharmacoresistance to AEDs two hypotheses have been put forward.[192] The *target hypothesis* states that due to a modification of the target structure (intrinsic or acquired) a drug loses its affinity and consequently its effectiveness. The *transporter hypothesis* suggests that an (intrinsic or acquired) overexpression of multidrug transporters and a resulting increased drug efflux prevents effective concentrations of the drug at the target site in the CNS. One example for the target hypothesis has been described by Remy et al. who showed that carbamazepine is not a substrate for drug transporters, but rather shows drug resistance due to a loss of Na^+-channel sensitivity.[193]

Regarding LEV-resistant epilepsy no data have been published so far, which would support the *target hypothesis* – and this is in agreement with our (preliminary) experimental results. With reference to the *transporter hypothesis* it has to be mentioned that certain published data suggest that LEV (in contrast to several other AEDs) is not a substrate for the human P-glycoprotein (Pgp), a membrane efflux pump belonging to the ABC transporters, which plays an important role in the blood-brain barrier.[194,195] Based on this finding Potschka et al. concluded that this might be one reason why LEV shows efficacy in patients, who did not satisfactorily respond to treatment with other AEDs.[194,196] Contradictorily, other data suggest that LEV is a substrate of Pgp as well as of MRP (multidrug resistance transporter), which only might not have been recognized earlier due to a low substrate affinity.[197] Still, this question has not been answered yet and, moreover, there are other transporters, which have been identified to potentially being involved in drug-resistant epilepsy (e.g. RLIP76, a non-ABC transporter)[198]. Furthermore, besides efflux pumps, transporters have been identified, which are responsible for facilitated brain uptake as described for the AED valproate.[199] According to Potschka et al. a transporter-facilitated brain uptake is also conceivable for LEV since it possesses high hydrophilicity and therefore does probably not penetrate passively into the brain.[194] A downregulation of such transporters could be another reason for pharmacoresistance. However, as suggested by Remy et al., drug resistance is a complex phenomenon, which may be caused by multiple mechanisms.[200]

3.3 Summary

Radioligand binding assays were established and optimized using the radioligands [³H]LEV, [³H]isoBRV and [³H]BRV at rat cortical membrane preparations. In preliminary experiments optimal concentrations of protein and radioligand were determined. Concerning the assay conditions several factors were identified, which have a remarkable influence on the quality of the outcome. Among these was, on the first place, the minimization of dissociation during the washing procedure (dissociative loss) by using ice-cold washing buffer and by keeping the total time of the washing procedure as short as possible.

In association binding experiments the following rank order was found regarding the speed of association: [³H]LEV > [³H]isoBRV > [³H]BRV. Based on these results the incubation times for radioligand binding studies were determined as 120 min for [³H]LEV, 180 min for [³H]isoBRV and 240 min for [³H]BRV.

By means of saturation studies it was shown that all of the three pyrrolidone radioligands showed saturable binding to a single site. K_D values (as a measure of affinity) as well as B_{max} values (maximum number of binding sites) were calculated to be $1.12 \pm 0.18\,\mu M$ and 3.7 ± 0.1 pmol/mg protein ([³H]LEV), 409 ± 23 nM and 10.4 ± 1.2 pmol/mg protein ([³H]isoBRV), and 70.0 ± 8.4 nM and 8.3 ± 1.5 pmol/mg protein ([³H]BRV), respectively.

In competition binding experiments concentration-response curves of LEV versus all of the three pyrrolidone radioligands were determined. Moreover, several compounds known for their ability to compete with potential SV2A ligands were investigated in competition binding experiments versus the radioligands [³H]LEV and [³H]BRV. Data were in agreement with published results. Thus, the present radioligands are appropriate for providing reliable data in competition binding studies. Moreover, [³H]BRV proved to be useful for the screening of compounds that compete with BRV for its binding site. Concerning the radioligands [³H]LEV and [³H]BRV, it can be concluded that both radioligands provide similar results for competing drugs indicating that they are labeling the same binding site. Therefore, [³H]BRV can be considered as a suitable surrogate for [³H]LEV with improved properties.

In further competition experiments the binding of LEV versus the radioligands [³H]LEV and [³H]BRV to membrane preparations of different species and brain areas was

investigated. From the obtained results it can be concluded that, in general, differences in binding affinities between different species and brain areas are moderate to low.

Human brain samples of pharmacoresistant patients obtained from epilepsy surgery were examined by competition binding experiments to determine the affinity of LEV versus the radioligand [³H]BRV. Highly reproducible results were obtained demonstrating concentration-dependent inhibition of radioligand binding by unlabeled LEV. Moreover, preliminary experiments did not show differences between samples classified as initial non-responder and those that initially had been responsive to LEV therapy.

4   [³H]LEV and [³H]BRV binding to recombinant SV2 proteins

4.1   Introduction

In 2004, the binding site of LEV was identified.[61] The fact that LEV binds to the SV2A protein suggested a completely different mechanism of action, which distinguishes this class of pyrrolidone drugs from conventional AEDs. As mentioned above (see 1.3) until today three isoforms of the synaptic vesicle protein are known (SV2A, SV2B and SV2C), which differ by size and sequence as well as their distribution pattern. So far, the precise role of all of the three isoforms of SV2 remains to be elucidated, thus, making it even more difficult to understand how the interaction of LEV with the SV2A protein is translated into an anticonvulsive effect. Additionally, to date there is only little information about amino acids that are essential for the interaction with the pyrrolidone ligands,[100] and a concrete domain of the SV2A protein, which is responsible for this interaction could not be identified yet.

Within this study the radioligands were further characterized by radioligand binding to recombinantly expressed SV2A proteins. Apart from the SV2A protein, its isoforms SV2B and SV2C were recombinantly expressed and examined in binding experiments to verify absence of interaction with the radioligands. Moreover, different mutants (deletion variants and variants with point mutations) were recombinantly expressed and their interaction with the radioligands was investigated to gather further information concerning the potential binding domain of the SV2A protein.

4.2   Molecular cloning and heterologous expression

4.2.1   Constructs of SV2 wild-type proteins

For heterologous expression of the **human SV2A** protein in CHO cells a cDNA clone was commercially acquired (pCMV-hSV2A, see 8.1.3.3). In a first step it was planned to introduce a *green fluorescent protein* (GFP) tag at the C-terminus (3' end). For that reason, while amplifying the sequence by PCR (see **Table 24**; primers: f-hSV2A-ATG-EcoRI, r-hSV2A-SalI; annealing T: 56 °C; elongation t: 135 s), the restriction sites EcoRI (at 5' end) and SalI (at 3' end) were inserted at the same time. The PCR product was then cloned into a pCMV vector containing the GFP sequence. In a second PCR the whole sequence (SV2A with GFP) was amplified (see **Table 24**; primers: f-hSV2A-NotI, r-GFP-BsiWI; annealing T: 60 °C; elongation t: 180 s), while flanking the ends

with a NotI (5' end) and BsiWI (3' end) restriction site. This PCR product was then cloned into the retroviral pQCXIH vector. After verification of the correct sequence (see 8.6.13), the construct was first linearized (see 8.6.11) and subsequently stably transfected into CHO cells via lipofection (see 8.7.6.1 d). Due to the presence of a gene for hygromycin resistance, it was possible to select clones stably expressing the human SV2A protein.

A plasmid containing the **rat SV2A** sequence along with the GFP sequence fused to the C-terminus (pCMV-rSV2A-GFP) was kindly provided by the group of Prof. Dr. S. Schoch. For cloning it into a retroviral vector, the SV2A sequence along with the GFP sequence was first amplified by PCR (see **Table 25**; primers: f-rSV2A-GFP-NotI, r-GFP-BsiWI; annealing T: 62 °C; elongation t: 180 s), attaching the restriction sites NotI (5' end) and BsiWI (3' end) to either end. The corresponding PCR product was cloned into the pQCXIH vector, followed by subsequent verification of the correct sequence (see 8.6.13). The plasmid was used for retroviral transfection of CHO cells (see 8.7.6.2).

The plasmid containing the sequence for the **human SV2B** protein was also provided by the group of Prof. Dr. S. Schoch (pBluescript-hSV2B, see 8.1.3.3). As an initial step, it needed to be fused with GFP at the C-terminus. Therefore, the sequence was amplified by PCR (see **Table 26**; primers: f-hSV2B-ATG-ClaI, r-hSV2B-SalI; annealing T: 56 °C; elongation t: 60 s), introducing ClaI (at 5' end) and SalI (at 3' end) restriction sites at the same time. The PCR product was then cloned into a pCMV vector containing the GFP sequence. After verification of the correct sequence (see 8.6.13) this plasmid was used for transient transfections (see 8.7.6.1 b).

In analogy, the **rat SV2C** sequence that was likewise obtained from the group of Prof. Dr. S. Schoch (pCMV-rSV2C) was cloned into the pCMV plasmid containing the GFP sequence. The conditions for the PCR, during which the restriction sites ClaI (at 5' end) and SalI (at 3' end) were attached, were as listed in **Table 26** (primers: f-rSV2C-ATG-ClaI, r-rSV2C-SalI; annealing T: 56 °C; elongation t: 60 s). After verification of the correct sequence (see 8.6.13), this plasmid was used for transient transfections (see 8.7.6.1 b).

4.2.2 Constructs of rSV2A with deletions of exons 5 and/or 6

Furthermore, variants of the rSV2A protein with deletions of exon 5 and/or 6 were investigated within this study. The variant containing a deletion of exon 5 (pCMV-rSV2Ad5-GFP) and the one that contained deletions of both, exon 5 and 6 (pCMV-rSV2Ad5u6-GFP), were obtained from the group of Prof. Dr. S. Schoch already tagged with the GFP protein at the 3' end (see 8.1.3.3). The variant containing a deletion of exon 6 (pCMV-rSV2Ad6-GFP) was constructed as follows: using the plasmid pCMV-rSV2A-GFP as a template the sequence comprising exons 1 to 5 flanked by the restriction sites EcoRI (at 5' end) and BamHI (at 3' end) was amplified by PCR (see **Table 24**; primers: f-rSV2A-ATG-EcoRI, r-rSV2A-exon5-BamHI; annealing T: 56 °C; elongation t: 160 s). The plasmid pCMV-rSV2Ad5u6-GFP was simultaneously digested with both restriction enzymes EcoRI and BamHI (see 8.6.11). Thus, besides the already deleted exons 5 and 6, also exons 1 to 4 within the SV2A sequence were removed. Subsequently, it was ligated with the obtained PCR product (exon 1 to 5) leading to plasmid pCMV-rSV2Ad6-GFP. All of the three rSV2A deletion variants tagged with GFP at the C-terminus were subsequently cloned into the retroviral pQCXIH vector (see **Figure 22**).
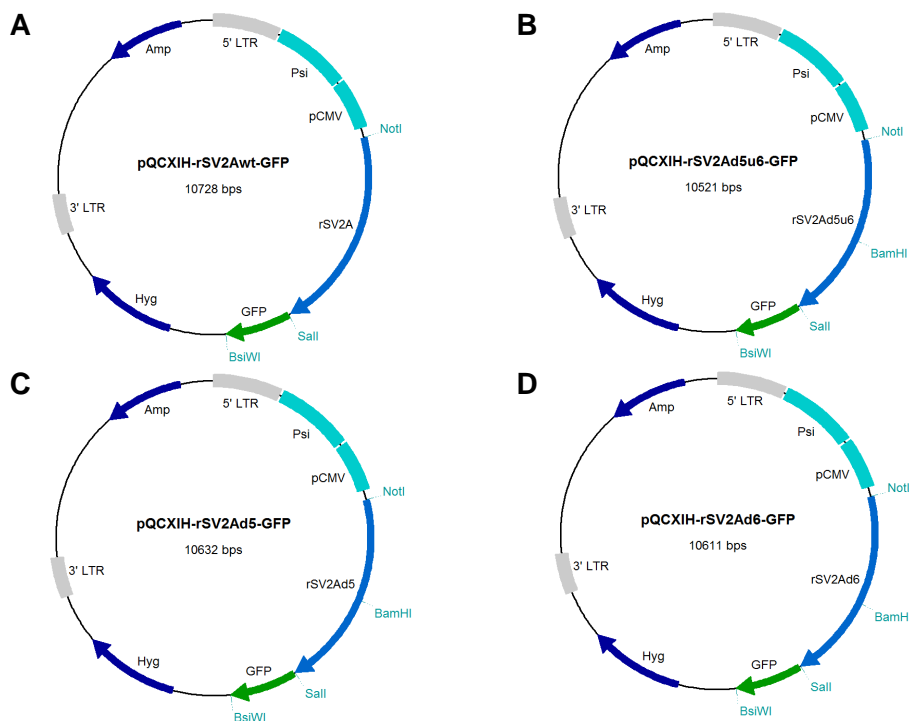
Figure 22: Vector maps of the constructs pQCXIH-rSV2Awt-GFP (**A**), pQCXIH-rSV2Ad5u6-GFP (**B**), pQCXIH-rSV2Ad5-GFP (**C**) and pQCXIH-rSV2Ad6-GFP (**D**). The regions of the packaging signal (Psi), the promoter (pCMV) and the long terminal repeats (5' LTR, and 3' LTR, respectively) are marked by boxes. Arrows indicate positions of genes encoding for the rSV2A variant, GFP and for antibiotic resistance (Hyg: hygromycin B and Amp: ampicillin). Restriction enzymes specified in the maps were used for cloning.

For this purpose, the coding sequence of each variant was amplified by PCR (see **Table 24**; primers: f-rSV2A-GFP-NotI, r-GFP-BsiWI; annealing T: 56 °C; elongation t: 180 s), introducing the restriction sites NotI (5' end) and BsiWI (3' end) to either end. The PCR product of each variant was then cloned into the pQCXIH vector. The correct sequence was verified (see 8.6.13) and the plasmids were applied for retroviral transfection (see 8.7.6.2).

4.2.3   Constructs of rSV2A with point mutations

In addition, variants of the rSV2A protein with point mutations within exons 5 and 6 were investigated by radioligand binding studies. The plasmids containing the mutants tagged with GFP at the C-terminus (see **Table 8** and 8.1.3.3) were constructed and kindly provided by the group of Prof. Dr. S. Schoch.

Table 8: Constructs of rSV2A with point mutations.

	point mutation	substitution	exon
pCMV-rSV2A_N364K-GFP	Asn364 → Lys	polar, uncharged → basic	5
pCMV-rSV2A_H387Q-GFP	His387 → Gln	basic → polar, uncharged	5
pCMV-rSV2A_H387Q_T395I-GFP	His387 → Gln Thr395 → Ile	basic → polar, uncharged polar, uncharged → non-polar	5 and 6
pCMV-rSV2A_T395I –GFP	Thr395 → Ile	polar, uncharged → non-polar	6
pCMV-rSV2A_E403D-GFP	Glu403 → Asp	acidic → acidic	6
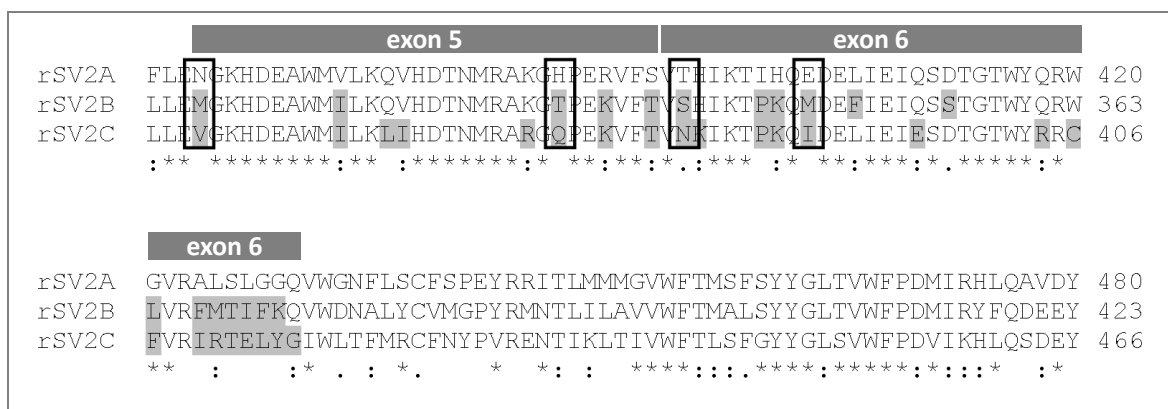
Figure 23: Extract of the sequence alignment (modified from Clustal W, see 8.1.1) of rSV2A, rSV2B and rSV2C, showing exon 5 and exon 6. Amino acids that differ from the SV2A sequence are highlighted in grey. Marked with black boxes are amino acids, which were exchanged by point mutations. Symbols below the sequences mark identical amino acids (*), conserved substitutions / same functional groups (:), and semi-conserved substitutions / similar shape (.).

4.2.4 Transfection method: lipofection versus retroviral transduction

Lipofection

Lipofection describes the lipid-mediated incorporation of nucleic acids into the cell. The first lipid applied was DOTMA (*N*-[1-(2,3-dioleoyloxy)propyl]-*N*,*N*,*N*-trimethyl-ammonium chloride), a cationic compound that forms unilamellar liposomes. After formation of complexes of this lipid with the nucleic acid molecules, the complex is taken up by the cell. The efficiency of the transfection could be improved by combining the cationic lipid molecule with a neutral helper lipid like e.g. DOPE (dioleoylphosphatidylethanolamine), which facilitates the fusion of the liposome with the membrane and therewith allows the entrapped nucleic acid molecules to be released into the cell. Nowadays, several further lipids are applied for lipofection, also nonliposomal compounds that are assumed to form complexes with the nucleic acid. Regarding the exact mechanism of nucleic acid uptake, there are still a lot of uncertainties. Moreover, many commercially available lipofection reagents are of unknown composition (proprietary formulation). However, in general the uptake is believed to proceed either by endocytosis or by fusion with the cell membrane via the lipid moieties of the liposome.[201–204]

Retroviral transfection (transduction)

Strictly spoken transduction does not belong to the transfection methods, because it is a virus-based method. Nevertheless, it is a further method by which nucleic acids can be introduced into eukaryotic cells and therefore it will be discussed at this point.

Viruses are non-living particles, which depend on infecting cells and introducing genetic material. Thus, transduction in general is an extremely efficient technique. Moreover, a lot of viruses integrate their genetic material into the genome of the host cell and hence are valuable tools for the stable expression of recombinant proteins. This is also the case for the murine leukemia virus (MuLV), a retrovirus that was used within this study.
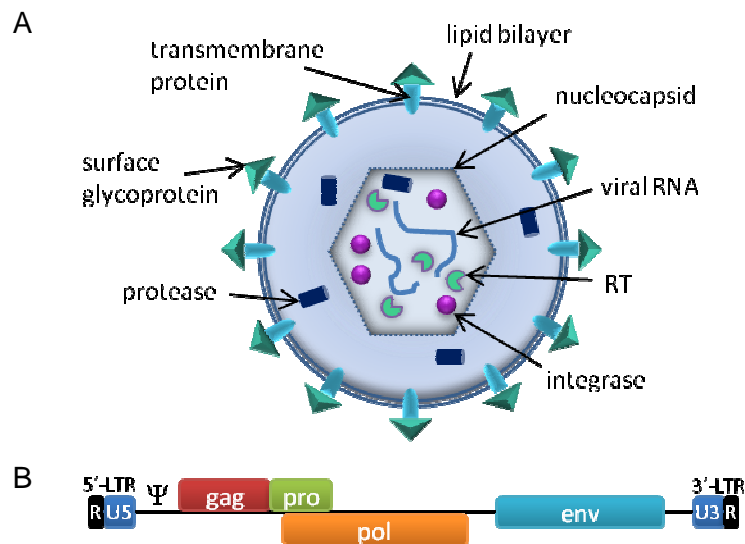
Figure 24: Morphologic structure and part of the genetic sequence from murine leukemia virus. **A:** Cross-section of a virus particle showing the nucleocapsid, which encloses the viral RNA as well as several viral proteins. It is surrounded by a lipid bilayer, which forms the viral envelope containing transmembrane and surface proteins. **B:** Genomic sequence containing regulatory elements and coding regions. gag encodes for capsid proteins as well as the protease. pol encodes RT and integrase. env encodes the transcription unit for the envelope protein. RT: reverse transcriptase, LTR: long terminal repeat, R: direct repeat, U3: 3'-unique sequence, U5: 5'-unique sequence, Ψ: packaging signal, pro: proteinase.

The MuLV is composed of a nucleocapsid, which contains the viral genome – single stranded RNA – as well as viral proteins. It is encompassed by a lipid bilayer, originating from the cell membrane of the host cell. The infectivity of a virus particle depends on several essential proteins, which are either components of envelope and core or responsible for transcription of RNA into DNA as well as for the integration into the host genome. These proteins are encoded by the viral genes gag (core proteins), env (envelope proteins) and pol (reverse transcriptase and integrase), shown in **Figure 24 A**.

A further essential factor is the packaging signal Ψ (psi), which is also encoded within the viral genome. In laboratory practice replication-incompetent viruses are used for safety reasons. These are modified viruses lacking the essential genes for replication, and therefore they cannot replicate outside of so-called packaging cells like e.g. GP[+]envAM-12 cells.
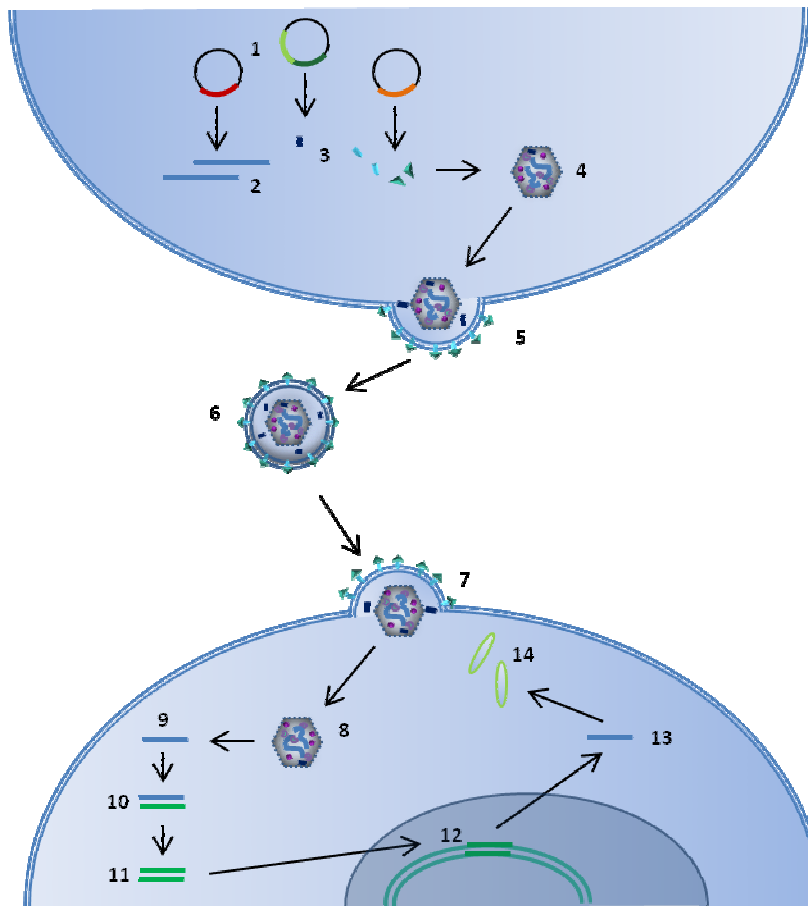
Figure 25: Production of virus particles with a helper cell and transduction of host cell. (**1**) A helper cell possessing plasmids with the env gene (orange) as well as the genes gag and pol (light and dark green) is transfected with a recombinant plasmid containing the gene of interest as well as the packaging signal Ψ (red). After transcription of the viral RNA (**2**) and expression of the viral proteins (**3**), a nucleocapsid is assembled (**4**). By budding the nucleocapsid is coated by a lipid bilayer (**5**) and afterwards released into the medium (**6**). This virus-containing supernatant can then be applied for the infection of host cells. After entry into the cell (**7**), the nucleocapsid (**8**) releases the RNA containing the gene of interest (**9**) followed by reverse transcription into DNA (**10, 11**). The DNA is stably integrated into the host cell genome (**12**) and along with the genome transcribed into mRNA (**13**). Subsequently, it is translated into the gene product and therewith the recombinant protein is expressed (**14**).

The helper cell line GP⁺envAM-12 is an amphotropic cell line deriving from the murine fibroblast (NIH 3T3), which has been transfected with two plasmids that separately encode the env gene of MuLV on one and gag and pol genes on the other plasmid (see **Figure 25**). To ensure that GP⁺envAM-12 cells do not degrade or lose these two plasmids during cultivation, both plasmids possess certain genes: the plasmid with the env gene also holds a gene that encodes resistance against the aminoglycoside hygromycin B, whereas the other plasmid possesses a gpt gene that encodes for xanthine-guanine phosphoribosyltransferase. The presence of hygromycin B, hypoxanthine, xanthine and mycophenolic acid in the culture medium (see **Table 27**, HXM medium) puts the cells under selection pressure, making the two plasmids essential for survival: hygromycin B enforces cells to possess hygromycin resistance.

Mycophenolic acid inhibits the endogenous purine synthesis, whereby only cells that can independently synthesize purines via xanthine-guanine phosphoribosyltransferase are capable of surviving. Thereby, hypoxanthine and xanthine are needed as substrates. Nevertheless, these packaging cells themselves can only produce empty, non-infectious virus envelopes, since they do not possess the genetic information for the packaging signal Ψ. For this purpose, the packaging signal Ψ is transfected (here: via lipofection) along with the gene of interest on the recombinant plasmid, like e.g., pQCXIH or pQCXIN, into the packaging cells. The packaging signal Ψ as well as the multiple cloning site (MCS) containing the gene of interest are flanked by long terminal repeats (LTR). These regions contain promoters and enhancers, as well as the initiation region for reverse transcription. Along with the recombinant plasmid the packaging cells are cotransfected with a plasmid that encodes for the envelope glycoprotein of the vesicular stomatitis virus (VSV-G). By integration of VSV-G proteins into the viral envelope the virus is capable of interacting with any phospholipids on the surface of the host cell and is not dependent on special receptors for docking (pseudotyping). That way, infectious, replication-incompetent virus particles are produced, which are capable of infecting target cells and transduction of genetic material that will be stably integrated into the host cell genome.[205–210]

Choice of transfection method

In general, lipofection belongs to the highly efficient transfection methods allowing transient as well as stable transfection of the nucleic acid molecules. Moreover, it is possible to transfect large inserts. A drawback is the cytotoxic effect of many transfection reagents leading to a decreased viability of the cells. Additionally, lipofection reagents are quite cost-intensive. On the contrary, the retroviral transfection system described above – once established – is a very cost-effective method. Since the applied vectors have the ability to integrate their genome into the host cell genome, a stable expression of the transgene is enabled. Furthermore, high transfection efficiencies can be achieved in a great number of cell lines. The capacity of the virus particle, however, limits the size of the insert to be transfected.

Within this study the first transfection attempts made use of the already established retroviral transfection system with helper cells. However, by control of the transfection efficiency as well as in subsequent experiments only poor expression levels were

determined (see 4.3.4). Since the capacity of retroviruses is limited to an insert size of about 9-12 kb,[211] it seems more than likely that the applied retroviral plasmids including the gene of interest (see e.g. **Figure 22**) exceeded the maximum capacity of the used MuLV and therefore were not sufficiently incorporated into the virus particle. Thus, in subsequent attempts it was decided to perform the transfection step by lipofection. While certain transfections were only done for transient expression of the recombinant protein, lipofection was also applied for stable expression of recombinant proteins. As described by Thomas et al., mammalian cells are capable of integrating exogenous DNA into their genome at random sites by non-homologous or illegitimate recombination.[212] Making use of the resistance gene present in the retroviral vectors (here: hygromycin B in pQCXIH) after lipofection with the corresponding construct, it was possible to subsequently select clones that stably integrated the transfected genes into their genome within an appropriate region. As shown further on by the results of the radioligand binding studies, with this method it was possible to obtain cell lines expressing the recombinant protein with very high expression levels.

4.3   Radioligand binding studies with [³H]LEV and [³H]BRV

In radioligand binding studies, applied for the investigation of recombinantly expressed SV2 proteins, intact cells were used. Therefore, on the day of the experiment, transiently or stably transfected cells were harvested and prepared as described in 8.7.7. Preliminary experiments showed that depending on the type of experiment one or two confluent dishes (152 cm^2) were needed for a 24-well assay. The expression level was controlled by fluorescence (flow cytometric analysis or fluorescence microscopy) emitted by the green fluorescent protein fused to the C-terminus of each recombinantly expressed SV2 variant.

4.3.1   Saturation studies at human SV2A protein

Binding of the radioligand [³H]BRV was investigated in a saturation binding experiment on intact CHO cells transiently expressing hSV2A tagged with GFP at the C-terminus. Therefore, CHO cells were transfected with the pCMV-hSV2A-GFP construct one day before the experiment (see 8.7.6.1 b). On the day of the experiment

for a 24-well assay two confluent dishes were harvested and prepared as described in 8.7.7. Saturation experiments were performed as described in 8.5.3.2.4.
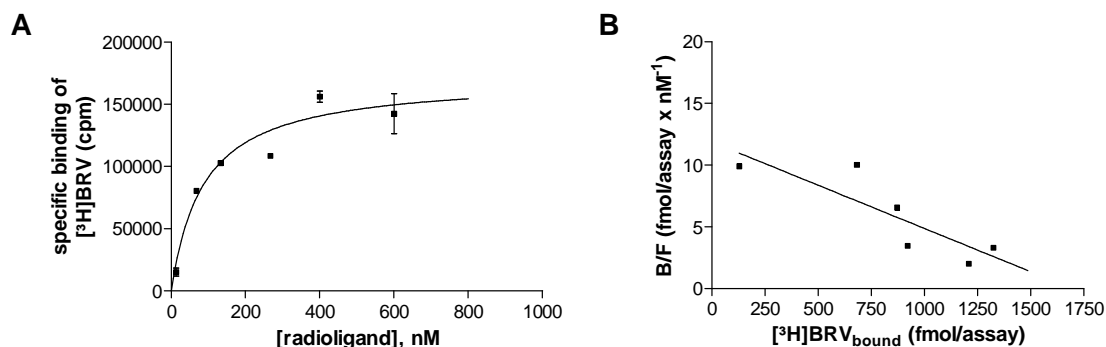
Figure 26, A: Specific binding of [³H]BRV obtained in saturation binding experiments using intact CHO cells transiently expressing GFP-tagged hSV2A protein. Different concentrations of the radioligand were incubated together with the cells at 4 °C for 240 min. Non-specific binding was determined for each radioligand concentration in the presence of unlabeled LEV (1 mM). Depicted in the graph is a representative curve of two single experiments ± SEM performed in duplicate. **B:** Rosenthal plot from transformed data.

The above described saturation experiments revealed a K_D value of **75.1** ± 12.2 **nM**. This is in the range of the data published from similar experiments (saturation experiment of [³H]BRV using intact CHO cells recombinantly expressing hSV2A protein), disclosing a K_D value of 152 ± 40 nM.[72] The obtained value is furthermore consistent with the K_D value (70.0 ± 8.4 nM) that earlier on was determined in saturation studies at rat cortical membrane preparations (see 3.2.3). This demonstrates that the affinity of the radioligand [³H]BRV to its native protein target lies within the same order of magnitude as the affinity to recombinantly expressed hSV2A tagged with GFP at its C-terminus. Taken together, it can be concluded that GFP attached to the C-terminus of the protein does not hinder binding of the radioligand. Regarding the course of the saturation curve, binding to a single site was observed, which is further demonstrated by a Rosenthal plot with transformed data of the saturation experiment (see **Figure 26 B**). This is also in agreement with findings according to the above mentioned published saturation study. A very high transfection efficiency resulting in a high expression level can be deduced from the observed B_{max} value that was determined to be **496000** ± 74000 **binding sites/cell.** This is several fold higher than for instance the stably transfected (retroviral transfection) CHO cells expressing the human A_{2A} or A_{2B} receptors (around 3200 to 3600 binding sites/cell) that are successfully used in our group for other studies (data not shown).

4.3.2 Competition experiments at rat and human SV2A protein

To further characterize the radioligand as well as the recombinantly expressed SV2A wild-type proteins (rat and human) in CHO cells, competition experiments with unlabeled LEV were performed. Binding to transiently expressed rSV2A-GFP and hSV2A-GFP as well as stably expressed hSV2A-GFP was investigated. Transient transfections were performed as described in 8.7.6.1 b) using pCMV-rSV2A-GFP or pCMV-hSV2A-GFP as DNAs. Stable expression of hSV2A-GFP was performed as described in 8.7.6.1 d). On the day of the experiment, two confluent dishes of cells were harvested for one 24-well experiment and prepared as described in 8.7.7. Competition binding experiments were performed as described in 8.5.4.1.1 and **Table 22**/**Table 23**.
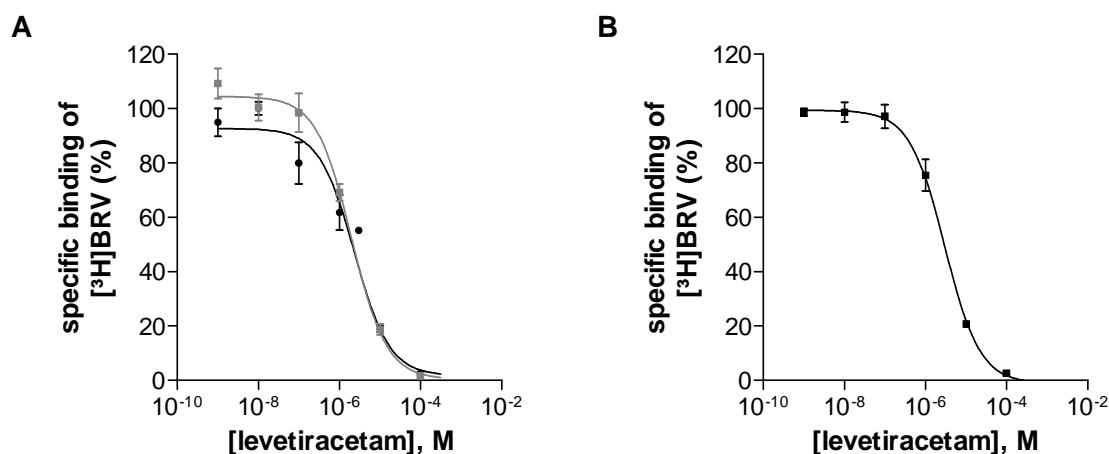
Figure 27: Specific binding of [³H]BRV (1 nM) to recombinantly expressed hSV2A-GFP (**A**) and rSV2A-GFP (**B**) obtained in competition binding experiments with unlabeled LEV. SV2A proteins were transiently (black) or stably (grey) expressed in CHO cells. Increasing concentrations of LEV were incubated with intact cells and the radioligand at 4 °C for 240 min. Non-specific binding was determined in the presence of unlabeled LEV (1 mM). All data are means ± SEM of 3-4 individual experiments performed in triplicate.

The competition experiments provided IC_{50} values for LEV of **2.64** ± 0.53 **µM** (hSV2A-GFP transient), **2.05** ± 0.26 **µM** (hSV2A-GFP stable) and **2.98** ± 0.63 **µM** (rSV2A-GFP transient). Based on **Equation 15** K_i values can be calculated for transiently expressed hSV2A-GFP and rSV2A-GFP (2.61, and 2.95 µM, respectively) in which the K_D value necessary for calculation was taken from the corresponding saturation experiments. Data from a published competition experiment of LEV vs. [³H]BRV at recombinantly expressed hSV2A protein suggest a K_i value of 3.16 µM.[72] With regard to these published data, accuracy of the herein obtained results can be assumed.

Comparing the experimentally obtained IC_{50} values with each other it is apparent that the affinity of LEV does only marginally differ between the recombinantly expressed

SV2A protein from rat and from human. This is in accordance with the high sequence homology between those orthologues (see **Table 9**). It furthermore confirms the results that earlier were determined by investigations of native brain membrane preparations from different species (see 3.2.5) suggesting only moderate to low differences for the affinity of LEV. Hence, these results indicate that data obtained from the rat SV2A protein are very likely transferable to the human SV2A protein.

Table 9: Homology of the amino acid sequence between human and rat SV2 proteins determined with the sequence alignment program Needle (see 8.1.1).

	identity	similarity
SV2A	98.8%	99.6%
SV2B	94.9%	97.7%
SV2C	97.0%	99.0%

4.3.3   Binding to SV2B and SV2C proteins

As outlined in chapter 1.3 two further isoforms of the SV2A protein have been identified. In contrast to SV2A, which is ubiquitously expressed in the brain, these isoforms exhibit more restricted (SV2B) distribution patterns or are found only in very few brain regions (SV2C).[86,87,90,96] Matching the amino acid sequences of these three isoforms with each other (see **Figure 4**), it becomes evident that a high sequence homology exists within TMDs, while non-conserved amino acids are present in main parts of the N-terminus and the luminal loop between TMDs 7 and 8, and to a lower extent also within the cytoplasmic loop between TMDs 6 and 7. In 2004, when SV2A was identified as the binding site for LEV, it was shown that [³H]ucb30889 (used as surrogate for LEV due to higher affinity,[159] see **Figure 8**), only binds to the SV2A isoform, while no binding to the isoforms SV2B and SV2C could be detected.[61] Therefore, it appears that amino acids that are not conserved between those three isoforms must be responsible for the interaction with LEV.

Within this study the interaction of the radioligands [³H]LEV and [³H]BRV with the recombinantly expressed GFP-tagged isoforms SV2B and SV2C was investigated by radioligand binding studies and compared to binding to SV2A-GFP. For this purpose the three isoforms SV2A, SV2B and SV2C (either human or rat) were recombinantly expressed by transient transfection (see 8.7.6.1 d) using pCMV-hSV2A-GFP, pCMV-hSV2B-GFP and pCMV-rSV2C-GFP as DNA. The efficiency of the transfection was

controlled for each cell line by fluorescence microscopy (exemplarily shown for hSV2B-GFP in **Figure 28**). Each SV2 isoform was expressed with the same efficiency with expression levels of approximately 60%.
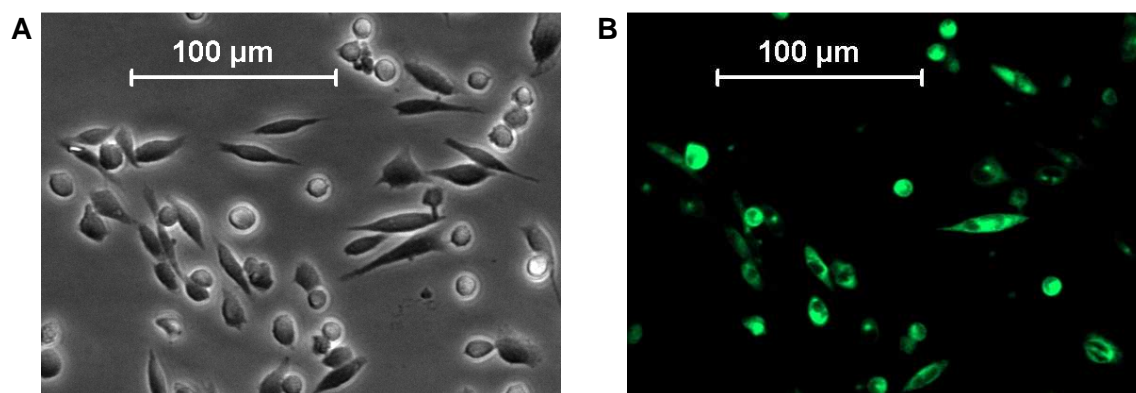
Figure 28: Microscope images of CHO cells transiently expressing recombinant GFP-tagged SV2 protein (here: hSV2B-GFP). **A**: transmitted light; **B**: GFP fluorescence.

On the day of the experiment, the cells were harvested and prepared as described in 8.7.7, in which one confluent dish was used for 12 wells (2 assays, each 6 wells). Binding studies were performed as described in 8.5.4.1.1 and **Table 21**.
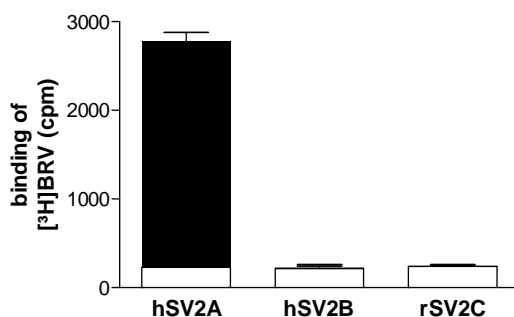
Figure 29: Binding of [³H]BRV to CHO cells transiently transfected with GFP-tagged hSV2A, hSV2B and rSV2C. Cells were incubated with [³H]BRV (1 nM) for 240 min at 4 °C. Non-specific binding (open bars) was determined in the presence of unlabeled LEV (1 mM). Specific binding (black/grey bars) was obtained by subtraction of non-specific binding from total binding, which was determined in the absence of unlabeled LEV. Data depicted in the graph show one representative of three individual experiments performed in triplicate; shown are means ± SEM.

The obtained data demonstrate very clearly the difference in binding of [³H]BRV to the three SV2 isoforms: as shown in **Figure 29** specific binding was reduced from 2550 cpm (SV2A) to about 15 cpm (SV2B and SV2C), which definitely falls below the limit of reliable signals. Binding in percentage was determined as hSV2A (92 ± 0%) compared to the proteins hSV2B (7 ± 3%) and rSV2C (5 ± 1%). Considering that also non-transfected CHO cells, which do not express SV2A proteins provide fluctuating

values for specific binding of 0-5% that – due to a very low absolute detected signal (in cpm) – must be considered neglectable, the detected specific binding to SV2B and SV2C isoforms can be interpreted as irrelevant. In an analogous experiment performed with the lower-affinity ligand [³H]LEV (data not shown) comparable results were obtained (specific binding of [³H]LEV in percent was $31 \pm 2\%$ at hSV2A, $0 \pm 0\%$ at hSV2B and $0 \pm 0\%$ at rSV2C). Thus, these results reveal likewise for [³H]LEV that the pyrrolidone drugs do not interact with those isoforms. Due to the remarkably high sequence homology between the orthologues of different species (human vs. rat, see also **Table 9**), which is $> 95\%$ for each of the three isoforms, it can be assumed that no different result would have been obtained for the human SV2C isoform. Consequently, these data support the finding that no binding of LEV and its analogues occurs to the lower-abundant isoforms SV2B and SV2C.

4.3.4   Binding to rat SV2A variants with deleted exons 5 and/or 6

As mentioned before, very recently the first study was published, which led to the identification of several amino acids of the SV2A protein that appeared to be essential for the interaction with pyrrolidone ligands.[100] In the study that combined modeling and mutagenesis experiments (based on a comparison with the structurally related transporter proteins lactose permease LacY, rat organic cation transporter 1, and human organic anion transporter 1 and 2) several positions in the SV2A protein, which correspond to functional residues in those related transporter proteins, were mutated (see **Figure 35**). Since the related transporter proteins – in contrast to the SV2A protein – do not possess long TMD-connecting loops, the examined mutations were mainly limited to regions of TMDs. Critically viewed must be the fact that the radioligands applied for investigations of the mutants (e.g. [³H]ucb30889, see **Figure 8**) differ structurally from the compounds of interest LEV and BRV: the rather bulky, aromatic phenyl-residue may exert different interactions than the AEDs LEV and BRV. Furthermore, it is debatable if functional residues of the related transporter proteins automatically represent important residues within the SV2A protein, which does not function as a transporter anymore.

In an attempt to further contribute to the identification of the pyrrolidone binding site within the SV2A protein, additional mutational approaches were performed in the present study. In contrast to the above mentioned approach we focused on the sequence

encompassing exons 5 and 6 (see **Figure 35**). This region mainly constitutes the long loop between TMDs 6 and 7, which is protruding into the cytoplasm. Like the N- and C-termini, this loop sequence might have a functional role in protein interactions and thus could potentially be modulated by interactions with small molecules. To further investigate this hypothesis, deletion variants of the rSV2A protein in which either exon 5 or 6 or both exons were deleted, were recombinantly expressed and investigated.

Initially, radioligand binding experiments were performed with CHO cells that were stably transfected with the deletion variants by retroviral transfection (see 8.7.6.2). However, with these cell lines no analyzable results could be obtained, since the observed transfection efficiencies and thus expression levels were very low. Therefore, CHO cells were transiently transfected (as described in 8.7.6.1 b) with the deletion variants as well as with rSV2A wild-type using the plasmids pCMV-rSV2Ad5u6-GFP, pCMV-rSV2Ad5-GFP, pCMV-rSV2Ad6-GFP, and pCMV-rSV2A-GFP, respectively. As verified by flow cytometric analysis, thereby much higher expression levels were achieved (see **Figure 30**).
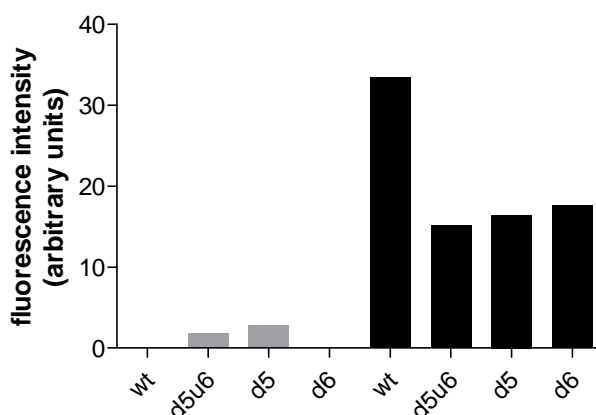
Figure 30: Fluorescence intensity (arbitrary units) as detected by flow cytometric analysis of CHO cells stably (grey) and transiently (black) transfected with GFP-tagged rSV2A wild-type (wt) and deletion variants with deleted exons 5 and 6 (d5u6), exon 5 (d5), and exon 6 (d6). Columns show the fluorescence intensities (geometric mean of analyzed sample) of each cell line without the autofluorescence, which was determined with non-transfected cells.

On the day of the experiment, transiently transfected cells were harvested and prepared for the binding studies as described in 8.7.7. Binding experiments were performed as described in 8.5.4.1.1 and **Table 21** using cells from one confluent dish for 12 wells (2 assays, each 6 wells).
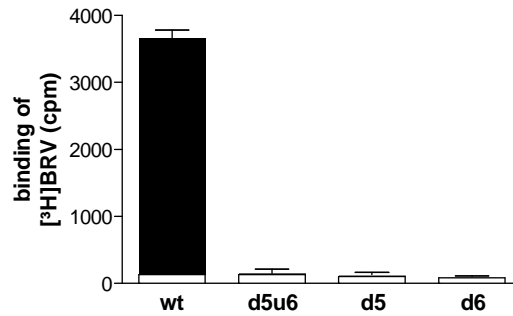
Figure 31: Binding of [³H]BRV to CHO cells transiently transfected with GFP-tagged rSV2A wild-type (wt), variant with deletion of exon 5 and 6 (d5u6), variant with deletion of exon 5 (d5), and variant with deletion of exon 6 (d6). Cells were incubated with [³H]BRV (1 nM) for 240 min at 4 °C. Non-specific binding (open bars) was determined in the presence of unlabeled LEV (1 mM). Specific binding (black/grey bars) was obtained by subtraction of non-specific binding from total binding, which was determined in the absence of unlabeled LEV. Data depicted in the graph show one representative of three individual experiments performed in triplicate; shown are means ± SEM.

Figure 31 very clearly illustrates the remarkable change in specific binding of [³H]BRV to rSV2A variants with deletions of exons 5 and/or 6 compared to the wild-type protein: specific binding in cpm decreases from 3500 cpm (wt) to less than 30 cpm (deletion variants). The remaining detected binding to the deletion variants, which definitely falls below the limit of reliable detection, can be considered as irrelevant. Thus, it can be concluded that no binding occurs to the rSV2A variants with deletions in exon 5 and/or exon 6.

As can be deduced from **Figure 30** the transfection efficiency for cells transiently expressing the rSV2A wild-type variant was determined to be about twice as high as for the deletion variants. Nevertheless, also cells that were transfected with the rSV2A deletion variants still exhibited relatively high expression levels. Thus, regardless of the obtained transfection efficiency if the investigated deletion variants presented a target site for [³H]BRV binding, at least specific binding in percentage should not have decreased in such a drastic manner.

Taken these results together, it can be summarized that [³H]BRV loses its affinity to recombinantly expressed rSV2A variants if deletions of exons within the cytoplasmic loop (between TMDs 6 and 7) are present. Therewith, these results suggest that exon 5 as well as exon 6 play an essential role for the interaction of BRV with the SV2A protein.

Nonetheless, certainly those results have to be interpreted with caution. By deletion of exons 5 and 6 a region of the protein is removed, which encompasses 67 amino acids.

Since the tertiary structure of a protein can be severely impaired by such interventions, it cannot be excluded that the removal of such a long region causes different folding resulting in an altered conformation of the protein. This in turn might lead to a limited access of a ligand to its binding site or a significant change of the binding site. Thus, the interaction of a ligand with its target site might be hindered even if a region apart from exons 5 and 6 is responsible for the binding. In subsequent investigations it is necessary to circumvent this potential problem. To examine exons 5 and 6 as region that potentially is involved in the interaction with the pyrrolidone ligands one approach would be to insert point mutations in positions of amino acids, which are likely to be involved in binding interactions (see 4.3.5). Thereby, occurring changes within the protein structure can be expected to be less marked.

Excursus: Subcellular localization of recombinantly expressed SV2 proteins
To investigate the localization of the recombinantly expressed SV2 proteins the cells were examined by fluorescence microscopy. The observation of the fluorescence excited by the GFP-tagged SV2 proteins confirmed that the subcellular localization was identical for each of the recombinantly expressed SV2 isoforms and SV2A mutants investigated in this study (exemplarily shown for GFP-tagged rSV2A and hSV2B in **Figure 32**).
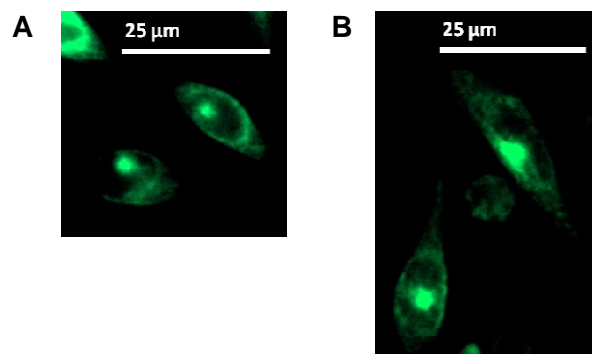
Figure 32: Fluorescence images of CHO cells transiently transfected with rSV2A-GFP (**A**), and hSV2B-GFP (**B**), respectively.

Based on these investigations it appears that the recombinantly expressed GFP-tagged SV2 proteins were mainly located intracellularly and a smaller number was present in the cell membrane of the transfected CHO cells.

4.3.5 Binding to rat SV2A variants with point mutations in exon 5 and 6

Keeping the focus on exons 5 and 6 as a region that potentially might be involved in the interaction with the pyrrolidone drugs, variants of GFP-tagged rSV2A with point mutations within exons 5 and/or 6 were investigated. The choice of positions where point mutations were placed was based on non-conserved amino acids that differ between the sequence of SV2A and its isoforms (see **Figure 23** and **Figure 35**). Since no binding of LEV and its pyrrolidone analogues occurs to the SV2B and SV2C isoform (see 4.3.3 and literature[61,72]), it can be assumed that non-conserved amino acids must play a major role for the interaction with the pyrrolidone drugs.

For radioligand binding studies CHO cells were transiently transfected (see 8.7.6.1 b) with mutants of pCMV-rSV2A-GFP (see **Table 8**). Prior to harvesting of the cells, the expression level was controlled for each cell line by fluorescence microscopy, which always proved to be about 60%.

On the day of the experiment, cells were harvested and prepared as described in 8.7.7, using two confluent dishes for a 24-well assay. Competition binding studies were performed with LEV versus [³H]BRV (see 8.5.4.1.1 and **Table 22**).
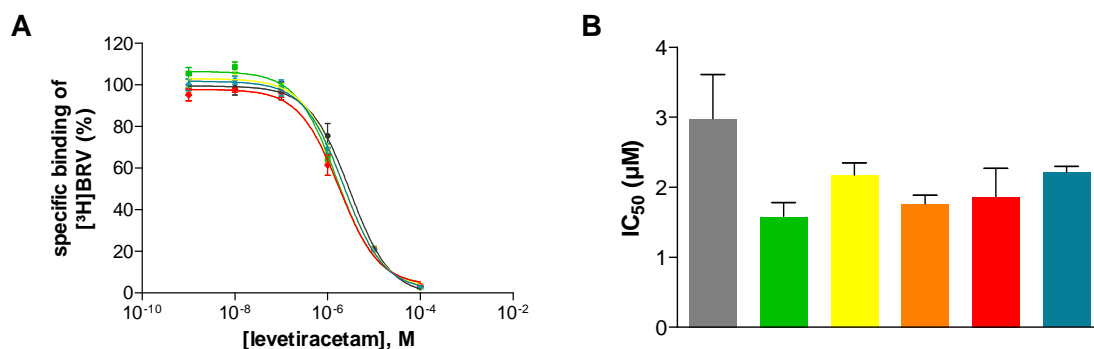
Figure 33 A: Specific binding of [³H]BRV (1 nM) to transiently expressed rSV2Awt-GFP (grey), rSV2A_N364K-GFP (green), rSV2A_H387Q-GFP (yellow), rSV2A_H387Q_T395I-GFP (orange), rSV2A_T395I-GFP (red) and rSV2A_E403D-GFP (blue) obtained in competition binding experiments with unlabeled LEV. Increasing concentrations of LEV were incubated with intact CHO cells expressing the corresponding SV2A mutant and with radioligand at 4 °C for 240 min. Non-specific binding was determined in the presence of unlabeled LEV (1 mM). All data are means ± SEM of 3 individual experiments performed in triplicate. **B:** IC_{50} values of LEV obtained in competition experiments versus [³H]BRV on rSV2A-GFP wild-type and point mutations (for color code refer to **A**). The columns show the mean IC_{50} values ± SEM of 3 independent experiments performed in triplicate.

Table 10: IC_{50} values of LEV vs. [³H]BRV to recombinantly expressed rSV2A wild-type protein and variants with point mutations.

	IC_{50} (μM)
pCMV-rSV2A-GFP	2.98 ± 0.63
pCMV-rSV2A_N364K-GFP	1.58 ± 0.20
pCMV-rSV2A_H387Q-GFP	2.17 ± 0.17
pCMV-rSV2A_H387Q_T395I-GFP	1.77 ± 0.12
pCMV-rSV2A_T395I –GFP	1.86 ± 0.41
pCMV-rSV2A_E403D-GFP	2.21 ± 0.08

As can be deduced from the competition experiments (see **Figure 33**), LEV exhibits quite similar affinity to all of the observed rSV2A variants, regardless if wild-type or mutant. The most aberrant change in affinity compared with the wild-type protein was obtained for mutant N364K. In order to assess the extent of these differences, a statistical analysis was performed applying a one-way ANOVA with Dunnett's test for multiple comparisons, in which the IC_{50} value obtained from the wild-type protein was used as control data to which the IC_{50} values of each mutant were compared. For none of these comparisons a statistically significant difference was found ($p > 0.05$). Hence, it can be concluded that the observed point mutations do not alter the affinity of LEV to its SV2A binding site. To further confirm these results, it was decided to compare the mutant with the largest change in affinity (pCMV-rSV2A_N364K-GFP) to the wild-type protein by means of saturation binding studies (see 4.3.6).

4.3.6 Saturation experiments with rat SV2A wild-type and mutant N364K

Binding to the rSV2A variant with mutation N364K, which exhibited the largest difference in the IC_{50} value of LEV in competition experiments (see 4.3.5), was investigated by means of saturation binding studies using [³H]BRV. Therefore, CHO cells were transiently transfected (see 8.7.6.1 b) with pCMV-rSV2A-GFP, and pCMV-rSV2A_N364K-GFP, respectively. On the day of the experiment, cells were harvested and prepared as described in 8.7.7, using one confluent dish for a 24-well assay. Saturation experiments were performed as described in 8.5.3.2.4.
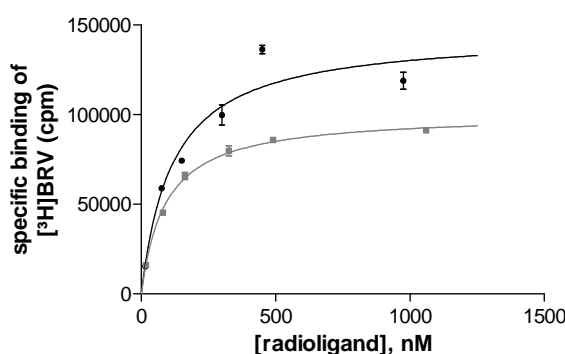
Figure 34: Saturation binding curves of [³H]BRV to intact CHO cells transiently transfected with GFP-tagged rSV2Awt-GFP wild-type (black) and rSV2A_N364K-GFP mutant (grey). Different concentrations of the radioligand were incubated together with the cells at 4 °C for 240 min. Non-specific binding was determined for each radioligand concentration in the presence of unlabeled LEV (1 mM). Each curve is a representative of two independent experiments performed in duplicate.

	K_D (nM)	B_{max} (binding sites/cell)
rSV2A-GFP	106 ± 11	510000 ± 53000
rSV2A_N364K-GFP	87 ± 3	497000 ± 74000

The results of the performed saturation binding studies illustrate that basically no difference exists between the wild-type and mutated protein concerning the affinity of [³H]BRV. Both K_D values fall within the same range. Therewith, it can be concluded that small differences observed within the competition experiments (see 4.3.5) can truly be considered as non-significant.

Consequently, the pyrrolidone ligands do not show altered binding behavior to the rSV2A variants possessing point mutations within exon 5 and/or 6, which have been investigated within this study. Hence, these results allow the conclusion that the positions of the examined point mutations do not influence a potential binding site and

thus are not essential for the interaction of the pyrrolidone ligands with the SV2A protein. However, there are several issues that have to be considered. First of all, the point mutations have been created with exchange of a defined amino acid randomly against another amino acid. Thereby, also functionalities of amino acids have been exchanged randomly (compare **Table 8**). This, after all, makes it impossible to interpret if an observed or non-observed effect is due to a change in the functionality of the amino acid, since too many variables are changed at the same time. It would be much easier to interpret an effect caused by systematic exchange, e.g. always against a neutral amino acid like alanine. Moreover, it is also evident that starting with an approach by which single amino acids are exchanged in a sequential manner might serve less likely for the identification of essential amino acids. In this context, it would rather be reasonable to exchange all of the non-constitutive amino acids within exons 5 and 6 against the corresponding amino acid present in the isoform SV2B or SV2C. Since it is known that LEV and its pyrrolidone analogues do not bind to these isoforms, it would be very interesting to observe how binding will be changed to such a mutant. Following this strategy, the potential of altering the conformation of the investigated protein could be reduced in comparison to complete deletion of the region comprising exons 5 and 6.
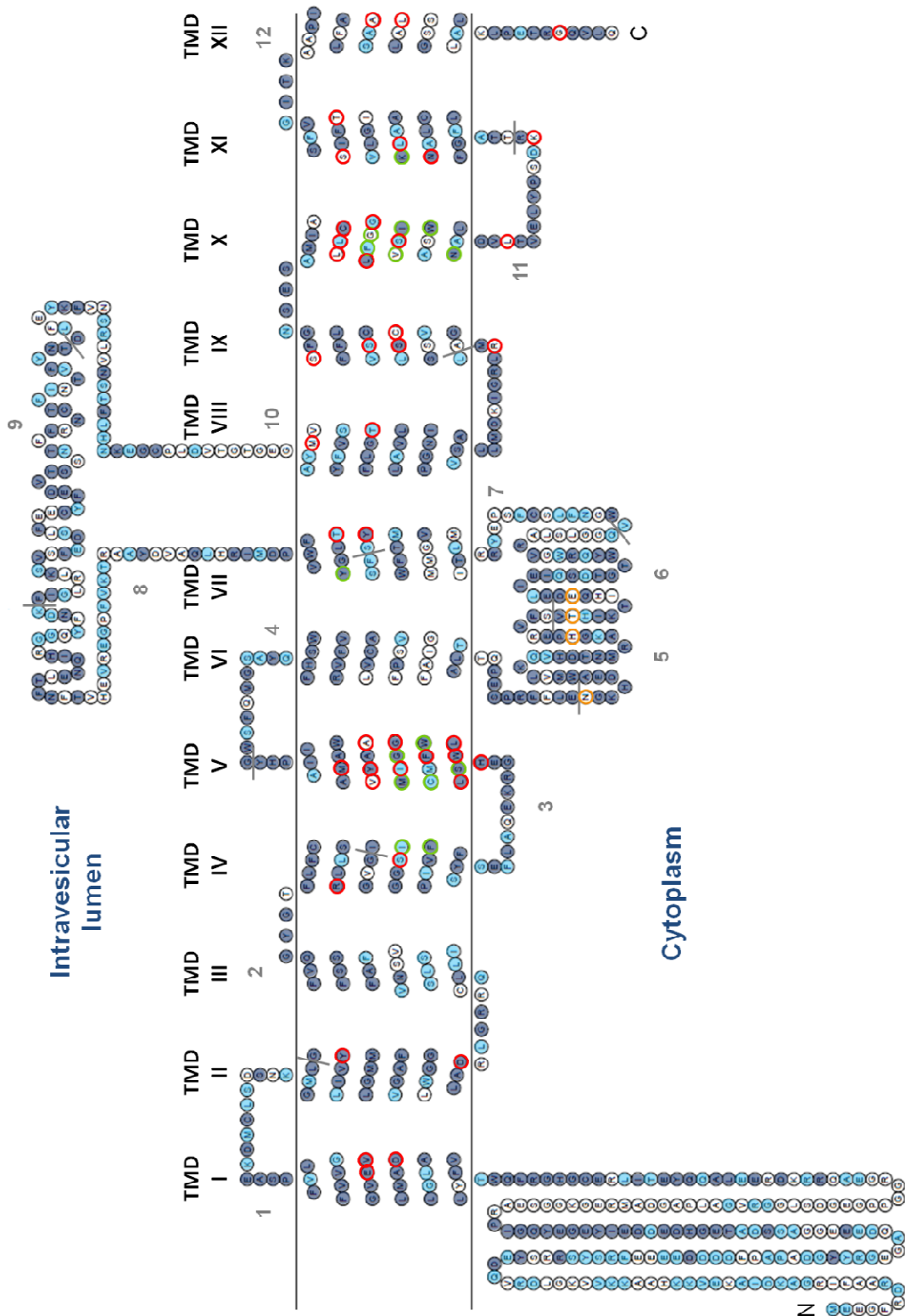
Figure 35: Topology model of the rat SV2A protein. The snakeplot diagram was drawn with TOPO2 with prediction of transmembrane domains based on TMHMM software[93,94] (see 8.1.1). Transmembrane domains are numbered TMD I to XII, exons are numbered in grey Arabic numbers from 1 to 12 and separated by lines, N- and C-termini are labeled with the corresponding letters. Amino acids colored in dark blue represent residues that are conserved among all three isoforms (SV2A, SV2B and SV2C), light blue colored ones are conserved in one other isoform besides SV2A, and white colored ones are non-conserved and only present in the SV2A isoform. Amino acids that were mutated in the study of Shi et al.[100] are circled in red (no change in ligand binding), and in green (altered ligand binding), respectively. Amino acids that are marked with a yellow circle were mutated and investigated in this study.

4.4 Summary

Molecular cloning and heterologous expression

For the investigation of the SV2 protein by binding studies to the recombinantly expressed protein, several different cDNA clones were obtained. SV2 wild-type cDNA clones were received of each isoform (A, B and C) representing either the human and/or the rat sequence. All of these sequences initially needed to be tagged with a GFP at the 3' end and, as fusion proteins, afterwards were cloned into a suitable vector for transfection. Moreover, plasmids containing sequences of rSV2A with deletions in exon 5 and/or 6 and a GFP-tag fused to the 3' end were acquired or constructed. Likewise, constructs with point mutations in exon 5 and/or 6 of rSV2A were provided, which were already tagged with GFP at the 3' end.

In order to introduce the genetic information into the target cell (transfection), initially it was planned to make use of a retroviral transfection. Therefore, the sequences of the genes of interest had to be cloned into a retroviral vector (here: pQCXIH). However, since the sizes of the constructs most likely exceeded the limit of the virion capacity, the target cells were not transfected with high efficiency. Thus, only very low expression levels were achieved. This problem was circumvented subsequently by transfecting the cells by lipofection. Thereby, cells were either transiently transfected (using the pCMV plasmid containing the gene of interest) and used directly for binding studies or stably transfected (using the pQCXIH plasmid containing the gene of interest in its linearized form) by a subsequent selection phase of stable clones.

Radioligand binding studies with [³H]LEV and [³H]BRV

By means of saturation binding studies, the affinity of [³H]BRV to recombinantly expressed hSV2A-GFP was investigated. The obtained K_D value corresponds well to the K_D value, which was obtained by saturation studies at rat cortical membrane preparations and therewith represents the affinity as determined in native tissue. Moreover, this value is comparable with a published K_D value from a saturation experiment at recombinantly expressed hSV2A protein. This allows the conclusion that the GFP, which is fused to the C-terminus of the protein, does not impair the binding of the pyrrolidone radioligand. In these assays high B_{max} values were determined, which

demonstrates a successful transfection of the CHO cells, yielding to high expression levels.

Heterologous competition experiments of LEV versus the radioligand [³H]BRV were performed to compare the binding behavior of LEV to recombinantly expressed SV2A proteins (rat and human). Within these experiments it was shown that no differences exist in the affinity of LEV between human and rat SV2A protein. This is consistent with the high sequence homology of these orthologues and furthermore suggests that results obtained from investigations on the rat protein are most likely transferable on the human protein.

Two further isoforms besides SV2A are known (SV2B and SV2C), which were investigated within this study. Using GFP-tagged recombinantly expressed hSV2B and rSV2C protein, it could be shown that no binding of the pyrrolidone radioligands occurs to either one of that isoforms.

Furthermore, investigations were made to elucidate potential domains of the SV2A protein, which might be involved in the interaction with LEV and its analogues. Looking at its domain structure (see **Figure 4**) the long loop between TMDs 6 and 7 (containing exons 5 and 6) was chosen to be examined, since it is protruding into the cytoplasm and might potentially interact with modulatory proteins. Additionally, it contains several non-conserved amino acids and thus differs from the loops of the isoforms SV2B and SV2C, which do not represent targets for LEV and its analogues. Three deletion variants of rSV2A-GFP were recombinantly expressed in which exons 5 and/or 6 were deleted. By means of radioligand binding studies it could be shown that the radioligand [³H]BRV does not bind to either one of the variants. As a preliminary conclusion this allows to assign to exons 5 and 6 an essential role in the interaction with the pyrrolidone ligands. However, it should further be considered that a deletion of exon 5 and/or exon 6 might lead to a major change in the protein's conformation. Therewith, it could also be conceivable that an evoked conformational change simply hinders the accessibility or changes the structure of a target site, which after all does not lie within exons 5 and 6.

Further focus was put on mutants of the rSV2A protein, in which non-conserved amino acids within exons 5 and 6 were exchanged by point mutations. This mutational approach – in contrast to deletion of whole regions – would less likely lead to severe

conformational changes of the protein. Five different mutants were provided (N364K, H387Q, H387Q/T395I, T395I, E403D) that were investigated within this study. The examination of the binding behavior of LEV versus [³H]BRV to these recombinantly expressed proteins in competition experiments revealed merely marginal differences. A subsequently performed saturation experiment of [³H]BRV, in which the mutant with the largest difference was compared to the wild-type variant, revealed affinities in the same order of magnitude. Therewith, it can be concluded that the obtained SV2A mutants, which were investigated within this study, do not evoke altered binding of the pyrrolidone ligands. Thus, the results suggest that the selected positions are not essential for the interaction with the pyrrolidone ligands – though, within the constraints discussed above.

As depicted in **Figure 23**, several further positions (besides the investigated residues) exist, in which the amino acid sequence is not conserved. Within these 12 further positions SV2B as well as SV2C possess amino acids that are different from those present in the SV2A isoform. For definite clarification of this matter it would be interesting to further analyze binding to rSV2A mutants in which all non-conserved amino acids in this loop are exchanged for those present in the isoforms SV2B or SV2C at the same time.

5 Binding to AMPA receptors

5.1 Introduction

Several years after the discovery of the SV2A protein as the binding site for LEV,[61] its mode of operation as well as the exact role of SV2A in transmitter release still remains to be elucidated. This certainly complicates the understanding of LEV's mode of action as an antiepileptic drug (AED). Concerning SV2A as a potential target for anticonvulsive agents, there is one main issue that still raises questions: since the SV2A protein, which is ubiquitously present in synaptic vesicles, is involved in excitatory as well as inhibitory neurotransmission, it is not apparent how the interaction of LEV can be exclusively translated into an anticonvulsive effect. Thus, it cannot be excluded that SV2A is not the main and/or not the only target structure of LEV and that further protein targets contribute to or are even responsible for its anticonvulsive effect. Bidlack and Rasheed supported this hypothesis by stating that LEV also directly interacts with AMPA receptors (AMPARs): based on an observed competitive binding behavior of different allosteric AMPAR modulators (obtained against [³H]LEV), they postulated that LEV binds to an allosteric modulator site on AMPARs.[115] Already earlier on an interaction of LEV with AMPARs was described in patch-clamp recordings using cultured cortical neurons: Carunchio et al. demonstrated that LEV significantly decreases AMPA-induced currents and hence, concluded that LEV interacts with certain AMPAR subunits.[83] On the other hand, Lee et al. suggested that an observed effect of LEV on the glutamate system is evoked presynaptically (by modulation of P/Q-type voltage-dependent Ca^{2+}-channels) leading to reduced glutamate release.[213] So far this issue has not been clarified yet. In any case, the structural similarity of LEV to its analogues piracetam and aniracetam (see **Figure 17**) would support the finding of Bidlack et al. that LEV could directly interact with AMPARs: piracetam and aniracetam bind to AMPARs at different allosteric binding sites, which are located at the dimer interface of the receptor complex. Based on crystal structures of piracetam with the AMPAR subunits GluR2 and GluR3 Ahmed et al. determined that the amide group as well as the carbonyl oxygen atom of the pyrrolidone ring participate in the interactions that are essential for the binding.[214] Based on these findings, it is conceivable that the structurally related compound LEV and its analogues likewise could interact with AMPARs.

In order to investigate this issue, in the present study potential direct binding of the pyrrolidone radioligands to AMPARs was investigated. For this purpose, AMPARs were recombinantly expressed in HEK cells, which were applied for radioligand binding studies. Since AMPARs can be composed in multiple ways by assembling different subunits in homomeric or heteromeric combinations, a representative subunit was chosen. For the reasons stated above (see 1.4.3), the GluR2 subunit was selected and applied for the expression of homomeric receptors. Regarding the interaction of the pyrrolidone compounds aniracetam and piracetam with the AMPAR essential amino acids have been identified, which contribute to the binding interaction.[214] These amino acids in parts are also located within the region encompassing the flip/flop sequence, hence, it was chosen to include both isoforms within this study. For all data shown in the following chapters that were experimentally determined within the present study, the radioligand [³H]AMPA and the non-labeled compound AMPA were both applied as racemic mixtures.

5.2 Binding of [³H]AMPA to native proteins in membrane preparations

5.2.1 Establishment of binding assays for [³H]AMPA

In order to characterize recombinantly expressed AMPARs, the radioligand [³H]AMPA (racemic mixture) was purchased. As an initial step, it was necessary to establish valid and reproducible binding assays, which are suitable for the evaluation of its binding properties. For this purpose, binding to membrane preparations of native brain tissue (rat cortex) was investigated, therewith establishing an assay system in analogy to formerly published binding studies.[215–218] Preliminary experiments revealed that the radioligand binding assay using [³H]AMPA is quite sensitive concerning the experimental conditions, which subsequently had to be optimized in a series of experiments.

One definite confounder is the **presence of glutamate**, which might still be present in the prepared membrane suspensions (according to 8.3.1 and 8.3.2), deriving from endogenous stores. Since binding of the radioligand [³H]AMPA would be significantly reduced by glutamate in a competitive manner, it is necessary to additionally wash and sonicate membrane preparations applied for studies with [³H]AMPA.

Concerning the influence of **repeated freezing and thawing cycles** of the membrane preparations (as well as preparations of cells recombinantly expressing AMPARs) on [³H]AMPA binding, contradictory information has been published.[215,216,219] Therefore, membranes were always treated in the same way: after production of membrane preparations as described in 8.3.1 and 8.3.2, aliquots were shock-frozen and stored at -80 °C. On the day of the experiment, the required aliquots were thawed, treated as described in 8.3.4 and directly used for the experiment without further freezing/thawing cycles. For later on performed experiments with recombinantly expressed AMPARs, cells were always harvested and prepared as described in 8.7.8 on the day of the experiment, thereby avoiding any freezing and thawing.

A lot of studies are published concerning the **influence of different anions** in the incubation buffer. Especially the chaotropic anion thiocyanate appears to have a large effect on [³H]AMPA binding and is suggested to be essential for investigations of [³H]AMPA binding to receptors in brain membranes.[216,217,220–222] The presence of thiocyanate clearly stimulates binding of [³H]AMPA, which is supposed to be caused by enhanced receptor desensitization.[223] Preliminary binding assays revealed results that underline these findings and thus the importance of the presence of KSCN in the incubation buffer: as demonstrated in **Figure 36** KSCN clearly enhanced the binding of [³H]AMPA by a factor of 3 to 4 (**A**) with an increase of specific binding from ca. 30% to ca. 70% (**B**).
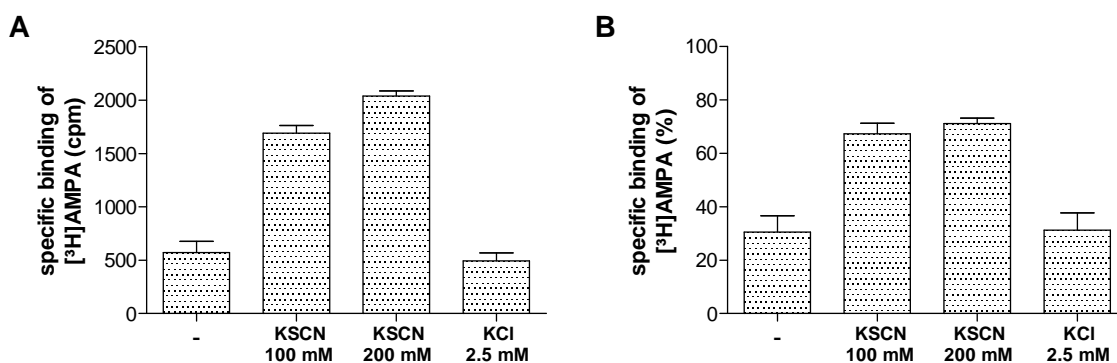
Figure 36: Specific binding of [³H]AMPA (50 nM) to rat brain cortical membrane preparations in the presence of different incubation buffer additives. The radioligand and membrane preparations (300 µg of protein/well) were incubated for 30 min at 4 °C in Tris-HCl buffer (50 mM, pH 7.4) in the presence of KSCN (100 or 200 mM), KCl (2.5 mM) or without additions of further salts (-). Non-specific binding was determined in the presence of L-glutamate (1 mM). Specific binding was calculated by subtraction of non-specific binding from total binding, which was determined in the absence of L-glutamate. All data are means ± SEM of an experiment performed in triplicate. **A**: Specific binding in cpm. **B**: Specific binding expressed as a percentage of total binding.

Furthermore, within different experiments it was confirmed that the presence of KSCN likewise in the washing buffer has great influence on the quality of the results as it minimizes the dissociative loss of binding during the **filtration procedure** (compare Kessler et al.).[217] To further keep the binding loss in filtration assays as low as possible Kessler et al. additionally suggested using a washing buffer close to freezing temperature. As experienced in a number of assays, this seems to be an essential point – as well as keeping the duration of the washing procedure to a minimum: following filtration, the filters should not be washed more than two quick rinses.

5.2.2 Homologous competition experiments with AMPA

In compliance with the above described assay conditions, radioligand binding studies were performed in the manner of homologous competition experiments as described in 8.5.4.1.2. Thereby, the affinity of AMPA to its native protein target in different membrane preparations was examined.
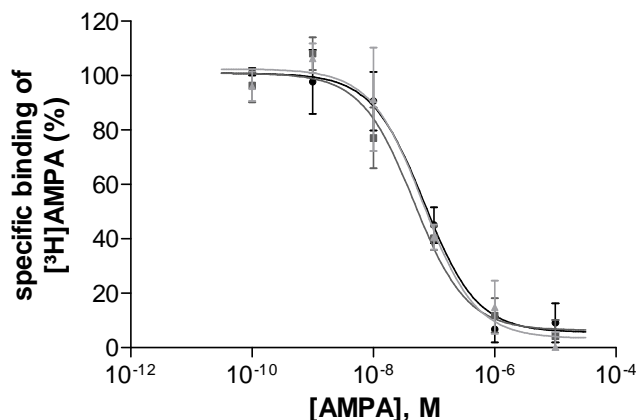
Figure 37: Specific binding of [³H]AMPA (20 nM) to membrane preparations from rat brain cortex (black), rat brain striatum (dark grey) and mouse brain (light grey) obtained in competition binding experiments with unlabeled AMPA. Increasing concentrations of AMPA were incubated with membrane preparations (300 µg of protein/well) and radioligand at 4 °C for 30 min. Non-specific binding was determined in the presence of L-glutamate (1 mM). All data are means ± SEM of 3-4 individual experiments performed in triplicate.

Table 11: IC_{50} and B_{max} values for AMPA versus [³H]AMPA obtained in competition experiments at brain membrane preparations.

	IC_{50} (nM)	K_D (nM)	B_{max} (fmol/mg protein)
rat cortical membrane	86.9 ± 33.8	66.9 ± 33.0	420 ± 174
rat striatal membrane	50.5 ± 22.7	31.0 ± 20.9	510 ± 269
mouse brain membrane	64.2 ± 29.2	44.7 ± 27.5	358 ± 187

From the above described homologous competition experiments (R,S-AMPA versus [³H]R,S-AMPA) IC_{50} values were obtained between 50 and 90 nM. Based on **Equation 16** this corresponds to K_D values in the range of 30 to 70 nM. Analysis of the data revealed binding to a single site for all membrane preparations examined. Within these homologous binding experiments likewise the maximum number of binding sites was determined, which, for all preparations investigated, proved to be between 0.4 and 0.5 pmol/mg protein. Comparison of the results with data from the literature, however, appears to be rather difficult, since various factors are discussed, which are assumed to have an influence on the results (e.g. protein treatment like detergents and freezing/thawing, buffer additives, centrifugation versus filtration assays etc.).[215–217,219,221,222,224,225] Examples for literature K_D values for [³H]AMPA at rat brain membranes (obtained in saturation binding experiments) are listed in **Table 12**.

Table 12: Exemplary K_D (nM) and B_{max} (fmol/mg protein) values published in literature[216,218,221] as obtained from saturation binding experiments with [³H]AMPA at rat brain membrane preparations with centrifugation assays. *indicates data obtained in filtration assays. In the last column it is specified if the applied radioligand was a racemic mixture (R,S) or applied in enantiopure (S) form.

	in the absence of KSCN		in the presence of KSCN		[³H]AMPA
Olsen et al.[216]	K_{D1} = 28	B_{max1} = 200	K_{D1} = 75	B_{max1} = 1000	R,S
	K_{D2} = 500	B_{max2} = 1800	K_{D2} ~3000	B_{max2} ~18000	
Murphy et al.[221]	K_{D1} = 28	B_{max1} = 330	K_D = 71*	B_{max} = 1100*	R,S
	K_{D2} = 3960	B_{max2} = 23600			
Kessler et al.[218]			K_{D1} = 11		S
			K_{D2} = 377		

For the most part in literature, binding of [³H]AMPA is described as binding to a high and a low affinity site. However, when performing a filtration assay, instead of a centrifugation assay, Murphy et al. only determined binding to a single site.[221] With regard to the published data, the obtained K_D values within this study (30 to 70 nM) represent the high affinity binding site. A detection of the low affinity binding site is not possible in competition binding studies applying a low concentration (20 nM) of [³H]AMPA. This site could only be obtained in saturation binding studies at high [³H]AMPA concentrations (as shown in **Table 12**). Data published by Kessler et al. were determined with the pure S-enantiomer of [³H]AMPA, therewith providing higher affinities for both binding sites. The maximum number of binding sites determined in the present experiments (0.4-0.5 pmol/mg protein) corresponds to the high affinity site.

As can be concluded from literature data (see **Table 12**), B_{max} values in the presence of KSCN in generally could be expected to be higher. However, as stated by Kessler et al., within filtration assays B_{max} is very likely to be reduced (up to 50%) due to a dissociative loss.[217] Finally, it has to be mentioned that published values also vary from each other to a certain extent, as can be seen from the exemplary data listed in **Table 12**. Hence, the here obtained data for AMPA binding overall corresponds to formerly published results gained by comparable experiments. Consequently, it can be concluded that the established binding assay for [³H]AMPA proved to be reliable and thus represents a suitable method for further investigations of AMPA binding sites.

5.3   Molecular cloning and heterologous expression

For several reasons that have been discussed above (see 1.4.3), the GluR2 subunit was chosen as a representative subunit for the heterologous expressions of homomeric AMPARs. Therefore, the flip as well as the flop isoforms of the human GluR2 subunit were purchased (pCMV-hGluR2flip and pCMV-hGluR2flop, see 8.1.3.3). For stable transfection both sequences needed to be cloned into suitable plasmids, which encode the resistance for a certain antibiotic; hence the plasmids pQCXIN and pQCXIH (encoding G418, and hygromycin B resistance, respectively) were chosen. By means of PCR, the hGluR2flip and hGluR2flop sequences were amplified (see **Table 24**; primers: f-hGluR2-ATG-NotI, r-hGluR2-TAG-BsiWI; annealing T: 56 °C; elongation t: 160 s), thereby flanking the ends with a NotI (5' end) and a BsiWI (3' end) restriction site. The hGluR2flip sequence was then cloned into the pQCXIN plasmid, while the hGluR2flop sequence was cloned into the pQCXIH plasmid. After verification of the correct sequence (see 8.6.13), both plasmids were linearized (see 8.6.11) and used for stable transfection of HEK cells as described in 8.7.6.1 c). Due to the presence of genes that encode for antibiotic resistance (G418 or hygromycin B), it was possible to select clones stably expressing the gene of interest.

Similarly as discussed above for the SV2 proteins (see 4.2.4), initial attempts proved that the constructs pQCXIN-hGluR2flip and pQCXIH-hGluR2flop exhibit too large sizes for the retroviral transfection method as explained above. Additionally, it has been described that recombinant expression of glutamate receptors appears to be toxic for the receptor-expressing cells,[219] which means a certain challenge for attempting a successful stable transfection of AMPARs. Nevertheless, after transfection of HEK cells

via lipofection, which already have been reported to represent a suitable cell line in several cases,[218,225] it was possible to generate cell lines stably expressing the homomeric AMPARs GluR2 flip and GluR2 flop.

5.4   Binding to recombinantly expressed AMPA receptors

Radioligand binding studies at HEK cells recombinantly expressing homomeric AMPARs of the GluR2 subunit were performed in agreement with the assay conditions established with protein membrane preparations (see 5.2). Cells were permeabilized with saponin and washed several times to remove endogenous glutamate (see 8.7.8). Upon this treatment, cells were directly used for binding studies without making membrane preparations. As determined in preliminary experiments (data not shown) cells from one confluent culture flask (175 cm^2) were used for one 24-well assay.

5.4.1   Homologous competition experiments with AMPA

A functional AMPAR consists of four subunits being composed of two dimers each comprising two identical subunits. As mentioned earlier on, here the GluR2 subunit was chosen for the heterologous expression of AMPARs, therewith providing homomeric AMPARs of either the flip or the flop isoform. By means of radioligand binding studies with the radioligand [³H]AMPA, the recombinantly expressed AMPARs were investigated. Competition experiments were performed as described in 8.5.4.1.2.
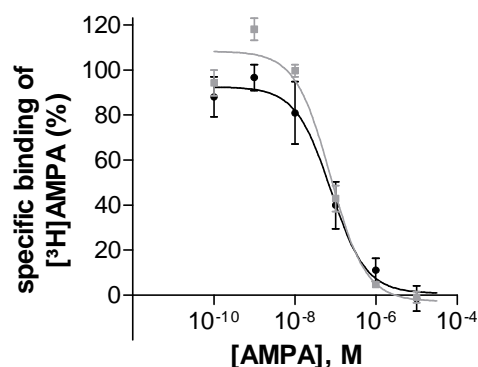
Figure 38: Specific binding of [³H]AMPA (20 nM) to HEK cells recombinantly expressing homomeric AMPARs comprised of GluR2 flip (black) and GluR2 flop (grey) obtained in competition binding experiments with unlabeled AMPA. Increasing concentrations of AMPA were incubated with cells and radioligand at 4 °C for 30 min. Non-specific binding was determined in the presence of unlabeled L-glutamate (1 mM). All data are means ± SEM of 3 individual experiments performed in triplicate.

Table 13: IC_{50} and B_{max} values for AMPA determined in homologous competition experiments at recombinantly expressed homomeric AMPARs (GluR2 flip and GluR2 flop) in HEK cells.

	IC_{50} (nM)	K_D (nM)	B_{max} (binding sites/cell)
GluR2 flip	98.1 ± 41.6	78.8 ± 42.1	55000 ± 1700
GluR2 flop	80.5 ± 20.6	61.8 ± 20.0	68000 ± 5000

In case of both isoforms it was determined that binding proceeds to a single site, providing IC_{50} values in a quite similar order of magnitude (80 to 100 nM). According to **Equation 16** this corresponds to K_D values in the range of 60 to 80 nM. The expression level gained by this stable transfection was lower than that obtained with various transient transfections (compare B_{max} values with values from transient transfections of SV2A variants, e.g. 4.3.6), however, absolutely sufficient since a maximum binding of 1000 to 3000 cpm was determined within these experiments. Moreover, it is conceivable that stable transfections cannot yield in much higher expression levels at all, since glutamate receptors (ion channels) appear to exert a toxic effect on the cells.[219]

In order to assess the experimentally obtained results, comparable binding studies from literature were taken as a reference. **Table 14** summarizes published K_D values from saturation binding experiments of [³H]AMPA at recombinantly expressed homomeric AMPARs of the GluR2 subunit.

Table 14: K_D values published in literature[218,219,225] as obtained from saturation binding experiments with [³H]AMPA at recombinantly expressed homomeric AMPARs of the GluR2 subunit (flip and flop isoform). In the last column it is specified if the applied radioligand was a racemic mixture or applied in enantiopure (*S*) form; n/a: no information available.

	GluR2 flip	GluR2 flop	[³H]AMPA
Andersen et al.[219]	K_{D1} = 2.9 nM K_{D2} = 40.7 nM	K_{D1} = 2.5 nM K_{D2} = 43.9 nM	n/a
Hennegriff et al.[225]	K_{D1} = 2.3 nM K_{D2} = 109 nM	K_{D1} = 4.7 nM K_{D2} = 28 nM	n/a
Kessler et al.[218]	K_{D1} = 2.2 nM K_{D2} = 34 nM	K_D = 4 nM	*S*

According to the above listed studies, in most cases it is suggested that [³H]AMPA is binding to two binding sites. Only Kessler et al. proposed binding to only one site for

the flop isoform. While for binding to the high-affinity site quite similar values were reported (2.3 to 4.7 nM), K_D values for the lower affinity site vary to a greater extent (28 to 109 nM). Unfortunately, only Kessler et al. provided information on the nature of the radioligand (*S*-enantiomer), which makes it even more difficult to interpret the other results. Moreover, only Andersen et al. defined the species from which the DNA used for transfection originated (rat), though, based on a sequence homology of > 99% for both isoforms between the human and the rat sequence, in this case identical binding behavior might be assumed. As discussed above (see 5.2.2), literature data might only be suitable as references to a certain extent, since numerous factors may influence the results obtained from [³H]AMPA binding. In general, however, the experimentally determined K_D values seem to correspond to the low-affinity sites published in the literature. This might be traced back to the observation by Hennegriff et al., showing that for membrane-embedded (in contrast to solubilized) receptors the low affinity site appears to be favored (e.g. low affinity site > 80% in case of GluR2 flip as determined in a saturation experiment).[225] Thus, it might be possible that a potentially present, but much lower abundant high affinity site was not detected at all within the performed binding studies.

Making overall comparisons between the binding affinities of [³H]AMPA to native brain receptors published in the literature, it has been concluded that affinities for recombinantly expressed homomeric receptors correspond to the high-affinity site of native receptors.[218] Concerning the high- and the low-affinity site in native AMPARs, it has been hypothesized that these two sites may represent receptors in distinct stages of trafficking. Supposedly, AMPARs exhibiting high-affinity sites are immature variants within the endoplasmatic reticulum, which need to undergo final processing in the Golgi apparatus and with insertion into the synaptic membrane undergo conversion into the functional low-affinity receptor.[218,224,226] Since the affinities determined for [³H]AMPA to recombinantly expressed AMPARs in general correspond to the high-affinity site of the native receptor, it has been postulated that cells used as expression systems (here: HEK cells) might lack a cellular factor, which initiates the maturation of the AMPARs.[225] Thus, it needs to be kept in mind that the question remains as to what extent recombinantly expressed AMPARs in general might reflect binding to their native analogues.

5.4.2 Investigations concerning potential binding of BRV to AMPAR

To examine if LEV and its pyrrolidone analogues are binding to AMPARs several experimental setups were performed. As mentioned above the subunit GluR2 was chosen as a representative for the recombinant expression of homomeric AMPARs. In radioligand binding studies the interaction of [³H]BRV with HEK cells recombinantly expressing GluR2 was investigated. Therefore, on the day of the experiment HEK cells were harvested and prepared as described in 8.7.8. One cell culture flask (175 cm^2, grown to confluence) was used for a 24-well assay. Binding studies were performed as described in 8.5.4.1.1 and **Table 21** with the following variations: in different experiments as a buffer for incubation Tris-HCl buffer was used, either with addition of MgCl$_2$ (2 mM) or with addition of KSCN (200 mM). Binding of the radioligand was investigated in different concentrations (1 nM and 2 nM). The time of the washing procedure of the glass fiber filter was always kept as short as possible using ice-cold Tris-HCl buffer with addition of 50 mM KSCN. The binding experiment was performed each time in triplicate.

Regardless of the examined modifications of buffer additives or radioligand concentrations, in neither experiment specific binding could be detected: for binding to the flip isoform the total binding (in cpm) was 97 ± 22 cpm with a specific binding of 18 ± 3 cpm. Binding to the flop isoform provided a total binding of 83 ± 23 cpm and a specific binding of 10 ± 8 cpm (data not shown). Considering that for binding of [³H]BRV to non-transfected HEK cells a total binding of 86 cpm and a specific binding of 12 cpm was determined (experiment in triplicate), it becomes evident that the observed marginal binding is irrelevant. Thus, based on these results it can be concluded that no binding of [³H]BRV occurs to homomeric AMPARs of the GluR2 subtype.

Consequently, as shown with the radioligand [³H]BRV as a potent antiepileptic pyrrolidone drug, those experimental observations reveal no direct binding to the AMPARs and therewith do not support the results described by Bidlack and Rasheed.[115] Surely, it is a question, if the results would have been different, if other subunits than the GluR2 subunit had been used for the investigation. However, for the structurally related allosteric AMPAR modulators piracetam and aniracetam subunit specificity has been determined to be low.[214] Bidlack and Rasheed published a brief abstract in which they summarized that LEV is binding to an allosteric site of AMPARs since binding of [³H]LEV was inhibited by allosteric AMPAR modulators in a concentration-dependent

manner. Unfortunately, this abstract does not give any details or show concrete results. Therefore, it also cannot be excluded that the examined AMPAR modulators competed with the [³H]LEV binding in a manner independent from their interaction with the allosteric AMPAR binding site. The experimental results that were obtained within this study therewith would rather be in agreement with findings by e.g. Lee et al. suggesting that an observed AMPAR modulation by LEV is conveyed by a presynaptical interaction leading to a decreased glutamate release.[213]

5.4.3   Potential modulation of [³H]AMPA binding by levetiracetam

In further binding studies it was planned to investigate if the antiepileptic compound LEV is modulating the binding of [³H]AMPA to its receptor. Therefore, rat cortical membrane preparations were purified as described in 8.3.4 to ensure the removal of endogenous glutamate. The experiment was performed in accordance with conditions described in 8.5.4.1.2, representing optimized conditions for the radioligand [³H]AMPA. Binding of [³H]AMPA was examined in the presence of LEV in concentrations from 100 nM to 1 mM.
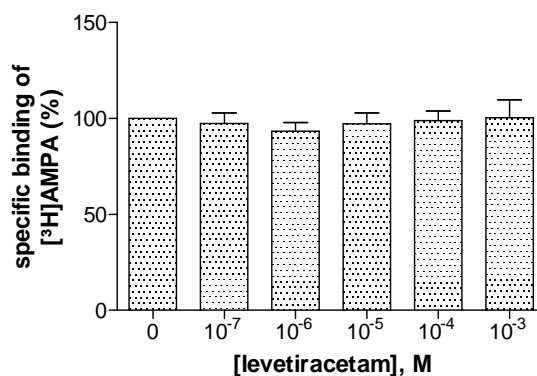
Figure 39: Specific binding expressed in % of [³H]AMPA (20 nM) to rat brain cortical membrane preparations in the presence of different concentrations of levetiracetam. Increasing concentrations of levetiracetam were incubated with the radioligand and membrane preparations (300 µg of protein/well) at 4 °C for 30 min. Non-specific binding was determined in the presence of L-glutamate (1 mM). All data are means ± SEM of 4-5 individual experiments performed in triplicate.

As can be deduced from the above described experiment, no modulatory effect of levetiracetam could be observed on the binding of [³H]AMPA under the investigated conditions.

5.4.4   Potential modulation of [³H]BRV binding by AMPA and L-glutamate

It was further intended to investigate if the presence of the glutamate receptor agonists AMPA and L-glutamate influences the binding of the pyrrolidone compound [³H]BRV. For these experiments rat cortical membrane preparations were purified as described in 8.3.4 to remove endogenous glutamate. Binding studies were performed as described in 8.5.4.1.1 and **Table 22** to ensure optimal conditions for [³H]BRV binding.
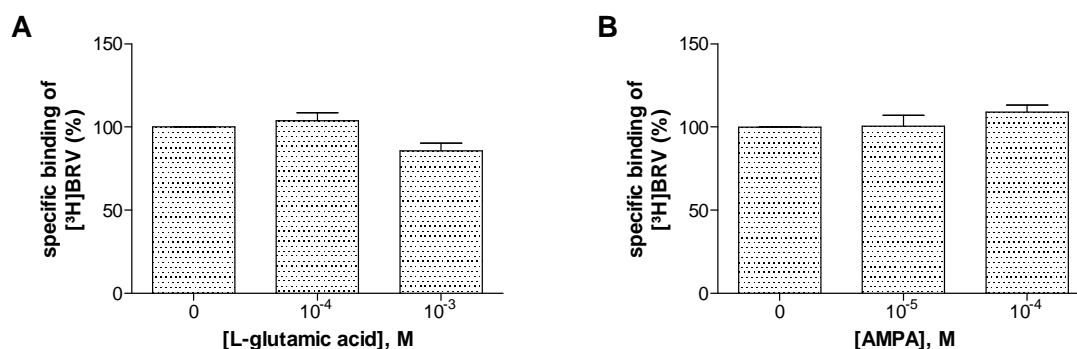
Figure 40: Specific binding expressed in % of [³H]BRV (1 nM) to rat brain cortical membrane preparations in the presence of L-glutamate (A), and AMPA (B), respectively. Different concentrations of the test compounds were incubated with the radioligand and membrane preparations (100 µg of protein/well) at 4 °C for 240 min. Non-specific binding was determined in the presence of LEV (1 mM). All data are means ± SEM of 3 individual experiments with six-fold determination.

As demonstrated above, slight modifications on [³H]BRV binding by L-glutamate or AMPA might be recognizable. In order to assess the significance of these effects, a statistical analysis was performed applying a one-way ANOVA with Dunnett's test for multiple comparisons: therefore specific binding of [³H]BRV in the absence of test compounds was used as control data to which specific binding in the presence of test compounds was compared. The analysis revealed that no statistically significant difference ($p > 0.05$) exists between binding of [³H]BRV in the presence or absence of L-glutamate or AMPA.

Consequently, it can be concluded that neither LEV appears to modulate the binding of the radioligand [³H]AMPA (see 5.4.3), nor do L-glutamate or AMPA exert any significant effect on the binding of [³H]BRV under the observed experimental conditions. These results, obtained with native tissue, are in agreement with the above mentioned observation (see 5.4.2) that no binding of [³H]BRV could be observed to AMPARs (represented by a homomeric receptor of the GluR2 subunit).

5.5 Summary

Since SV2A is a ubiquitously expressed synaptic vesicle protein, which – as far as it is known today – contributes to inhibitory as well as excitatory neurotransmission, questions have been raised if further potential targets of LEV exist that are involved and contribute to its potent anticonvulsive effect. Based on postulated interactions between LEV and AMPARs, it was decided to investigate if direct binding of the new pyrrolidone radioligands, which show high specific activity, to AMPARs can be observed.

Molecular cloning and heterologous expression

For the recombinant expression of the AMPAR, for which the subunit GluR2 was chosen as a representative, the DNA sequences encoding both isoforms (flip and flop) were subcloned into retroviral vectors. Since the initially planned retroviral transfection turned out to be not suitable for these constructs due to the limited capacity of the virus particles, stable transfection was performed via lipofection. Thereby, it was possible to generate cell lines stably expressing the recombinant homomeric AMPAR of the subunit GluR2 in its flip as well as flop isoform.

Radioligand binding studies

Initially, a suitable assay system to perform [³H]AMPA binding studies had to be established. Therefore, several factors were examined, some of which proved to have a large influence on the outcome of the experiments. Using native protein preparations (rat cortical membrane preparations), optimal conditions for a reliable assay system were determined.

By means of homologous competition experiments, binding of [³H]AMPA to native protein from rat cortical membrane preparations was investigated and compared to data in the literature obtained from saturation experiments. Competition binding experiments allowed the detection of a single binding site, providing values that are consistent with the high affinity binding site reported in the literature. Since in competition binding experiments in general only a relatively low concentration of radioligand is applied, the detection of the low affinity site described in the literature can only be achieved in saturation experiments. Taken together, it can be concluded that the established assay

system proves to be reliable and hence represents a valuable system for the investigation of the binding of [³H]AMPA to its molecular target structures.

Furthermore, HEK cells recombinantly expressing homomeric AMPARs of the GluR2 subunit (flip and flop isoform) were applied in binding studies with [³H]AMPA. Thereby, it was confirmed that the transfection was successful, providing cell lines stably expressing homomeric AMPARs with sufficient expression levels. As far as comparisons were possible, the experimentally obtained data were consonant with data published in the literature. Consequently, it can be assumed that the recombinantly expressed AMPARs are suitable for investigations of drug-target interactions.

To examine if AMPARs exhibit a potential binding site for the pyrrolidone drugs, binding of [³H]BRV to the recombinantly expressed homomeric AMPAR was investigated. Repeated experiments under varying conditions revealed that no binding of the radioligand could be detected. As far as GluR2 can be considered to be a representative subunit for AMPARs, these results imply that the pyrrolidone drugs do not directly interact with AMPARs, neither by binding to an allosteric nor to an orthosteric binding site. This is also consistent with results obtained from further studies on native membrane preparations: under the observed conditions no modulatory effect on [³H]AMPA binding to its protein target could be observed in the presence of LEV. Likewise, the presence of L-glutamate and AMPA did not significantly influence the binding of [³H]BRV to its protein target.

6 Binding to SV2A knockout brain tissue

With the identification of the SV2A protein as the target structure for levetiracetam (LEV) and its analogues[61] it was suggested that these pyrrolidone drugs apparently exert their antiepileptic effects via a novel mechanism of action. By radioligand binding studies involving brain tissue from SV2A KO mice it was demonstrated that the SV2A protein appeared to represent the only target of the pyrrolidone drugs since no binding could be detected in the absence of SV2A.[61,72] However, the validity of these studies was limited by the relatively low signal (~900 dpm, which corresponds to ~450 cpm) that was observed in control tissue (wild-type mice),[61] and the low specific activity of the applied radioligand (8 Ci/mmol),[72] respectively. Other studies, which showed that the affinity of different pyrrolidone drugs to the SV2A protein positively correlated with their antiepileptic potency,[61,75] have been criticized with regard to the missing information on the actual cerebrospinal fluid levels of the investigated compounds.[76] As discussed in chapter 5.1, so far it cannot be excluded that further targets besides the SV2A protein are involved in the antiepileptic effect evoked by LEV and its analogues. Considering that the SV2A protein is ubiquitously present in the brain with very high expression levels of approximately 9 to 11 pmol/mg protein,[60,72] it is likely that potentially present low-abundant protein targets (expressed e.g. in femtomolar concentrations) may not have been detectable with the applied radioligands under the so far applied experimental conditions.

Having a radioligand in hand with high specific activity, it was intended to reinvestigate brain tissue from SV2A KO mice with the new radioligand [³H]BRV. Due to its remarkably high specific activity, the radioligand is supposed to be more suitable than the previously used ones[61,72] to detect potential protein targets with low expression levels. For this purpose membrane preparations were made as described in 8.3.2 from brains of SV2A wild-type (+/+), heterozygous SV2A KO (+/-) and homozygous SV2A KO (-/-) mice, which were provided by the group of Prof. Dr. S. Schoch. Binding studies were performed similarly as described in 8.5.4.1.1, **Table 21** and **Table 23** with the following modifications: the radioligand [³H]BRV was applied in concentrations of 10 and 50 nM; the amount of protein was increased to 200 µg per well.
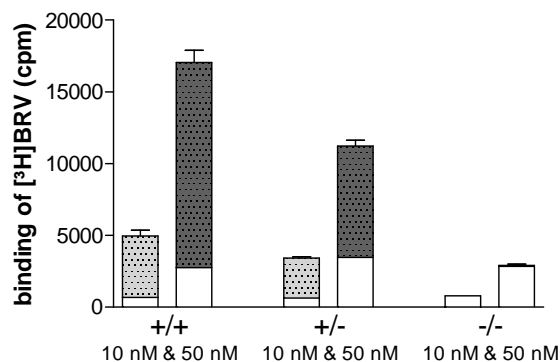
Figure 41: Binding of [³H]BRV in cpm to brain membrane preparations of SV2A wild-type mice (+/+), heterozygous SV2A KO mice (+/-), and homozygous SV2A KO mice (-/-), respectively. The radioligand [³H]BRV (10 nM, and 50 nM, respectively) was incubated with membrane preparations (200 µg of protein/well) at 4 °C for 240 min. Non-specific binding was determined in the presence of unlabeled LEV (1 mM). Depicted is a representative result of two individual experiments performed in triplicate; data points represent means ± SEM.

From the above described experiments the following results were obtained: in brain membrane preparations of SV2A wild-type mice (+/+) very high specific binding was achieved ranging from ~4300 cpm (10 nM radioligand) to ~14300 cpm (50 nM radioligand). In preparations of heterozygous SV2A KO mice (+/-) binding was reduced to ~2800 cpm (10 nM radioligand), and ~7700 cpm (50 nM radioligand), respectively. No specific binding of the radioligand [³H]BRV was detected to brain membrane preparations of homozygous SV2A KO mice (-/-), for none of the applied radioligand concentrations. Thus, no additional binding sites for [³H]BRV – besides SV2A – could be detected in these experiments.

The experimental conditions for this analysis were chosen in analogy to conditions of previous investigations at membrane preparations of SV2A KO mice,[61,72] which were optimized for binding of the pyrrolidone drugs to the SV2A protein. Hence, it has to be considered that this experimental setup might not provide the ideal conditions for the detection of potentially present low-abundant target proteins other than the SV2A protein. As discussed in chapter 5.2 (for the AMPAR) and the therein cited literature, binding of radioligands to proteins can be strongly influenced by a number of factors: for instance Olsen et al. determined a B_{max} value of 200 fmol/mg protein for the high affinity binding site of [³H]AMPA in the absence of KSCN as compared to 1000 fmol/mg protein in the presence of KSCN with otherwise optimal conditions for [³H]AMPA binding (see **Table 12**).[216] Assuming that [³H]BRV was binding with the same affinity as it binds to the SV2A protein to a potentially low-abundant target site

with similarly low expression levels (e.g. 200 fmol/mg protein, which is ~ 50 times lower than the expression level of the SV2A protein), the signal determined in the above described experimental setup would still be below 300 cpm. Considering that, in addition, the applied conditions might not be ideal for binding to such an unknown target, it is conceivable that the signal would be lower than the limit of detection and hence, the "unknown" target site may not be measurable by the applied approach. Moreover, in antiepileptic therapy, Keppra® (LEV) is administered in very high doses of 1-3 g/day (plasma level: 35-100 µM, peak concentrations: 90-250 µM).[213,227] Thus, it is conceivable that also lower affinity target proteins could be addressed at therapeutic doses.

Due to the limited amount of available brain tissue from SV2A KO mice, it has only been possible so far to perform a very limited number of experiments without the required variations of experimental conditions. In future studies, it will be interesting to investigate binding to the tissue under systematically varied conditions, representing optimized conditions for binding to diverse protein targets. As can be concluded from the above described experiment, the new radioligand [³H]BRV proves to be suitable for the performance of these experiments and hence for the investigation of potentially present low-abundant protein targets besides the SV2A protein.

7   Summary and outlook

Since levetiracetam (LEV) was approved in 1999 by the FDA, it has become one of the most successful of the newer antiepileptic drugs (AEDs). Nevertheless, its mode of action has still not been fully elucidated. In 2004, Lynch et al.[61] discovered that the pyrrolidone drug is binding to the synaptic vesicle protein SV2A, thereby suggesting a completely novel mechanism of antiepileptic action. So far little is known about the exact role of this protein in neurotransmitter release and how LEV might affect its function. Very recently, the first study was published in which several amino acids were identified that supposedly participate in the interaction with pyrrolidone drugs,[100] however, the exact site of ligand binding remains to be elucidated. Furthermore, it is under discussion if the SV2A protein represents the main and only target for the pyrrolidone drugs: radioligand binding studies at membrane preparations of SV2A KO mice argue for the SV2A protein as the only target structure.[61,72] However, in these studies radioligands of limited sensitivity were applied. Moreover, based on another study it has been suggested that LEV is also binding to an allosteric site of AMPARs.[115]

To contribute to the clarification of these matters, it was planned to synthesize tritium-labeled radioligands of the AEDs LEV and its higher-affinity analogue brivaracetam (BRV), which should possess high specific activity and thus represent sensitive tools for binding studies. Within this study, synthetic routes were developed, which allowed the preparation of the radioligands **[³H]LEV**, **[³H]BRV**, as well as its stereoisomer **[³H]isoBRV** with very high specific activity of 94-98 Ci/mmol (see **Schemes S1 and S2**).
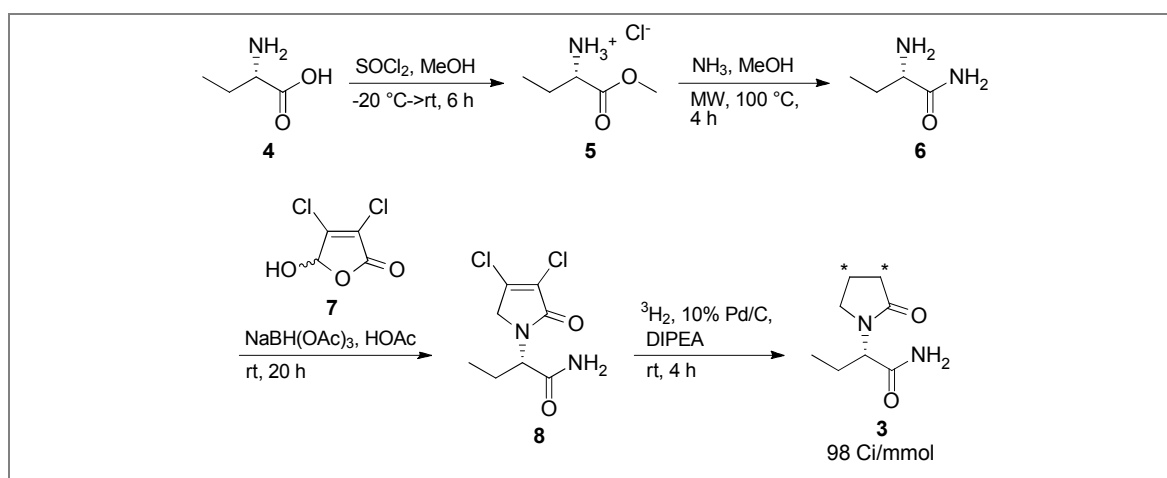
Scheme S1: Synthesis of [³H]LEV (3); MW: microwave, DIPEA: *N,N*-diisopropylethylamine (*denotes positions of ³H).
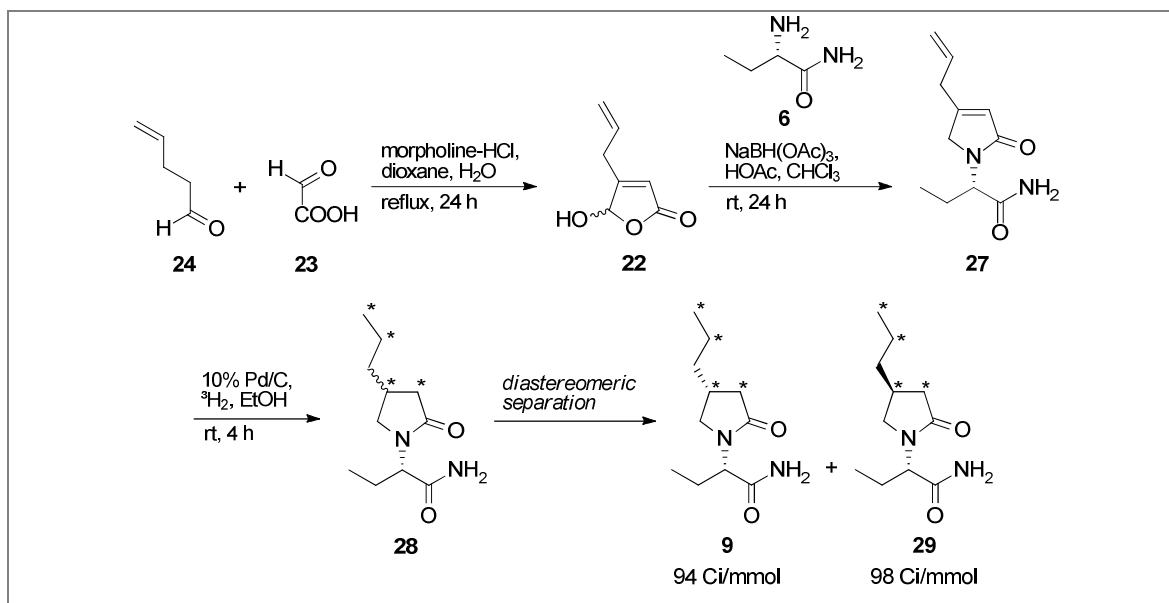
Scheme S2: Synthesis of [³H]BRV (9) and [³H]isoBRV (29);*denotes positions of ³H.

An assay system, suitable for the application of all these three radioligands in binding studies, was established. The radioligands were characterized in kinetic studies and saturation binding experiments. It was confirmed that the affinity to the target protein (SV2A) increased in the order [³H]LEV < [³H]isoBRV < [³H]BRV based on K_D values of $1.12 \pm 0.18\ \mu M$, $409 \pm 23\ nM$, and $70.0 \pm 8.4\ nM$, respectively.

Subsequently, the new radioligand [³H]BRV was applied in different competition binding experiments, in which it proved to be **valuable for the screening of compounds** providing highly reproducible results. Moreover, it was confirmed that [³H]BRV can be considered as a **suitable surrogate for the low-affinity ligand [³H]LEV** with superior properties due to its ~15-fold higher affinity. In competition experiments with unlabeled LEV at diverse brain membrane preparations [³H]BRV proved to be a reliable tool providing IC_{50} values of $1.73 \pm 0.23\ \mu M$ (rat cortex), $0.693 \pm 0.131\ \mu M$ (rat striatum), $0.948 \pm 0.144\ \mu M$ (mouse brain), $1.43 \pm 0.33\ \mu M$ (human thalamus) and $2.69 \pm 0.55\ \mu M$ (human putamen) for the antiepileptic drug LEV.

[³H]BRV was further employed to examine **brain samples from patients with pharmacoresistant epilepsy** obtained by surgery. Competition binding experiments (unlabeled LEV versus [³H]BRV) provided highly reproducible binding curves, demonstrating **concentration-dependent binding inhibition** with IC_{50} values between 0.7 and 1.2 μM. No significant difference in affinity of LEV to its target protein was observed among different samples, including initial Keppra®-therapy (LEV) responsive as well as non-responsive patients.

To investigate the interaction of LEV with the SV2A protein, several different native and mutant SV2 proteins were subcloned, expressed in CHO cells and subjected to radioligand binding studies. Saturation binding experiments of the radioligand [³H]BRV to the recombinantly expressed human wild-type SV2A protein showed binding to a single saturable binding site with a K_D value of 75.1 ± 12.2 nM, which was comparable to literature values as well as to data obtained at native membrane preparations. Competition binding experiments of LEV versus [³H]BRV at recombinantly expressed human and rat SV2A protein showed that **no species differences** exist (IC_{50}: 2.64 ± 0.53 µM, and 2.98 ± 0.63 µM, respectively), which is in accordance with the high sequence homology between these orthologues.
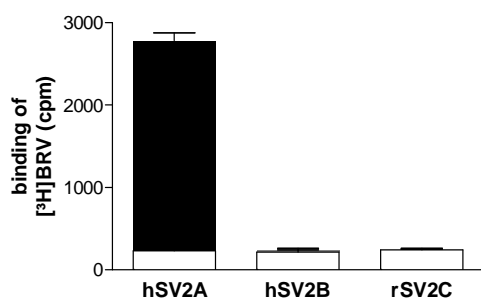
Binding of [³H]BRV (1 nM) to GFP-tagged SV2A, SV2B, and SV2C proteins expressed in CHO cells; h: human, r: rat.

By binding experiments at the different recombinantly expressed SV2 protein isoforms SV2A, SV2B and SV2C it could be confirmed that the pyrrolidone drugs **only bind to the SV2A**, but not to the SV2B or SV2C isoforms at radioligand concentrations of 1 nM ([³H]BRV) and 10 nM ([³H]LEV).

To contribute to the identification of the ligand binding site at the SV2A protein it was investigated if the long cytoplasmic loop comprising exons 5 and 6 (see **Figure S1**) is involved in this interaction.
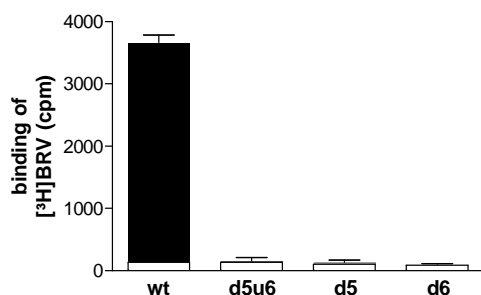
Binding of [³H]BRV (1 nM) to GFP-tagged rat SV2A wild-type protein (wt), and variants with deletions of exons 5 and/or 6 (d5u6, d5, d6) expressed in CHO cells.

Therefore, studies were performed in which binding of [³H]BRV to deletion mutants of the rat **SV2A protein lacking exons 5 and/or 6** were investigated. In the absence of this region **no binding** of the pyrrolidone radioligands could be detected, which may suggest an essential role of this area in the ligand-target interaction.
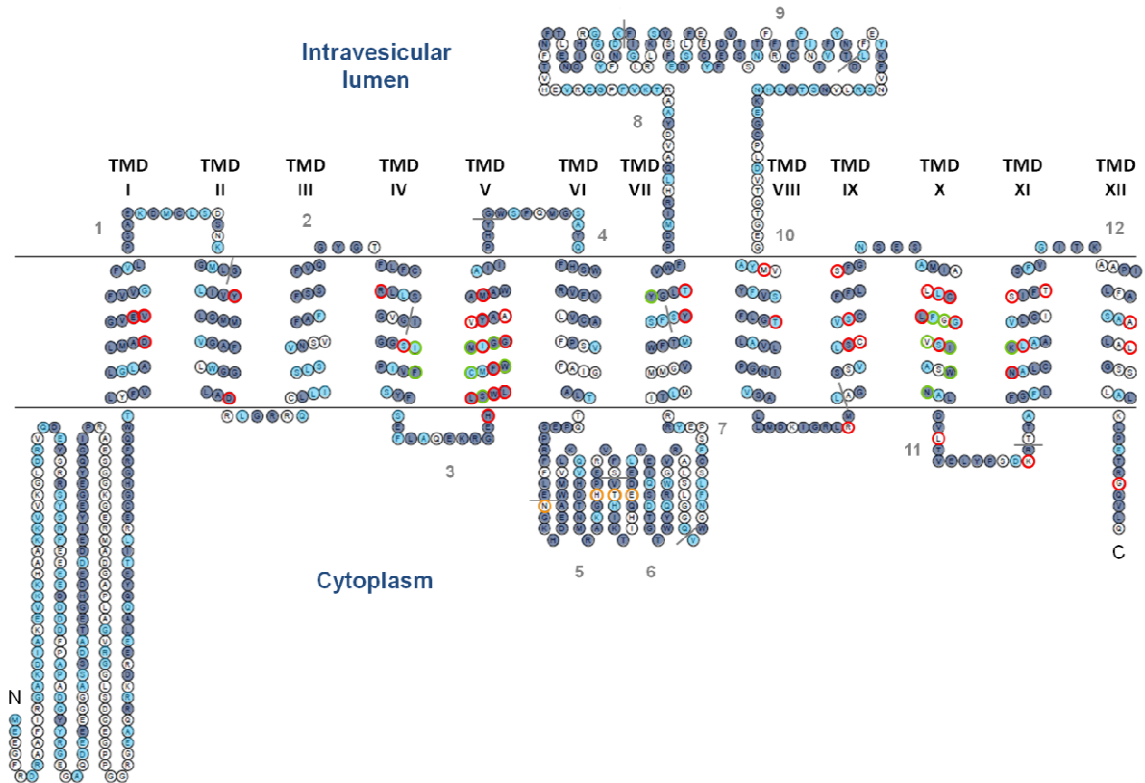
Figure S1: Topology model of the rat SV2A protein. The snakeplot diagram was drawn with TOPO2 with prediction of transmembrane domains based on TMHMM software[93,94] (see 8.1.1). Exons are numbered in grey from 1 to 12 and separated by lines, N- and C-termini are indicated with the corresponding letters. Amino acids colored in dark blue represent residues that are conserved among all three isoforms (SV2A, SV2B and SV2C), light blue colored ones are conserved in one other isoform besides SV2A, and white colored ones are non-conserved and only present in the SV2A isoform. Residues that were mutated and investigated in the study of Shi et al.[100] are marked with red (no change in ligand binding), and green (altered ligand binding), respectively. Residues that are marked with a yellow circle were mutated and investigated in this study.

However, deletion of a longer sequence might potentially evoke a conformational change of the resulting protein mutant. Therefore, it is not clear, whether the drugs actually bind to the deleted sequence or whether conformational changes cause these effects. Subsequently, several point mutants of the rat SV2A protein were investigated (see **Figure S1**): certain amino acids, which are non-conserved among the SV2 isoforms, and therefore might have an essential function in the interaction of the SV2A protein with its ligands, were exchanged (N364K, H387Q, H387Q/T395I, T395I, E403D). All of these mutants behaved like the wild-type protein and thus do not appear to be involved in ligand binding. In future studies, it may be a reasonable approach to create a mutant in which all non-conserved amino acids of exons 5 and 6 are exchanged for the corresponding ones from the isoforms SV2B or SV2C.

Concerning the hypothesis that the pyrrolidone drugs might bind to an allosteric site of AMPARs, it was planned to investigate binding of [³H]BRV to recombinantly expressed AMPARs. Therefore, initially an assay system for [³H]AMPA using membrane preparations of rat and mouse brain was established: in competition binding experiments with unlabeled AMPA, IC_{50} values were obtained that are comparable with published data. Recombinant AMPARs were stably expressed in HEK cells (assembled from the subunit GluR2 as flip and flop isoform) and were characterized by homologous competition experiments with [³H]AMPA. The radioligand [³H]BRV did not show any specific binding to HEK cells recombinantly expressing AMPARs. In binding studies at native protein preparations (rat cortex) LEV (100 nM to 1 mM) also did not modulate the binding of [³H]AMPA, nor did AMPA or L-glutamate modulate the binding of [³H]BRV. Thus, the results of the present study **do not reveal evidence for direct binding of LEV and BRV to AMPA receptors**.

Finally, the radioligand [³H]BRV was applied to investigate binding to membrane preparations of brains from **SV2A KO mice**, and thus to repeat investigations, which so far were of limited validity due to the available radioligands.[61,72]
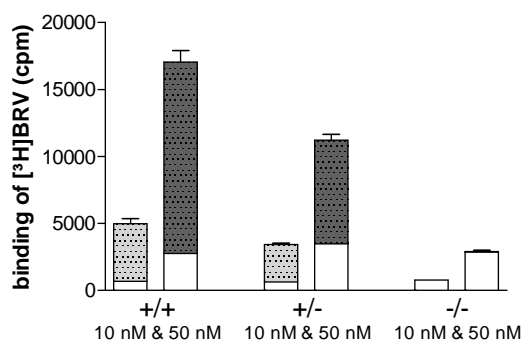
Binding of [³H]BRV (10 nM, and 50 nM, respectively) to brain membrane preparations of wild-type mice (+/+), heterozygous SV2A KO mice (+/-), and homozygous SV2A KO mice (-/-).

Under identical experimental conditions with the new radioligand [³H]BRV high-affinity specific binding could also not be detected in the absence of the SV2A protein (-/-), while the same concentrations of radioligand (10 nM or 50 nM) provided high binding in control tissue from wild-type mice (+/+) and reduced binding in heterozygous KO mice (+/-).

The limited amount of so far available SV2A KO mice brain tissue only allowed a small number of experiments (performed only under optimal conditions for binding to SV2A). In future studies repetitions of this investigation with systematical variations of experimental conditions will help to clarify, if additional targets are addressed by the antiepileptic pyrrolidone drugs. As demonstrated within this thesis the new radioligand [³H]BRV represents a most valuable tool for that kind of investigations.

8   Experimental part

8.1   General

8.1.1   Software

Microsoft Office 2007 (Excel, Word, PowerPoint, Picture Manager)

ChemBioDraw Ultra 11.0.1, Cambridge Software

WIN-NMR 6.2.0.0, Bruker Daltonik GmbH

GraphPad Prism 5.01, GraphPad Software, San Diego, California, USA

DNAtrans 2.1, http://www.b-und-s-software.de/

Clone Manager Basic for Windows, version 9, Scientific & Educational Software

Plasmid Map Enhancer for Windows, version 3.1, Scientific & Educational Software

Oligoanalyzer 3.1, http://eu.idtdna.com/analyzer/Applications/OligoAnalyzer/

Chromas Lite 2.01, http://www.technelysium.com.au/chromas_lite.html

ClustalW, EMBL-EBI, http://www.ebi.ac.uk/Tools/msa/clustalw2/

Needle, EMBL-EBI, http://www.ebi.ac.uk/Tools/psa/emboss_needle/

TOPO2, http://www.sacs.ucsf.edu/cgi-bin/tmhmm.py

8.1.2   Material for synthesis

8.1.2.1   Chemicals and solvents

Chemicals for synthesis have been purchased from Acros Organics (Nidderau, Germany), Alfa Aesar (Karlsruhe, Germany), Bachem (Weil am Rhein, Germany), Fluka (Buchs, Schweiz), Merck (Darmstadt, Germany), Sigma Aldrich (Steinheim) and TCI Europe (Eschborn, Germany). If not stated otherwise chemicals were used without further purification.

Solvents were obtained from various commercial sources. If not indicated otherwise, they were used without further purification.

8.1.2.2 Material and instruments

Microwave instrument

Chemical reactions with microwave radiation were performed in a Discover microwave instrument (CEM GmbH, Kamp-Lintfort, Germany).

Hydrogenation apparatus

Catalytic hydrogenation was performed with a Hogen® GC Hydrogen Generator (Proton Energy Systems, Wallingford, USA).

TLC

Analytical thin layer chromatography (TLC) was performed on silica-coated aluminum plates containing a fluorescent indicator (Merck silica gel 60 F_{254}, Darmstadt, Germany).

Column chromatography

For column chromatography silica gel 60 (0.063-0.200 mm) from Merck (Darmstadt, Germany) was used.

Preparative HPLC

For preparative HPLC a Knauer HPLC system (Knauer GmbH, Berlin, Germany) was used comprising a Wellchrome K-1800 pump, injection and switching valves, a Wellchrome K-2600 spectrophotometer, a Eurospher 100 C18 precolumn (30 mm x 20 mm, particle size 10 μm) and a Eurospher 100 C18 column (250 mm x 20 mm, particle size 10 μm). As mobile phase a mixture of methanol (HPLC grade, Merck, Darmstadt, Germany) and deionised water with a flow rate of 20 ml/min was used.

Lyophilization

Lyophilization of compounds was performed with Alpha 1-4 LSC (Martin Christ Gefriertrocknungsanlagen GmbH, Osterode, Germany).

Polarimeter

Optical rotation of chiral compounds was measured with 241 Polarimeter (PerkinElmer).

Melting point apparatus

For the determination of melting points Büchi Melting Point B-545 was used.

NMR

NMR spectra were recorded on a Bruker Avance 500 spectrometer (^{1}H: 500 MHz, ^{13}C: 125 MHz) at room temperature. Spectra were recorded at room temperature in CDCl$_3$, or CD$_3$OD, respectively, and the remaining protons of the deuterated solvent were used as an internal standard (^{1}H: δ (ppm) CDCl$_3$: 7.24; CD$_3$OD: 3.35 and ^{13}C: δ (ppm) CDCl$_3$: 77.0; CD$_3$OD: 49.3). Coupling constants are given in Hertz (Hz) and chemical shifts in parts per million (ppm). Spin multiplicities are abbreviated with s (singlet), d (doublet), t (triplet), m (multiplet), br (broad).

HPLC-MS

Low-resolution mass spectra were obtained on an API 2000 mass spectrometer (electrospray ionization, Applied Biosystems, Darmstadt, Germany) coupled to an HPLC system (Agilent 1100) using the following procedure: compounds were dissolved in methanol (0.5 mg/ml). A 10 μl sample of this solution was injected into the HPLC system containing a Phenomenex Luna C18 column (50 mm x 2.00 mm, particle size 3 μm). It was chromatographed using a gradient of water : methanol (containing 2 mM ammonium acetate, if not stated otherwise) from 90 : 10 to 0 : 100 in 30 min. The gradient was started after 10 min, the flow rate was 250 μl/min. UV absorption was detected using a diode array detector (from 190 to 900 nm) and purity was determined at 254 nm.

8.1.3 Material for biological work

8.1.3.1 Chemicals and additives

Acetic acid	Merck, 1.00063.1011
Agarose	Roth, 2267.2
(*R,S*)-AMPA	Enzo Life Sciences, EA-110
Ampicillin sodium salt	Roth, K029.1
Aniracetam	Sigma, A9950
ATP disodium salt	AppliChem, A1348
Bemegride	TCI Europe, E0284
Bromophenol blue sodium salt	AppliChem, 3640
BSA/Albumin fraction V	Roth, 8076.4
Calcium chloride, anhydrous	AppliChem, A3652

Calcium chloride dihydrate	Fluka, 21097
Calf serum	Sigma, C8056
Copper(II) sulfate pentahydrate	AppliChem, A1034
Disodium hydrogen phosphate, anhydrous	AppliChem, A1046
DMSO (binding studies)	Roth, 4720.3
DMSO (cell culture)	AppliChem, A3672
EDTA	Roth, 8040.3
Ethanol p.a.	Merck, 1.00983.1000
Ethosuximide	Sigma, E7138
Fetal Bovine Serum	Sigma, F7524
Folin & Ciocalteau's phenol reagent	Sigma, F 9252
D-(+)-Glucose	Sigma, G-7021
L-Glutamic acid	Sigma, G1251
Glycerol	AppliChem, A1123
HEPES	Roth, 9105.4
H_2O, sterile	VWR, AX021376
Hydrochloric acid 37%	Sigma-Aldrich, 30721
Hypoxanthine	AppliChem, A0700
LB agar	Roth, X965.3
LB medium	Roth, X968.2
Levetiracetam	Chemos GmbH, Art No. 134992
Liquid Scintillation Cocktail	LumaSafe[TM] Plus, Lumac
Magnesium chloride	Sigma, M8266
Magnesium chloride hexahydrate	Fluka, 63068
Mycophenolic acid	AppliChem, A3801
PEI solution (50% in H_2O)	Sigma, P-3143
Penicillin-Streptomycin, liquid	Gibco, 15140
Pentylenetetrazole	Sigma, P6500
Phenobarbital	Sigma, P1636
Phenol red solution	Sigma, P0290
Piracetam	Sigma, P5295
Polybrene (Hexadimethrine bromide)	Aldrich, 10,768-9
Potassium chloride	Fluka, 60128
Potassium phosphate monobasic	Sigma, P9791

Potassium thiocyanate	Sigma-Aldrich, 20779-9
Saponin	Fluka, 84510
SDS solution 20%	AppliChem, A0675
Sodium butyrate	Alfa Aesar, A11079
Sodium chloride	Roth, 9265.1
Sodium hydroxide	Fluka, 71689
D(+)-Sucrose	AppliChem, A4734,5
Tris(hydroxymethyl)aminomethane	Roth, AE15.3 / 5429.3
Xanthine	Sigma, X7375

8.1.3.2 Material and instruments

Autoclave	VX-95, Systec
	3850 ELV, Systec
Balance, analytical	XA205DU Excellence, Mettler Toledo
Balance, precision	SBC 42, SCALTEC
	440-47N, KERN
Centrifuges	Mikro 200, Hettich
	AllegraTM 21 R, Beckman Coulter
	AvantiTM J-201, Beckman
	Rotofix 32, Hettich
Dismozon$^®$ pur	975400, Bode Chemie
Drying cabinet	T6120, Heraeus
Electrophoresis chamber	Schütt Labortechnik
Electrophoresis power supply	Power Pac 300, ELITE 300 Plus,
	Schütt Labortechnik
Gel documentation system	Universal Hood II Geldoc, BioRad
Glass-fiber filters	Whatman$^®$, Schleicher und Schüll (GF/C)
Glass homogenizer, Potter	Sartorius
Harvester	Brandel M24 Gaithersburg, MD, USA
	Brandel M48 Gaithersburg, MD, USA
Hemocytometer (cell counting chamber)	Marienfeld Germany
Incubator for cells	Jouan IG 650, Heraeus,
	INC 246, Memmert

Incubator shaker	Innova 4200 Incubator shaker,
	New Brunswick Scientific
Liquid scintillation analyzer	Tri-Carb 2810 TR, Perkin-Elmer
Liquid scintillation cocktail	LumaSafe®, Perkin-Elmer
Microscope	Wilovert, Hund Wetzlar
	Axiovert 25, Zeiss
Microscope for fluorescence images	Leica, DM IL LED Fluo
MilliQ	PURELAB flex, ELGA
pH-meter	691 pH Meter, Metrohm
	Seven Easy, Mettler Toledo
Pipets	Eppendorf
Photometer	DU-530, Beckman
Rocking shaker	ELMI Digital Rocking Shaker DRS-12
Safety cabinet	NUNC® Safe flow 1.2
	NUNC® MICROFLOW
Steril filter	Filtropur 0.22 µm, 831826001, Sarstedt
Thermal block	Thermomixer comfort, Eppendorf
Thermocycler	T Personal, Biometra
Tip Sonicator	Sonoplus HD2070, Bandelin
Tissue homogenizer	RW 16 basic, IKA,
	Ultra-turrax T25 basic, IKA
Vortex mixer	UNIMAG Zx³, UniEquip
	Vortex Genius 3, IKA
	MS2 Minishaker, IKA
Water bath	WNB 14, Memmert

Flow cytometer

For flow cytometric analysis the flow cytometer FACScalibur (BD Biosciences, USA) was used, equipped with an argon laser (excitation at 488 nm). Emission was detected between 515-545 nm. Cells were injected suspended in PBS buffer. Autofluorescence, which was subtracted from the determined fluorescence intensity of each sample, was determined with non-transfected CHO cells.

8.1.3.3 Material for molecular biology

Plasmids

pCMV-hSV2A (NM_014849.3)

pCMV-hGluR2_flip (NM_000826.2)   AMS Biotechnology, UK

pCMV-hGluR2_flop (NM_001083619.1)

pCMV-rSV2Awt-GFP (NM_057210.2)

pCMV-rSV2Ad5u6-GFP

pCMV-rSV2Ad5-GFP

pBluescript-hSV2B (NM_014848.4)
                                                    provided by Prof. Dr. S. Schoch,
pCMV-rSV2C (NM_031593.1)
                                                    Institut für Neuropathologie,
pCMV-rSV2A_N364K-GFP
                                                    Universitätsklinikum Bonn
pCMV-rSV2A_H387Q-GFP

pCMV-rSV2A_H387Q_T395I-GFP

pCMV-rSV2A_T395I-GFP

pCMV-rSV2A_E403D-GFP

Enzymes

BamHI

BsiWI

ClaI

EcoRI
                                                    New England BioLabs
FspI

NotI

SalI

StuI

Pyrobest^{TM} DNA Polymerase   TaKaRa

AccuPrime^{TM} Pfx DNA Polymerase   Invitrogen

KOD Hot Start DNA Polymerase   Novagen

T4 DNA ligase   New England BioLabs

Primer for cloning

name	sequence (5' to 3')	restriction site
f-rSV2A-GFP-NotI	GAGCTAGCGGCCGCACCATGGAAGAAGGCTTTCGAG	NotI
r-GFP-BsiWI	CATCATCGTACGTTACTTGTACAGCTCGTCCATGC	BsiWI
f-rSV2A-ATG-EcoRI	ATTCAGAATTCACCATGGAAGAAGGCTTTCGAG	EcoRI
f-rSV2A-Exon5-BamHI	ATAGTGGATCCTGAGAAGACTCGCTCAGGATGG	BamHI
f-hSV2A-ATG-EcoRI	ATTCAGAATTCATGGAAGAGGGCTTCCGAG	EcoRI
r-hSV2A-SalI	AGTTTGTGTCGACCTGCAGCACCTGCCCCC	SalI
f-hSV2A-NotI	GAGCTAGCGGCCGCACCATGGAAGAGGGCTTCCGAGAC	NotI
f-hSV2B-ATG-ClaI	ATTCAATCGATATGGATGACTACAAGTATCAG	ClaI
r-hSV2B-SalI	AGTTTGTGTCGACCATCAGGACCTGTTCTCGA	SalI
f-rSV2C-ATG-ClaI	ATTCAATCGATATGGAAGACTCCTACAAGGATAG	ClaI
r-rSV2C-SalI	AGTTTGTGTCGACCATCAGAACCTGGGTTCTTGTG	SalI
f-hGluR2-ATG-NotI	TCAATCAGCGGCCGCATGCAAAAGATTATGCATATTTCTG	NotI
r-hGluR2-TAG-BsiWI	CATTCACGTACGCTAAATTTTAACACTTTCGATGCC	BsiWI

Primer for sequencing

name	sequence (5' to 3')
f-pQCXI-Seq	ACGCCATCCACGCTGTTTTGACCT
r- pQCXI-Seq	GGCCTTATTCCAAGCGGCTTCG
f-pCMV	CGCAAATGGGCGGTAGGCGTG
r-pCMV	ACAAGGCTGGTGGGCACTGG
r-rSV2A-Seq1	GGAACACTTTGGTTCGGGCTG
f- rSV2A Seq2	GATTGGTGGCGTGTATGCAGC
f-rSV2A-Seq3	CAGCCCGAACCAAAGTGTTCC
f-rSV2A-Seq4	TCAGCTTCTTGGGGACACTGG
f-rSV2A-Seq5	GCTCTGAAGCTGCCTGAGACC
f-hSV2A-Seq1 (f-hSV2A-ATG-EcoRI)	ATTCAGAATTCATGGAAGAGGGCTTCCGAG
r-hSV2A-Seq2	GGAACACTTTGGTGCGGGATG
f- hSV2A-Seq3	GATTGGTGGCGTGTACGCAGC
f-hSV2A-Seq4	CATCCCGCACCAAAGTGTTCC
f-hSV2A-Seq5	GCCCTGAAGCTGCCTGAGACC
f-hSV2B-Seq1 (f-hSV2B-ATG-ClaI)	ATTCAATCGATATGGATGACTACAAGTATCAG
f-hSV2B-Seq2	GGAGAACACCTCAGTTGGC
f-hSV2B-Seq3	CACCAACATGGGAAACTTGTG
f-hSV2B-Seq4	CCTTCGACTGCCAGAGACT
f-rSV2C-Seq1 (f-rSV2C-ATG-ClaI)	ATTCAATCGATATGGAAGACTCCTACAAGGATAG
f-rSV2C-Seq2	AGACAAAGTGGGAAGGAAGC
f-rSV2C-Seq3	ATGGACTGTCCGTTTGGTTC
f-rSV2C-Seq4	GAACGCACTCTGTAAAGCAG
f-hGluR2-Seq1	CATTCACGTACGAGAAAGATCCTCAGCACTTTCG
f-hGluR2-Seq2	TTTCCTTGGGTGCCTTTATG

marker, dyes, antibodies, reagents, kits

Lambda DNA/EcoRI+HindIII marker	Fermentas, SM0191
ΦX174 DNA-HaeIII Digest	New England BioLabs, N3026S
6x Gel Loading Dye, blue	New England BioLabs, B7021S
GelRed^{TM} nucleic acid gel stain	New England Biotium, 41003
Lipofectamine^{TM} 2000 Transfection Reagent	Invitrogen, 11668019
Zymoclean^{TM} Gel DNA Recovery Kit	Zymo Research, D4001
DNA clean & concentrator^{TM} -5 Kit	Zymo Research, D4003
ZR Plasmid Miniprep^{TM} - Classic	Zymo Research, D4015
S.N.A.P.^{TM} Midi Prep Kit	Invitrogen, K1910-01
Pure Link^{TM} HiPure Plasmid Filter Midiprep Kit	Invitrogen, K2100-15
Zyppi Plasmid Maxiprep Kit	Zymo Research, D4028
Pure Link^{TM} HiPure Plasmid Filter Maxiprep Kit	Invitrogen, K2100-17

8.1.3.4 Media, supplements and solutions for cell culture

DMEM	Dulbecco's Modified Eagle Medium, Gibco/Invitrogen
DMEM/F12	Dulbecco's Modified Eagle Medium – Nutrient Mixture F-12, Gibco/Invitrogen
Opti-MEM	Opti-MEM I Reduced Serum Medium, Gibco/Invitrogen
FCS	Fetal Bovine Serum, Sigma F7524
PS	Penicillin-Streptomycin solution, Gibco 15140
Hygromycin B	Hygromycin B Solution (100 mg/ml), Merck, 400052
G418	G418 solution (100 mg/ml), InvivoGen, ant-gn-5
CS	Calf Serum, Sigma, C8056
HXM	Hypoxanthine Xanthine Mycophenolic acid solution, see 8.1.3.5
Trypsin/EDTA	Trypsin (0.05%) / EDTA (0.6 mM) solution, see 8.1.3.5

8.1.3.5 Buffer and solutions for membrane preparations and binding studies

Sucrose solution (0.32 M)

D(+)-Sucrose	$M_r = 342.30$	0.32 M	110 g
Water, deionized, autoclaved			1 l

The solution needs to be prepared freshly prior to use.

HEPES buffer (10 mM, pH 7.4)

HEPES	$M_r = 238.30$	10 mM	2.38 g
NaCl	$M_r = 58.44$	80 mM	4.68 g
KCl	$M_r = 74.55$	3.6 mM	0.27 g
$MgCl_2 \cdot 6\ H_2O$	$M_r = 203.30$	0.53 mM	0.11 g
$CaCl_2 \cdot 2\ H_2O$	$M_r = 147.01$	1.2 mM	0.18 g
Water, deionized			1 l

pH is adjusted to 7.4 at 4 °C with saturated NaOH solution. The buffer is stored at 4 °C.

Tris-HCl buffer (50 mM, pH 7.4)

Tris	$M_r = 121.14$	50 mM	6.05 g
Water, deionized			1 l

pH is adjusted to 7.4 with HCl 37%. The buffer is stored at 4 °C.
If not indicated otherwise, Tris-HCl buffer used in this study always was 50 mM, pH 7.4

MgCl₂ solution (10 mM)

$MgCl_2$	$M_r = 95.21$	10 mM	95 mg
Tris-HCl buffer (50 mM, pH 7.4)			100 ml

The solution is stored at 4 °C.

Levetiracetam solution (5 and 50 mM) for non-specific binding

Levetiracetam	$M_r = 170.21$	5 mM	8.5 mg
		50 mM	85 mg
Tris-HCl buffer (50 mM, pH 7.4)			10 ml

The solution is stored at 4 °C.

PEI solution (0.1%)

PEI solution (50% in H_2O)			1 ml
Water, deionized			ad 500 ml

The solution is stored at 4 °C.

KSCN solution (1 M)

KSCN	$M_r = 97.18$	1 M	9.72 g
Tris-HCl buffer (50 mM, pH 7.4)			100 ml

100 µl of this solution in a final volume of 500 µl equal a concentration of 250 mM. The solution is stored at 4 °C

L-Glutamic acid solution (5 mM) for non-specific binding

L-Glutamic acid	$M_r = 147.13$	5 mM	74 mg
Tris-HCl buffer (50 mM, pH 7.4)			100 ml

100 µl of this solution in a final volume of 500 µl equal a concentration of 1 mM. The solution is stored at 4 °C.

Tris (20 mM) / Sucrose (250 mM) solution

D(+)-Sucrose	$M_r = 342.30$	250 mM	8.6 g
Tris-HCl buffer (50 mM, pH 7.4)			40 ml
Water, deionized			60 ml

pH is adjusted to 7.4 with HCl 37%. The solution is stored at 4 °C.

Tris (10 mM) / NaCl (150 mM) solution

NaCl	$M_r = 58.44$	150 mM	877 mg
Tris-HCl buffer (50 mM, pH 7.4)			20 ml
Water, deionized			80 ml

pH is adjusted to 7.4 with HCl 37%. The solution is stored at 4 °C.

Saponin solution (1%)

Saponin	1%	0.1 g
Water, deionized		10 ml

Saponin is dissolved in water. The solution is stored at 4 °C.

Reagent A for *Lowry* protein determination

Na_2CO_3	2%	10 g
NaOH solution (0.1 N)		ad 500 ml

The solution is stored at rt.

Reagent B for *Lowry* protein determination

CuSO$_4$ · 5 H$_2$O	0.5%	0.25 g
Sodium tartrate	1%	0.5 g
Water, deionized		ad 50 ml

Both salts are dissolved in water separately and combined afterwards. The solution is stored at 4 °C.

Reagent C for *Lowry* protein determination

Reagent A	50 parts
Reagent B	1 part

The reagent needs to be prepared freshly prior to use.

Reagent D: Folin & Ciocalteau's phenol reagent working solution

Folin reagent	18 ml
Water, deionized	ad 90 ml

The solution is stored at rt.

8.1.3.6 Buffer/solutions for molecular biology, cell and bacteria culture

LB medium

LB medium	25 g
Water, deionized	ad 1 l

LB medium is given into deionized water and the suspension is autoclaved. The solution is stored at 4 °C.

LB medium with ampicillin (100 μg/ml)

LB medium	25 g
Water, deionized	ad 1 l
Ampicillin (100 mg/ml)	1 ml

LB medium is given into deionized water and the suspension is autoclaved. Ampicillin is added after the solution has cooled down < 50 °C. The solution is stored at 4 °C.

LB agar plates with ampicillin

LB agar		32 g
Water, deionized		ad 1 l
Ampicillin (100 mg/ml)		1 ml

LB agar is given into deionized water and the suspension is autoclaved. Ampicillin is added after the solution has cooled down $< 50\,°C$. Approximately 15-20 ml of this solution is poured into each petri dish of 10 mm diameter. After the agar solidified the plates are stored face down in a plastic bag at $4\,°C$.

CaCl$_2$ solution (0.1 M), sterile

CaCl$_2$	$M_r = 110.98$	0.1 M	1.1 g
Water, deionized			ad 100 ml

CaCl$_2$ is dissolved in deionized water, sterilized via sterile filtration and stored at $4\,°C$.

TAE buffer 50x (for agarose gel electrophoresis)

Tris	$M_r = 121.14$	2 M	242 g
EDTA	$M_r = 292.24$	50 mM	14.6 g
Acetic acid			57.1 ml
Water, deionized			ad 1 l

The buffer is autoclaved and diluted 1:50 prior to use. It is stored at rt.

6x loading dye (for agarose gel electrophoresis)

Bromophenol blue sodium salt	0.25%	
Glycerol		5 ml
Water, deionized		5 ml

The loading dye is stored at $4\,°C$.

Sodium butyrate solution (500 mM)

Sodium butyrate	$M_r = 110.09$	500 mM	55 mg
Water, deionized			1 ml

After sterile filtration, the solution is stored at -20° C.

Polybrene solution (4 mg/ml)

Polybrene	20 mg
Water, deionized	5 ml

After sterile filtration, the solution is stored at -20° C.

EDTA stock solution (0.1 M)

EDTA	$M_r = 292.24$	0.1 M	2.9 g
Water, deionized			100 ml

After pH adjustment to 7.6, the solution is stored at rt.

Hypoxanthine Xanthine Mycophenolic acid solution (HXM)

Hypoxanthine	75 mg
Xanthine	1250 mg
Mycophenolic acid	125 mg
NaOH solution (6 N)	q.s.
Methanol	5 ml
Water, deionized	45 ml

To a suspension of hypoxanthine and xanthine in 40 ml of deionized water NaOH solution (6 N) is added dropwise until the solution becomes clear. Deionized water is added ad 45 ml. In a separate vial mycophenolic acid is dissolved in methanol and the two solutions are mixed. After sterile filtration, aliquots (à 5 ml) of the solution are prepared and stored at -20° C, protected from light.

PBS buffer

NaCl	$M_r = 58.44$	1.5 M	8.8 g
KCl	$M_r = 74.55$	25 mM	0.2 g
Na_2HPO_4	$M_r = 141.96$	75 mM	1.1 g
KH_2PO_4	$M_r = 136.09$	15 mM	0.2 g
Water, deionized			1 l

After pH adjustment to 7.4 with HCl 37%, the buffer is autoclaved and stored at rt.
PBS 10x buffer is prepared in analogy except that amounts of salts are multiplied by 10.

Trypsin (0.05%) / EDTA (0.6 mM) solution

EDTA stock solution (0.1 M)	0.6 mM	6 ml
Trypsin (2.5%)	0.05%	20 ml
Phenol red solution (0.5%)		750 µl
PBS buffer		ad 1 l
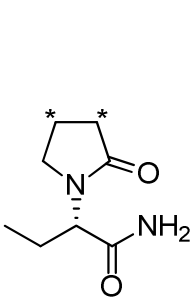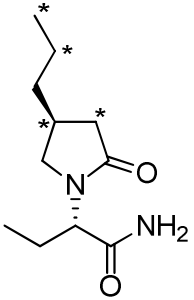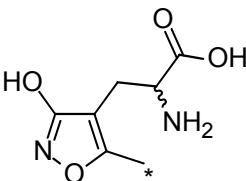
EDTA stock solution is given into PBS buffer and the solution is autoclaved. After the solution has cooled down to rt, trypsin (sterile filtrated) and phenol red solution (sterile filtrated) are added under laminar air-flow. The solution is stored at 4 °C.

8.1.3.7 Radioligands

The radioligands [³H]LEV, [³H]isoBRV and [³H]BRV were obtained from Quotient Bioresearch (UK) by labeling previously synthesized precursors (see chapter 8.2). These radioligands are solved in ethanol (1 mCi/ml). Radioligand [³H]AMPA (racemic mixture) was obtained from PerkinElmer (USA) in a solution of ethanol : water (1 : 1) in a concentration of 1 mCi/ml.

Table 15: Chemical structures of radioligands applied within this study.

name	[³H]levetiracetam		[³H]brivaracetam	[³H]R,S-AMPA
internal code	[³H]LEV	[³H]isoBRV	[³H]BRV	[³H]AMPA
code (supplier)	TRQ40411	TRQ40412	TRQ40419	
specific activity	98 Ci/mmol	98 Ci/mmol	94 Ci/mmol	45.8 Ci/mmol
radiochem. purity	99.7%	99.3%	99.5%	> 97%

8.1.3.8 Tissue

Sprague-Dawley rat brain	56004-2, Pel Freez®, Rogers, Arkansas, USA
Black 6 mouse brain	provided by Prof. Dr. V. Gieselmann,
	Institut für Biochemie und Molekularbiologie,
	Universität Bonn
SV2A KO mouse brain	provided by Prof. Dr. S. Schoch,
	Institut für Neuropathologie,
	Universitätsklinikum Bonn
human brain from epilepsy surgery	Institut für Neuropathologie,
	Universitätsklinikum Bonn
human post-mortem brain	Institut für Neuropathologie,
	Universitätsklinikum Bonn

8.2   Syntheses

8.2.1   Synthesis of [³H]levetiracetam

(S)-Methyl 2-aminobutanoate hydrochloride (5)[167]
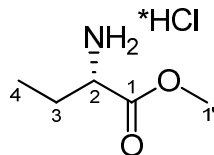
The ester was prepared in analogy to Klieger and Gibian.[167] Freshly distilled thionyl chloride (30 mmol, 2.6 ml) was added dropwise to 10 ml of methanol previously cooled to -20 °C. (S)-2-aminobutyric acid (10 mmol, 1.0 g) was added and the mixture was stirred at room temperature for several hours. The reaction progress was monitored by TLC and if needed additional thionyl chloride was added until the reaction was completed. At the end of the reaction the solvent was removed by distillation. The remaining residue is recrystallized from diethylether giving the product in nearly quantitative yield (lit.: 80%).[167]

Appearance: white crystalline powder. **Solubility:** soluble in chloroform, methanol, water. **Detection:** Ninhydrin reagent. **Melting point:** 116 °C (lit.: 116-117 °C).[167] **^{1}H NMR (500 MHz, CDCl$_3$)** δ ppm 1.08 (t, 3H, J = 7.43, C4H), 2.07-2.13 (m, 2H, C3H), 3.78 (s, 3H, C1'H), 4.09-4.13 (m, 1H, C2H), 8.73 (s, 3H, NH$_3^+$Cl$^-$). **^{13}C NMR (125 MHz, CDCl$_3$)** δ ppm 9.63 (CH, C4), 23.78 (CH, C3), 53.04 (CH, C1'), 54.40 (CH, C2), 169.77 (Cq, C1).

(S)-2-Aminobutanamide (6)[228]
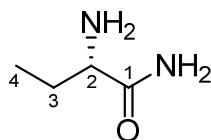
(S)-Methyl 2-aminobutanoate hydrochloride (1 mmol, 153 mg) was dissolved in 6 ml of ammonia (7 M) in methanol. The solution was stirred under microwave irradiation (70 W) at 100 °C for 240 min. The mixture was evaporated to dryness and the residue was purified by column chromatography (gradient of dichloromethane : methanol of 100 : 0 to 70 : 30, containing 2% aqueous ammonia solution). Pure fractions were

combined, evaporated to dryness and subsequently dissolved in water and lyophilized (yield 77%).

Appearance: clear liquid. **Solubility:** soluble in chloroform, methanol, water. **Detection:** Ninhydrin reagent. **^{1}H NMR (500 MHz, CDCl$_3$)** δ ppm 0.95 (t, 3H, J = 7.55, C4H), 1.52-1.60 (m, 1H + 2H, C3H + NH$_2$), 1.78-1.87 (m, 1H, C3H), 3.28-3.30 (m, 1H, C2H), 5.79, 7.03 (2 s, 1H each, CONH$_2$). **^{13}C NMR (125 MHz, CDCl$_3$)** δ ppm 9.94 (CH, C4), 27.97 (CH, C3), 56.32 (CH, C2), 178.16 (Cq, C1). Obtained data corresponded to published data.[228]

(*S*)-2-(3,4-Dichloro-2,5-dihydro-2-oxo-1*H*-pyrrol-1-yl)butanamide (8)[165]
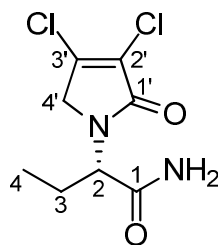
Mucochloric acid (2 mmol, 338 mg) and (*S*)-2-aminobutanamide (2 mmol, 204 mg) were dissolved in a mixture of 10 ml of chloroform and 0.2 ml of acetic acid. After addition of sodium triacetoxyborohydride (3 mmol, 636 mg, 1.5 equiv.) the mixture was stirred at room temperature for several hours. The reaction progress was monitored by TLC. After approximately 20 h a saturated solution of ammonium chloride (20 ml) was added to the reaction mixture. The product was extracted from the aqueous phase with chloroform (3 x 20 ml). The organic layers were collected and washed with water (20 ml) and subsequently with brine (10 ml). After drying over Na$_2$SO$_4$, the solvent was evaporated, and the residue purified by column chromatography eluting with cyclohexane : ethyl acetate (1 : 4). Yield 75% (lit.: 62%).[165]

Appearance: white crystalline powder. **Solubility:** soluble in chloroform, ethanol, methanol. **TLC:** R$_f$ = 0.38 (cyclohexane : ethyl acetate, 1:4). **Detection:** UV absorption at 254 nm, Ninhydrin reagent. **Melting point**: > 140 °C (decomp.). **^{1}H NMR (500 MHz, CDCl$_3$)** δ ppm 0.94 (t, 3H, J = 7.43, C4H), 1.70-1.79, 1.95-2.04 (2 m, 1H each, C3H), 4.04, 4.34 (AB-system, 2H, J = 18.9, C4'H), 4.55-4.59 (m, 1H, C2H), 5.42, 6.17 (2 br, 1H each, NH$_2$). **^{13}C NMR (125 MHz, CDCl$_3$)** δ ppm 10.42 (CH, C4), 22.42 (CH, C3), 50.98 (CH, C4'), 56.39 (CH, C2), 124.73 (Cq, C2'), 141.37 (Cq, C3'), 165.00

(Cq, C1'), 171.40 (Cq, C1). **LC-MS** *m/z* 237 ([M + H]$^+$). **[α]$^{20}_D$:** -21.2 (c = 0.33, CHCl$_3$).

(2*S*)-2-(2-Oxopyrrolidin-1-yl)butanamide (1)[165]
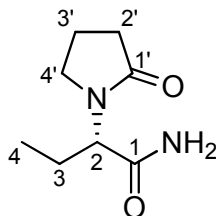
(*S*)-2-(3,4-Dichloro-2,5-dihydro-2-oxo-1*H*-pyrrol-1-yl)butanamide (50 mg, 0.2 mmol) was dissolved in 2 ml ethanol. Triethylamine (0.07 ml, 0.5 mmol) and dry 10% Pd/C (5 mg) were added and the mixture was hydrogenated at 50 psi for 2 hours while stirring at room temperature. The mixture was filtrated (elution with dichloromethane) through a short column of silica gel, which previously has been washed with hexane to remove lipophilic impurities. The filtrate was evaporated to dryness giving the product with nearly quantitative yield (lit.: 91%).[165]

Appearance: white crystalline powder. **Solubility:** soluble in chloroform, ethyl acetate, methanol, water. **Melting point:** 116-119 °C (lit.: 115-117 °C).[229] **^{1}H NMR (500 MHz, CDCl$_3$)** δ ppm 0.89 (t, 3H, *J* = 7.40, C4H), 1.67, 1.95 (2 m, 1H each, C3H), 2.02 (m, 2H, C3'H), 2.40 (m, 2H, C2'H), 3.41 (m, 2H, C4'H), 4.43 (dd, 1H, *J* = 8.85, 6.95, C2H), 5.47, 6.28 (2 s, 1H each, CONH$_2$). **^{13}C NMR (125 MHz, CDCl$_3$)** δ ppm 10.5 (CH, C4), 18.1 (CH, C3'), 20.9 (CH, C3), 31.1 (CH, C2'), 43.9 (CH, C4'), 56. 1 (CH, C2), 172.1 (Cq, C1'), 176. 1 (Cq, C1).

(2*S*)-[3,4-^{3}H]2-(2-Oxopyrrolidin-1-yl)butanamide (3)
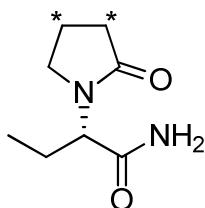
The labeling of (2*S*)-2-(2-oxopyrrolidin-1-yl)butanamide with tritium was performed by Quotient Bioresearch, UK using the following procedure: (2*S*)-2-(2-oxopyrrolidin-1-

yl)butanamide (3 mg) and 10% palladium on charcoal (20 mg) were stirred in ethanol (2 ml) containing *N,N*-diisopropylethylamine (100 µl) in the presence of tritium gas (10 Ci) for 4 hours. Labile tritium was removed by repeated evaporation to dryness from ethanol. The crude yield was 850 mCi and the radiochemical purity was 60%. Purification of the radioligand was performed by HPLC (detection at 205 nm) leading to a radiochemical purity of 99.7%. The specific activity was determined to be 98 Ci/mmol (3.6 TBq/mmol).

8.2.2 Synthesis of [^{3}H]brivaracetam

4-Allyl-5-hydroxyfuran-2(5*H*)-one (22)
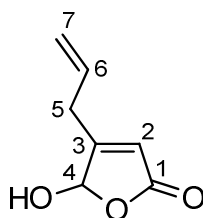
The synthesis was performed in analogy to the procedure described by Bourguignon and Wermuth.[180] Glyoxylic acid monohydrate (10 mmol, 0.92 g) and morpholine hydrochloride (11 mmol, 1.4 g) were suspended in 8 ml dioxane. Under continuous stirring 2.5 ml of water and freshly distilled pent-4-enal (10.5 mmol, 1.0 ml) were added dropwise. The mixture was stirred for 1 h at room temperature until it became homogenous. It was then heated under reflux for 24 h. For the workup dioxane was removed by evaporation under vacuum. The product was extracted from the remaining aqueous residue with diethyl ether (3 x 20 ml). The organic phases were combined and washed with water. After drying with Mg$_2$SO$_4$ it was evaporated to dryness. Purification was performed by column chromatography using dichloromethane : ethyl acetate (9 : 1) for elution. Yield 42%.

Appearance: yellowish liquid. **Solubility:** soluble in diethyl ether, chloroform, methanol. **TLC:** R$_f$ = 0.49 (cyclohexane : ethyl acetate, 1:1). **Detection:** UV absorption at 254 nm, Ninhydrin reagent. **^{1}H NMR (500 MHz, CDCl$_3$)** δ ppm 3.02-3.25 (m, 2H, C5H), 5.19-5.21, 5.22-5.23 (2 m, 1H each, C7H), 5.80-5.88 (m, 2H, C2H+C6H), 6.01 (s, 1H, C4H). **^{13}C NMR (125 MHz, CDCl$_3$)** δ ppm 31.8 (CH, C5), 98.8 (CH, C4), 118.1 (CH, C2), 119.4 (CH, C7), 131.3 (CH, C6), 167.8 (Cq, C3), 171.4 (Cq, C1). **LC-MS** *m/z* 138.9 ([M - H]$^-$).

(*S*)-2-(4-Allyl-2-oxo-2,5-dihydro-1*H*-pyrrol-1-yl)butanamide (27)
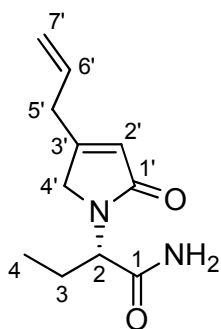
The reaction is performed essentially as described in 8.2.1 applying similar conditions as described by Das Sarma et al.:[165] 4-allyl-5-hydroxyfuran-2(5*H*)-one (3.6 mmol, 0.50 g) and (*S*)-2-aminobutanamide (3.6 mmol, 0.37 g) were given into a mixture of 15 ml of chloroform and 0.4 ml of acetic acid. Sodium triacetoxyborohydride (5.4 mmol, 1.1 g, 1.5 equiv.) was added and the mixture was stirred at room temperature for several hours, while reaction progress was monitored by TLC. After completion of the reaction (approximately 24 h), a saturated solution of ammonium chloride (15 ml) was added to the reaction mixture. The product was extracted from the aqueous phase with chloroform (3 x 15 ml). The organic layers were combined and after washing with water (2 x 20 ml) and subsequently with brine (20 ml), the organic phase was dried over Mg_2SO_4. The solvent was evaporated under vacuum and the remaining residue purified by column chromatography eluting with dichloromethane : methanol (9 : 1). Yield 53%.

The sample used for labeling with tritium was further purified by preparative HPLC: Elution was performed with methanol : H_2O, 30 : 70 for 10 min, then a gradient to a final ratio of 50 : 50 was run over 40 min. The product was eluted at a retention time of 19.6 min, detection was performed by UV absorption at 254 nm.

Appearance: yellow waxy solid. **Solubility:** soluble in chloroform, methanol. **TLC:** R_f = 0.51 (dichloromethane : methanol, 9:1). **Detection:** UV absorption at 254 nm, Ninhydrin reagent. **Melting point:** 72-74 °C. **¹H NMR (500 MHz, CDCl₃)** δ ppm 0.89 (t, 3H, *J* = 7.43, C4H), 1.67-1.76, 1.94-2.03 (2 m, 1H each, C3H), 3.09-3.11 (m, 2H, C5'H), 3.84-3.88, 4.01-4.05 (2 m, 1H each, C4'H), 4.48-4.51 (m, 1H, C2H), 5.12-5.16 (m, 2H, C7'H), 5.54 (br, 1H, NH₂), 5.77-5.86 (m, 2H, C6'H+C2'H), 6.44 (br, 1H, NH₂). **¹³C NMR (125 MHz, CDCl₃)** δ ppm 10.6 (CH, C4), 22.2 (CH, C3), 34.1 (CH, C4'), 51.6 (CH, C5'), 55.8 (CH, C2), 118.4 (CH, C7'), 121.9 (CH, C2'), 132.8 (CH, C6'), 159.2 (Cq, C3'), 172.4, 172.6 (Cq, C1'+C1). **LC-MS** *m/z* 207.1 ([M - H]⁻).

(2*S*)-2-(2-Oxo-4-propylpyrrolidin-1-yl)butanamide (21)

(diastereomeric mixture of brivaracetam[70])
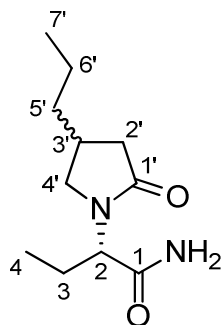
The precursor molecule **27** (0.18 mmol, 37 mg) was given into a hydrogenation vial containing 2 ml of ethanol. A catalytic amount of dry 10% palladium on charcoal (40 mg) was added and the suspension was hydrogenated at 50 psi for 1 h while stirring at room temperature. The reaction mixture was then filtered through Celite® eluting with methanol. The obtained filtrate was evaporated to dryness under vacuum and subsequently purified by preparative HPLC: elution was performed with methanol : H_2O, 30 : 70 for 20 min, continuing with a gradient to a ratio of 50 : 50 within 40 min, then a gradient to a final concentration of 100% methanol was run over 10 min. The product was eluted at a retention time of 42.5 min, detection was performed by UV absorption at 205 nm.

Appearance: white crystalline solid. **Solubility:** soluble in chloroform, ethyl acetate, methanol. **Melting point:** 77 °C. **^{1}H NMR (500 MHz, CDCl$_3$)** δ ppm 0.87-0.91 (m, 6H, C7'H+C4H), 1.27-1.34 (m, 2H, C6'H), 1.36-1.43 (m, 2H, C5'H), 1.62-1.71, 1.88-1.97 (2 m, 1H each, C3H), 2.03-2.14 (m, 1H, C2'H), 2.28-2.36 (m, 1H, C3'H), 2.48-2.59 (m, 1H, C2'H), 2.97-3.00, 3.45-3.53 (2 m, 1H each, C4'H), 4.39-4.44 (m, 1H, C2H), 5.39, 6.20 (2 br, 1H each, NH$_2$). **^{13}C NMR (125 MHz, CDCl$_3$)** δ ppm 10.4, 10.5 (CH, C4)*, 14.0 (CH, C7'), 20.5, 20.6 (CH, C6')*, 20.8, 20.9 (CH, C3)*, 31.8, 31.9 (CH, C3')*, 36.6, 36.8 (CH, C5')*, 37.6, 37.9 (CH, C2')*, 49.5, 49.7 (CH, C4')*, 56.0 (CH, C2), 171.9, 172.2 (Cq, C1')*, 175.5, 175.7 (Cq, C1)* [*double signals result from diastereomeric mixture]. **LC-MS** *m/z* 213.3 ([M + H]$^+$).

(2S)-[³H]2-(2-Oxo-4-propylpyrrolidin-1-yl)butanamide (28, mixture of **9** and **29)**
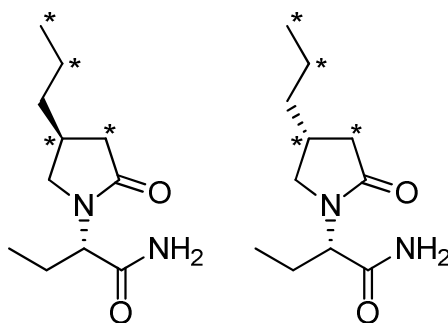
Compound (S)-2-(4-allyl-2-oxo-2,5-dihydro-1H-pyrrol-1-yl)butanamide was labeled with tritium by Quotient Bioresearch according to the following procedure: 3 mg of (S)-2-(4-allyl-2-oxo-2,5-dihydro-1H-pyrrol-1-yl)butanamide and 10 mg 10% palladium on charcoal were given into 2 ml of ethanol and stirred in the presence of tritium gas (10 Ci) for 4 h. The suspension was filtered to remove catalyst and subsequently repeatedly evaporated to dryness from ethanol to remove labile tritium. The crude yield obtained was 1.5 Ci and radiochemical purity was determined to be greater than 90%. Separation of diastereomers was achieved by chiral HPLC (Chiralpak AD-H 5 µm, 250 x 46 mm column, isocratic elution with ethanol : hexane (55 : 45) at 25 °C with a flow rate of 1 ml/min, UV detection at 205 nm). [³H]BRV was eluted after 8.75 min with a radiochemical purity of 99.5% and a specific activity of 94 Ci/mmol (3.5 TBq/mmol). [³H]isoBRV was obtained with a retention time of 6.52 min with a radiochemical purity of 99.3% and a specific activity of 98 Ci/mmol (3.6 TBq/mmol).

8.2.3   Synthesis of brivaracetam

4-n-Propylbutyrolacton (13)[70] (via Grignard reagent)
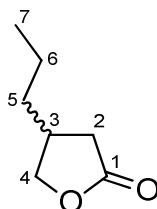
Reaction conditions for the preparation of the Grignard reagent n-propylmagnesiumbromide (**11**) were adopted from a published procedure of a Grignard reagent.[230] Therefore, magnesium turnings (100 mmol, 2.43 g) were placed in a reaction vial, which was flame-dried and flushed with argon afterwards. 12 ml of diethyl ether were added to cover the turnings. Under continuous stirring, 1 ml of a solution of

n-propylbromide (88 mmol, 8.0 ml) in 28 ml of diethyl ether was added and the reaction was started by cautious heating. The n-propylbromide solution was then added dropwise in a rate to maintain a gentle reflux. After addition has been completed the mixture was gently refluxed for 30 more minutes. The freshly prepared Grignard reagent (assumed concentration: 1.76 mmol/ml in diethyl ether) was directly used for the next reaction step.

To prepare the propyl-substituted lactone (**13**) in accordance to the procedure described by Kenda et al.[70] copper(I) iodide (8.2 mmol, 1.6 g) was placed in a reaction vessel, which was flame-dried and filled with argon afterwards. 3 ml of diethyl ether were added to cover the copper(I) iodide. The suspension was cooled down to -20 °C (acetone/dry ice) and the Grignard reagent **11** (16.4 mmol, 9.32 ml) was added dropwise under stirring. It was then stirred for 30 more minutes at -20 °C, before the mixture was cooled down to -40 °C and trimethylsilyl chloride (8.2 mmol, 1.1 ml) was added dropwise. Subsequently, a solution of the furanone **12** (8.2 mmol, 0.58 ml) in 5 ml of diethyl ether was added dropwise. The cooling system was removed and after stirring at room temperature for 30 more minutes saturated ammonium chloride solution (20 ml) was added for cleavage of the formed trimethylsilyl ester. The mixture was filtered to remove copper salts and then the product was obtained by extraction (3 x 20 ml) with ethyl acetate. The organic layers were combined, washed with H_2O, dried over Na_2SO_4 and evaporated to dryness in vacuum. The lactone was used for the following reaction step without further purifications.

Appearance: clear liquid. **Solubility:** soluble in dichloromethane, ethyl acetate. **^{1}H NMR (500 MHz, CDCl$_3$)** δ ppm 0.92 (t, 3H, J = 7.25, C7H), 1.25-1.44 (m, 4H, C5H+C6H), 2.16 (dd, 1H, J = 17.0, 7.85, C2H), 2.50-2.63 (m, 2H, C2H+C3H), 3.90, 4.39 (2 dd, 1H each, J = 9.15, 6.95, C4H). **^{13}C NMR (125 MHz, CDCl$_3$)** δ ppm 13.9 (CH, C7), 20.6 (CH, C6), 34.5, 35.2, 35.5 (CH, C5, C2, C3), 73.4 (CH, C4), 177.3 (Cq, C1). **LC-MS** *m/z* 126.8 ([M - H]$^-$).

3-(Iodomethyl)-hexanoic acid (14)[70]
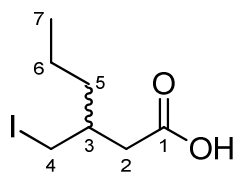
The crude lactone **13** (6.5 mmol, 0.83 g) was dissolved in 6 ml dichloromethane and the solution was cooled down to 0 °C. Under stirring, trimethylsilyl iodide (7.2 mmol, 1.0 ml, 1.1 equiv.) was added dropwise. It was stirred for 2 further hours at room temperature. Afterwards, 7.2 ml HCl 1 M was added followed by 2.5 ml 10% sodium thiosulfate solution. The product was extracted from the aqueous phase with dichloromethane (3 x 10 ml). Organic layers were combined, washed with brine, dried over Na_2SO_4 and evaporated to dryness under vacuum. The product was used without further purification.

Appearance: dark yellow liquid. **Solubility:** soluble in dichloromethane. **^{1}H NMR (500 MHz, CDCl$_3$)** δ ppm 0.89-0.93 (m, 3H*, C7H), 1.25-1.36 (m, 4H*, C5H+C6H), 1.69-1.76 (m, 1H, C3H), 2.36, 2.45 (2 dd, 1H each, *J* = 16.4, 7.25, C2H), 3.29, 3.38 (2 dd, 1H each, *J* = 10.1, 4.10, C4H) [*signals superimposed by impurity from reactant (Grignard)]. **^{13}C NMR (125 MHz, CDCl$_3$)** δ ppm 13.9 (CH, C7), 14.6 (CH, C4), 19.6 (CH, C6), 35.3 (CH, C3), 36.5 (CH, C5), 38.9 (CH, C2), 176.3 (Cq, C1). Obtained data corresponded to published data.[70]

(*S*)-2-(*tert*-Butoxycarbonylamino)butanoic acid (15)[231]
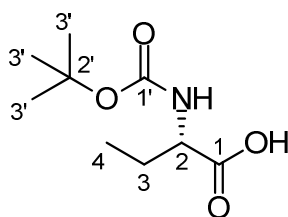
For N-protection of the amino acid, (*S*)-2-aminobutyric acid (50 mmol, 5.2 g) was given into a mixture of 25 ml dioxane and 20 ml H_2O, which was cooled down to 0 °C. Sodium hydroxide (55 mmol, 2.2 g, 1.1 equiv.) was dissolved in 10 ml of H_2O and given into the reaction mixture. After addition of di-*tert*-butyl dicarbonate (55 mmol, 12 g, 1.1 equiv.), the vessel was rinsed with 5 ml dioxane and the reaction mixture stirred at room temperature for 24 h. Dioxane was removed under vacuum, some more

H_2O was added and by addition of 10% sodium hydrogen sulfate solution the mixture was acidified to ~ pH 3. The product was extracted with ethyl acetate (3 x 30 ml), organic layers were combined and washed with brine. After drying with Mg_2SO_4, it was evaporated to dryness under vacuum. Yield: almost quantitative (lit.: 100%).[231]

Appearance: clear high-viscosity oil. **Solubility:** soluble in dichloromethane, chloroform, ethyl acetate, methanol. **TLC:** R_f = 0.28 (hexane : ethyl acetate, 2:1 + 1 drop acetic acid). **Detection:** Ninhydrin reagent. **^{1}H NMR (500 MHz, CDCl$_3$)** δ ppm 0.96 (t, 3H, *J* = 7.40, C4H), 1.43 (s, 9H, C3'H), 1.67-1.76, 1.85-1.93 (2 m, 1H each, C3H), 4.05-4.28 (2 m, 1H, C2H), 5.00, 6.17 (br d + br, 1H, *J = 7.5*, NH). **^{13}C NMR (125 MHz, CDCl$_3$)** δ ppm 9.6 (CH, C4), 25.6 (CH, C3), 28.3 (CH, C3'), 54.5 (CH, C2), 80.2 (Cq, C2'), 155.6 (Cq, C1'), 177.3 (Cq, C1). Obtained data corresponded to published data.[231] **LC-MS** *m/z* 202.1 ([M - H]$^-$).

(S)-4-Methoxybenzyl 2-(tert-butoxycarbonylamino)butanoate (17)
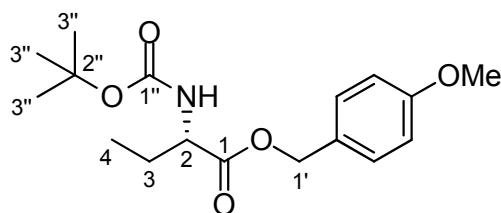
In analogy to esterification procedures described by Dutton et al.,[174] a solution of (*S*)-2-(*tert*-butoxycarbonylamino)butanoic acid (20 mmol, 4.1 g) in 30 ml anhydrous DMF was cooled down to 0 °C and cesium carbonate (20 mmol, 6.5 g, 1 equiv.) was added. After stirring for 1 h at 0 °C, 4-methoxybenzyl chloride (20 mmol, 2.7 ml, 1 equiv.) was given into the suspension and stirred for 30 further minutes at 0 °C. It was then left stirring at room temperature over night. For the workup the reaction mixture was poured into 100 ml H_2O and the product extracted with cyclohexane. The organic layers were combined, washed with saturated sodium hydrogen carbonate solution, brine and water, dried over Mg_2SO_4 and evaporated to dryness under vacuum. Absence of reactant (amino acid) was confirmed by TLC, before the product was precipitated as hydrochloride without further purifications.

Appearance: white crystalline solid. **Solubility:** soluble in cyclohexane, chloroform, dioxane, methanol. **TLC:** R_f = 0.71 (cyclohexane : ethyl acetate, 1:1). **Detection:** UV absorption at 254 nm, Ninhydrin reagent. **Melting point:** 61 °C. **^{1}H NMR (500 MHz,**

CD₃OD) δ ppm 0.86 (t, 3H, *J* = 7.25, C4H), 1.41 (s, 9H, C3''H), 1.61-1.69, 1.77-1.85 (2 m, 1H each, C3H), 3.79 (s, 3H, OMe), 4.23-4.28 (m, 1H, C2H), 4.98-5.13 (2 m, 3H, NH+C1'H), 6.86, 7.26 (2 d, 2H each, *J* = 8.80, Ar). **¹³C NMR (125 MHz, CD₃OD)** δ ppm 9.5 (CH, C4), 25.9 (CH, C3), 28.3 (CH, C3''), 54.6 (CH, C2), 55.3 (CH, OMe), 66.8 (CH, C1'), 79.7 (Cq, C2''), 113.9 (CH, Ar), 127.6 (Cq, Ar), 130.1 (CH, Ar), 155.3 (Cq, C1''), 159.7 (Cq, Ar), 172.7 (Cq, C1). **LC-MS** *m/z* 324.4 ([M + H]⁺).

(*S*)-4-Methoxybenzyl 2-aminobutanoate (base of **18**)
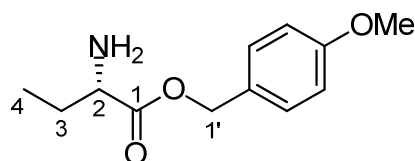
(S)-4-Methoxybenzyl 2-(*tert*-butoxycarbonylamino)butanoate was dissolved in 10 ml HCl/dioxane (4 M) and stirred at room temperature. After approximately 1.5 hours 20 ml diethyl ether were added dropwise and stirred for 2 additional hours. The formed precipitate was filtered, washed with diethyl ether and dried at 30 °C. To remove the carboxylic acid, which partially formed by acidic hydrolysis of the ester, the filtrate was dissolved in some H₂O, alkalized with saturated sodium hydrogen carbonate solution and directly extracted from the aqueous phase with dichloromethane.

Appearance: colorless liquid. **Solubility:** soluble in THF, chloroform. **Melting point (18):** > 235 °C (decomp.). **Detection:** UV absorption at 254 nm, Ninhydrin reagent. **¹H NMR (500 MHz, CDCl₃)** δ ppm 0.90 (t, 3H, *J* = 7.43, C4H), 1.55-1.64, 1.69-1.78 (2 m, 1H each, C3H), 3.38-3.40 (m, 1H, C2H), 3.79 (s, 3H, OMe), 5.04-5.09 (m, 2H, C1'H), 6.87 (d, 2H, *J* = 8.55, Ar), 7.27 (d, 2H , *J* = 8.85, Ar). **¹³C NMR (125 MHz, CDCl₃)** δ ppm 9.8 (CH, C4), 28.0 (CH, C3), 55.3 (CH, OMe), 55.7 (CH, C2), 66.4 (CH, C1'), 114.0 (CH, Ar), 127.9 (Cq, Ar), 130.1 (CH, Ar), 159.7 (Cq, Ar), 176.0 (Cq, C1). **LC-MS** *m/z* 223.9 ([M + H]⁺).

(2*S*)-4-Methoxybenzyl 2-(3-(iodomethyl)hexanamido)butanoate (19)
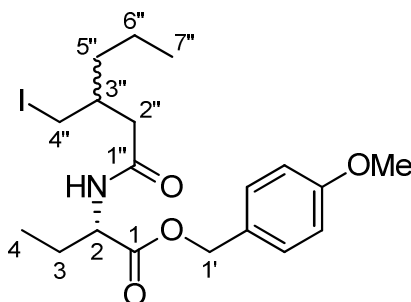
For the amide coupling reaction conditions were applied as formerly described by Herrmann et al.[175] 3-(Iodomethyl)-hexanoic acid (2.2 mmol, 0.56 g) was dissolved in 10 ml anhydrous THF and *N*-methylmorpholine (2.2 mmol, 0.22 g, 1 equiv.) was added. After the solution has been cooled down to -25 °C (dry ice/isopropanol) isobutyl chloroformate (2.2 mmol, 0.30 ml, 1 equiv.) was added under stirring. Approximately 1 min later a solution of (*S*)-4-methoxybenzyl 2-aminobutanoate (2.5 mmol, 0.56 g, 1.1 equiv.) in 10 ml THF, which previously has been cooled on ice, was added and the vessel rinsed with THF. The reaction mixture was stirred for 3 more hours, while it was allowed to gradually warm to room temperature. For the workup THF was removed under vacuum and some H_2O (20 ml) was added. The mixture was acidified to pH 1-2 with 10% sodium hydrogen sulfate solution and extracted with ethyl acetate (3 x 20 ml). The organic layers were combined and washed three times each with saturated sodium hydrogen carbonate solution and H_2O. Subsequently, it was dried over Mg_2SO_4 and evaporated to dryness under vacuum. Due to instability the product was only roughly purified by a short chromatographic column eluting with cyclohexane : ethyl acetate (2 : 1). Yield: 59%.

Appearance: yellow waxy solid. **Solubility:** soluble in THF, chloroform, ethyl acetate. **TLC:** R_f = 0.53 (cyclohexane : ethyl acetate, 2:1). **Detection:** UV absorption at 254 nm, Ninhydrin reagent. **^{1}H NMR (500 MHz, CDCl3)** δ ppm 0.84-0.93 (m, 6H*, C7''H+C4H), 1.22-1.35 (m, 4H*, C6''H+C5''H), 1.60-1.74 (2 m, 1H each, C3''H+C3H), 1.82-1.90 (m, 1H, C3H), 2.13-2.25 (m, 2H, C2''H), 3.27-3.40 (m, 2H, C4''H), 3.79 (s, 3H, OMe), 4.52-4.60 (m, 1H, C2H), 5.04-5.14 (m, 2H, C1'H), 6.00-6.04 (m, 1H, NH), 6.86 (d, 2H, *J* = 8.50, Ar), 7.27 (d, 2H, *J* = 8.50, Ar) [*signals superimposed by impurity from reactant (lactone)]. **^{13}C NMR (125 MHz, CDCl3)** δ ppm 9.5 (CH, C4), 13.9 (CH, C7''), 16.4, 16.6 (CH, C4'')*, 19.6, 19.7 (CH, C6'')*,

25.4, 25.6 (CH, C3)*, 35.2, 35.5 (CH, C3'')*, 36.5, 36.6 (CH, C5'')*, 41.8, 41.9 (CH, C2'')*, 53.2, 53.4 (CH, C2)*, 55.3 (CH, OMe), 67.0 (CH, C1'), 114.0 (CH, Ar), 127.4 (Cq, Ar), 130.2 (CH, Ar), 159.8 (Cq, Ar), 170.9 (Cq, C1), 172.1 (Cq, C1'') [*double signals result from diastereomeric mixture].

(2S)-4-Methoxybenzyl 2-(2-oxo-4-propylpyrrolidin-1-yl)butanoate (20)
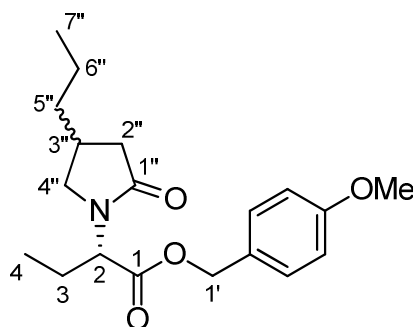
The cyclization reaction was perfomed applying similar conditions as described by Sánchez et al.[176] (2S)-4-Methoxybenzyl 2-(3-(iodomethyl)hexanamido)butanoate (1.2 mmol, 0.55 g) was dissolved in 50 ml THF, anhydrous and cooled down to 0 °C. After gradual addition of potassium *tert*-butoxide (1.3 mmol, 0.15 g) under stirring, the mixture was allowed to warm to room temperature and it was stirred for 2 additional hours. At the end of the reaction time 30 ml saturated ammonium chloride solution were added and the product was extracted with ethyl acetate (3 x 30 ml). The organic layers were collected and washed with 10% sodium thiosulfate solution and H_2O. Finally, it was dried with Mg_2SO_4 and evaporated to dryness under vacuum. Purification was done by column chromatography using cyclohexane : ethyl acetate (1 : 1) as eluant. The product was further purified by HPLC: elution was performed using methanol : H_2O (25 : 75) for 20 min, continuing with a gradient to a ratio of 50 : 50 within 20 min, followed by a second gradient to 100% methanol within 10 min, which was maintained for 20 more minutes. The product was eluted after 51.0 min, detection was performed by UV absorption at 254 nm. The ratio of the two isomers was 1:1 (determined by NMR).

Appearance: white crystalline solid. **Solubility:** soluble in toluene, diethyl ether, chloroform, ethyl acetate. **TLC:** $R_f = 0.50$ (cyclohexane : ethyl acetate, 1:1). **Detection:** UV absorption at 254 nm. **Melting point:** 44 °C. **^{1}H NMR (500 MHz, CDCl$_3$)** δ ppm 0.85-0.90 (m, 6H, C7''H+C4H), 1.25-1.39 (m, 4H, C6''H+C5''H), 1.59-1.66, 1.94-2.00 (2 m, 1H each, C3H), 2.03-2.09 (m, 1H, C2''H), 2.23-2.34 (m, 1H, C3''H), 2.47-2.53

(m, 1H, C2''H), 2.88, 3.01, 3.35, 3.51 (4 dd*, 2H, *J* = 9.45, 9.15, 7.90, 6.65, C4''H), 3.78, 3.79 (2 s*, 3H, OMe), 4.66-4.69 (m, 1H, C2H), 5.00-5.04, 5.06-5.09 (2 m, 1H each, C1'H), 6.86 (d, 2H, *J* = 8.50, Ar), 7.25 (d, 2H, *J* = 8.20, Ar) [*double signals result from diastereomeric mixture]. **¹³C NMR (125 MHz, CDCl₃)** δ ppm 10.4 (CH, C4), 13.7 (CH, C7''), 20.2, 20.3 (CH, C6'')*, 21.6, 21.9 (CH, C3)*, 31.5 (CH, C3''), 36.2, 36.5, 37.1, 37.2 (CH, C2'', C5'')*, 48.7, 49.1 (CH, C4''), 54.7, 54.9 (CH, C2, OMe), 66.3 (CH, C1'), 113.6 (CH, Ar), 127.3 (Cq, Ar), 129.7, 129.8 (CH, Ar), 170.7 (Cq, C1), 175.2 (Cq, C1'') [*double signals result from diastereomeric mixture]. **LC-MS** *m/z* 334.3 ([M + H]⁺).

(2*S*)-2-(2-Oxo-4-propylpyrrolidin-1-yl)butanamide (21)

(diastereomeric mixture of brivaracetam[70])
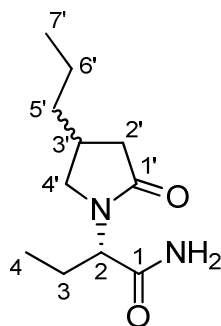
The general performance of the following reaction was done according to a procedure described by Levin et al.[178] For the preparation of the aluminum amide reagent (assumed: 0.67 M) ammonium chloride was suspended in 4 ml toluene, anhydrous and cooled to 5 °C. 2 ml of a trimethylaluminum solution (2 M in toluene) were added dropwise, before the cooling was removed and the mixture stirred for 2 h at room temperature.

(2*S*)-4-Methoxybenzyl 2-(2-oxo-4-propylpyrrolidin-1-yl)butanoate (0.41 mmol, 0.14 g) was dissolved in 4 ml anhydrous toluene and flooded with argon. After addition of 2 ml of the previously *in situ* prepared aluminum amide reagent (1.3 mmol, 3 equiv.) it was heated up to 50 °C and stirred over night. The reaction was stopped by cautious addition of water. The formed precipitate was removed by filtration followed by washing with ethyl acetate and saturated sodium hydrogen carbonate solution. The product was extracted from the obtained filtrate with ethyl acetate (3 x 10 ml), the organic layers were combined, dried over Mg₂SO₄ and evaporated to dryness under vacuum. The final

product was purified by HPLC: elution was performed with methanol : H_2O (30 : 70) for 20 min, continuing with a gradient to a ratio of 50 : 50 within 40 min, then a gradient to a final concentration of 100% methanol was run over 10 min. The product was eluted with a retention time of 42.5 min, detection was performed by UV absorption at 210 nm. Yield: 20%.

For chemical properties see 8.2.2

8.3 Membrane preparation of native tissue

8.3.1 Rat brain membrane

For radioligand binding studies rat brain membrane preparations from cortex as well as striatum were utilized. During the whole preparation procedure brains were kept on ice.

After thawing frozen brains (-80 °C) in ice-cold sucrose solution (0.32 M), they were put on an ice-cold glass plate for dissection. Brains were carefully cut on the top side along the two hemispheres with a scalpel, allowing the removal of the cortex on either half. Cortical tissue was collected and stored in ice-cold sucrose solution (0.32 M) until further preparation. In the meanwhile, the striatum – a subcortical, striped brain region located in the forebrain – was dissected out. Striatal tissue was collected in ice-cold Tris-HCl buffer.

Striatum

After determination of the wet weight, the collected striatal tissue was placed in ice-cold Tris-HCl buffer and disrupted (Ultraturrax, setting 3, 10 s). The obtained suspension was centrifuged (37000 g, 4 °C for 15 min) and the supernatant was discarded. The remaining pellet was resuspended in ice-cold Tris-HCl buffer and centrifuged again (37000 g, 4 °C for 15 min). The pellet was resuspended in ice-cold Tris-HCl buffer (100 mg per 1 ml buffer) and homogenized (Ultraturrax, setting 3, 10 s). The obtained homogenate was aliquoted, shock-frozen and stored at -80 °C until use.

Cortex

The collected cortical tissue in ice-cold sucrose solution (0.32 M) was disrupted with a Potter glass homogenizer and afterwards centrifuged at 1000 g, 4 °C for 10 min. Whereas the pellet P1 – containing e.g. cell debris and nuclei – was discarded, the supernatant was transferred into a new tube and was centrifuged at 37000 g, 4 °C for

1 h. The resulting pellet was resuspended and homogenized (Ultraturrax, setting 3, 10 s) in ice-cold deionized water. After centrifugation at 37000 g, 4 °C for 1 h, a second wash step was performed in which the pellet was resuspended and homogenized (Ultraturrax, setting 3, 10 s) in ice-cold Tris-HCl buffer and again centrifuged at 37000 g, 4 °C for 1 h. After removal of the supernatant, the pellet was resuspended and homogenized (Ultraturrax, setting 3, 10 s) in a small amount of ice-cold Tris-HCl buffer. The homogenized membrane suspension was aliquoted, shock-frozen and stored at -80 °C until use.

8.3.2 Mouse brain membrane

Like all membrane preparations of native tissue, the whole procedure of mouse brain membrane preparation was performed on ice. For whole brain membrane preparations, frozen (-80 °C) brains of Black 6 wild-type mice, or brains of SV2A KO mice, respectively, were thawed in Tris-HCl buffer stored on ice. After disruption of the brains with a Potter glass homogenizer, the suspension was centrifuged (37000 g, 4 °C, 15 min). The supernatant was discarded and the pellet was resuspended in ice-cold Tris-HCl buffer and homogenized (Ultraturrax, setting 3, 10 s). The obtained suspension was centrifuged (37000 g, 4 °C, 15 min) and the supernatant was discarded. After resuspension, it was once more centrifuged and the remaining pellet was resuspended in a small amount of ice-cold Tris-HCl buffer and homogenized (Ultraturrax, setting 3, 10 s). The suspension was aliquoted, shock-frozen and stored at -80 °C until use.

8.3.3 Human brain membrane

Preparation of human brain tissue was performed under elevated precautionary safety measures (under the hood, face mask, double layer of gloves etc.). All waste was collected (S2) and autoclaved prior to disposal. Implements and place of work were sterilized with Dismozon® afterwards.

Membrane preparations from human thalamus and human putamen each were prepared separately by pooling tissue from three different brain samples. As far as it is known, utilized brain samples originated from males as well as females, aged 25-46 years without relevant underlying conditions. Indicated causes of death were accident, cardiac death/arteriosclerosis and hypothermia.

Membrane preparations from tissue obtained by epilepsy surgery from pharmacoresistant epileptic patients were prepared for each sample separately. The following information were provided along with the tissue: the brain tissue was resected during epilepsy surgery from people with focal pharmacoresistant epilepsy after standard presurgical assessment including cerebral 3 Tesla magnetic resonance imaging, neuropsychological testing and video-EEG telemetry using scalp electrodes. In all patients, tissue resection was clinically indicated with the goal to treat epilepsy. In six of the eight patients (samples 1-4, 6 and 7) selective amygdala-hippocampectomy (in one patient (sample 7) together with a resection of two thirds of the temporal lobe) was performed. In one patient (sample 5) a tailored lesionectomy of a cavernoma in the frontal lobe was carried out. Sample 8 was resected from a patient suffering from a glioblastoma in the temporomesial region.

Brains were kept on ice during the whole preparation procedure. Initially, brain tissue, which was stored at -80 °C, was thawed on ice. After determination of the wet weight, ice-cold HEPES buffer was added and the tissue was homogenized (Ultraturrax, setting 6, 10 s). The obtained suspension was centrifuged (35000 g, 4° C, 20 min). The supernatant was discarded and the pellet resuspended in HEPES buffer and homogenized (Ultraturrax, setting 6, 10 s). The washing procedure was repeated until the supernatant remained clear. The final pellet was then resuspended in a small volume of HEPES buffer and homogenized (Ultraturrax, setting 1, 5 s). The homogenate was aliquoted, shock-frozen in liquid nitrogen and stored at -80 °C until use.

When needed for binding studies, required amounts of aliquots were thawed at room temperature, diluted with Tris-HCl buffer and homogenized (vortex mixer). After centrifugation (35000 g, 4 °C, 20 min) the supernatant was discarded and the remaining pellet was resuspended (vortex mixer) in Tris-HCl buffer to a final concentration of 5 mg/ml.

8.3.4   Treatment of membrane preparations for studies with [³H]AMPA

Protein membrane preparations used for binding studies with [³H]AMPA were additionally purified by washing and sonication. Therefore, membrane preparations (8.3.1 and 8.3.2) were diluted with additional Tris-HCl buffer to a volume of 10 ml and were sonicated, while cooling with ice. The suspension was spun down (30000 g, 4 °C,

20 min) and after resuspension of the pellet in 10 ml of Tris-HCl buffer the sonification and centrifugation procedure was repeated. The resulting pellet was resuspended in a defined volume of Tris-HCl buffer and was directly used for binding studies.

8.4 Protein determination (Lowry)

To determine the protein amount in a prepared membrane suspension a protein determination according to Lowry[232] was performed. This method is based on a colorimetric reaction in which the protein concentration directly correlates with the developing intensity of a color. It consists of two partial reactions: under alkaline conditions copper(II) cations interact with free electron pairs of the nitrogens in peptide bonds. The emerging complex is square planar and blue colored (Biuret reaction). This copper protein complex acts as reducing agent, which reduces the likewise added yellow Folin-Ciocalteau reagent, containing molybdenum(VI)- and wolfram(VI)-heteropolyacids (molybdenum blue reaction). The exact mechanism of this reaction is not completely understood. It is assumed that complexed copper, which previously has been reduced to copper(I), as well as the aromatic amino acid residues of tyrosine and tryptophan (independent from complex formation) are involved in the reduction of the Folin-Ciocalteau reagent. By determination of the extinction of several samples with known protein concentration, a sample with unknown protein concentration can be determined according to Lambert-Beer Law, which describes the proportionality between extinction and concentration:

$$E_\lambda = \varepsilon_\lambda \cdot c \cdot l$$

Equation 1: Lambert-Beer Law

E_λ: extinction at wavelength λ
ε_λ: absorption coefficient
c: concentration
l: path length

One should be aware that several non-proteinogenic compounds like EDTA, ammonium sulfate, Tris, sucrose, citrate and phenols falsify the protein determination. If this is the case, in protein suspensions where these compounds are present, proteins should be precipitated with trichloroacetic acid and resolubilized in water.

In this present study BSA was used as standard for generation of a calibration line: the actual concentration of a solution with a supposed concentration of 1 mg/ml was determined by measuring the extinction at 280 nm, based on the knowledge that a 1 mg/ml solution of BSA possesses an extinction of 0.66. This standard solution was used for the preparation of a series of dilutions ranging from 50 to 500 µg/ml. The series of dilutions as well as dilutions from the protein samples with unknown concentration (in a total volume of 200 µl) were complexed according to the following protocol:

To each sample (BSA standard and protein samples), as well as to a blank (no protein), 1 ml of freshly prepared reagent C (see 8.1.3.5) was added, homogenized and the solution incubated for 20 min at room temperature. Thereafter, 100 µl of reagent D (see 8.1.3.5) was added, immediately homogenized and incubated for 30 more minutes. The extinction was then determined at a wavelength of 500 nm.

8.5   Radioligand binding studies

8.5.1   Introduction

Radioligand binding studies[156–158] are broadly used for the investigation of ligand-receptor interaction *in vitro*. The availability of a radioactively labeled ligand allows to easily examine and characterize its binding behavior in native tissue as well as to recombinantly expressed receptors. In principle, the radioligand simply needs to be incubated with a preparation of the protein of interest for a certain amount of time. After separation of protein-bound from protein-unbound radioligand, it is possible to draw conclusions on the binding behavior by measuring the remaining quantity of radioactivity. Ligands labeled with the radioactive isotope tritium can be considered biologically identical to the unlabeled compound and thus, provide valuable information for understanding ligand-receptor interactions on a molecular level.

As simple the principle concept, there are several demands that are indispensable for reliable and reproducible binding studies, above all on the radioligand itself. Ideally, radioligands should possess high affinity (< 5 nM), combined with a high specific activity (tritiated ligands: 30 to 100 Ci/mmol) and low non-specific binding (< 10-30%). It is furthermore important to optimize the procedure that enables separation of bound from free radioligand. The lower the affinity of a radioligand, the bigger the effect caused by dissociation during delayed separation times (dissociative loss).

The underlying principle of a ligand binding to its receptor is described by **Equation 2** (based on the law of mass action):

$$R + L \xrightleftharpoons[k_{-1}]{k_{+1}} RL$$
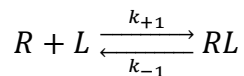
Equation 2: Equilibrium of receptor-ligand binding

R: receptor

L: unbound ligand ≙ Free

RL: receptor-ligand complex ≙ Bound

k_{+1}: association rate constant

k_{-1}: dissociation rate constant

General procedure

If not indicated otherwise, all experiments were performed in polypropylene test tubes in a total volume of 0.5 ml. After completion of incubation period (at 4 °C), protein-bound ligand was recovered by vacuum filtration through glass fiber filters, followed by a wash step. For the filtering process with GF/C filters, always a double layer of this filter type was used, from which the upper one was continued to be used for analysis. Subsequently, the filters were dried (50 °C, 90 min) and filter pieces of each individual well were given into a separate vial and filled with scintillation cocktail (LumaSafe™). After incubation for at least 6 hours, radioactivity was determined by liquid scintillation counting. Non-specific binding was determined by measuring radioligand binding in the presence of a high concentration of a coldligand (non-labeled compound). Specific binding was determined by subtracting non-specific binding from total binding for each single value. Data were analyzed by GraphPad Prism® 5.01.

8.5.2 Kinetic experiments

8.5.2.1 Background

In kinetic experiments binding of a constant concentration of radioligand to a protein preparation is measured after different time intervals. Association experiments (see **Figure 42 A**) describe the binding of a radioligand to a receptor starting from time t_0 until steady state has been reached, whereas dissociation experiments (see **Figure 42 B**)

start at binding in steady state, when dissociation of radioligand from the receptor is
initiated until no more radioligand remains bound to the receptor.
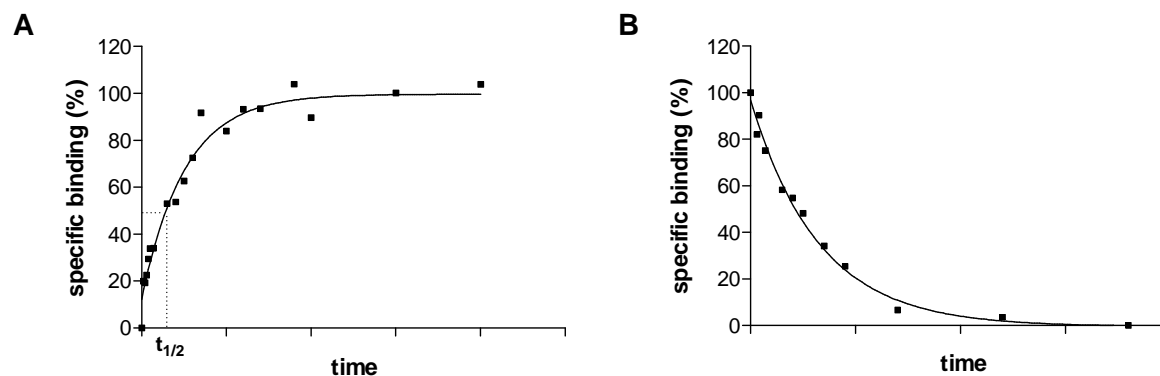
Figure 42: Example curves of association binding (**A**) and dissociation binding (**B**); $t_{1/2}$ indicates
association half-life.

From association experiments the association half life $t_{1/2}$ can be determined, which
allows the calculation of the observed kinetic constant k_{obs} (min^{-1}) from **Equation 3**:

$$k_{obs} = \frac{\ln 2}{t_{1/2}}$$

Equation 3: Calculation of k_{obs}

k_{obs}: observed kinetic constant (min^{-1})
$t_{1/2}$: half-life of association (min)

By determination of the dissociation half-life $t_{1/2}$ from the dissociation experiment, it is
possible to calculate the dissociation kinetic constant k_{off} (**Equation 4**):

$$k_{off} = \frac{\ln 2}{t_{1/2}}$$

Equation 4: Calculation of k_{off}

k_{off}: dissociation kinetic constant (min^{-1})
$t_{1/2}$: half-life of dissociation (min)

Via **Equation 5**

$$k_{on} = \frac{k_{obs} - k_{off}}{L}$$

Equation 5: Calculation of k_{on}

k_{on}: association kinetic constant (M^{-1} min^{-1})

k_{obs}: observed kinetic constant (min^{-1})

k_{off}: dissociation kinetic constant (min^{-1})

L: concentration of radioligand (M)

the association kinetic constant k_{on} is obtained, which allows calculation of the kinetic equilibrium dissociation constant K_D (**Equation 6**):

$$K_D = \frac{k_{off}}{k_{on}}$$

Equation 6: Calculation of kinetic K_D

K_D: kinetic equilibrium dissociation constant (M)

k_{off}: dissociation kinetic constant (min^{-1})

k_{on}: association kinetic constant (M^{-1} min^{-1})

8.5.2.2 Performance of kinetic experiments

Kinetic experiments were performed essentially as described by Noyer et al.[60] For association experiments the radioligand was given into buffer solution. The protein preparation (rat cortical membrane preparations, see 8.3.1) was added at different time intervals prior to vacuum filtration. Non-specific binding was determined for several time intervals by addition of unlabeled levetiracetam (1 mM) and subtracted from each measured value (total binding) to obtain the specific binding. For dissociation experiments the radioligand was first incubated together with the protein preparation in the buffer solution until steady state was reached. Dissociation was then started by addition of unlabeled levetiracetam (1 mM) at different time intervals prior to vacuum filtration. For determination of specific binding, the value, which asymptotically is approximated by the function, was subtracted from each measured value (total binding). For filtration GF/C glass fiber filters, pre-soaked for 30 min in 0.1% aqueous PEI solution, were used. After filtration the filters were washed three times with Tris-HCl buffer. Given results were obtained from three individual experiments performed in triplicate ([³H]LEV), three individual experiments performed in duplicate

([³H]isoBRV), or four individual experiments performed in duplicate ([³H]BRV), respectively.

Table 16: Conditions for kinetic binding studies.

	[³H]LEV	[³H]isoBRV	[³H]BRV
buffer solution	Tris-HCl buffer containing MgCl$_2$ (2 mM)		
radioligand concentration	10 nM	5 nM	1 nM
amount of protein per well	200 μg	100 μg	100 μg
incubation time until dissociation was started	120 min	180 min	240 min

8.5.3 Saturation experiments

8.5.3.1 Background

Saturation experiments constitute a further subgroup of receptor binding experiments, by which the affinity (K_D value) of a radioligand for a receptor as well as the density of a receptor (B_{max} value) in a certain protein preparation can be determined.
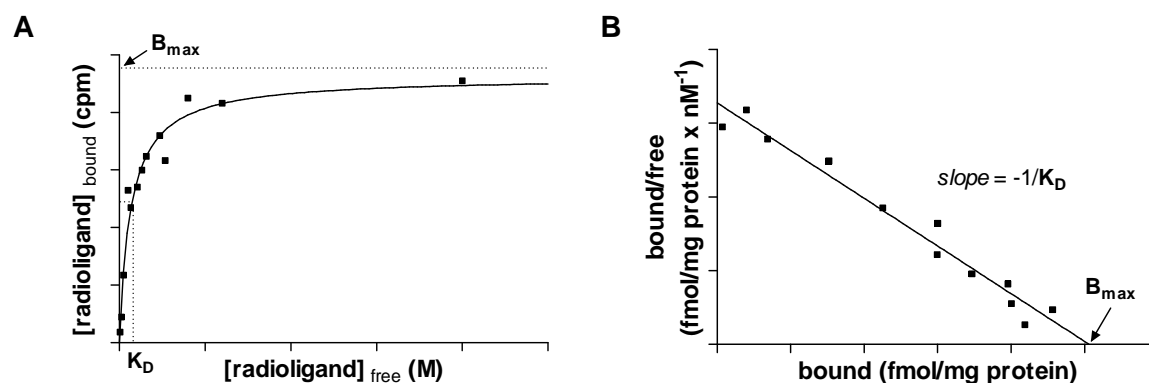
Figure 43: Example curve of saturation binding experiment (**A**) and linear transformation to a Rosenthal plot (**B**); K_D indicates the concentration of the equilibrium dissociation constant and B_{max} indicates the maximum number of binding sites.

Therefore, the radioligand is incubated with the protein preparation in increasing concentrations, covering a range of 0.1 x K_D to 10 x K_D, if possible. The resulting function is a hyperbola (see **Figure 43 A**), described by **Equation 7**:

$$R - L \ = \ \frac{B_{max} \cdot L}{K_D \ + \ L}$$

Equation 7: Mathematical function of saturation binding curve

> R-L: receptor-ligand complex ≙ Bound
> B_{max}: maximum number of binding sites (cpm)
> L: unbound ligand ≙ Free
> K_D: equilibrium dissociation constant (M)

As indicated in **Figure 43** the K_D value corresponds to the concentration of radioligand at which 50% of the receptors are occupied, whereas B_{max} equals the value that is asymptotically approximated by the hyperbola. B_{max} (cpm) can subsequently be used for the calculation of B_{max} (pmol/mg protein) (**Equation 8 to Equation 10**):

$$pM \ Bound \ = \ \frac{B_{max} \ (cpm)}{V \ (ml) \cdot \ efficiency \ (\%) \cdot 2.2 \cdot spec. \ activity \ (Ci/mmol)}$$

Equation 8: Calculation of pM Bound

> B_{max}: maximum number of binding sites (cpm)
> V: volume per well (ml)
> efficiency: counter efficiency (cpm/dpm ≙ cpm in %)
> 2.2: factor for converting cpm in Bq
>   →for details see Deupree et al.[155]
> spec. activity: specific activity of radioligand (Ci/mmol)

$$B_{max} \ (pmol/well) = \ pM \ Bound \ \cdot V \ (l)$$

Equation 9: Calculation of B_{max} (pmol/well)

$$B_{max} \ (pmol/mg \ protein) \ = \ \frac{B_{max} \ (pmol/well)}{protein \ (mg/well)}$$

Equation 10: Calculation of B_{max} (pmol/mg protein)

By plotting the concentration of bound radioligand against the quotient of bound/free radioligand (see **Figure 43 B**) a Rosenthal plot is obtained.[233] In case of ligand binding to a single site a linear correlation can be observed. Thereby, the slope of the line equals -1/K_D, while the x-intercept corresponds to the value of B_{max}. If the ligand is binding to

more than one binding site, the Rosenthal plot will deviate from a linear function and express a bent curve. However, it should be mentioned that the Rosenthal plot should only be used for visualizing not analyzing data, since the transformation is more prone to errors.

For saturation experiments, in which intact cells instead of membrane preparations are used, B_{max} (binding sites/cell) can be calculated using the following equations (**Equation 8, Equation 11** and **Equation 12**):

$$B_{max}\ (pmol/cell)\ =\ \frac{pM\ Bound\ \cdot V\ (l)}{cells\ per\ well}$$

Equation 11: Calculation of B_{max} (pmol/cell)

$$B_{max}\ (binding\ sites/cell)\ =\ B_{max}\ (pmol/cell)\ \cdot\ 10^{-12}\ \cdot\ N_A$$

Equation 12: Calculation of B_{max} (binding sites/cell)

N_A: Avogadro constant $(6.022 \cdot 10^{23})$

8.5.3.2 *Performance of saturation experiments*

All saturation experiments were performed in analogy to the procedure described by Noyer et al.[60] The protein preparation was incubated for a certain amount of time at 4 °C in a total volume of 0.5 ml Tris-HCl buffer, containing $MgCl_2$ (2 mM) and the radioligand. Non-specific binding was determined for all radioligand concentrations separately in the presence of unlabeled levetiracetam (1 mM). Separation of bound from unbound radioligand was achieved by filtration through GF/C glass fiber filters pre-soaked for 30 min in 0.1% aqueous PEI solution. Subsequently, it was washed three times with ice-cold Tris-HCl buffer.

8.5.3.2.1 Saturation studies with [³H]LEV at rat brain cortical membrane preparations

The saturation experiment of [³H]LEV at rat brain cortical membrane preparations (RC) was performed with radioligand diluted with a constant percentage of unlabeled levetiracetam (isotopic dilution). This is a convenient method to decrease the amount of radioligand applied in the assay, if unlabeled ligand for dilution is available. In this case

the radioligand [³H]LEV (98 Ci/mmol) was diluted by a factor of 100 according to **Equation 13**:

$$radioligand\ (\mu Ci) = \frac{spec.\,activity_d\ (Ci/mmol)\ \cdot\ L_d\ (nM) \cdot f\ \cdot\ V_{L\,total}\ (ml)}{1000}$$

Equation 13: Calculation of the amount of radioligand (µCi)

    spec. activity$_d$: desired specific activity after dilution (Ci/mmol)

    L_d: highest desired concentration of radioligand in the assay (nM)

    f: assay dilution factor (here: 5, since 100 µl are given into a total volume of 500 µl)

    $V_{L\,total}$: required volume of the highest concentrated radioligand solution

$$[^3H]LEV\ (\mu Ci) = \frac{0.98\ Ci/mmol\ \cdot\ 30000\ nM \cdot 5\ \cdot\ 1.1\ ml}{1000} = 161.7\ \mu Ci$$

Since the original radioligand [³H]LEV solution possesses a concentration of 1 mCi/ml according to **Equation 13** a total amount of 162 µl of [³H]LEV was needed.

The required amount of unlabeled levetiracetam (mg) for dilution can be calculated by **Equation 14**:

$$unlabeled\ ligand\ (mg) = M\ \cdot L\ (\frac{1}{a_d} - \frac{1}{a_o})$$

Equation 14: Calculation of the amount of unlabeled ligand (mg)

        M: molecular weight of unlabeled ligand (mg/mmol)

        L: required amount of radioligand as calculated (mCi)

        a_d: desired specific activity after dilution (mCi/mmol)

        a_o: specific activity of original radioligand solution (mCi/mmol)

$$LEV\ (mg) = 170.11\ mg/mmol\ \cdot 0.1617\ mCi\ (\frac{1}{980} - \frac{1}{98000})\ (mmol/mCi)$$
$$= 28\ \mu g$$

Consequently, for the preparation of 1100 µl of the highest concentrated radioligand solution 162 µl [³H]LEV and 28 µl of levetiracetam solution (1 mg/ml) were given into 910 µl Tris-HCl buffer.

The series of dilution starting from the highest concentrated radioligand solution was prepared according to the following table:

Table 17: Preparation of dilution series for [³H]LEV solutions (30000-5 nM); f.c.: final concentration in the assay, f: dilution factor with regard to previous solution. From the radioligand solution with the highest concentration (first row), 300 µl are taken (see last column) to prepare the next dilution (second row). Since this requires to dilute the first solution by the factor of 3 (second column), 600 µl of Tris-HCl buffer need to be added (third column). This adds up to a volume of 900 µl (fourth column), from which 130 µl are taken (last column) for the preparation of the next dilution (third row), and so on.

f.c. (nM)	f	dilution step (previous solution + Tris-HCl) (µl)	prepared V (µl)	remaining V (µl)
30000			1100	(-300) = 800
10000	3	300 + 600	900	(-130) = 770
1000	10	130 + 1170	1300	(-550) = 750
500	2	550 + 550	1100	(-260) = 840
100	5	260 + 1040	1300	(-500) = 800
50	2	500 + 500	1000	(-240) = 760
10	5	240 + 960	1200	(-400) = 800
5	2	400 + 400	800	

For saturation experiments with [³H]LEV at rat cortical membrane preparations (RC) 200 µg of protein membrane preparation (see 8.3.1) per well were used. The assay was incubated for 120 min. The actual concentration of radioligand in the assay, which was determined by measuring aliquots of each radioligand dilution, was used for plotting the saturation curve. Obtained K_D and B_{max} values are means of two individual experiments performed in triplicate.

8.5.3.2.2 Saturation studies with [³H]isoBRV at rat brain cortical membrane preparations

Since no unlabeled ligand was available for dilution of the radioligand the saturation experiment with [³H]isoBRV was performed without isotopic dilution. In order to reduce the amount of applied radioligand, the saturation experiment was not performed until a highest concentration of 10 times the expected K_D value. Instead, a total amount of 1000 µl of the original radioligand solution in ethanol was vaporized to dryness at ambient pressure over several days. The residue was dissolved in the determined volume of Tris-HCl buffer required for the highest concentration (see **Table 18**) and the series of dilution was prepared as described in the following table:

Table 18: Preparation of dilution series for [³H]isoBRV solutions; relative f.c.: final concentration in the assay in relation to lowest concentrated solution (second last row), f: dilution factor with regard to previous solution. For a detailed explanation see **Table 17**.

relative f.c.	f	dilution step (previous solution + Tris-HCl) (µl)	prepared V (µl)	remaining V (µl)
200			1235	(-785) = 450
100	2	785 + 785	1570	(-1116) = 454
80	5/4	1116 + 279	1395	(-945) = 450
60	4/3	945 + 315	1260	(-810) = 450
40	3/2	810 + 405	1215	(-765) = 450
30	4/3	765 + 255	1020	(-570) = 450
20	3/2	570 + 285	855	(-405) = 450
10	2	405 + 405	810	(-360) = 450
5	2	360 + 360	720	(-270) = 450
2	5/2	270 + 405	675	(-225) = 450
1	2	225 + 225	450	
0		only Tris-HCl		

For saturation experiments with [³H]isoBRV at rat cortical membrane preparations (RC) 100 µg of protein membrane preparation (see 8.3.1) per well were used. The assay was incubated for 180 min. Final concentrations (nM) of the radioligand in the assay were determined by measuring an aliquot of each dilution. The results from two individual experiments performed in duplicate were plotted against determined actual concentrations.

8.5.3.2.3 Saturation studies with [³H]BRV at rat brain cortical membrane preparations

As already described for the saturation experiment with [³H]isoBRV, likewise no isotopic dilution was done for the saturation experiment with [³H]BRV, since no unlabeled ligand was available. For a required radioligand concentration of 650 nM (final concentration in the assay) the amount of original radioligand solution was determined according to **Equation 13**:

$$[^3H]BRV \; (\mu Ci) = \frac{94 \; Ci/mmol \; \cdot \; 650 \; nM \cdot 5 \; \cdot \; 1.37 \; ml}{1000} = 419 \; \mu Ci$$

The corresponding amount (419 µl) of original [³H]BRV solution was given into 951 µl Tris-HCl buffer to add up to the determined total volume (1370 µl) for the highest concentration (see **Table 19**), which was diluted as described in the following table:

Table 19: Preparation of dilution series for [³H]BRV solutions (650-1 nM); f.c.: final concentration in the assay, f: dilution factor with regard to previous solution. For a detailed explanation see **Table 17**.

f.c. (nM)	f	dilution step (previous solution + Tris-HCl) (µl)	prepared V (µl)	remaining V (µl)
650			1370	(-920) = 450
400	13/8	920 + 575	1495	(-1035) = 460
300	4/3	1035 + 345	1380	(-930) = 450
200	3/2	930 + 465	1395	(-945) = 450
150	4/3	945 + 315	1260	(-810) = 450
100	3/2	810 + 405	1215	(-765) = 450
75	4/3	765 + 255	1020	(-560) = 460
50	3/2	560 + 280	840	(-370) = 470
25	2	370 + 370	740	(-288) = 452
10	5/2	288 + 432	720	(-270) = 450
5	2	270 + 270	540	(-90) = 450
1	5	90 + 360	450	

For saturation experiments with [³H]BRV at rat cortical membrane preparations (RC), 100 µg of protein membrane preparation (see 8.3.1) per well were used. The assay was incubated for 240 min. The results from two individual experiments performed in duplicate were plotted against determined actual concentrations.

8.5.3.2.4 Saturation studies with [³H]BRV on intact cells

Saturation experiments with [³H]BRV on intact CHO cells recombinantly expressing the protein of interest were performed as following: transiently transfected CHO cells (see 8.7.6.1 b) were prepared for binding studies as described in 8.7.7. For saturation experiments on CHO cells recombinantly expressing hSV2A-GFP cells of two dishes (152 cm^2) grown to confluence suspended in Tris-HCl buffer were used for a 24-well assay, whereas for experiments on CHO cells recombinantly expressing rSV2A-GFP and rSV2A_N364K-GFP the amount of cells was reduced to one confluent dish per

24-well assay. The incubation time for the assay was 240 min. K_D and B_{max} values are means of two individual experiments performed in duplicate. The radioligand was used without isotopic dilution by vaporizing a certain amount (~500 - 750 µl) of original radioligand solution at ambient pressure over several days and dissolving the residue in a defined volume of Tris-HCl buffer as described in **Table 20**. Final concentrations (nM) of the radioligand in the assay were determined by measuring an aliquot of each dilution.

Table 20: Preparation of dilution series for [³H]BRV solutions; relative f.c.: final concentration in the assay in relation to lowest concentrated solution (last row), f: dilution factor with regard to previous solution. For a detailed explanation see **Table 17**.

relative f.c.	f	dilution step (previous solution + Tris-HCl) (µl)	prepared V (µl)	remaining V (µl)
65			912	(-462) = 450
30	13/6	462 + 539	1001	(-540) = 461
20	3/2	540 + 270	810	(-360) = 450
10	2	360 + 360	720	(-270) = 450
5	2	270 + 270	540	(-90) = 450
1	5	90 + 360	450	

8.5.4 Competition experiments

8.5.4.1 Background

Competition experiments enable the determination of the affinity of an unlabeled compound (competitor) to a receptor by measuring its ability to displace a radioligand from its receptor. Therefore, a constant concentration of radioligand is exposed to increasing concentrations of the competitor. If both, radioligand and competitor, compete for the same binding site, radioligand binding is decreased with increasing amounts of added competitor.
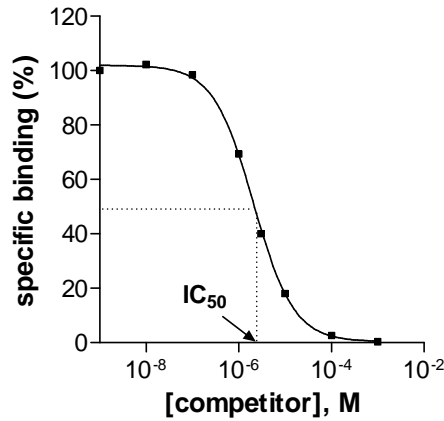
Figure 44: Example curve of competition binding experiment; IC_{50} indicates the concentration of competitor at which specific binding of the radioligand is reduced to 50%.

By logarithmic application of the concentration (M) of the competitor against the specific binding of the radioligand (cpm or %), a sigmoidal curve is obtained whose inflection point marks the concentration, which corresponds to the IC_{50} value (see **Figure 44**). This value indicates the concentration of the competitor at which specific binding of the radioligand is reduced by 50%. Since the IC_{50} value is dependent of the concentration of the radioligand and its K_D value and therewith is not comparable with IC_{50} values from other experiments, whenever possible the independent value K_i should be indicated. The K_i value (equilibrium inhibition constant of competitor) is obtained from the Cheng-Prusoff equation[234] (see **Equation 15**):

$$K_i = \frac{IC_{50}}{1 + \dfrac{L}{K_D}}$$

Equation 15: Cheng-Prusoff equation

K_i: equilibrium inhibition constant (M)
IC_{50}: half maximal inhibitory concentration (M)
L: concentration of radioligand (M)
K_D: equilibrium dissociation constant of radioligand (M)

Besides experiments in which the competitor structurally differs from the radioligand (heterologous binding experiment), it is also common to perform homologous competition experiments in which the radioligand competes with a coldligand that is structurally identical. Basically, homologous binding experiments are comparable with saturation experiments and therewith allow the determination of the K_D and B_{max} value

of a compound. Since in a homologous competition experiment K_i is identical to K_D **Equation 15** simplifies to **Equation 16**:

$$K_D = IC_{50} - L$$

Equation 16: Calculation of K_D in homologous competition experiments

K_D: equilibrium dissociation constant (M)

IC_{50}: half maximal inhibitory constant (M)

L: concentration of radioligand (M)

As further explained by De Blasi et al.[235] the calculation of the maximum number of binding site B_{max} in homologous competition experiments can be done according to **Equation 17**:

$$B_{max} = \frac{B_0 \cdot IC_{50}}{L}$$

Equation 17: Calculation of B_{max} in homologous competition experiments

B_{max}: maximum number of binding sites (cpm)

B_0: specific binding (cpm)

IC_{50}: half maximal inhibitory constant (M)

L: concentration of radioligand (M)

For the determination of B_{max} in fmol/mg protein, or binding sites per cell, respectively, the obtained B_{max} in cpm can be substituted into **Equation 8**.

8.5.4.1.1 General performance of competition experiments with radioligands [³H]LEV, [³H]BRV and [³H]isoBRV

In general, all competition experiments with [³H]LEV, [³H]BRV and [³H]isoBRV were performed as described by Noyer et al.[60] A constant amount of radioligand was given into Tris-HCl buffer containing $MgCl_2$ (2 mM) and in case of competition experiments, various concentrations of the competitor. After addition of the protein preparation, it was incubated for a certain amount of time at 4 °C. Total binding was determined in the absence of competitive compounds, whereas non-specific binding was determined in the

presence of LEV (1 mM). In general, the stock solutions as well as the dilutions of the competitor were prepared in Tris-HCl buffer. In competition experiments, in which the competitor was added in DMSO solution, the same amount of DMSO (here 10 µl) was also added to wells used for determination of total and non-specific binding. DMSO concentration in the assay was always kept $\leq 2\%$. Separation of bound from unbound radioligand was achieved by filtration through GF/C glass fiber filters pre-soaked for 30 min in aqueous PEI solution (0.1%). Subsequently, it was washed three times with ice-cold Tris-HCl buffer. If not indicated otherwise, results were obtained from three individual experiments performed in triplicate.

Table 21: General pipetting scheme for sole determination of total and non-specific binding (pyrrolidone radioligands).

	total binding [µl]	non-specific binding [µl]
MgCl$_2$ solution (10 mM)	100	100
Tris-HCl buffer	200	100
Levetiracetam solution (5 mM)	-	100
radioligand in Tris-HCl buffer	100	100
protein in Tris-HCl buffer	100	100
total volume	500	500

Table 22: General pipetting scheme for competition experiments (pyrrolidone radioligands).

	total binding [µl]	non-specific binding [µl]	competitive binding [µl]
MgCl$_2$ solution (10 mM)	100	100	100
Tris-HCl buffer	200	190	190
Levetiracetam solution (50 mM)	-	10	-
dilution of competitor	-	-	10
radioligand in Tris-HCl buffer	100	100	100
protein in Tris-HCl buffer	100	100	100
total volume	500	500	500

Table 23: Conditions for competitive binding experiments. As protein components membrane preparations from rat cortex (RC), rat striatum (RS), mouse brain (M), post-mortem human brain of thalamus (HT) and putamen (HP) and human brain from surgery of epileptic patients (HEB) were applied. Cells investigated were CHO cells recombinantly expressing the gene of interest.

		[³H]LEV	[³H]isoBRV	[³H]BRV
buffer solution		Tris-HCl buffer containing MgCl$_2$ (2 mM)		
radioligand concentration		10 nM	5 nM	1 nM
amount of protein (per well)	RC (8.3.1)	200 µg	100 µg	100 µg
	RS (8.3.1)	200 µg		100 µg
	M (8.3.2)	200 µg		100 µg
	HT, HP (8.3.3)	400 µg		200 µg
	HEB (8.3.3)	200 µg		100 µg
	cells (8.7.7)			2 dishes (152 cm^2) grown to conflucence per 24-well assay
incubation time		120 min	180 min	240 min

8.5.4.1.2 General performance of competition experiments with [^{3}H]AMPA

For competition binding experiments with [³H]AMPA (20 nM) the radioligand was given into Tris-HCl buffer containing KSCN (200 mM) and the competitor in various concentrations. After addition of either 300 µg protein membrane preparations (RC, RS, or M, see 8.3.4) or permeabilized cell preparation (see 8.7.8), the assay was incubated at 4 °C for 30 min. Total binding of the radioligand was determined in the absence of competitive compounds, non-specific binding was determined in the presence of L-glutamate (1 mM). In experiments in which the competitor was added in DMSO solution, the same amount of DMSO was also added to wells for the determination of total and non-specific binding. The total amount of DMSO in the assay was always ≤ 2%. After incubation time was completed, the assay was filtered through GF/C glass fiber filters, which afterwards were quickly washed twice with ice-cold (~0 °C) Tris-HCl buffer containing KSCN (50 mM). Results were obtained from three to four individual experiments performed in triplicate.

8.6   Molecular biology

8.6.1   Production of competent bacteria

In general, bacterial cell walls are impermeable for nucleic acids. If DNA needs to be introduced into bacteria cells, these bacteria first have to be treated in a way that they become transformation competent, which facilitates the uptake of DNA under certain conditions.

In this study the E.Coli genotype TOP10 was used, from which 50 µl of a glycerol culture were given into 4 ml LB medium (without antibiotics), which was incubated in the bacteria shaker at 37 °C, 220 rpm over night. The following day, 500 µl of this preculture were transferred into 40 ml LB medium (without antibiotics) and again incubated in the bacteria shaker (37 °C, 220 rpm). After approximately 45 min, the optical density of this suspension at 550 nm (OD_{550}) was measured against a blank (LB medium without bacteria). If necessary the incubation time was extended until an OD_{550} of 0.5 was obtained. At this time, it can be assumed that bacterial reproduction is within the exponential phase of the bacteria growth curve. The suspension was centrifuged (1700 g, 4 °C, 20 min) and the resulting pellet resuspended in 20 ml cold $CaCl_2$ solution (0.1 M). After incubation on ice for 30 min, the suspension again was centrifuged (1700 g, 4 °C, 20 min). The obtained pellet was resuspended in 2 ml cold $CaCl_2$ solution (0.1 M). After addition of 0.5 ml glycerol and quick homogenization, the suspension was aliquoted à 100 µl and stored at -80 °C.

8.6.2   Transformation

Replication of a plasmid of interest can efficiently be achieved by incorporation into bacterial cells. With each cell cycle of the transformed bacterium, the plasmid is replicated and passed on to the daughter cell. Thus, an emerged bacterial colony, which derived from a single transformed bacterial clone, contains multiple copies of the plasmid. There are several different chemical and physical methods to enforce a bacterium to take up a plasmid (transformation), which will not be discussed here in detail. On either way, only a marginal number of bacteria will actually take up the DNA, why it is important to make use of antibiotic resistance (here: ampicillin resistance, which is encoded on the plasmid) to select clones that successfully incorporated the plasmid of interest.

For transformation of bacteria cells, in this study the method of heat shock was applied. Therefore, 100 µl of a suspension of competent E.Coli TOP10 (see 8.6.1) were thawed on ice. The plasmid (10-50 ng) was added and carefully mixed with a pipette tip. After incubation on ice for 30 min, the bacteria were exposed to the heat shock: the tube containing the bacteria suspension was incubated at 37 °C in a water bath for 2 min, followed by two minutes incubation on ice. Subsequently, 200 µl of LB medium (without antibiotics) were added and carefully mixed with a pipette tip. The suspension was incubated in a thermal block at 300 rpm, 37 °C for 1 h, before it was spread on a LB agar plate with ampicillin (100 µg/ml), which was incubated at 37 °C over night. Since these agar plates contained ampicillin, only successfully transformed bacteria possessing recombinant plasmids with an ampicillin resistance gene survived.

8.6.3 Cultivation of bacteria

Bacteria (e.g. a selected colony from an agar plate or an aliquot of a glycerol stock) were given into 4 ml LB medium with ampicillin (100 µg/ml). The suspension was incubated over night in a bacteria shaker (220 rpm, 37 °C).

8.6.4 Plasmid isolation

One of the most frequently used methods to isolate plasmid DNA from bacteria is based on the principle of alkaline lysis.[236] Therefore, bacteria containing the plasmid of interest are first centrifuged and obtained as a pellet. This pellet is resuspended in a specific buffer containing NaOH and SDS, which cause lysis of the cells as well as denaturation of the DNA, RNA and proteins due to the high pH level. RNA is degraded in the presence of RNAse. In the presence of EDTA divalent cations are complexed and thus removed from the environment, whereby bacterial nucleases are hindered in their function to degrade plasmid DNA. Subsequently, an acetic acid/acetate buffer is added, which neutralizes the pH level. In this milieu, small plasmid DNA renaturates and passes into solution, while genomic bacterial DNA only renaturates incompletely and remains precipitated as do proteins and other cellular components. By centrifugation plasmid DNA can then be separated from the precipitated material. Adsorption of plasmid DNA to silica membrane columns allows purification of the DNA with ethanol based washing buffers and a final elution with pure H_2O.

Isolation of plasmid DNA in this study was performed with different kits (see 8.1.3.3) according to the manufacturer's protocol. These kits are all based on the above described principle.

8.6.5 Determination of DNA concentration

A 1:500 dilution (2 µl DNA solution + 998 µl water) of the DNA solution was prepared to determine the concentration photometrically. The measurement was made at 260 nm using water as a blank.

8.6.6 Preparation of glycerol stocks

For long-term storage of bacteria, an aliquot of the culture was conserved as glycerol stock. Therefore, 800 µl of a bacteria culture were mixed with 200 µl glycerol and stored at -20 °C. To recultivate bacteria, a small amount of the glycerol culture was given into LB medium with ampicillin (100 µg/ml) and incubated in the bacteria shaker (220 rpm, 37 °C) over night.

8.6.7 Primer design

All primers applied in this study were either designed as primer for PCR or for DNA sequencing reactions (see 8.1.3.3). What they all have in common, is the requirement to bind as specific as possible to a certain sequence of the DNA. Only that way it can be guaranteed that the DNA polymerase, which uses the primer as starter oligonucleotide for elongation of the complementary strand, will exclusively amplify the DNA sequence of interest. For the performance of a PCR as well as a sequencing reaction, a pair of primers had to be designed (forward and reverse), which are complementary to the 3' end of the sense and anti-sense strand and therewith flank the DNA sequence of interest. Ideally, a primer possesses a GC-content (guanine-cytosine content) in a range of 45 to 60%, a melting temperature between 55 and 70 °C and comprises a length of 18 to 22 nucleotides. Furthermore, it should not form any stable hairpins (intramolecular base pairing), nor stable dimers with other primer molecules (intermolecular base pairing). Primers designed for this study have been analyzed with the online program Oligoanalyzer 3.1, Integrated DNA Technologies (see 8.1.1).

8.6.8 Polymerase chain reaction

The polymerase chain reaction (PCR), which was invented by Kary Mullis in 1983 (nobel prize 1993), is an efficient and fast method for the amplification of DNA. It is based on a heat program, which – depending on the present temperature – causes denaturation or renaturation of the DNA template. In the presence of a heat stable DNA polymerase, DNA strands are amplified by elongation in 5'- to 3'-direction. Therefore, a pair of specific primers (see 8.1.3.3) is needed, which flank the template sequence and serve as starter oligonucleotides for the polymerase. As building blocks for the emerging strand the polymerase requires nucleotides of the four bases A, T, G and C, which are added in form of dNTPs (ATP, TTP, GTP and CTP) into the reaction mixture. It is further important to choose an appropriate buffer system with additions like e.g. certain cations, providing an optimized working environment for the polymerase.

In a typical PCR, the reaction mixture, which is placed in a thermocycler, is first heated up to a temperature that lies above the melting temperature (T_m) of the DNA strand. This step (e.g. 94 °C for a couple of seconds) causes the double-stranded DNA to denaturate into two single strands. Subsequently, the thermocycler cools down to a temperature that is just a few degrees beneath the melting temperature (T_m) of the primers. The temperature, which roughly lies between 55 and 65 °C, is dependent on the GC-content of the primers. During this second step the primers anneal to the 3' end of the sense or anti-sense strand, respectively. Afterwards, the elongation of the DNA strand is achieved by heating up to a temperature (e.g. 72 °C) that represents the temperature optimum for the DNA polymerase. The duration of the third step is dependent on how quickly the polymerase can work under the given conditions (e.g. proceeding speed of 1 kbp/min) and should be modified according to the template's size. This three-step cycle (denaturation, annealing, elongation) is repeated several times (typically 30 to 35 cycles), which causes an exponential amplification of the DNA template.

In this study the PCR protocols listed in the following were used. Annealing temperatures ($T_{ann.}$) were chosen based on the T_m of the applied primers. The duration of the elongation step was determined by the size of the template and the proceeding speed of the polymerase.

Table 24: PCR with Pyrobest^{TM} DNA polymerase.

PCR mixture			temperature program			
x µl	template DNA	20 ng				
2 µl	f-primer	10 pmol		98 °C	10 s	denaturation
2 µl	r-primer	10 pmol	30 x	$T_{ann.}$	30 s	annealing
0.5 µl	Pyrobest^{TM} DNA Polymerase			72 °C	1 kbp/min	elongation
5 µl	10x Pyrobest^{TM} Buffer II					
4 µl	dNTPs Mixture (2.5 mM)			72 °C	10 min	final elongation
ad 50 µl	H₂O, sterile					

Table 25: PCR mit AccuPrime^{TM} *Pfx* DNA polymerase.

PCR mixture			temperature program			
				95 °C	2 min	initial denaturation
x µl	template DNA	20 ng				
2 µl	f-primer	10 pmol		95 °C	15 s	denaturation
2 µl	r-primer	10 pmol	35 x	$T_{ann.}$	30 s	annealing
0.8 µl	Accu Prime^{TM} *Pfx* DNA Polymerase			68 °C	1 kbp/min	elongation
5 µl	10x Accu Prime^{TM} *Pfx* DNA mix					
ad 50 µl	H₂O, sterile			68 °C	5 min	final elongation

Table 26: KOD Hot Start DNA polymerase.

PCR mixture			temperature program			
x µl	template DNA	20 ng				
3 µl	f-primer	15 pmol		94 °C	2 min	initial denaturation
3 µl	r-primer	15 pmol				
1 µl	KOD Hot Start DNA polymerase			94 °C	20 s	denaturation
5 µl	10x buffer		35 x	$T_{ann.}$	15 s	annealing
5 µl	dNTPs Mixture (2 mM)			70 °C	3 kbp/min	elongation
4 µl	MgSO₄ (25 mM)					
5 µl	DMSO			70 °C	10 min	final elongation
ad 50 µl	H₂O, sterile					

In this study, after the PCR has been completed, the reaction mixture was mixed with 6x loading dye (see 8.1.3.3 and 8.1.3.6, 1 µl per final volume of 6 µl) and loaded onto an agarose gel (see 8.6.9) for purification.

8.6.9   Agarose gel electrophoresis

Agarose gel electrophoresis is a simple method for the separation of nucleic acids using a gel, whose pore size can be varied by the concentration of added agarose. For separation, the samples are given into small wells on the upper end of the gel placed in TAE buffer (pH ~ 8). When subjected to an electrical voltage, the negatively charged nucleic acid molecules migrate in the electrical field towards the anode. Short and small molecules migrate faster and therewith run further in the gel as do long and bulky molecules, which are stronger retained by the gel matrix. By addition of an intercalating dye (e.g. ethidium bromide) into the gel, it is possible to visualize the nucleic acids by light emission under UV light afterwards.

Within this study 1% agarose gels were used, for which agarose was given into TAE buffer (e.g. 500 mg in 50 ml) and carefully heated in the microwave until agarose had completely dissolved. After short cooling-down, the intercalation dye (here GelRed®) was added (1:20000 dilution, here 2.5 µl) and homogeneously distributed. The gel was poured into a gel chamber and after hardening, was transferred to the electrophoresis chamber filled with TAE buffer. 6x loading dye (see 8.1.3.3 and 8.1.3.6) was added to the DNA samples as well as to the respective DNA ladder (molecular weight size marker, see 8.1.3.3) and each sample was transferred into a well of the gel. The electrophoresis was run at 100 to 200 V depending on the size of the electrophoresis chamber. Subsequently, the gels were analyzed under UV light.

8.6.10 Gel extraction

After separation by gel electrophoresis, the band of interest was cut out of the agarose gel. From this piece of gel the DNA was regained using the Zymoclean™ Gel DNA Recovery kit according to the manufacturer's protocol. Thereby, the agarose gel is solubilized in a high-salt binding buffer liberating the DNA, which afterwards is purified on small silica columns.

8.6.11 Restriction enzyme digestion

Restriction endonucleases are enzymes that recognize certain sequences on the DNA molecule and thereupon cleave the strands in an enzyme specific manner. In this study for restriction endonuclease digestion, enzymes from New England BioLabs (see 8.1.3.3) were used in combination with supplied buffers and additives according to the manufacturer's protocol. If two enzymes were used that needed different reaction conditions the digestion was performed sequentially. In general, the following protocol was used:

DNA (plasmid or PCR product)	x µl
reaction buffer (10x)	1 µl
restriction enzymes	10 U, each
(BSA solution 10x, if needed)	1 µl
H_2O, sterile	ad 10 µl

If not indicated otherwise in the manufacturer's protocol, after incubation at 37 °C for 1 h, the enzymes were heat inactivated by incubation at 65 °C for 20 min. The digested product was either purified by agarose gel electrophoresis (see 8.6.9) or – as was the case for digested PCR products – using the DNA clean & concentrator^{TM}-5 kit (see 8.1.3.3).

For plasmid DNA that was linearized in order to be applied for stable transfections (see 8.7.6.1, c and d), 50 µg of the plasmid was cleaved using 50 U of the below mentioned restriction enzyme in the presence of 1x BSA at 37 °C for 3 h.

pQCXIH-hSV2A-GFP:	FspI	NEbuffer 4
pQCXIN-hGluR2flip:	StuI	NEbuffer 4
pQCXIH-hGluR2flop:	FspI	NEbuffer 4

8.6.12 Ligation

For ligation of two nucleic acid sequences (e.g. a digested PCR product with a digested plasmid), the ATP-dependent enzyme ligase, was used. This enzyme ligates the 3'-hydroxy terminus of one fragment with the 5'-phosphate terminus of the other fragment under formation of a phosphodiester bond. The reaction mixture was prepared according to the following protocol:

plasmid, digested	50 ng
PCR product, digested	150 ng
10 x ligation buffer	1 µl
T4 DNA ligase	2 U
ATP (10 mM)	1 µl
H$_2$O, steril	ad 10 µl

The ligation mixture was incubated at 16 °C over night and afterwards directly used for transformation of competent bacteria (see 8.6.2).

8.6.13 Sequencing

Analysis of DNA sequences was performed by GATC Biotech AG, Konstanz.

8.7   Cell Culture

8.7.1   Revitalization of cells

Cells that have been frozen in FCS/DMSO (see 8.7.4) and stored in liquid nitrogen for long-time storage were revitalized according to the following procedure: a cryovial of frozen cell suspension was thawed in a water bath at 37 °C. Immediately before the cell suspension was thawed completely, the suspension was transferred into a falcon tube containing 10 ml of culture medium prewarmed to 37 °C. The suspension was pelleted (5 min, 200 g) and the supernatant containing the cell toxic DMSO was discarded. The cell pellet was resuspended in new culture medium, which afterwards was transferred into a cell culture flask. For cultivation the culture flask was placed into a cell incubator (37 °C, 95% humidity, 5-10% CO$_2$).

8.7.2   Cultivation of cells

Table 27: Cultivation of cells.

cell type	cultivation medium	preparation of medium*	incubation and passaging ratio
CHO-K1	*basal medium*		
	DMEM/F12 ~ 10% FCS ~ 100 U/ml penicillin ~ 100 µg/ml streptomycin	500 ml DMEM/F12 50 ml FCS 5 ml PS	37 °C, 5% CO$_2$, 95% humidity 1:30

cell type	cultivation medium	preparation of medium*	incubation and passaging ratio
HEK293	*basal medium*		
	DMEM ~ 10% FCS ~ 100 U/ml penicillin ~ 100 µg/ml streptomycin	500 ml DMEM 50 ml FCS 5 ml PS	37 °C, 10% CO_2, 95% humidity 1:10
GP$^+$envAM-12	*HXM medium*		
	DMEM ~ 10% CS ~ 100 U/ml penicillin ~ 100 µg/ml streptomycin ~ 200 µg/ml hygromycin B ~ 15 µg/ml hypoxanthine ~ 250 µg/ml xanthine ~ 25 µg/ml mycophenolic acid	500 ml DMEM 50 ml CS 5 ml PS 1 ml Hygromycin B 5 ml HXM	37 °C, 5% CO_2, 95% humidity 1:6
	basal medium		
	DMEM ~ 10% CS ~ 100 U/ml penicillin ~ 100 µg/ml streptomycin	500 ml DMEM 50 ml FCS 5 ml PS	37 °C, 5% CO_2, 95% humidity
CHO_hSV2A-GFP	*selection medium*		
	DMEM/F12 ~ 10% FCS ~ 100 U/ml penicillin ~ 100 µg/ml streptomycin ~ 500 µg/ml hygromycin B	500 ml DMEM/F12 50 ml FCS 5 ml PS 2.78 ml hygromycin B	37 °C, 5% CO_2, 95% humidity 1:30
HEK_hGluR2flip	*selection medium*		
	DMEM ~ 10% FCS ~ 100 U/ml penicillin ~ 100 µg/ml streptomycin ~ 400 µg/ml G418	500 ml DMEM 50 ml FCS 5 ml PS 2.22 ml G418	37 °C, 10% CO_2, 95% humidity 1:10
HEK_hGluR2flop	*selection medium*		
	DMEM ~ 10% FCS ~ 100 U/ml penicillin ~ 100 µg/ml streptomycin ~ 300 µg/ml hygromycin B	500 ml DMEM 50 ml FCS 5 ml PS 1.67 ml hygromycin B	37 °C, 10% CO_2, 95% humidity 1:10

*For information on culture medium and supplements see 8.1.3.4.

8.7.3   Passaging of cells

After removal of old culture medium, cells attached to the flask were washed with PBS buffer and afterwards incubated with 1-2 ml trypsin/EDTA solution at 37 °C for a few minutes until cells began to detach. New culture medium was added and cell aggregates in the suspension were separated by pipetting up and down. A certain amount of cell suspension was then transferred into a new cell culture flask containing prewarmed culture medium in a total volume of 5-25 ml depending on the flask's size. For cultivation, cells were stored in the incubator (see 8.7.2).

8.7.4   Cryopreservation of cells

For long-term storage of cells, backup aliquots were prepared according to the following procedure: cells grown to confluence (80-90%) in a cell culture flask (175 cm^2) were washed with PBS buffer and incubated with 2 ml of trypsin/EDTA solution at 37 °C for a few minutes. When cells began to detach, the trypsin reaction was stopped by addition of new culture medium and cell aggregates in the suspension were separated by pipetting up and down for several times. The suspension was pelleted by centrifugation (200 g, 5 min) and the supernatant was discarded. The cell pellet was resuspended in 4 ml of freezing medium consisting of FCS containing 10% DMSO. Being aware that the cryoprotectant DMSO is toxic to the cells, the suspension was quickly transferred into cryovials (à 1 ml). For gentle freezing the cryovials were put into a freezing box filled with isopropanol, which was stored at -80 °C over night, allowing the suspension to cool down at an approximate rate of 1 °C/min. The following day, the cryovials were transferred into a liquid nitrogen tank.

8.7.5   Cell counting

To determine the number of cells in a given solution, a hemocytometer (Neubauer chamber) was used. Therefore, the chamber was filled with cell suspension and cells within a square of the dimension 1 x 1 mm were counted under the microscope. Since a square of these dimensions – due to a depth of 0.1 mm – contains 100 nl, the number of cells counted in this square multiplied by 10^4 corresponds to the number of cells per ml. To increase the accuracy of the determination, cells within two or more of these squares were counted and the mean was used for calculation of cells per ml.

8.7.6 Transfection

The term transfection refers to the introduction of nucleic acids into eukaryotic cells by non-viral methods. If, as a result thereof, the nucleic acid molecule is integrated into the host genome (stable transfection), the transfected nucleic acid will be replicated along with the host genome with each cell cycle and the gene product will be stably expressed. If the nucleic acid molecule is not integrated into the host genome (transient transfection), it will only temporarily remain within the cell and will get lost during mitosis or will be degraded by time. Several different transfection methods are known at present, which make use of various electrical, chemical or physical principles. Furthermore, nucleic acids can also be introduced into a host cell by viruses (transduction).

Within this study, liposome transfection (lipofection) and transduction were used as methods for the introduction of DNA into eukaryotic cells.

8.7.6.1 Lipofection

In general, lipofection with Lipofectamine^{TM} 2000 was performed according to the manufacturer's protocol, as described in the following: one day before transfection, cells were seeded in seeding medium (no antibiotics) and cultivated over night (**1**). On the following day, the culture medium was exchanged against OptiMEM$^®$ (**2**). In a tube Lipofectamine^{TM} 2000 was added to OptiMEM$^®$, mixed by inverting and incubated for 5 min (**3**). In the meanwhile, the DNA solution was prepared by adding the required amount of DNA into OptiMEM$^®$ in a second tube (**4**). Subsequently, the Lipofectamine^{TM} 2000 solution was given into the DNA solution, mixed by inverting and the mixture was incubated for 20 min at room temperature. At the end of the incubation time, liposome-DNA complexes have formed, which were given drop-by-drop onto the cells. After incubation for 6 h the medium was exchanged against basic culture medium (**5**).

a) Conditions for transient transfection for production of virus particles

The performance and the conditions for the transient transfection of GP$^+$envAM12 cells are described in detail below (see 8.7.6.2).

b) Conditions for transient transfections for radioligand binding studies

1	number/type of cells	15×10^6 CHO-K1 cells
	seeding medium	DMEM/F12 + 10% FCS, 20 ml
	dish/cell culture flask	152 cm^2 culture dish
	cultivation conditions	5% CO_2, 37 °C, 95% humidity
2	amount of Opti-MEM$^®$	20 ml
3	Lipofectamine solution	3.6 ml Opti-MEM$^®$ + 150 µl Lipofectamine^{TM} 2000
4	DNA solution	3.75 ml Opti-MEM$^®$ + 66 µg DNA
5	culture medium	see **Table 27**, cultivation medium of CHO-K1 cells, 20 ml

CHO cells transiently transfected for radioligand binding studies were cultivated over night. On the next day, they were prepared as described in 8.7.7.

c) Conditions for stable transfection of hGluR2 flip/flop into HEK293 cells

1	number/type of cells	3.5×10^6 HEK293 cells
	seeding medium	DMEM + 10% FCS, 5 ml
	dish/cell culture flask	25 cm^2 cell culture flask
	cultivation conditions	10% CO_2, 37 °C, 95% humidity
2	amount of Opti-MEM$^®$	5 ml
3	Lipofectamine solution	25 µl Lipofectamine^{TM} 2000 + 600 µl Opti-MEM$^®$
4	DNA solution	10 µg DNA (linearized pQCXIH-hGluR2flop, see 8.6.11) + Opti-MEM$^®$ ad 625 µl, or
		10 µg DNA (linearized pQCXIN-hGluR2flip, see 8.6.11) + Opti-MEM$^®$ ad 625 µl
5	culture medium	see **Table 27**, cultivation medium of HEK293 cells, 20 ml

Cells transfected with linearized DNA (pQCXIH-hGluR2flop or pQCXIN-hGluR2flip) were cultivated over night (37 °C, 95% humidity, 10% CO_2). The following day, they were detached and transferred into a big cell culture flask (175 cm^2) containing 25 ml cultivation medium for HEK cells (see **Table 27**). 24 h later, the medium was exchanged against selection medium containing hygromycin B or G418, respectively

(selection medium for HEK_hGluR2flip, or HEK_hGluR2flop, see **Table 27**). The medium was replaced every two days by new selection medium until selection was finished. For cultivation, stably transfected cells were kept in selection medium and passaged twice a week.

d) Conditions for stable transfection of hSV2A-GFP into CHO-K1 cells

1	number/type of cells	2.5×10^6 CHO-K1 cells
	seeding medium	DMEM/F12 + 10% FCS, 5 ml
	dish/cell culture flask	$25\ cm^2$ cell culture flask
	cultivation conditions	5% CO_2, 37 °C, 95% humidity
2	amount of Opti-MEM®	5 ml
3	Lipofectamine solution	25 µl Lipofectamine™ 2000 + 600 µl Opti-MEM®
4	DNA solution	10 µg DNA (linearized pQCXIH-hSV2A-GFP, see 8.6.11) + Opti-MEM® ad 625 µl
5	culture medium	see **Table 27**, cultivation medium of CHO-K1 cells, 20 ml

CHO cells transfected with linearized pQCXIH-hSV2A-GFP were cultivated over night (37 °C, 95% humidity, 5% CO_2). The following day, they were detached and transferred into a big cell culture flask (175 cm^2) containing 25 ml cultivation medium for CHO-K1 cells (see **Table 27**). After 6 h of cultivation (37 °C, 95% humidity, 5% CO_2), the cells had attached onto the flask's ground (~60% confluent) and the medium was exchanged by 25 ml selection medium for CHO_hSV2A-GFP (see **Table 27**). The medium was replaced by new selection medium every two days until selection was finished. Stably transfected cells were cultivated in selection medium and passaged twice a week.

8.7.6.2 *Retroviral transfection and infection*

For retroviral transfection, it was first necessary to produce virus particles containing the gene of interest, which can be used for infection of a cell line. Therefore, on *day one* 1.2×10^6 packaging cells (GP⁺envAM-12 cells) were seeded in a small cell culture flask (25 cm^2) in a total volume of 5 ml basal medium (see **Table 27**, basal medium of GP⁺envAM-12 cells). On the morning of *day two*, the medium was exchanged against

6.25 ml medium without antibiotics (DMEM + 10% CS). A few hours later, the packaging cells were cotransfected (by lipofection) with 6.25 µg of the recombinant plasmid and 3.75 µg of the plasmid containing the gene for the VSV-G protein. Therefore, 600 µl DMEM and 25 µl Lipofectamine^{TM} 2000 were mixed in a tube by inverting and incubated for 5 min at room temperature. In the meanwhile, in a second tube the DNA (gene of interest + VSV-G) was mixed with DMEM in a total volume of 625 µl. Subsequently, the Lipofectamine solution was added into the DNA solution, mixed by inverting the tube and was incubated for 20 min at room temperature. The whole mixture containing the DNA-Lipofectamine complexes was then given dropwise onto the packaging cells and was homogenously distributed by gentle rocking. The cells were incubated at 37 °C, 5% CO_2 over night. On *day three*, the medium was replaced by 3 ml basal medium (see **Table 27**, basal medium of GP$^+$envAM-12 cells) and 30 µl sodium butyrate solution (500 mM) were added and homogenously distributed. For production of virus particles, from then on the packaging cells were incubated at 32 °C, 5% CO_2 for 48 h. On *day four*, the target cell line (3 x 10^5 CHO-K1 cells) was seeded in a small cell culture flask (25 cm^2) in 5 ml basal medium (see **Table 27**) and incubated over night at 37 °C, 5% CO_2. On *day five*, the target cells were infected with the virus particles (transduction). Therefore, the medium of the target cell line was removed. The supernatant of the packaging cells containing the virus particles was sterile filtered and transferred onto the target cells. Additionally, 6 µl polybrene solution were added and homogenously distributed. After incubation at 32 °C for 2.5 h, the medium was removed and displaced by 5 ml basal medium (see **Table 27**, basal medium of CHO-K1 cells). Cells were then incubated at 37 °C for 48 to 72 h before selection of successfully transfected cells was started: therefore, the transfected cells were detached from the flask and transferred into a big cell culture flask (175 cm^2) containing selection medium (basal medium with addition of hygromycin B). The medium was replaced by new selection medium every two days until selection was finished. Stably transfected cells were cultivated in selection medium (basal medium with addition of hygromycin B) and passaged twice a week.

8.7.7 Preparation of cells for binding studies: intact cells

Cells for radioligand binding studies on intact cells were prepared as described by Gillard et al.[161] The culture medium of 1-2 cell culture dishes (152 cm^2) grown to confluence was aspirated and the cells were washed with PBS buffer. 2 ml of trypsin/EDTA solution was distributed onto the cells and incubated at 37 °C until cells began to detach. New cell culture medium was added to stop the trypsin reaction and cells were carefully scraped off with a cell scraper. The cell suspension was given into a falcon tube and cell aggregates were separated by pipetting up and down. Subsequently, cells were spun down (500 g, 4 °C, 10 min) and the resulting pellet was resuspended in PBS buffer. Again, the cell suspension was centrifuged (500 g, 4 °C, 10 min) and the cell pellet was resuspended in cold Tris (20 mM) / Sucrose (250 mM) solution (2.8 ml per 24-well assay).

8.7.8 Preparation of cells for binding studies: permeabilized cells

Cells for radioligand binding studies using permeabilized cells were prepared essentially as described by Kessler et al.[218] The culture medium of a dish (152 cm^2) grown to confluence was aspirated and cells were washed with PBS buffer. 2 ml of trypsin/EDTA solution was given onto the cells, which were then incubated at 37 °C until cells began to detach. New cell culture medium was added to stop the trypsin reaction and cells were carefully scraped off with a cell scraper. The cell suspension was given into a falcon tube and cell aggregates were separated by pipetting up and down. Cells were spun down (2000 g, 10 min) and the resulting pellet was resuspended in 10 ml Tris (10 mM) / NaCl (150 mM) solution. Again, it was centrifuged (2000 g, 10 min) and the cell pellet was resuspended in 9 ml Tris (10 mM) / NaCl (150 mM) solution and 1 ml saponin solution (1%). After centrifugation (2000 g, 10 min) the resulting pellet was twice again resuspended in 10 ml Tris (10 mM) / NaCl (150 mM) solution and the suspension spun down in the centrifuge (2000 g, 10 min). After the last centrifugation step, the pellet was resuspended in cold Tris-HCl buffer (2.8 ml per 24 well assay).

9 Abbreviations

ABC	ATP binding cassette
ad	up to (*Latin*)
ADA	adenosine deaminase
AED	antiepileptic drug
AMPA	α-amino-3-hydroxy-5-methyl-4-isoxazole propionate
AMPAR	AMPA receptor
ANOVA	analysis of variance
ATP	adenosine-5'-triphosphate
b	base(s)
B_{max}	maximum number of binding sites
bp	base pair(s)
Bq	Becquerel
br	broad
BRV	brivaracetam
BSA	bovine serum albumin
$CDCl_3$	chloroform, deuterated
cDNA	copy DNA
CHO	Chinese hamster ovary
Ci	Curie
CNS	central nervous system
cpm	counts per minute
CS	calf serum
d	doublet
Da	Dalton
decomp.	decomposition
DIPEA	*N*,*N*-diisopropylethylamine
DMEM	Dulbecco's Modified Eagle's Medium
DMF	dimethylformamide
DMSO	dimethyl sulfoxide
DNA	deoxyribonucleic acid
dNTP	deoxyribonucleotide triphosphate
DOPE	dioleoylphosphatidylethanolamine

DOTMA	*N*-[1-(2,3-dioleoyloxy)propyl]-*N*,*N*,*N*-trimethylammonium chloride
dpm	disintegrations per minute
E.coli	*Escherichia coli*
EDTA	ethylenediaminetetraacetic acid
EEG	electroencephalography
e.g.	*exempli gratia* (for example)
EPSP	excitatory postsynaptic potential
et al.	*et alii* (and others)
EtOH	ethanol
f	forward
f.c.	final concentration
FCS	fetal calf serum
FDA	Food and Drug Administration
g	gram
G418	geneticin
GABA	γ-aminobutyric acid
GABAT	GABA transaminase
GAD	glutamate decarboxylase
GAT	GABA transporter
GF/C	glass fiber filter type C
GFP	green fluorescent protein
GluR	glutamate receptor
GPCR	G protein-coupled receptor
G protein	guanine nucleotide-binding protein
h	hour(s)
h	human
HEK	human embryonic kidney
HEPES	*N*-(2-hydroxyethyl)piperazine-*N′*-(2-ethanesulfonic acid)
HOAc	acetic acid
HP	human post-mortem membrane preparation from putamen
HPLC	high performance liquid chromatography
HT	human post-mortem membrane preparation from thalamus
HVA	high-voltage activated

HXM	hypoxanthine xanthine mycophenolic acid solution
Hz	hertz
IC_{50}	half maximal inhibitory concentration
ILAE	International League Against Epilepsy
i.p.	intraperitoneal
i.v.	intravenous
J	coupling constant
KA	kainic acid
K_D	equilibrium dissociation constant
K_i	equilibrium inhibition constant
KO	knockout
k_{obs}	observed kinetic constant
k_{off}	dissociation kinetic constant
k_{on}	association kinetic constant
l	liter
L	ligand
LB medium	lysogeny broth medium
LC	liquid chromatography
LEV	levetiracetam
lit.	literature
LSC	liquid scintillation counter
LTR	long terminal repeat
LVA	low-voltage activated
m	meter
m	multiplet
M	mouse brain membrane preparations
M	Molar
MCS	multiple cloning site
Me	methyl
MeOH	methanol
MES	maximal electroshock
min	minute(s)
M_r	relative molecular mass
mRNA	messenger RNA

MRP	multidrug resistance protein
MRT	magnetic resonance tomography
MS	mass spectroscopy
MuLV	murine leukemia virus
MW	microwave
n	number of experiments
N	normal
n/a	not available
nd	no data
NMDA	*N*-methyl-*D*-aspartate
N-MM	*N*-methylmorpholine
NMR	nuclear magnetic resonance
OAc	acetate
OD	optical density
p.a.	*pro analysi*
PBS	phosphate buffered saline
PCR	polymerase chain reaction
PEI	polyethyleneimine
Pgp	P-glycoprotein
PS	Penicillin-Streptomycin solution
PTZ	pentylenetetrazol
q.s.	*quantum satis* (as much as needed)
r	rat
r	reverse
R	receptor
RC	rat cortical membrane preparations
R_f	retention factor
RNA	ribonucleic acid
rpm	rounds per minute
RS	rat striatal membrane preparations
rt	room temperature
RT	reverse transcriptase
s	singlet
s	second(s)

s.c.	subcutaneous(ly)
SDS	sodium dodecyl sulfate
SEM	standard error of the mean
SV2	synaptic vesicle protein 2
SVOP	$\underline{SV}$tw$\underline{o}$-related $\underline{p}$rotein
t	triplet
$T_{ann.}$	annealing temperature
TAE	Tris Acetate EDTA buffer
THF	tetrahydrofuran
TLC	thin layer chromatography
T_m	melting temperature
TMA	trimethylaluminum
TMD	transmembrane domain
TMSCl	trimethylsilyl chloride
TMSI	trimethylsilyl iodide
Tris	tris(hydroxymethyl)aminomethane
U	units
UV	ultraviolet
V	volume
Vis	visible
vs.	versus
VSV-G	vesicular stomatitis virus
wt	wild-type

10 References

1. Brodie, M. J.; Shorvon, S. D.; Canger, R.; Halász, P.; Johannessen, S.; Thompson, P.; Wieser, H. G.; Wolf, P. Commission on European Affairs: appropriate standards of epilepsy care across Europe: ILEA. *Epilepsia* **1997**, *38*, 1245-1250.

2. World Health Organization. Epilepsy: key facts. http://www.who.int/mediacentre/factsheets/fs999/en/ (accessed April 2012).

3. Ngugi, A. K.; Kariuki, S. M.; Bottomley, C.; Kleinschmidt, I.; Sander, J. W.; Newton, C. R. Incidence of epilepsy: a systematic review and meta-analysis. *Neurology* **2011**, *77*, 1005-1012.

4. Leitlinien für Diagnostik und Therapie in der Neurologie. 4. überarbeitete Auflage. ISBN 978-3-13-132414-6. Georg Thieme Verlag: Stuttgart, 2008, 654ff.

5. Kelso, A. R. C.; Cock, H. R. Advances in epilepsy. *Br. Med. Bull.* **2004**, *72*, 135-148.

6. Olafsson, E.; Ludvigsson, P.; Gudmundsson, G.; Hesdorffer, D.; Kjartansson, O.; Hauser, W. Incidence of unprovoked seizures and epilepsy in Iceland and assessment of the epilepsy syndrome classification: a prospective study. *Lancet Neurol.* **2005**, *4*, 627–634.

7. Sander, J. W. The epidemiology of epilepsy revisited. *Curr. Opin. Neurol.* **2003**, *16*, 165-170.

8. Werhahn, K. J. Epilepsy in the elderly. *Dtsch. Arztebl. Int.* **2009**, *106*, 135-142.

9. Fisher, R. S.; van Emde Boas, W.; Blume, W.; Elger, C.; Genton, P.; Lee, P.; Engel, J. Epileptic seizures and epilepsy: definitions proposed by the International League Against Epilepsy (ILAE) and the International Bureau for Epilepsy (IBE). *Epilepsia* **2005**, *46*, 470-472.

10. Böhme, I.; Lüddens, H. Zielstrukturen für Antiepileptika. *Pharm. Unserer Zeit* **2007**, *36*, 262-268.

11. Dannhardt, G.; Kiefer, W. Antiepileptika - Wirkprinzipien und strukturelle Parameter. *Pharm. Unserer Zeit* **2007**, *36*, 270-281.

12. Gutierrez-Delicado, E.; Serratosa, J. M. Genetics of the epilepsies. *Curr. Opin. Neurol.* **2004**, *17*, 147-153.

13. Sánchez-Carpintero Abad, R.; Sanmartí Vilaplana, F. X.; Serratosa Fernández, J. M. Genetic causes of epilepsy. *Neurologist* **2007**, *13*, S47-S51.

14. Hauser, W. A. Seizure disorders: the changes with age. *Epilepsia* **1992**, *33 Suppl 4*, S6-S14.

15. Reynolds, E. H.; Rodin, E. The clinical concept of epilepsy. *Epilepsia* **2009**, *50 Suppl 3*, 2-7.

16. ILAE Commission on Classification and Terminology. Proposal for revised clinical and electroencephalographic classification of epileptic seizures. *Epilepsia* **1981**, *22*, 489–501.

17. ILAE commission on classification and terminology. Proposal for revised classification of epilepsies and epileptic syndromes. *Epilepsia* **1989**, *30*, 389-399.

18. Mutschler, E. Arzneimittelwirkungen. Lehrbuch der Pharmakologie und Toxikologie; Wissenschaftliche Verlagsgesellschaft: Stuttgart, 2008.

19. Sasa, M. A new frontier in epilepsy: novel antiepileptogenic drugs. *J. Pharmacol. Sci.* **2006**, *100*, 487-494.

20. Callaghan, B. C.; Anand, K.; Hesdorffer, D.; Hauser, W. A.; French, J. A. Likelihood of seizure remission in an adult population with refractory epilepsy. *Ann. Neurol.* **2007**, *62*, 382-389.

21. Luciano, A. L.; Shorvon, S. D. Results of treatment changes in patients with apparently drug-resistant chronic epilepsy. *Ann. Neurol.* **2007**, *62*, 375-381.

22. Kwan, P.; Brodie, M. J. Early identification of refractory epilepsy. *N. Engl. J. Med.* **2000**, *342*, 314-319.

23. Shorvon, S. D. Drug treatment of epilepsy in the century of the ILAE: the second 50 years, 1959-2009. *Epilepsia* **2009**, *50 Suppl 3*, 93-130.

24. Greenwood, R. S. Adverse effects of antiepileptic drugs. *Epilepsia* **2000**, *41 Suppl 2*, S42-S52.

25. Löscher, W.; Schmidt, D. New horizons in the development of antiepileptic drugs: innovative strategies. *Epilepsy Res.* **2006**, *69*, 183-272.

26. Catterall, W. A. Ion channel voltage sensors: structure, function, and pathophysiology. *Neuron* **2010**, *67*, 915-928.

27. Yu, F. H.; Catterall, W. A. Overview of the voltage-gated sodium channel family. *Genome Biol.* **2003**, *4*, 207.

28. Kuo, C. C. A common anticonvulsant binding site for phenytoin, carbamazepine, and lamotrigine in neuronal Na^+ channels. *Mol. Pharmacol.* **1998**, *54*, 712-721.

29. Catterall, W. A. Voltage-gated calcium channels. *Cold. Spring. Harb. Perspect. Biol.* **2011**, *3*, a003947.

30. Gee, N. S.; Brown, J. P.; Dissanayake, V. U.; Offord, J.; Thurlow, R.; Woodruff, G. N. The novel anticonvulsant drug, gabapentin (Neurontin), binds to the $\alpha_2\delta$ subunit of a calcium channel. *J. Biol. Chem.* **1996**, *271*, 5768-5776.

31. Field, M. J.; Cox, P. J.; Stott, E.; Melrose, H.; Offord, J.; Su, T. Z.; Bramwell, S.; Corradini, L.; England, S.; Winks, J.; Kinloch, R. A.; Hendrich, J.; Dolphin, A. C.; Webb, T.; Williams, D. Identification of the α_2-δ-1 subunit of voltage-dependent calcium channels as a molecular target for pain mediating the analgesic actions of pregabalin. *Proc. Natl. Acad. Sci. U.S.A.* **2006**, *103*, 17537-17542.

32. Huguenard, J. R. Low-threshold calcium currents in central nervous system neurons. *Annu. Rev. Physiol.* **1996**, *58*, 329-348.

33. Coulter, D. A.; Huguenard, J. R.; Prince, D. A. Characterization of ethosuximide reduction of low-threshold calcium current in thalamic neurons. *Ann. Neurol.* **1989**, *25*, 582-593.

34. Wickenden, A. D. Potassium channels as anti-epileptic drug targets. *Neuropharmacology* **2002**, *43*, 1055-1060.

35. Rundfeldt, C. The new anticonvulsant retigabine (D-23129) acts as an opener of K^+ channels in neuronal cells. *Eur. J. Pharmacol.* **1997**, *336*, 243-249.

36. Main, M. J.; Cryan, J. E.; Dupere, J. R.; Cox, B.; Clare, J. J.; Burbidge, S. A. Modulation of KCNQ2/3 potassium channels by the novel anticonvulsant retigabine. *Mol. Pharmacol.* **2000**, *58*, 253-262.

37. Ben-Ari, Y.; Holmes, G. L. The multiple facets of γ-aminobutyric acid dysfunction in epilepsy. *Curr. Opin. Neurol.* **2005**, *18*, 141-145.

38. Rudolph, U.; Crestani, F.; Benke, D.; Brünig, I.; Benson, J. A.; Fritschy, J. M.; Martin, J. R.; Bluethmann, H.; Möhler, H. Benzodiazepine actions mediated by specific γ-aminobutyric acid$_A$ receptor subtypes. *Nature* **1999**, *401*, 796-800.

39. Rho, J. M.; Donevan, S. D.; Rogawski, M. A. Direct activation of GABA$_A$ receptors by barbiturates in cultured rat hippocampal neurons. *J. Physiol.* **1996**, *497.2*, 509-522.

40. Wikinski, S. I.; Acosta, G. B.; Rubio, M. C. Valproic acid differs in its in vitro effect on glutamic acid decarboxylase activity in neonatal and adult rat brain. *Gen. Pharmacol.* **1996**, *27*, 635-638.

41. Gale, K.; Iadarola, M. J. Seizure protection and increased nerve-terminal GABA: delayed effects of GABA transaminase inhibition. *Science* **1980**, *208*, 288-291.

42. De Biase, D.; Barra, D.; Bossa, F.; Pucci, P.; John, R. A. Chemistry of the inactivation of 4-aminobutyrate aminotransferase by the antiepileptic drug vigabatrin. *J. Biol. Chem.* **1991**, *266*, 20056-20061.

43. Nielsen, E. B.; Suzdak, P. D.; Andersen, K. E.; Knutsen, L. J. S.; Sonnewald, U.; Braestrup, C. Characterization of tiagabine (NO-328), a new potent and selective GABA uptake inhibitor. *Eur. J. Pharmacol.* **1991**, *196*, 257-266.

44.   Hayashi, T. Effects of sodium glutamate on the nervous system. *Keio J. Med.* **1954**, *3*, 183-192.

45.   Qian, A.; Johnson, J. W. Channel gating of NMDA receptors. *Physiol. Behav.* **2002**, *77*, 577-582.

46.   Subramaniam, S.; Rho, J. M.; Penix, L.; Donevan, S. D.; Fielding, R. P.; Rogawski, M. A. Felbamate block of the *N*-methyl-*D*-aspartate receptor. *J. Pharmacol. Exp. Ther.* **1995**, *273*, 878-886.

47.   Keinänen, K.; Wisden, W.; Sommer, B.; Werner, P.; Herb, A.; Verdoorn, T. A.; Sakmann, B.; Seeburg, P. H. A family of AMPA selective glutamate receptors. *Science* **1990**, *249*, 556-560.

48.   Bialer, M.; Johannessen, S. I.; Levy, R. H.; Perucca, E.; Tomson, T.; White, H. S. Progress report on new antiepileptic drugs: a summary of the Tenth Eilat Conference (EILAT X). *Epilepsy Res.* **2010**, *92*, 89-124.

49.   Gryder, D. S.; Rogawski, M. A. Selective antagonism of GluR5 kainate-receptor-mediated synaptic currents by topiramate in rat basolateral amygdala neurons. *J. Neurosci.* **2003**, *23*, 7069-7074.

50.   Lasoń, W.; Dudra-Jastrzębska, M.; Rejdak, K.; Czuczwar, S. J. Basic mechanisms of antiepileptic drugs and their pharmacokinetic/pharmacodynamic interactions: an update. *Pharmacol. Rep.* **2011**, *62*, 271-292.

51.   Rogawski, M. A.; Löscher, W. The neurobiology of antiepileptic drugs. *Nature Rev. Neurosci.* **2004**, *5*, 553-564.

52.   Stafstrom, C. E. Mechanisms of action of antiepileptic drugs: the search for synergy. *Curr. Opin. Neurol.* **2010**, *23*, 157-163.

53.   Landmark, C. J. Targets for antiepileptic drugs in the synapse. *Med. Sci. Monit.* **2007**, *13*, RA1-RA7.

54.   Micromedex® Healthcare Series. Thomson Reuters (Healthcare) Inc. http://www.thomsonhc.com (accessed May 2012).

55.   Giurgea, C.; Lefevre, D.; Lescrenier, C.; David-Remacle, M. Pharmacological protection against hypoxia induced amnesia in rats. *Psychopharmacologia* **1971**, *20*, 160-168.

56.   Gower, A. J.; Noyer, M.; Verloes, R.; Gobert, J.; Wülfert, E. ucb L059, a novel anti-convulsant drug: pharmacological profile in animals. *Eur. J. Pharmacol.* **1992**, *222*, 193-203.

57.   Löscher, W.; Hönack, D. Profile of ucb L059, a novel anticonvulsant drug, in models of partial and generalized epilepsy in mice and rats. *Eur. J. Pharmacol.* **1993**, *232*, 147-158.

58. Klitgaard, H.; Matagne, A.; Gobert, J.; Wülfert, E. Evidence for a unique profile of levetiracetam in rodent models of seizures and epilepsy. *Eur. J. Pharmacol.* **1998**, *353*, 191-206.

59. Food and Drug Administration. FDA approves new epilepsy drug. Rockville, Md: National Press Office; December 1, 1999. FDA Talk Paper T99-54.

60. Noyer, M.; Gillard, M.; Matagne, A.; Hénichart, J. P.; Wülfert, E. The novel antiepileptic drug levetiracetam (ucb L059) appears to act via a specific binding site in CNS membranes. *Eur. J. Pharmacol.* **1995**, *286*, 137-146.

61. Lynch, B. A.; Lambeng, N.; Nocka, K.; Kensel-Hammes, P.; Bajjalieh, S. M.; Matagne, A.; Fuks, B. The synaptic vesicle protein SV2A is the binding site for the antiepileptic drug levetiracetam. *Proc. Natl. Acad. Sci. U.S.A.* **2004**, *101*, 9861-9866.

62. Klitgaard, H. Levetiracetam: the preclinical profile of a new class of antiepileptic drugs? *Epilepsia* **2001**, *42 Suppl 4*, 13-18.

63. Ben-Menachem, E.; Falter, U. Efficacy and tolerability of levetiracetam 3000 mg/d in patients with refractory partial seizures: a multicenter, double-blind, responder-selected study evaluating monotherapy. *Epilepsia* **2000**, *41*, 1276-1283.

64. Alsaadi, T. M.; Shatzel, A.; Marquez, A. V.; Jorgensen, J.; Farias, S. Clinical experience of levetiracetam monotherapy for adults with epilepsy: 1-year follow-up study. *Seizure* **2005**, *14*, 139-142.

65. Rocamora, R.; Wagner, K.; Schulze-Bonhage, A. Levetiracetam reduces frequency and duration of epileptic activity in patients with refractory primary generalized epilepsy. *Seizure* **2006**, *15*, 428-433.

66. Alexandre, V.; Capovilla, G.; Fattore, C.; Franco, V.; Gambardella, A.; Guerrini, R.; La Briola, F.; Ladogana, M.; Rosati, E.; Specchio, L. M.; Striano, S.; Perucca, E. Characteristics of a large population of patients with refractory epilepsy attending tertiary referral centers in Italy. *Epilepsia* **2010**, *51*, 921-925.

67. Malerba, A.; Ciampa, C.; De Fazio, S.; Fattore, C.; Frassine, B.; La Neve, A.; Pellacani, S.; Specchio, L. M.; Tiberti, A.; Tinuper, P.; Perucca, E. Patterns of prescription of antiepileptic drugs in patients with refractory epilepsy at tertiary referral centres in Italy. *Epilepsy Res.* **2010**, *91*, 273-282.

68. De Smedt, T.; Raedt, R.; Vonck, K.; Boon, P. Levetiracetam: part II, the clinical profile of a novel anticonvulsant drug. *CNS Drug Rev.* **2007**, *13*, 57-78.

69. Matagne, A.; Margineanu, D. G.; Kenda, B.; Michel, P.; Klitgaard, H. Anti-convulsive and anti-epileptic properties of brivaracetam (ucb 34714), a high-affinity ligand for the synaptic vesicle protein, SV2A. *Br. J. Pharmacol.* **2008**, *154*, 1662-1671.

70. Kenda, B. M.; Matagne, A. C.; Talaga, P. E.; Pasau, P. M.; Differding, E.; Lallemand, B. I.; Frycia, A. M.; Moureau, F. G.; Klitgaard, H. V.; Gillard, M. R.; Fuks, B.; Michel, P. Discovery of 4-substituted pyrrolidone butanamides as new agents with significant antiepileptic activity. *J. Med. Chem.* **2004**, *47*, 530-549.

71. von Rosenstiel, P. Brivaracetam (UCB 34714). *Neurotherapeutics* **2007**, *4*, 84-87.

72. Gillard, M.; Fuks, B.; Leclercq, K.; Matagne, A. Binding characteristics of brivaracetam, a selective, high affinity SV2A ligand in rat, mouse and human brain: relationship to anti-convulsant properties. *Eur. J. Pharmacol.* **2011**, *664*, 36-44.

73. Rogawski, M. A. Brivaracetam: a rational drug discovery success story. *Br. J. Pharmacol.* **2008**, *154*, 1555-1557.

74. Rogawski, M. A.; Bazil, C. W. New molecular targets for antiepileptic drugs: $\alpha_2\delta$, SV2A, and K_v7/KCNQ/M potassium channels. *Curr. Neurol. Neurosci. Rep.* **2008**, *8*, 345-352.

75. Kaminski, R. M.; Matagne, A.; Leclercq, K.; Gillard, M.; Michel, P.; Kenda, B.; Talaga, P.; Klitgaard, H. SV2A protein is a broad-spectrum anticonvulsant target: functional correlation between protein binding and seizure protection in models of both partial and generalized epilepsy. *Neuropharmacology* **2008**, *54*, 715-720.

76. Surges, R.; Volynski, K. E.; Walker, M. C. Is levetiracetam different from other antiepileptic drugs? Levetiracetam and its cellular mechanism of action in epilepsy revisited. *Ther. Adv. Neurol. Disord.* **2008**, *1*, 13-24.

77. Lukyanetz, E. A.; Shkryl, V. M.; Kostyuk, P. G. Selective blockade of N-type calcium channels by levetiracetam. *Epilepsia* **2002**, *43*, 9-18.

78. Pisani, A.; Bonsi, P.; Martella, G.; De Persis, C.; Costa, C.; Pisani, F.; Bernardi, G.; Calabresi, P. Intracellular calcium increase in epileptiform activity: modulation by levetiracetam and lamotrigine. *Epilepsia* **2004**, *45*, 719-728.

79. Madeja, M.; Margineanu, D. G.; Gorji, A.; Siep, E.; Boerrigter, P.; Klitgaard, H.; Speckmann, E. J. Reduction of voltage-operated potassium currents by levetiracetam: a novel antiepileptic mechanism of action? *Neuropharmacology* **2003**, *45*, 661-671.

80. Zona, C.; Pieri, M.; Carunchio, I.; Curcio, L.; Klitgaard, H.; Margineanu, D. G. Brivaracetam (ucb 34714) inhibits Na^+ current in rat cortical neurons in culture. *Epilepsy Res.* **2010**, *88*, 46-54.

81. Angehagen, M.; Margineanu, D. G.; Ben-Menachem, E.; Rönnbäck, L.; Hansson, E.; Klitgaard, H. Levetiracetam reduces caffeine-induced Ca^{2+} transients and epileptiform potentials in hippocampal neurons. *Neuroreport* **2003**, *14*, 471-475.

82. Rigo, J. M.; Hans, G.; Nguyen, L.; Rocher, V.; Belachew, S.; Malgrange, B.; Leprince, P.; Moonen, G.; Selak, I.; Matagne, A.; Klitgaard, H. The anti-epileptic

drug levetiracetam reverses the inhibition by negative allosteric modulators of neuronal GABA- and glycine-gated currents. *Br. J. Pharmacol.* **2002**, *136*, 659-672.

83. Carunchio, I.; Pieri, M.; Ciotti, M. T.; Albo, F.; Zona, C. Modulation of AMPA receptors in cultured cortical neurons induced by the antiepileptic drug levetiracetam. *Epilepsia* **2007**, *48*, 654-662.

84. Lowe, A. W.; Madeddu, L.; Kelly, R. B. Endocrine secretory granules and neuronal synaptic vesicles have three integral membrane proteins in common. *J. Cell Biol.* **1988**, *106*, 51-59.

85. Buckley, K.; Kelly, R. B. Identification of a transmembrane glycoprotein specific for secretory vesicles of neural and endocrine cells. *J. Biol. Chem.* **1985**, *100*, 1284-1294.

86. Bajjalieh, S. M.; Frantz, G. D.; Weimann, J. M.; McConnell, S. K.; Scheller, R. H. Differential expression of synaptic vesicle protein 2 (SV2) isoforms. *J. Neurosci.* **1994**, *14*, 5223-5235.

87. Bajjalieh, S. M.; Peterson, K.; Shinghal, R.; Scheller, R. H. SV2, a brain synaptic vesicle protein homologous to bacterial transporters. *Science* **1992**, *257*, 1271-1273.

88. Feany, M. B.; Lee, S.; Edwards, R. H.; Buckley, K. M. The synaptic vesicle protein SV2 is a novel type of transmembrane transporter. *Cell* **1992**, *70*, 861-867.

89. Bajjalieh, S. M.; Peterson, K.; Linial, M.; Scheller, R. H. Brain contains two forms of synaptic vesicle protein 2. *Proc. Natl. Acad. Sci. U.S.A.* **1993**, *90*, 2150-2154.

90. Janz, R.; Südhof, T. C. SV2C is a synaptic vesicle protein with an unusually restricted localization: anatomy of a synaptic vesicle protein family. *Neuroscience* **1999**, *94*, 1279-1290.

91. Scranton, T. W.; Iwata, M.; Carlson, S. S. The SV2 protein of synaptic vesicles is a keratan sulfate proteoglycan. *J. Neurochem.* **1993**, *61*, 29-44.

92. Janz, R.; Hofmann, K.; Südhof, T. C. SVOP, an evolutionarily conserved synaptic vesicle protein, suggests novel transport functions of synaptic vesicles. *J. Neurosci.* **1998**, *18*, 9269-9281.

93. Möller, S.; Croning, M. D. R.; Apweiler, R. Evaluation of methods for the prediction of membrane spanning regions. *Bioinformatics* **2001**, *17*, 646-653.

94. Krogh, A.; Larsson, B.; von Heijne, G.; Sonnhammer, E. L. Predicting transmembrane protein topology with a hidden Markov model: application to complete genomes. *J. Mol. Biol.* **2001**, *305*, 567-580.

95. Lynch, B. A.; Matagne, A.; Brännström, A.; von Euler, A.; Jansson, M.; Hauzenberger, E.; Söderhäll, J. A. Visualization of SV2A conformations in situ by the use of protein tomography. *Biochem. Biophys. Res. Commun.* **2008**, *375*, 391-395.

96. Janz, R.; Goda, Y.; Geppert, M.; Missler, M.; Südhof, T. C. SV2A and SV2B function as redundant Ca^{2+} regulators in neurotransmitter release. *Neuron* **1999**, *24*, 1003-1016.

97. Iezzi, M.; Theander, S.; Janz, R.; Loze, C.; Wollheim, C. B. SV2A and SV2C are not vesicular Ca^{2+} transporters but control glucose-evoked granule recruitment. *J. Cell Sci.* **2005**, *118*, 5647-5660.

98. Yao, J.; Bajjalieh, S. M. Synaptic vesicle protein 2 binds adenine nucleotides. *J. Biol. Chem.* **2008**, *283*, 20628-20634.

99. Krupinski, J.; Coussen, F.; Bakalyar, H. A.; Tang, W. J.; Feinstein, P. G.; Orth, K.; Slaughter, C.; Reed, R. R.; Gilman, A. G. Adenylyl cyclase amino acid sequence: possible channel- or transporter-like structure. *Science* **1989**, *244*, 1558-1564.

100. Shi, J.; Anderson, D.; Lynch, B. A.; Castaigne, J. G.; Foerch, P.; Lebon, F. Combining modelling and mutagenesis studies of synaptic vesicle protein 2A to identify a series of residues involved in racetam binding. *Biochem. Soc. Trans.* **2011**, *39*, 1341-1347.

101. Dong, M.; Yeh, F.; Tepp, W. H.; Dean, C.; Johnson, E. A.; Janz, R.; Chapman, E. R. SV2 is the protein receptor for botulinum neurotoxin A. *Science* **2006**, *312*, 592-596.

102. Jahn, R. A neuronal receptor for botulinum toxin. *Science* **2006**, *312*, 540-541.

103. Crowder, K. M.; Gunther, J. M.; Jones, T. A.; Hale, B. D.; Zhang, H. Z.; Peterson, M. R.; Scheller, R. H.; Chavkin, C.; Bajjalieh, S. M. Abnormal neurotransmission in mice lacking synaptic vesicle protein 2A (SV2A). *Proc. Natl. Acad. Sci. U.S.A.* **1999**, *96*, 15268-15273.

104. Kaminski, R. M.; Gillard, M.; Leclercq, K.; Hanon, E.; Lorent, G.; Dassesse, D.; Matagne, A.; Klitgaard, H. Proepileptic phenotype of SV2A-deficient mice is associated with reduced anticonvulsant efficacy of levetiracetam. *Epilepsia* **2009**, *50*, 1729-1740.

105. Xu, T.; Bajjalieh, S. M. SV2 modulates the size of the readily releasable pool of secretory vesicles. *Nat. Cell Biol.* **2001**, *3*, 691-698.

106. Morgans, C. W.; Kensel-Hammes, P.; Hurley, J. B.; Burton, K.; Idzerda, R.; McKnight, G. S.; Bajjalieh, S. M. Loss of the synaptic vesicle protein SV2B results in reduced neurotransmission and altered synaptic vesicle protein expression in the retina. *PloS One* **2009**, *4*, e5230.

107. Custer, K. L.; Austin, N. S.; Sullivan, J. M.; Bajjalieh, S. M. Synaptic vesicle protein 2 enhances release probability at quiescent synapses. *J. Neurosci.* **2006**, *26*, 1303-1313.

108. Fernández-Chacón, R.; Königstorfer, A.; Gerber, S. H.; García, J.; Matos, M. F.; Stevens, C. F.; Brose, N.; Rizo, J.; Rosenmund, C.; Südhof, T. C. Synaptotagmin I functions as a calcium regulator of release probability. *Nature* **2001**, *410*, 41-49.

109. Schivell, A. E.; Batchelor, R. H.; Bajjalieh, S. M. Isoform-specific, calcium-regulated interaction of the synaptic vesicle proteins SV2 and synaptotagmin. *J. Biol. Chem.* **1996**, *271*, 27770-27775.

110. Schivell, A. E.; Mochida, S.; Kensel-Hammes, P.; Custer, K. L.; Bajjalieh, S. M. SV2A and SV2C contain a unique synaptotagmin-binding site. *Mol. Cell. Neurosci.* **2005**, *29*, 56-64.

111. Südhof, T. C. The synaptic vesicle cycle: a cascade of protein-protein interactions. *Nature* **1995**, *375*, 645-653.

112. Südhof, T. C. The synaptic vesicle cycle. *Annu. Rev. Neurosci.* **2004**, *27*, 509-547.

113. Chang, W. P.; Südhof, T. C. SV2 renders primed synaptic vesicles competent for Ca^{2+}-induced exocytosis. *J. Neurosci.* **2009**, *29*, 883-897.

114. Yang, X. F.; Weisenfeld, A.; Rothman, S. M. Prolonged exposure to levetiracetam reveals a presynaptic effect on neurotransmission. *Epilepsia* **2007**, *48*, 1861-1869.

115. Bidlack, J. M.; Rasheed, I. Y. [^{3}H]Levetiracetam binds to AMPA glutamate receptors at a site that modulates the AMPA receptor desensitization. *Epilepsia* **2009**, *50 Suppl 11*, 251-252 (abstract 2.207).

116. Sugiyama, H.; Ito, I.; Watanabe, M. Glutamate receptor subtypes may be classified into two major categories: a study on Xenopus oocytes injected with rat brain mRNA. *Neuron* **1989**, *3*, 129-132.

117. Tanabe, Y.; Masu, M.; Ishii, T.; Shigemoto, R.; Nakanishi, S. A family of metabotropic glutamate receptors. *Neuron* **1992**, *1*, 169-179.

118. Nicoletti, F.; Bockaert, J.; Collingridge, G. L.; Conn, P. J.; Ferragut, F.; Schoepp, D. D.; Wroblewski, J. T.; Pin, J. P. Metabotropic glutamate receptors: from the workbench to the bedside. *Neuropharmacology* **2011**, *60*, 1017-1041.

119. Hansen, K. B.; Yuan, H.; Traynelis, S. F. Structural aspects of AMPA receptor activation, desensitization and deactivation. *Curr. Opin. Neurobiol.* **2007**, *17*, 281-288.

120. Dingledine, R.; Borges, K.; Bowie, D.; Traynelis, S. F. The glutamate receptor ion channels. *Pharmacol. Rev.* **1999**, *51*, 7-61.

121. Sommer, B.; Keinänen, K.; Verdoorn, T. A.; Wisden, W.; Burnashev, N.; Herb, A.; Köhler, M.; Takagi, T.; Sakmann, B.; Seeburg, P. H. Flip and flop: a cell-specific functional switch in glutamate-operated channels of the CNS. *Science* **1990**, *249*, 1580-1585.

122. Hollmann, M.; Heinemann, S. Cloned glutamate receptors. *Annu. Rev. Neurosci.* **1994**, *17*, 31-108.

123. Sun, Y.; Olson, R.; Horning, M.; Armstrong, N.; Mayer, M.; Gouaux, E. Mechanism of glutamate receptor desensitization. *Nature* **2002**, *417*, 245-253.

124. Kaae, B. H.; Harpsoe, K.; Kastrup, J. S.; Sanz, A. C.; Pickering, D. S.; Metzler, B.; Clausen, R. P.; Gajhede, M.; Sauerberg, P.; Liljefors, T.; Madsen, U. Structural proof of a dimeric positive modulator bridging two identical AMPA receptor-binding sites. *Chem. Biol.* **2007**, *14*, 1294–1303.

125. Jin, R.; Clark, S.; Weeks, A. M.; Dudman, J. T.; Gouaux, E.; Partin, K. M. Mechanism of positive allosteric modulators acting on AMPA receptors. *J. Neurosci.* **2005**, *25*, 9027-9036.

126. Sobolevsky, A. I.; Rosconi, M. P.; Gouaux, E. X-ray structure, symmetry and mechanism of an AMPA-subtype glutamate receptor. *Nature* **2009**, *462*, 745-758.

127. Rogawski, M. A. Revisiting AMPA receptors as an antiepileptic drug target. *Epilepsy Curr.* **2011**, *11*, 56-63.

128. Seal, A. J.; Collingridge, G. L.; Henley, J. M. An investigation of the membrane topology of the ionotropic glutamate receptor subunit GluR1 in a cell-free system. *Biochem. J.* **1995**, *312*, 451-456.

129. Ayalon, G.; Stern-Bach, Y. Functional assembly of AMPA and kainate receptors is mediated by several discrete protein-protein interactions. *Neuron* **2001**, *31*, 103-113.

130. Mano, I.; Lamed, Y.; Teichberg, V. I. A venus flytrap mechanism for activation and desensitization of α-amino-3-hydroxy-5-methyl-4-isoxazole propionic acid receptors. *J. Biol. Chem.* **1996**, *271*, 15299-15302.

131. Armstrong, N.; Mayer, M.; Gouaux, E. Tuning activation of the AMPA-sensitive GluR2 ion channel by genetic adjustment of agonist-induced conformational changes. *Proc. Natl. Acad. Sci. U.S.A.* **2003**, *100*, 5736-5741.

132. Balannik, V.; Menniti, F.; Paternain, A.; Lerma, J.; Stern-Bach, Y. Molecular mechanism of AMPA receptor noncompetitive antagonism. *Neuron* **2005**, *48*, 279–288.

133. Kohda, K.; Wang, Y.; Yuzaki, M. Mutation of a glutamate receptor motif reveals its role in gating and δ2 receptor channel properties. *Nat. Neurosci.* **2000**, *3*, 315-322.

134. Leonard, A. S.; Davare, M. A.; Horne, M. C.; Garner, C. C.; Hell, J. W. SAP97 is associated with the α-amino-3-hydroxy-5-methylisoxazole-4-propionic acid receptor GluR1 subunit. *J. Biol. Chem.* **1998**, *273*, 19518-19524.

135. Monyer, H.; Seeburg, P. H.; Wisden, W. Glutamate-operated channels: developmentally early and mature forms arise by alternative splicing. *Neuron* **1991**, *6*, 799-810.

136. Mosbacher, J.; Schoepfer, R.; Monyer, H.; Burnashev, N.; Seeburg, P. H.; Ruppersberg, J. P. A molecular determinant for submillisecond desensitization in glutamate receptors. *Science* **1994**, *266*, 1059-1062.

137. Koike, M.; Tsukada, S.; Tsuzuki, K.; Kijima, H.; Ozawa, S. Regulation of kinetic properties of GluR2 AMPA receptor channels by alternative splicing. *J. Neurosci.* **2000**, *20*, 2166-2174.

138. Shi, S.; Hayashi, Y.; Esteban, J. A.; Malinow, R. Subunit-specific rules governing AMPA receptor trafficking to synapses in hippocampal pyramidal neurons. *Cell* **2001**, *105*, 331–343.

139. Tichelaar, W.; Safferling, M.; Keinänen, K.; Stark, H.; Madden, D. R. The three-dimensional structure of an ionotropic glutamate receptor reveals a dimer-of-dimers assembly. *J. Mol. Biol.* **2004**, *344*, 435-442.

140. Lu, W.; Shi, Y.; Jackson, A.; Bjorgan, K.; During, M.; Sprengel, R.; Seeburg, P.; Nicoll, R. Subunit composition of synaptic AMPA receptors revealed by a single-cell genetic approach. *Neuron* **2009**, *62*, 254-268.

141. Craig, A.; Blackstone, C.; Huganir, R.; Banker, G. The distribution of glutamate receptors in cultured rat hippocampal neurons: postsynaptic clustering of AMPA-selective subunits. *Neuron* **1993**, *10*, 1055–1068.

142. Wenthold, R. J.; Petralia, R. S.; Blahos, J.; Niedzielski, A. S. Evidence for multiple AMPA receptor complexes in hippocampal CA1/CA2 neurons. *J. Neurosci.* **1996**, *76*, 1982-1989.

143. Köhler, M.; Kornau, H. C.; Seeburg, P. H. The organization of the gene for the functionally dominant α-amino-3-hydroxy-5-methylisoxazole-4-propionic acid receptor subunit GluR-B. *J. Biol. Chem.* **1994**, *269*, 17367-17370.

144. Gold, S. J.; Ambros-Ingerson, J.; Horowitz, J. R.; Lynch, G.; Gall, C. M. Stoichiometries of AMPA receptor subunit mRNAs in rat brain fall into discrete categories. *J. Comp. Neurol.* **1997**, *385*, 491-502.

145. Sommer, B.; Kohler, M.; Sprengel, F.; Seeburg, P. H. RNA editing in brain controls a determinant of ion flow in glutamate-gated channels. *Cell* **1991**, *67*, 11-19.

146. Hume, R. I.; Dingledine, R.; Heinemann, S. F. Identification of a site in glutamate receptor subunits that controls calcium permeability. *Science* **1991**, *253*, 1028-1031.

147. Verdoorn, T. A.; Burnashev, N.; Monyer, H.; Seeburg, P. H.; Sakmann, B. Structural determinants of ion flow through recombinant glutamate receptor channels. *Science* **1991**, *252*, 1715-1718.

148. Higuchi, M.; Maas, S.; Single, F. N.; Hartner, J.; Rozov, A.; Burnashev, N.; Feldmeyer, D.; Sprengel, R.; Seeburg, P. H. Point mutation in an AMPA receptor gene rescues lethality in mice deficient in the RNA-editing enzyme ADAR2. *Nature* **2000**, *406*, 78-81.

149. Burnashev, N.; Monyer, H.; Seeburg, P. H.; Sakmann, B. Divalent ion permeability of AMPA receptor channels is dominated by the edited form of a single subunit. *Neuron* **1992**, *8*, 189-198.

150. Seeburg, P. H. The role of RNA editing in controlling glutamate receptor channel properties. *J. Neurochem.* **1996**, *66*, 1-5.

151. Jia, Z.; Agopyan, N.; Miu, P.; Xiong, Z.; Henderson, J.; Gerlai, R.; Taverna, F. A.; Velumian, A.; MacDonald, J.; Carlen, P.; Abramow-Newerly, W.; Roder, J. Enhanced LTP in mice deficient in the AMPA receptor GluR2. *Neuron* **1996**, *17*, 945-956.

152. Gerlai, R.; Henderson, J. T.; Roder, J. C.; Jia, Z. Multiple behavioral anomalies in GluR2 mutant mice exhibiting enhanced LTP. *Behav. Brain Res.* **1998**, *95*, 37-45.

153. Brusa, R.; Zimmermann, F.; Koh, D. S.; Feldmeyer, D.; Gass, P. H.; Seeburg, P. H.; Sprengel, R. Early-onset epilepsy and postnatal lethality associated with an editing-deficient GluR-B allele in mice. *Science* **1995**, *270*, 1677-1680.

154. Feldmeyer, D.; Kask, K.; Brusa, R.; Kornau, H. C.; Kolhekar, R.; Rozov, A.; Burnashev, N.; Jensen, V.; Hvalby, O.; Sprengel, R.; Seeburg, P. H. Neurological dysfunctions in mice expressing different levels of the Q/R site-unedited AMPAR subunit GluR-B. *Nat. Neurosci.* **1999**, *2*, 57-64.

155. Deupree, J. D.; Bylund, D. B. Basic principles and techniques for receptor binding. *Tocris Reviews* **2002**, *18*, 1-7.

156. Bylund, D. B.; Toews, M. L. Radioligand binding methods: practical guide and tips. *Am. J. Physiol.* **1993**, *265*, L421-429.

157. Yamamura, H. I.; Enna, S. J.; Kuhar, M. J., Eds. Neurotransmitter receptor binding. Raven Press: New York, 1985; pp 62-89.

158. Davenport, A. P.; Russell, F. D. Radioligand binding assays: theory and practice. In *Current directions in radiopharmaceutical research and development*, 1st ed.; Mather, S. J., Ed.; Springer: Netherlands, 1996; pp 169-179.

159. Gillard, M.; Fuks, B.; Michel, P.; Vertongen, P.; Massingham, R.; Chatelain, P. Binding characteristics of [³H]ucb 30889 to levetiracetam binding sites in rat brain. *Eur. J. Pharmacol.* **2003**, *478*, 1-9.

160. Lambeng, N.; Gillard, M.; Vertongen, P.; Fuks, B.; Chatelain, P. Characterization of [³H]ucb 30889 binding to synaptic vesicle protein 2A in the rat spinal cord. *Eur. J. Pharmacol.* **2005**, *520*, 70-76.

161. Gillard, M.; Chatelain, P.; Fuks, B. Binding characteristics of levetiracetam to synaptic vesicle protein 2A (SV2A) in human brain and in CHO cells expressing the human recombinant protein. *Eur. J. Pharmacol.* **2006**, *536*, 102-108.

162. Hulme, E. C., Ed. Receptor-ligand interactions. A practical approach; University Press: Oxford, 1992.

163. Wilzbach, K. E. Tritium-labeling by exposure of organic compounds to tritium gas. *J. Am. Chem. Soc.* **1957**, *79*, 1013.

164. Loveland, W. D.; Morrissey, D.; Seaborg, G. T. Modern nuclear chemistry; Wiley: New Jersey, 2006.

165. Das Sarma, K.; Zhang, J.; Huang, Y.; Davidson, J. G. Amino acid esters and amides for reductive amination of mucochloric acid: synthesis of novel γ-lactams, short peptides and antiseizure agent levetiracetam (Keppra®). *Eur. J. Org. Chem.* **2006**, *37*, 3730-3737.

166. Zhang, J.; Blazecka, P. G.; Davidson, J. G. First direct reductive amination of mucochloric acid: a simple and efficient method for preparing highly functionalized α,β-unsaturated γ-butyrolactams. *Org. Lett.* **2003**, *5*, 553-556.

167. Klieger, E.; Gibian, H. Über Peptidsynthesen, VIII Weitere Synthesen von Glutamylpeptiden mit Carbobenzoxy-l-Pyroglutaminsäure. *Liebigs Ann. Chem.* **1961**, *649*, 183-202.

168. Hildenbrand, S.; Baqi, Y.; Müller, C. E. Synthesis of tritium-labeled levetiracetam ((2S)-2-(2-oxopyrrolidin-1-yl)butanamide) with high specific activity. *J. Labelled Comp. Radiopharm.* **2012**, *55*, 48-51.

169. Kharasch, M. S.; Tawney, P. O. Factors determining the course and mechanisms of Grignard reactions. II. The effect of metallic compounds on the reaction between isophorone and methylmagnesium bromide. *J. Am. Chem. Soc.* **1941**, *63*, 2308-2316.

170. Corey, E. J.; Boaz, N. W. Evidence for a reversible d, π*-complexation, β-cupration sequence in the conjugate addition reaction of Gilman reagents with α,β-enones. *Tetrahedron Lett.* **1985**, *26*, 6015-6018.

171. Alexakis, A.; Berlan, J.; Besace, Y. Organocopper conjugate addition reaction in the presence of trimethylchlorosilane. *Tetrahedron Lett.* **1986**, *27*, 1047-1050.

172. Frantz, D. E.; Singleton, D. A. Isotope effects and the mechanism of chlorotrimethylsilane-mediated addition of cuprates to enones. *J. Am. Chem. Soc.* **2000**, *122*, 3288-3295.

173. Munch-Petersen, J. Conjugate additions to Grignard reagents to α,β-unsaturated esters. *J. Org. Chem.* **1957**, *22*, 170-176.

174. Dutton, F. E.; Lee, B. H.; Johnson, S. S.; Coscarelli, E. M.; Lee, P. H. Restricted conformation analogues of an anthelmintic cyclodepsipeptide. *J. Med. Chem.* **2003**, *46*, 2057-2073.

175. Herrmann, M.; Ehrler, J.; Kayser, H.; Rindlisbacher, A.; Höfle, G. Chemical modification of thiangazole A in the oxazole and styryl region. *Eur. J. Org. Chem.* **1999**, *14*, 3381-3392.

176. Sánchez, V. M.; Rebolledo, F.; Gotor, V. Candida antarctica lipase-catalyzed doubly enantioselective aminolysis reactions. Chemoenzymatic synthesis of 3-hydroxypyrrolidines and 4-(silyloxy)-2-oxopyrrolidines with two stereogenic centers. *J. Org. Chem.* **1999**, *64*, 1464-1470.

177. Basha, A.; Lipton, M.; Weinreb, S. M. A mild, general method for conversion of esters to amides. *Tetrahedron Lett.* **1977**, *48*, 4171-4174.

178. Levin, J.; Turos, E.; Weinreb, S. An alternative procedure for the aluminum-mediated conversion of esters to amides. *Synth. Commun.* **1982**, *12*, 989-993.

179. Vyas, D. M.; Chiang, Y.; Doyle, T. W. A practical synthesis of racemic vinylglycine from (Z)-2-butene-1,4-diol. *J. Org. Chem.* **1984**, *49*, 2037-2039.

180. Bourguignon, J. J.; Wermuth, C. G. Lactone chemistry. Synthesis of β-substituted, γ-functionalized butanolides and butenolides and succinaldehydic acids from glyoxylic acid. *J. Org. Chem.* **1981**, *46*, 4889-4894.

181. Löscher, W. Animal models of intractable epilepsy. *Prog. Neurobiol.* **1997**, *53*, 239-258.

182. Gören, M. Z.; Onat, F. Ethosuximide: from bench to bedside. *CNS Drug Rev.* **2007**, *13*, 224-239.

183. Löscher, W. Preclinical assessment of proconvulsant drug activity and its relevance for predicting adverse events in humans. *Eur. J. Pharmacol.* **2009**, *610*, 1-11.

184. Mandhane, S. N.; Aavula, K.; Rajamannar, T. Timed pentylenetetrazol infusion test: a comparative analysis with s.c.PTZ and MES models of anticonvulsant screening in mice. *Seizure* **2007**, *16*, 636-644.

185. Wilson, C. W. Drug antagonism and audiogenic seizures in mice. *Brit. J. Pharm. Chemoth.* **1959**, *14*, 415-419.

186. Peuvot, J.; Schanck, A.; Deleers, M.; Brasseur, R. Piracetam-induced changes to membrane physical properties. A combined approach by ^{31}P nuclear magnetic resonance and conformational analysis. *Biochem. Pharmacol.* **1995**, *50*, 1129-1134.

187. Coq, J. O.; Xerri, C. Acute reorganization of the forepaw representation in the rat SI cortex after focal cortical injury: neuroprotective effects of piracetam treatment. *Eur. J. Neurosci.* **1999**, *11*, 2597-2608.

188. Kessler, J.; Thiel, A.; Karbe, H.; Heiss, W. D. Piracetam improves activated blood flow and facilitates rehabilitation of poststroke aphasic patients. *Stroke* **2000**, *31*, 2112-2116.

189. Winblad, B. Piracetam: a review of pharmacological properties and clinical uses. *CNS Drug Rev.* **2005**, *11*, 169-182.

190. Wieser, H. G.; Yaşargil, M. G. Selective amygdalohippocampectomy as a surgical treatment of mesiobasal limbic epilepsy. *Surg. Neurol.* **1982**, *17*, 445-457.

191. Hajek, M.; Yaşargil, M. G.; Yonekawa, Y.; Wieser, H. G. Epileptologisches Outcome der Zürcher Amygdala-Hippokampektomie-Serie. *Schweiz. Arch. Neurol. Psychatr.* **1999**, *150*, 79-82.

192. Schmidt, D.; Löscher, W. Drug resistance in epilepsy: putative neurobiologic and clinical mechanisms. *Epilepsia* **2005**, *46*, 858-877.

193. Remy, S.; Gabriel, S.; Urban, B. W.; Dietrich, D.; Lehmann, T. N.; Elger, C. E.; Heinemann, U.; Beck, H. A novel mechanism underlying drug resistance in chronic epilepsy. *Ann. Neurol.* **2003**, *53*, 469-479.

194. Potschka, H.; Baltes, S.; Löscher, W. Inhibition of multidrug transporters by verapamil or probenecid does not alter blood-brain barrier penetration of levetiracetam in rats. *Epilepsy Res.* **2004**, *58*, 85-91.

195. Baltes, S.; Gastens, A. M.; Fedrowitz, M.; Potschka, H.; Kaever, V.; Löscher, W. Differences in the transport of the antiepileptic drugs phenytoin, levetiracetam and carbamazepine by human and mouse P-glycoprotein. *Neuropharmacology* **2007**, *52*, 333-346.

196. Betts, T.; Yarrow, H.; Greenhill, L.; Barrett, M. Clinical experience of marketed levetiracetam in an epilepsy clinic — a one year follow up study. *Seizure* **2003**, *12*, 136-140.

197. Luna-Tortós, C.; Fedrowitz, M.; Löscher, W. Several major antiepileptic drugs are substrates for human P-glycoprotein. *Neuropharmacology* **2008**, *55*, 1364-1375.

198. Awasthi, S.; Hallene, K. L.; Fazio, V.; Singhal, S. S.; Cucullo, L.; Awasthi, Y. C.; Dini, G.; Janigro, D. RLIP76, a non-ABC transporter, and drug resistance in epilepsy. *BMC Neurosci.* **2005**, *6*, 61.

199. Fischer, W.; Praetor, K.; Metzner, L.; Neubert, R. H. H.; Brandsch, M. Transport of valproate at intestinal epithelial (Caco-2) and brain endothelial (RBE4) cells: mechanism and substrate specificity. *Eur. J. Pharm. Biopharm.* **2008**, *70*, 486-492.

200. Remy, S.; Beck, H. Molecular and cellular mechanisms of pharmacoresistance in epilepsy. *Brain* **2006**, *129*, 18-35.

201. Felgner, P. L.; Gadek, T. R.; Holm, M.; Roman, R.; Chan, H. W.; Wenz, M.; Northrop, J. P.; Ringold, G. M.; Danielsen, M. Lipofection: a highly efficient, lipid-mediated DNA-transfection procedure. *Proc. Natl. Acad. Sci. U.S.A.* **1987**, *84*, 7413-7417.

202. Karra, D.; Dahm, R. Transfection techniques for neuronal cells. *J. Neurosci.* **2010**, *30*, 6171-6177.

203. Wheeler, C. J.; Sukhu, L.; Yang, G.; Tsai, Y.; Bustamente, C.; Felgner, P.; Norman, J.; Manthorpe, M. Converting an alcohol to an amine in a cationic lipid dramatically alters the co-lipid requirement, cellular transfection activity and the ultrastructure of DNA-cytofectin complexes. *Biochim. Biophys. Acta* **1996**, *1280*, 1-11.

204. Gao, X.; Huang, L. Cationic liposome-mediated gene transfer. *Gene Ther.* **1995**, *2*, 710-722.

205. Li, K. J.; Garoff, H. Production of infectious recombinant Moloney murine leukemia virus particles in BHK cells using Semliki Forest virus-derived RNA expression vectors. *Proc. Natl. Acad. Sci. U.S.A.* **1996**, *93*, 11658-11663.

206. Markowitz, D.; Goff, S.; Bank, A. Construction and use of a safe and efficient amphotropic packaging cell line. *Virology* **1988**, *167*, 400-406.

207. Hu, W. S.; Pathak, V. K. Design of retroviral vectors and helper cells for gene therapy. *Pharmacol. Rev.* **2000**, *52*, 493-511.

208. Miller, A. D. Retrovirus packaging cells. *Hum. Gene Ther.* **1990**, *1*, 5-14.

209. Julius, M. A.; Yan, Q.; Zheng, Z.; Kitajewski, J. Q vectors, bicistronic retroviral vectors for gene transfer. *BioTechniques* **2000**, *28*, 702-707.

210. Emi, N.; Friedmann, T.; Yee, J. K. Pseudotype formation of murine leukemia virus with the G protein of vesicular stomatitis virus. *J. Virol.* **1991**, *65*, 1202-1207.

211. Tanabe, K. K.; Cusack, J. C. Jr. Gene Therapy. In *Surgery: basic science and clinical evidence*; Norton, J. A., Bollinger, R. R., Chang, A. E., Lowry, S. F., Mulvihill, S. J., Pass, H. I., Thompson, R. W., Eds.; Springer: Berlin, 2001; pp 1881-1895.

212. Thomas, K. R.; Folger, K. R.; Capecchi, M. R. High frequency targeting of genes to specific sites in the mammalian genome. *Cell* **1986**, *44*, 419-428.

213. Lee, C. Y.; Chen, C. C.; Liou, H. H. Levetiracetam inhibits glutamate transmission through presynaptic P/Q-type calcium channels on the granule cells of the dentate gyrus. *Br. J. Pharmacol.* **2009**, *158*, 1753-1762.

214. Ahmed, A. H.; Oswald, R. E. Piracetam defines a new binding site for allosteric modulators of alpha-amino-3-hydroxy-5-methyl-4-isoxazole-propionic acid (AMPA) receptors. *J. Med. Chem.* **2010**, *53*, 2197-2203.

215. Honoré, T.; Lauridsen, J.; Krogsgaard-Larsen, P. The binding of [³H]AMPA, a structural analogue of glutamic acid, to rat brain membranes. *J. Neurochem.* **1982**, *38*, 173-178.

216. Olsen, R. W.; Szamraj, O.; Houser, C. R. [³H]AMPA binding to glutamate receptor subpopulations in rat brain. *Brain Res.* **1987**, *402*, 243-254.

217. Kessler, M.; Arai, A. C. Use of [³H]fluorowillardiine to study properties of AMPA receptor allosteric modulators. *Brain Res.* **2006**, *1076*, 25-41.

218. Kessler, M.; Suzuki, E.; Montgomery, K.; Arai, A. C. Physiological significance of high- and low-affinity agonist binding to neuronal and recombinant AMPA receptors. *Neurochem. Int.* **2008**, *52*, 1383-1393.

219. Andersen, P. H.; Tygesen, C. K.; Rasmussen, J. S.; Soegaard-Nielsen, L.; Hansen, A.; Hansen, K.; Kiemer, A.; Stidsen, C. E. Stable expression of homomeric AMPA-selective glutamate receptors in BHK cells. *Eur. J. Pharmacol.* **1996**, *311*, 95-100.

220. Nielsen, E. O.; Cha, J. H.; Honoré, T.; Penney, J. B.; Young, A. B. Thiocyanate stabilizes AMPA binding to the quisqualate receptor. *Eur. J. Pharmacol.* **1988**, *157*, 197-203.

221. Murphy, D. E.; Snowhill, E. W.; Williams, M. Characterization of quisqualate recognition sites in rat brain tissue using DL-[³H]alpha-amino-3-hydroxy-5-methylisoxazole-4-propionic acid (AMPA) and a filtration assay. *Neurochem. Res.* **1987**, *12*, 775-781.

222. Hall, R. A.; Massicotte, G.; Kessler, M.; Baudry, M.; Lynch, G. Thiocyanate equally increases affinity for two DL-alpha-amino-3-hydroxy-5-methylisoxazolepropionic acid (AMPA) receptor states. *Mol. Pharmacol.* **1993**, *43*, 459-464.

223. Arai, A.; Silberg, J.; Kessler, M.; Lynch, G. Effect of thiocyanate on AMPA receptor mediated responses in excised patches and hippocampal slices. *Neuroscience* **1995**, *66*, 815-827.

224. Hall, R. A.; Kessler, M.; Lynch, G. Evidence that high- and low-affinity DL-alpha-amino-3-hydroxy-5-methylisoxazole-4-propionic acid (AMPA) binding sites reflect membrane-dependent states of a single receptor. *J. Neurochem.* **1992**, *59*, 1997-2004.

225. Hennegriff, M.; Arai, A.; Kessler, M.; Vanderklish, P.; Mutneja, M. S.; Rogers, G.; Neve, R. L.; Lynch, G. Stable expression of recombinant AMPA receptor subunits: binding affinities and effects of allosteric modulators. *J. Neurochem.* **1997**, *68*, 2424-2434.

226.   Standley, S.; Tocco, G.; Wagle, N.; Baudry, M. High- and low-affinity alpha-[^{3}H]amino-3-hydroxy-5-methylisoxazole-4-propionic acid ([^{3}H]AMPA) binding sites represent immature and mature forms of AMPA receptors and are composed of differentially glycosylated subunits. *J. Neurochem.* **1998**, *70*, 2434-2445.

227.   Patsalos, P. N. Pharmacokinetic profile of levetiracetam: toward ideal characteristics. *Pharmacol. Ther.* **2000**, *85*, 77-85.

228.   Acharyulu, P. V. R.; Raju, C. M. H. Preparation of amino acid amides. US Patent 20050182262, **2005**.

229.   Boschi, F.; Camps, P.; Comes-Franchini, M.; Munoz-Torrero, D.; Ricci, A.; Sanchez, L. A synthesis of levetiracetam based on (*S*)-N-phenylpantolactam as a chiral auxiliary. *Tetrahedron Asymmetry* **2005**, *16*, 3739-3745.

230.   Charette, A. B.; Lebel, H. (2*S*,3*S*)-(+)-(3-phenylcyclopropyl)methanol. *Org. Synth.* **2004**, *Coll. Vol. X.*, 613-620.

231.   Cushman, M.; Jurayj, J.; Moyer, J. D. Synthesis, biological testing, and stereochemical assignment of an end group modified retro-inverso bombesin C-terminal nonapeptide. *J. Org. Chem.* **1990**, *55*, 3186-3194.

232.   Lowry, O. H.; Rosebrough, N. J.; Farr, A. L.; Randall, R. J. Protein measurement with the Folin phenol reagent. *J. Biol. Chem.* **1951**, *193*, 265-275.

233.   Rosenthal, H. E. A graphic method for the determination and presentation of binding parameters in a complex system. *Anal. Biochem.* **1967**, *20*, 525-532.

234.   Cheng, Y.; Prusoff, W. H. Relationship between the inhibition constant (K_i) and the concentration of inhibitor which causes 50 per cent inhibition (I_{50}) of an enzymatic reaction. *Biochem. Pharmacol.* **1973**, *22*, 3099-3108.

235.   DeBlasi, A.; O'Reilly, K.; Motulsky, H. J. Calculating receptor number from binding experiments using same compound as radioligand and competitor. *Trends Pharmacol. Sci.* **1989**, *10*, 227-229.

236.   Birnboim, H. C.; Doly, J. A rapid alkaline extraction procedure for screening recombinant plasmid DNA. *Nucleic Acids Res.* **1979**, *7*, 1513-1523.

Register of Publications

Publications

Hildenbrand, S.; Baqi, Y.; Müller, C. E. Synthesis of tritium-labeled levetiracetam ((2S)-2-(2-oxopyrrolidin-1-yl)butanamide) with high specific activity. *J. Labelled Comp. Radiopharm.* **2012**, *55*, 48-51.

Hildenbrand, S.; Schoch, S.; von Lehe, M; Surges, R.; Müller, C. E. Tritium-labeled brivaracetam with high specific activity: preparation, characterization and application in human brain samples. *submitted*.

Scientific contribution to a congress

Hildenbrand, S.; Müller, C. E. Preparation of [³H]-Levetiracetam and [³H]-Brivaracetam with high Specific Radioactivity for studying Drug-Target Interactions. *17th Workshop of the International Isotope Society – Central European Division* **2010**, Bad Soden (oral presentation).

Erklärung

Hiermit versichere ich, dass ich die vorliegende Dissertation selbstständig angefertigt und nur die in der Arbeit ausdrücklich benannten Quellen und Hilfsmittel benutzt habe. Wörtlich oder inhaltlich übernommenes Gedankengut habe ich als solches kenntlich gemacht.